TJ-positive neurons implication in Drosophila larva locomotor behaviour

Hélène Babski

THÈSE POUR OBTENIR LE GRADE DE DOCTEUR DE L'UNIVERSITÉ DE MONTPELLIER

En Neurosciences

École doctorale n°168 Sciences Chimiques et Biologiques pour la Santé (CBS2)

Unité de recherche INSERM U1051, Institut des Neurosciences de Montpellier

Implication des neurones TJ-positifs dans le comportement locomoteur de la larve de Drosophile

TJ-positive neurons implication in *Drosophila* larva locomotor behaviour

Présentée par Hélène BABSKI
Le 01 octobre 2018

Sous la direction de Patrick CARROLL
Et Alain GARCÈS

Devant le jury composé de

Stéphanie BAULAC, DR, Institut du Cerveau et de la Moelle Epinière, Paris	Présidente
Patrick CARROLL, DR, U1051, Institut des Neurosciences de Montpellier	Directeur de thèse
Alain GARCÈS, CR, U1051, Institut des Neurosciences de Montpellier	Co-directeur de thèse
Matthias LANDGRAF, Lecturer, Zoology Department, University of Cambridge	Rapporteur
Laurent FASANO, DR, UMR7288, Institut de Biologie du Développement de Marseille	Rapporteur
Jonathan ENRIQUEZ, CR, Institut de Génomique Fonctionnelle de Lyon	Examinateur

UNIVERSITÉ DE MONTPELLIER

To my grandmother

Acknowledgments

First I would like to thank the members of my thesis jury: Mr Landgraf, Mr Fasano, Ms Baulac and Mr Enriquez. Thank you for agreeing to take part to this jury and sparing the time to read this manuscript.

This project was made possible by a three years funding from the AFM-Téléthon; I truly am thankful for that.

I am indebted to Patrick Carroll and Alain Garcès for their time, availability and commitment to the supervision of my thesis. I am grateful for the opportunity you gave me and for the enthusiasm you showed for my thesis project.

I thank the members of the team (past and present), especially Stéphanie, Alex, Willy, Fred and Ilana for their kindness and help. I have a thought for Lucie too, with whom I shared so many hours in the lab.

I would like to thank my PhD fellows of the Institute with whom I went through the sometimes painful, sometimes exhilarating experience of growing as a trainee scientist. I also would like to thank Valeria and Marion for their support and friendship.

Outside the lab, I have to cite former flatmates and current flatmates that made life so much easier and fun; if you ever get to read this page (Oh dear, in English, no less!), you will recognize yourselves.

My warmest thanks go to the Edmond family for simply making me feel welcome and loved (and also feeding me every single Monday evening…). Thank you for setting such an inspiring example of what my life could be. Many memories may fade but never the ones attached to you.

I wouldn't be here without my family, so I need to thank:

My brother lost in his countryside, who should just admit by now that I have the highest diploma; my sister across the ocean, who tilted the balance and convinced me to do a PhD; my brother across the border who will without a doubt teasingly call me 'Herr Doktor' from now on; my mother for being so understanding and supportive, and simply the best of mothers (always); and my father for not understanding at all sometimes, but still trusting blindly. Having you as a family is the greatest gift ever; I feel blessed.

Finally, I dedicate this thesis to my grandmother, great lover of six-legged creatures. I hope one day we finally get the answer to the "Does the butterfly remember it was a caterpillar?" question.

Table of contents

Abbreviation list

ALMA Alternating Leg Muscle Activation

ALS Amyotrophic Lateral Schlerosis

AN ascending neuron

AP1 superfamily Activator protein 1 superfamily

BarH1/2 BarH-like Homeobox 1/2

BOs Bolwig's organs

bZIP basic leucine zipper

CaMP Cyclic adenosine monophosphate

ch neurons chordotonal neurons

CiA Circumferential Ascending

CiD Circumferential Descending

CL cerebellar lobes

CLI 1/2 Cholinergic Lateral Interneuron 1/2

CNS Central Nervous System

CoB Commissural Bifurcating

CoBLCommissural Bifurcating Longitudinal

CoLA commissural longitudinal ascending

CoLo Commissural Local

CoPA Commissural Primary Ascending

CoSA Commissural Secondary Ascending

CPG Central Pattern Generator

CRISPR Clustered Regularly Interspaced Short Palindromic Repeats

Crx cone-rod homeobox

CSF-cN CerebroSpinal Fluid-Contacting neuron

CVJ CranioVertebral Junction

dbd sensory neurons dorsal bipolar dendritic sensory neurons

dbx1 developing brain homeobox 1

DN descending neuron

DoLA dorsal longitudinal ascending

DV channel DorsoVentral channel

eIN excitatory interneuron

EL Eve lateral

en engrailed

es external sensory

Eve Even-skipped

GDL GABAergic Dorso-Lateral interneuron

GFP Green Fluorescent Protein

GRASP GFP Reconstruction Across Synaptic Partners

GVLI Glutamatergic Ventro-Lateral Interneurons

HB9 Homeobox 9

iIN inhibitory Interneuron

IN interneuron

Isl Islet

ISN Intersegmental Nerve

iVUM Ventral Unpaired median interneuron

KA Kolmer-Agduhr

LLN Lateral Locomotor Neurons

Maf musculo-aponeurotic fibrosarcoma

MafL large Maf

MARE Maf recognition element

MCoD Multipolar Commissural Descending

mCSIs medial clusters of C4 da second-order INs

md sensory neuron multidendritic sensory neuron

MN motoneuron

MNB progeny Median NeuroBlast progeny

MS Multiple Sclerosis

mVUM Ventral Unpaired Median motoneuron

Nrl neural retina leucine zipper

OSNs olfactory sensory neurons

Otd Orthodenticle

PBS Phosphate Buffered Saline

PLMS Periodic Limb Movements during Sleep

PMSI *Period*-positive Median Segmental Interneurons

RC Renshaw cells

Rfx regulatory factor X

RLS Restless Leg Syndrome

RT room temperature

SA saaghi

SEZ subesophageal zone

SIDS Sudden Infant Death Syndrome

SN Segmental Nerve

SOG suboesophageal ganglion

spGFP1-10 split Green Fluorescent Protein 1-10

spGFP11 split Green Fluorescent Protein 11

TEM Transmission Electron Microscopy

TF transcription factor

TJ Traffic Jam

TJ-Flp *TJ-Flippase*

TRP transient receptor potential

UCoD Unipolar Commissural Descending

vbd sensory neurons ventral bipolar dendritic sensory neurons

VeLD Ventral Longitudinal Descending

VeMe Ventral Medial

VNC Ventral Nerve Cord

Zfh1 Zinc Finger Homeodomain 1

Chapter 1: General introduction

I. Central Pattern Generators

A - General organization and function

CPGs (for Central Pattern Generators) are neuronal circuits involved in the generation of crucial automatic rhythmic behaviours such as locomotion (walking, swimming, crawling, flying), breathing, scratching and chewing to cite only the most obvious (Bucher, 2009). CPGs are able to generate activity “on their own”, even in the absence of sensory feed-back or activation by descending neurons (Bucher, 2009). However, inputs coming from the higher centres and the sensory system can modulate their activity to respond to physiological conditions or environmental cues. Fig.1 displays the simplified organization of a CPG.

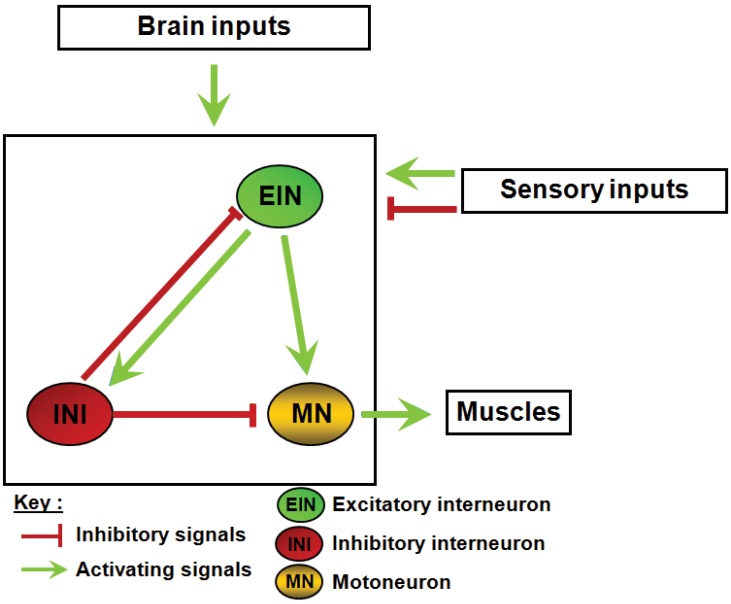

Fig.1: Schematic of a basic simplified CPG

A CPG comprises three types of neurons: motoneurons (MNs) and inhibitory and excitatory interneurons (INs). MNs are the last effectors of the system. They innervate muscles and allow for their contraction. MNs represent the tiniest neuronal population of the CPG; the greatest majority of the CPGs neurons are inhibitory or excitatory INs that innervate each other and/or MNs, and integrate signals coming from the higher centres or the sensory system. Although the basic components of the

CPG (MNs+INs) are able to generate activity on their own, inputs coming from the brain and the sensory system allow for the modulation of this activity to answer to environmental cues for example.

In vertebrates, the core components of the CPGs are located either in the spinal cord (or its equivalent in invertebrates) for the locomotor CPG or in the brainstem for the breathing and chewing CPGs. CPGs are highly complex and the basic cellular and network mechanisms of rhythm generation remain generally poorly characterized. Nowadays, defining and understanding them is of paramount importance for two main reasons. The first is medicine-related, to treat patients with CPG dysfunction. The second is more fundamental, with the purpose to understand how a neuronal circuit generates behaviour and how different behaviours are prioritised. In that respect the CPG is an attractive model, with which it seems possible to link “basic” behaviours (that can be easily seen and quantified) to circuit operation. Fundamental knowledge gathered during the study of CPGs could then be used to decipher other circuits involved in more complex behaviours (Bucher, 2009).

B - Human diseases of dysfunctional CPGs and implications of the study of CPGs

Here we will give a quick overview of some of the diseases linked to or potentially involving CPG dysfunction.

Medullar traumas are the most obvious disorders linked to locomotor CPG dysfunction. Although in most cases the core components of the locomotor CPG itself seem to be spared, connections between them and the higher centres are severed; here what is lacking for the CPG to function is the initial impulse that will start its rhythmic activity. Backing this hypothesis, it seems that stimulating the locomotor CPG directly in the spinal cord with neurotransmitters and forced physical activity (treadmill) leads to the reorganization of CPG circuits and improvement of some medullar trauma patients (Marder and Bucher, 2001). Involuntary CPG activation may be involved in the locomotor-related behaviours that are sometimes observed during epileptic seizures (Tassinari et al., 2005). Abnormal or involuntary CPG activation may also induce symptoms like Restless Legs Syndrome (RLS), Alternating Leg Muscle Activation (ALMA) or Periodic Limb Movements during Sleep (PLMS) found in individuals with Multiple Sclerosis (MS), sleep disorders and other

neurological problems (Chervin et al., 2003; Cosentino et al., 2006; Tassinari et al., 2009; Tassinari et al., 2005). This remains only hypothetical, as many of these pathological conditions are generally considered to be associated with several mechanisms beyond a malfunction of the CPG (Guertin, 2013). A better understanding of the CPG organization would undoubtedly help develop better treatments to improve the condition of patients with locomotor CPG malfunction.

More references can be found on diseases affecting the respiratory CPG. Sudden Infant Death Syndrome (SIDS) is the most common cause of post-neonatal deaths in developed countries. SIDS deaths commonly occur during a sleep period in infants aged less than a year and the actual mechanism of death is still unknown (Spinelli et al., 2017). SIDS is thought to depend on multiple factors but neurochemical abnormalities affecting the catecholaminergic, peptidergic, cholinergic, glutamatergic and serotoninergic systems in the brainstem networks controlling cardiac and/or respiratory functions may increase infants vulnerability (Spinelli et al., 2017; Machaalani and Waters, 2008; Machaalani and Waters, 2014). In some pathologies like axis rheumatoid arthritis, Arnold-Chiari type 1 malformation, anterio C1-2 osteochondroma, os odontoideum and occipital encephalocele, the craniovertebral junction (CVJ), which is the region lying between the skull and the cervical spine, is affected. This CVJ area encloses the soft-tissue structures of the cervicomedullary junction, including the medulla, spinal cord and lower cranial nerves. Central apnea syndrome is a common symptom found in those pathologies and might be related to respiratory centre dysfunction, as the CVJ area encompasses the region containing the respiratory CPG (Smoker, 1994; Visocchi et al., 2017). Rett syndrome is a genetic disorder affecting females and characterized by severe neurodevelopmental defects leading to problems with language, coordination and repetitive movements (Neul et al., 2010). It was found that dysfunction of the breathing CPG associated with a mutation in the methyl-CpG binding protein2 (*MECP2* gene) affects rhythm-generating networks and causes breathing complications (Guertin, 2013).

Amyotrophic Lateral Schlerosis (ALS) is a degenerative MN disease and is characterized by a loss of MNs that eventually leads to the patient death by respiratory insufficiency. Dysfunction of swallowing CPG was found in dysphagic ALS patients (Aydogdu et al., 2011). Deficient coordination between CPGs can also be problematic; coordination between swallowing and breathing CPGs is altered in

Parkinson's disease (Wang et al., 2017) as well as in ALS patients (Erdem et al., 2016).

Our lack of knowledge in CPG neuronal composition and networking might lead us to underestimate the number of diseases linked to dysfunctional CPGs. The study of CPG has therefore long-term fundamental implications to understand motor-function related disorders and injuries affecting the central nervous system (CNS) (Bucher, 2009).

II. Approaches to studying locomotor CPG

A - Model organisms

Several models have been traditionally used and are currently used to study locomotor CPG. The state of knowledge, strong points and disadvantages of each of them will be discussed in the following paragraphs.

1. Cat

Several preparations of decerebrate cats have been traditionally used to study the locomotor CPG; they differ from the level at which the nervous system is transected. The decerebrate cat model brought the uncompromising proof of existence of a CPG that can generate locomotion in absence of descending inputs, as cats transected immediately caudally to the thalamus (therefore "lacking" the cortex and thalamus) display spontaneous walking in response to a moving treadmill (Whelan, 1996). This model is still used but considering its complex set-up and the absence of tools for genetic manipulation, other "easier to use" models might nowadays be preferred.

2. Mouse

The mouse is used to a great extent for the study of locomotor CPG cellular composition and wiring. Its handling is easier than the cat and it remains a vertebrate and a mammal. Moreover, genetic tools are available in the mouse to study the function of locomotor CPG neurons in live individuals; and more genetic tools are being constantly created, adding to the already existing pool. Locomotion in mouse can be studied in wake, freely moving animals but also in isolated spinal cords that

provide potent fictive locomotion models for electrophysiological studies (Grossmann et al., 2010). Numerous studies focus on the development of discrete classes of INs and accordingly the bulk of information currently available is quite consequent (Lu et al., 2015). It allows one to know with precision the identity and in some cases the function of a neuronal population according to the specific transcription factor (TF) combinatorial code expressed by this population (Fig.2). The current viewpoint is that locomotor INs are divided into 4 large classes V_0, V_1, V_2 and V_3, depending on their lineage origin (Lu et al., 2015) (fig.2).

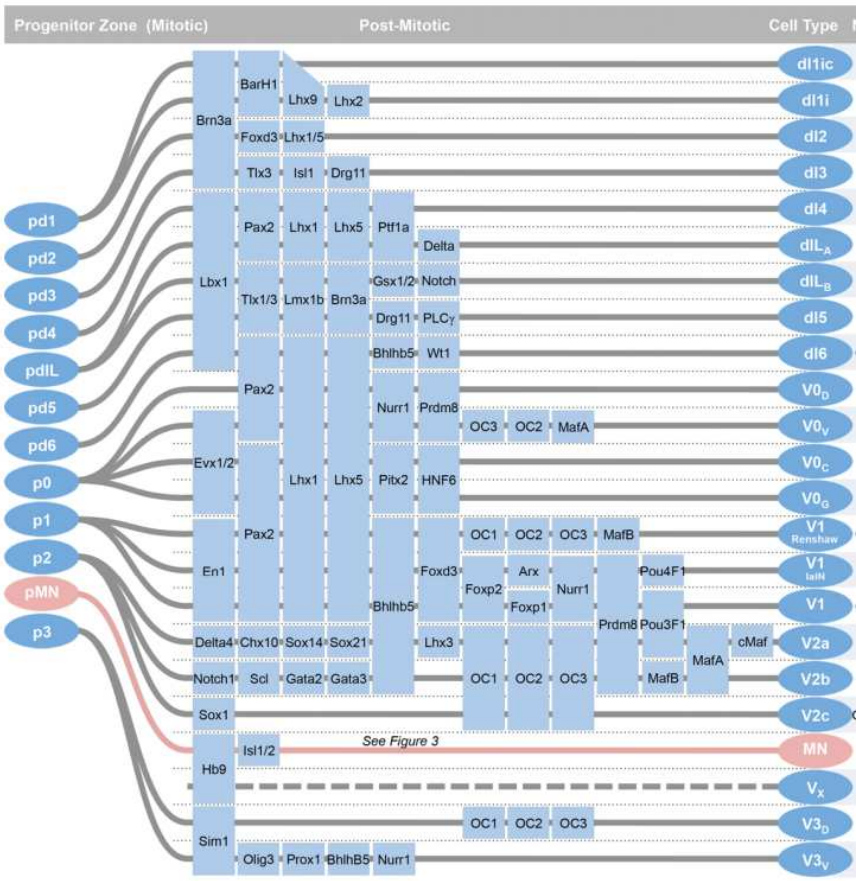

Fig.2: IN classes in the mouse spinal cord identified by their progenitor domain and their specific transcription factor combinatorial code. From (Lu et al., 2015)

Mouse IN populations can be identified thanks their specific transcription factor combinatorial code.

V_0 IN class arises from the dorsal-most progenitor pool of the ventral spinal cord. They form a heterogeneous population, with excitatory or inhibitory identity; however they are mostly contralateral-projecting, commissural neurons. The whole V_0 domain is characterized by its expression of *dbx1* (developing brain homeobox 1) homeodomain TF (Lu et al., 2015). V_0 INs can be subdivided in three populations:

commissural inhibitory *Pax7*$^{+}$ V_{0D}, commissural excitatory *Evx1/2*$^{+}$ V_{0V} and ipsilaterally-projecting cholinergic *Pitx2*$^{+}$ V_{0C} (Lanuza et al., 2004; Moran-Rivard et al., 2001; Pierani et al., 1999; Pierani et al., 2001; Zagoraiou et al., 2009). When the whole V_0 population is ablated, quadrupedal hopping is observed at all frequencies of locomotion in wake, freely moving mice: left/right alternation is abolished (Talpalar et al., 2013). Such results confirm previous observations of left/right alternation disruption in a model of *dbx1* deletion in spinal neurons that prevents V_0 population differentiation (Lanuza et al., 2004). The excitatory V_{0V} INs constitute the main V_0 subpopulation (Griener et al., 2015). Selective ablation of V_{0V} INs does not modify left/right alternation at low locomotion frequencies but leads to hopping gait at medium and high frequencies. Selective ablation of the inhibitory V_{0D} subpopulation does not alter left-right alternation at high frequencies but does disrupt left-right alternation at low frequencies (Talpalar et al., 2013). Control of left/right alternation might therefore be organized in a modular fashion, with two subgroups of V_0 INs involved at different speeds of locomotion. Computational modelling of the locomotor CPG suggests that V_{0D} and V_{0V} are recruited in an ascending order when locomotion speed increases, with V_{0D} active during walk while V_{0V} are active at higher speeds of locomotion, generating trot (Fig 3) (Shevtsova et al., 2015). V_{0C} subpopulation does not seem to be involved in left/right alternation but is rather premotor and makes C-boutons on MNs, thus promoting the firing of MN at higher frequency (Zagoraiou et al., 2009).

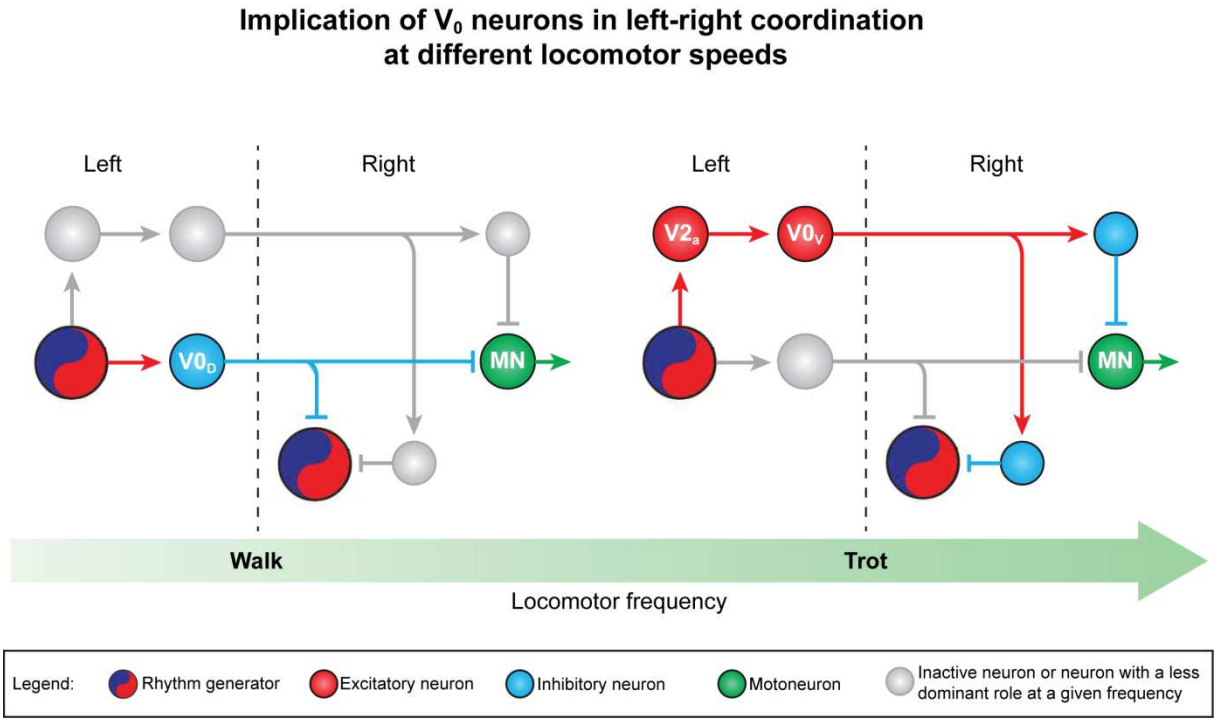

Fig 3: Schematic representation of the implication of V_0 INs in left-right coordination at different speeds. Current data suggest that inhibitory commissural V_{0D} INs are involved in the regulation of left-right alternation at lower locomotor frequencies that correspond to walk. Their activation on one side of the spinal cord (left on the schematics) leads to the inhibition of the locomotor CPG located on the other side of the spinal cord (right on the schematics). Excitatory commissural V_{0V} take in charge alternation at high locomotor speed that correspond to trot, thanks to the recruitment of inhibitory INs (blue) on the contralateral part of the spinal cord (right on the schematics). V_{2a} INs are involved in the left-right alternation as well, as they are placed upstream of V_{0V} INs. Dotted line denotes the midline. Single neurons represent the entire neuronal population considered. Adapted from (Kiehn, 2016).

The V_1 population is characterized by its expression of the homeodomain transcription factor *en1*. There are currently two characterized V_1 subpopulations: the premotor GABAergic Renshaw cells (RC) and glycinergic Ia INs. RC were characterized very early on, when their affiliation to V_1 population was still unknown (Eccles et al., 1957). They are inhibitory ipsilateral premotor INs that receive inputs from α-MNs axon collaterals. In turn, RCs form reciprocal synaptic contacts on the MNs that innervate them, establishing a negative feedback that adjusts the firing rate of MNs (Fig 4) (Eccles et al., 1957; Hultborn, 2006). This negative feedback might be instrumental to avoid MNs hyper-excitation that could lead to their death by excitotoxicity (Ramírez-Jarquín et al., 2014). RCs also innervate the other characterized Ia INs V1 population (Fig 4) (Eccles et al., 1957). Ia INs themselves are activated by proprioceptive information arising from muscle spindles and provide

inhibitory input onto MNs innervating antagonist muscles. By this process, they enable reciprocal inhibition between flexor and extensor MNs, therefore permitting flexor/extensor muscles alternating contractions (Fig 4) (Eccles et al., 1956; Feldman and Orlovsky, 1975). By losing Ia INs, we would expect to see flexor-extensor co-activation, but surprisingly, it is not the case: flexor-extensor alternating pattern is unchanged upon V_1 population ablation (Gosgnach et al., 2006). Loss of alternation is only observed when synaptic outputs of both V_1 and V_{2b} IN populations is blocked. As V_{2b} synaptic blockage does not disrupt flexor-extensor activity, it seems that the blockage of the two populations at the same time is required, thus proving that alternating flexor-extensor motor activity is secured by coordinated activity of both V_1 and V_{2b} INs (Zhang et al., 2014). Although initially Ia INs were thought to strictly originate from p1 domain that gives V_1 population (Fig 2), V_{2b} INs involved in flexor-extensor coordination actually fit the morphological characteristics of Ia INs; therefore it is now admitted that subpopulations of both V_1 and V_{2b} INs collectively constitute the whole Ia INs population (Zhang et al., 2014). Despite the wealth of knowledge on RC and Ia INs, the function of the majority of V_1 INs remains elusive. Indeed, RC and Ia INs subpopulations only account for about 25% of the V_1, leaving 75% still uncharacterized (Alvarez et al., 2005; Sapir et al., 2004; Zhang et al., 2014). Ablation of the V_1 whole population leads to a marked slowing of locomotion in fictive locomotion model (Gosgnach et al., 2006). This result is supported by the inability of *en1* knock-out mice to walk and maintain their balance during high speed locomotion (Gosgnach et al., 2006). Among the 75% of V_1 INs still uncharacterized, there might therefore be a subpopulation regulating the speed of locomotion. Interestingly, two recent studies have shown that the V_1 IN population displays a high variability in terms of molecular combinatorial code, with 50 hypothetical V_1-candidate subtypes (Bikoff et al., 2016; Gabitto et al., 2016). This also hints that V_1 might be divided into numerous functional IN subtypes involved in different aspects of locomotion. Also, if such diversity is seen in the V_1 IN population, might it be the same for the other IN populations?

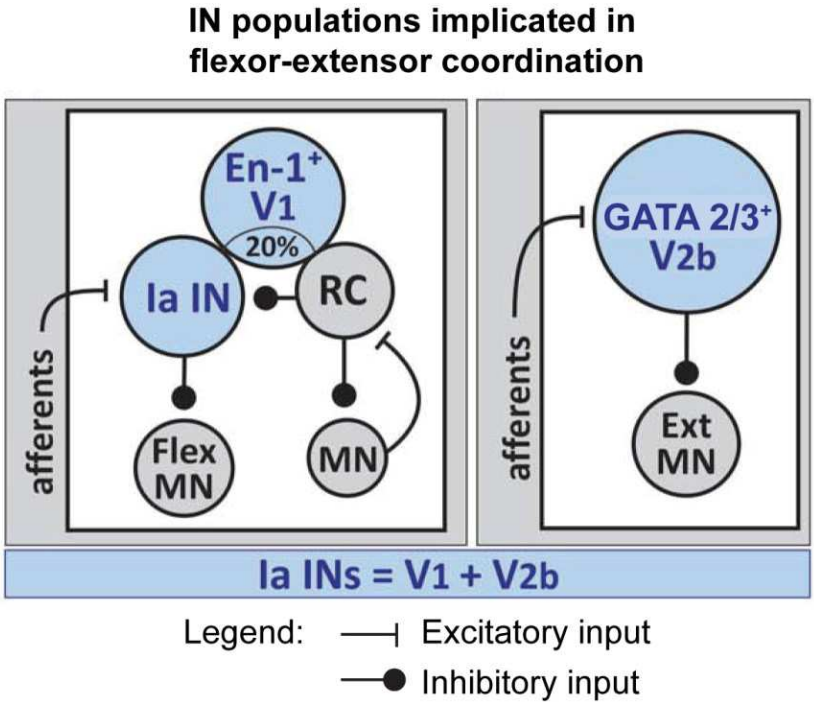

Fig 4: Schematic representation of the IN populations involved in flexor-extensor coordination

Flexor-extensor coordination is mediated by V1 Ia INs subpopulation that receive proprioceptive inputs and make inhibitory innervations on flexor MNs. Reciprocal inhibition of the extensor muscles is mediated by a *Gata2/3*$^{+}$ V_{2b} subpopulation that is now admitted as part of the Ia INs population. V_1 RC subpopulation apply recurrent inhibition on MNs and Ia INs. V_1 Ia INs and RCs only account for about 20% of the total V_1 population; the function of the remaining 75% remains unclear. Adapted from (Ziskind-Conhaim and Hochman, 2017).

The V_2 IN class is subdivided into two groups: the excitatory glutamatergic V_{2a} and the inhibitory V_{2b} that use both GABA and glycine (Al-Mosawie et al., 2007; Lundfald et al., 2007). V_{2a} INs are singled out by their expression of *Chx10* and are ipsilaterally-projecting neurons (Al-Mosawie et al., 2007; Lundfald et al., 2007). Functionally, they seem to be involved in left-right coordination at high locomotion speed, possibly through their excitatory drive on V_{0v} commissural INs (Fig 3 and 5) (Crone et al., 2008). During fictive locomotion only half of the V_{2a} population is rhythmically active, but this proportion increases at higher cycle frequencies, suggesting that V_{2a} subpopulations might be recruited at increasing speeds (Fig 5) (Zhong et al., 2010) much like what is currently thought to happen in Zebrafish (discussed in the following paragraph). As elimination of the whole V_{2a} population does not modify the frequency of the ongoing rhythm, V_{2a} are probably placed downstream to rhythm-generating neurons in the locomotor CPG (Crone et al., 2008; Crone et al., 2009). The other subpopulation of V_2 INs, the inhibitory ipsilaterally-

projecting V_{2b}, can be recognized by their expression of *Gata2/3* (Al-Mosawie et al., 2007). V_{2b} INs make direct synapses on MNs and as explained above, mouse model lacking both V_1 and V_{2b} show significant difficulty with limb articulation in flexion and extension (Fig 4) (Zhang et al., 2014).

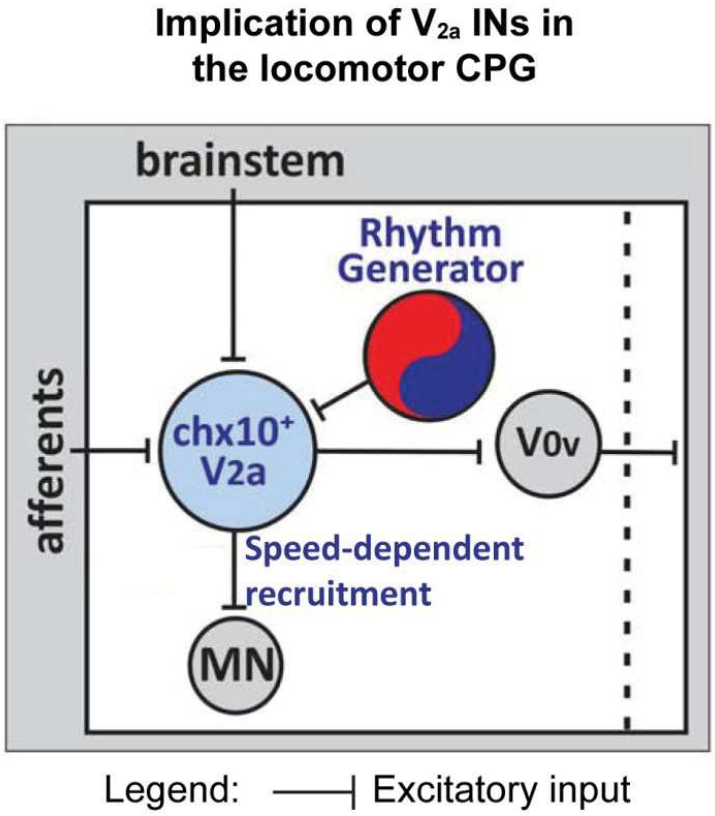

Fig 5: Schematic representation of the implication of V_{2a} INs in the locomotor CPG

V_{2a} INs characterized by their expression of *Chx10* have no implication in rhythm generation and are therefore probably placed downstream of rhythm-generating INs. They are premotor INs increasingly recruited upon increase of the locomotion speed. Additionally, V_{2a} influence left-right alternation through their connection on commissural excitatory V_{0V} INs. Adapted from (Ziskind-Conhaim and Hochman, 2017).

The V_3 IN class is characterized by it expression of *sim1* (a basic helix-loop-helix-PAS domain TF) (Briscoe et al., 1999; Goulding et al., 2002; Sugimori et al., 2007) and subdivided in two commissural glutamatergic V_{3V} and V_{3D} subpopulations with distinct intrinsic properties, morphologies and dorso-ventral distributions (Borowska et al., 2013; Grossmann et al., 2010). V_{3V} have simpler morphology and contact contralateral MNs while V_{3D} display large and complex dendritic arborisation and do not make synapses onto contralateral MNs. Extrapolating from their morphology, V_{3V} are thought to be implicated in the synchronization of motor outputs,

while V_{3D} would function as sensory relay INs (Borowska et al., 2013). Experimentally, locomotion output loses robustness when the whole V_3 population is silenced in a fictive locomotion model. In freely behaving mice, this translates by an irregular gait (Zhang et al., 2008). In a *Nkx2.2* and *Nkx2.9* mutant mouse that causes loss of V_3 INs, mice displayed hopping gait, implying that V_3 are likely to mediate left-right coordination as well (Holz et al., 2010).

An additional class of INs belonging to the locomotor CPG has been characterized recently: the *Shox2*$^+$ INs. They are ipsilaterally projecting excitatory INs that partially overlap with V_{2a} IN class (Dougherty et al., 2013). Optogenetic silencing or synaptic output blockade of the whole *Shox2*$^+$ population substantially reduces the rhythm of the locomotor-like activity in a fictive locomotion model, without modifying the left-right or flexor-extensor alternating patterns. In contrast, ablation of the *Shox2*$^+$ V_{2a} subpopulation does not disrupt the rhythm frequency nor the pattern of left-right or flexor-extensor coordination, but causes irregular amplitude and locomotor cycles. By deduction, one can surmise that non-V_{2a} *Shox2*$^+$ INs are part of the rhythm-generating circuits in the mouse spinal cord (Fig 6) (Dougherty et al., 2013). However, as silencing of the *Shox2*$^+$ population only partially reduces rhythm and does not completely abolishes it, it is likely that other neuronal populations are involved in rhythm generation.

The last IN class possibly involved in locomotion is exclusively located in thoracic and upper lumbar segments: the V_x INs. The developmental origin of these glutamatergic INs, characterized by their postnatal expression of *HB9*, is unknown (Hinckley and Ziskind-Conhaim, 2006; Thaler et al., 1999; Wichterle et al., 2002; Wilson et al., 2005). *HB9* is expressed in embryonic stages in multiple IN classes (Caldeira et al., 2017), therefore V_x INs could derive from any of them. They show oscillatory properties, probably synapse on MNs and are associated with motor rhythms (Brocard et al., 2010; Hinckley et al., 2005; Hinckley and Ziskind-Conhaim, 2006; Wilson et al., 2005; Ziskind-Conhaim et al., 2010). Clustered *HB9*$^+$ INs activity is furthermore synchronized by electrical coupling (Fig 6) (Hinckley and Ziskind-Conhaim, 2006). In addition, V_x IN rhythmic activity is generated by persistent sodium current (Tazerart et al., 2008; Ziskind-Conhaim et al., 2008), a prevalent current in various rhythmogenic CNS neurons (Ziskind-Conhaim and Hochman, 2017). Silencing glutamate release from V_x INs induces in a notable diminution of the frequency of drug-induced and descending fiber-evoked rhythms in newborn mice

(Caldeira et al., 2017). This strongly suggests that V_x INs, maybe alongside non-V_{2a} *Shox2*$^+$ INs, are involved in rhythm generation in the mouse locomotor CPG.

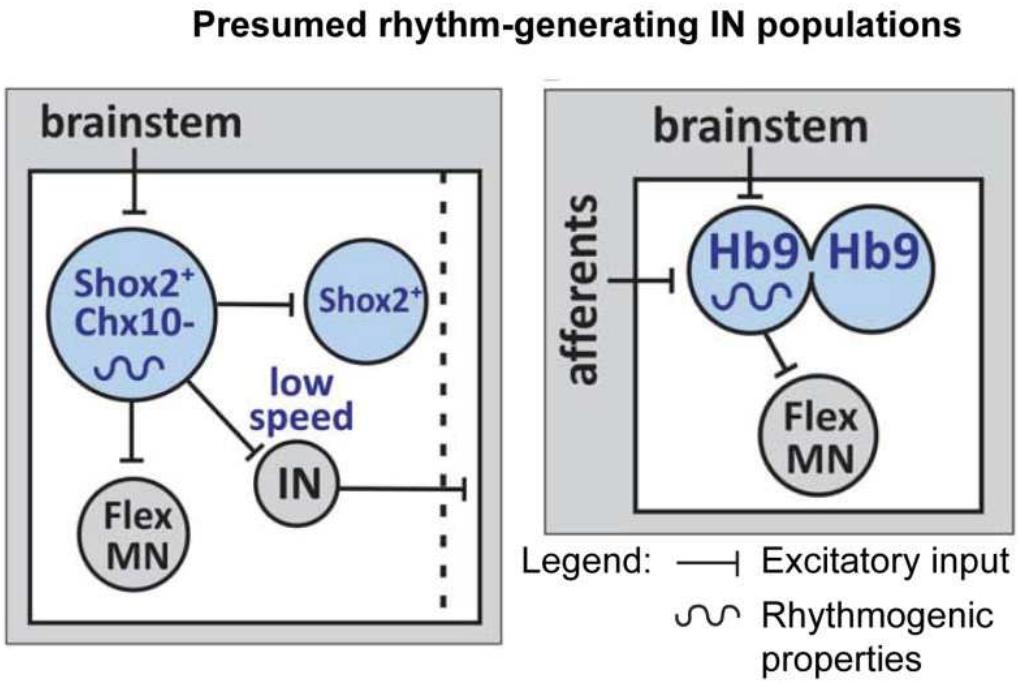

Fig 6: Schematic representation of the presumed rhythm-generating IN populations in the mouse spinal cord

Shox2$^+$ non-V_{2a} INs (*Chx10*$^-$) are one of the presumed rhythm-generating IN populations that innervate flexor MNs and INs including presumed commissural INs and V_{2a} *Shox2*$^+$ INs. The second presumed population is the *HB9*$^+$ V_x population: *HB9* neurons display synchronized activity through electrical coupling and innervate flexor MNs. Both populations might co-exist to generate rhythm, as ablation of *Shox2*$^+$ non-V_{2a} (*Chx10*$^-$) IN population only decreases rhythm without abolishing it. Adapted from (Ziskind-Conhaim and Hochman, 2017).

A recapitulative table of the IN populations implicated in locomotor CPG in the mouse spinal cord is presented below. The list is limited to the neuronal populations described in the text above; some populations have not been discussed.

Neuronal population	Neurotransmitter	Proposed role in locomotor CPG
Ipsilateral excitatory interneurons		
Chx10$^+$ V_{2a}	Glutamate	High speed left-right coordination
Shox2$^+$ non-V_{2a} (Chx10$^-$)	Glutamate	Rhythm generators
V_{0C}	Acetylcholine	Modulation of motor output via C-boutons
HB9$^+$ V_x	Glutamate	Rhythm generators
Ipsilateral inhibitory interneurons		
En1$^+$ V_1	GABA/glycine	Locomotion speed
Renshaw cells (V_1)	GABA/glycine	Recurrent inhibition on MNs
Ia INs (V_1)	GABA/glycine	Flexor-entensor coordination
Gata2/3$^+$ V_{2b} (Ia INs)	GABA/glycine	Flexor-entensor coordination
Commissural excitatory interneurons		
Dbx1$^+$ *Evx1*$^+$ V_{0V}	Glutamate	High speed left-right coordination
Sim1$^+$ V_{3V}	Glutamate	Left-right coordination
Sim1$^+$ V_{3D}	Glutamate	Left-right coordination (sensory relay?)
Commissural inhibitory interneurons		
Dbx$^+$ V_{0D}	GABA/glycine	Low speed left-right coordination

Table 1: Recapitulative table of the mouse IN populations discussed in this thesis

Adapted from (Ziskind-Conhaim and Hochman, 2017)

3. Lamprey

Lampreys are part of the oldest branch of vertebrates (Pombal and Megías, 2018) and move by undulating swimming. Their nervous system is simpler, with fewer neurons compared to other studied vertebrates; however it still displays the same ground plan (Grillner et al., 1991). This model has high historical value; indeed the detailed spinal circuitry responsible for the segmental generation of locomotion in a vertebrate was first identified in lamprey (Buchanan and Grillner, 1987). Lamprey has been used to study locomotion for four decades and continues to be used as a

model (Dubuc et al., 2008; Grillner et al., 1995; Grillner et al., 1998). As lampreys are located at a pivotal place in the evolution, studying locomotion in this model could also bring to light evolutionary conserved mechanisms, neuronal population and network organization (Pombal and Megías, 2018).

4. Zebrafish

Just like lamprey, Zebrafish (*Danio rerio*) moves by undulating locomotion and is a “simpler” vertebrate. Compared to lamprey, Zebrafish presents the additional advantage of being a genetically modifiable model. Indeed, an increasing number of genetic tools generated thanks to the chimeric-CRISPR/Cas9 technologies are now available to manipulate neurons potentially involved in locomotion (Wyatt et al., 2015). The time and expense required to generate a transgenic line are decreased compared to mice models. Zebrafish is therefore a cheaper model with which results can be obtained faster, while retaining the advantage of being a vertebrate (Wyatt et al., 2015). In the past 10 years a number of IN populations involved in Zebrafish locomotion have been characterized, some of them potential counterparts to defined mouse IN populations.

Baseline information on the morphology of INs was initially obtained by retrograde dye labelling in living Zebrafish larva (Hale et al., 2001), setting the foundation for further studies. As a consequence, Zebrafish INs are categorized either morphologically (Fig 7) or depending on the progenitor domain they arise from (similar to what is done in the mouse). These two types of classification can intersect, combine and be slightly confusing; for example, V_{2a} in Zebrafish are comprised of two morphologically distinct populations of INs: Multipolar Commissural Descending (MCoD) neurons and Circumferential Descending (CiD) INs (Kimura et al., 2006).

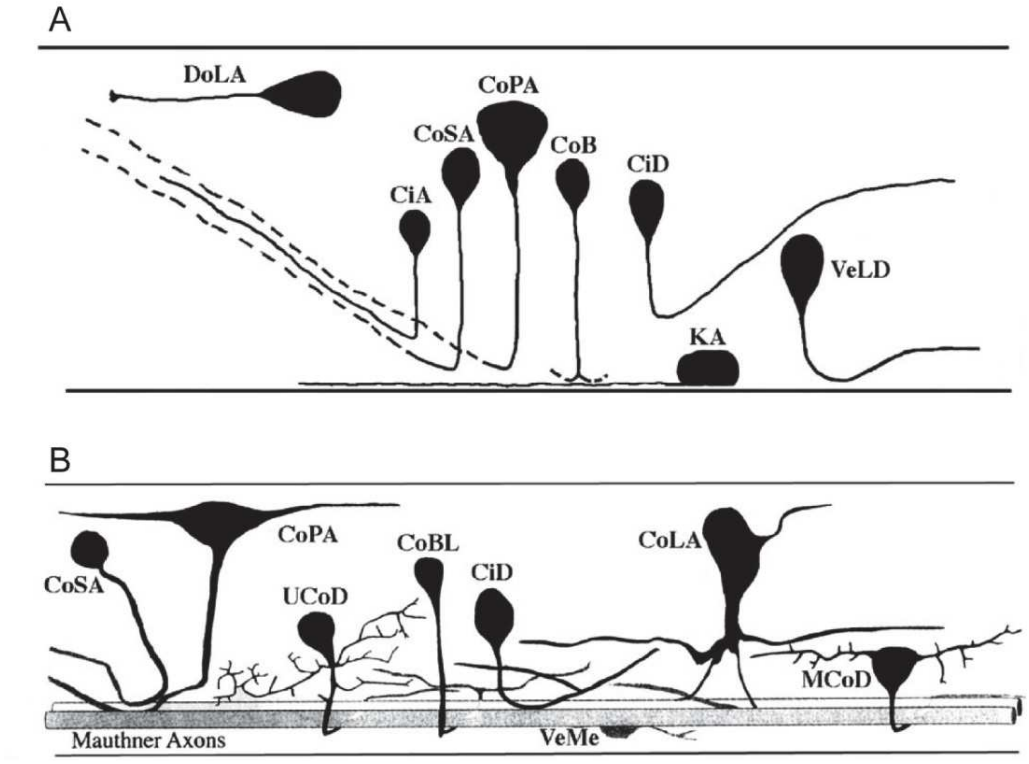

Fig 7: Lateral schematic representation of embryonic and larval INs in Zebrafish spinal cord.

This figure illustrates the morphological diversity of locomotor INs found in the spinal cord of Zebrafish at different developmental times.

A. Different morphologies of INs found in embryonic Zebrafish spinal cord. Dashed lines show contralateral axons that cross the midline. DoLA= Dorsal Longitudinal Ascending; CiA=Circumferential Ascending; CoSA= Commissural Secondary Ascending; CoPA= Commissural Primary Ascending; CoB= Commissural Bifurcating; CiD= Circumferential Descending; KA= Kolmer–Agduhr= CSF-cNs, VeLD= Ventral Longitudinal Descending **B**. Different morphologies of INs found in larval Zebrafish spinal cord. Axons of descending neurons, the Mauther reticulospinal INs, are represented as well. UCoD= Unipolar Commissural Descending; CoBL= Commissural Bifurcating Longitudinal; CoLA= commissural longitudinal ascending; VeMe= Ventral Medial; MCoD= Multipolar Commissural Descending. In both A and B, dorsal is up and anterior is left.

In Zebrafish several classes of commissural glycinergic inhibitor INs are implicated in escape, swimming and “struggle” behaviours. Some neurons are active and implicated in a single behaviour; for example the Commissural Longitudinal Ascending INs (CoLAs) in “struggle” or the Commissural Local INs (CoLos) during escape (Fig 7B) (Liao and Fetcho, 2008; Satou et al., 2009). Some like the Commissural Bifurcating Longitudinal INs (CoBLs) (Fig 7B) are involved in both swimming and struggling but not escape. Finally, some seem to be activated for all types of behaviours, for example the Commissural Secondary Ascending INs (CoSAs) (Fig 7) (Liao and Fetcho, 2008). Collectively, this organization of the

glycinergic commissural INs supports the idea that activity generated by a core of shared spinal neurons may be shaped by more specialized INs to produce an assortment of motor behaviours (Liao and Fetcho, 2008).

The V_0 IN population in Zebrafish is molecularly highly reminiscent of the V_0 in mouse, as it expresses *evx1* (Suster et al., 2009) and is divided in commissural ventral excitatory V_{0v} and commissural dorsal inhibitory V_{0D} subgroups. The V_{0v} population itself is divided in three subpopulations that are active at low, intermediate and fast swimming speed respectively (Björnfors and El Manira, 2016). This principle of sequential recruitment of IN populations depending on the speed of locomotion is found within other classes of INs, for exemple in the V_{2a} population in adult Zebrafish (Fig 8) (Ampatzis et al., 2014; Ausborn et al., 2012; Gabriel et al., 2010). In this respect, recruitment of different pools of V_{0v} and V_{2a} in Zebrafish mediates changes in the speed of locomotion in Zebrafish. Despite V_0 role in mouse in left-right coordination, there is currently no proof that V_0 INs are playing a similar role in Zebrafish (Kiehn, 2016).

The V_1 population in Zebrafish is comprised mainly of the class of Circumferential Ascending glycinergic INs (CiAs) (Fig 7A). This population expresses the *En1* ortholog *Engrailed-1b* (*En1b*), is inhibitory and has high molecular correspondence with the V_1 population in the mouse. It moreover directly synapses onto MNs (Fidelin and Wyart, 2014; Higashijima et al., 2004). Ablation of those neurons leads to exaggerated escape behaviour in larvae and inability to organize productive swimming movements. Therefore, although molecularly related, the V_1 population in Zebrafish might not be the functional counterpart of V_1 in mouse; keeping in mind however that the type of locomotion generated in both models is highly divergent (Zannino et al., 2014).

V_2 neurons in Zebrafish are subdivided into two subgroups: the excitatory *alx*$^+$ V_{2a} (molecular counterpart of the *Chx10*$^+$ V_{2a} in mouse) (Kimura et al., 2006) and the inhibitory *gata2a/3*-positive V_{2b}, also called Ventral Longitudinal Descending (VeLDs) (Fig 7A) (molecular counterpart to the *Gata2/3*$^+$ V_{2b} in mouse) (Andrzejczuk et al., 2018). As was briefly stated above, different V_{2a} populations are recruited at different speeds of locomotion.

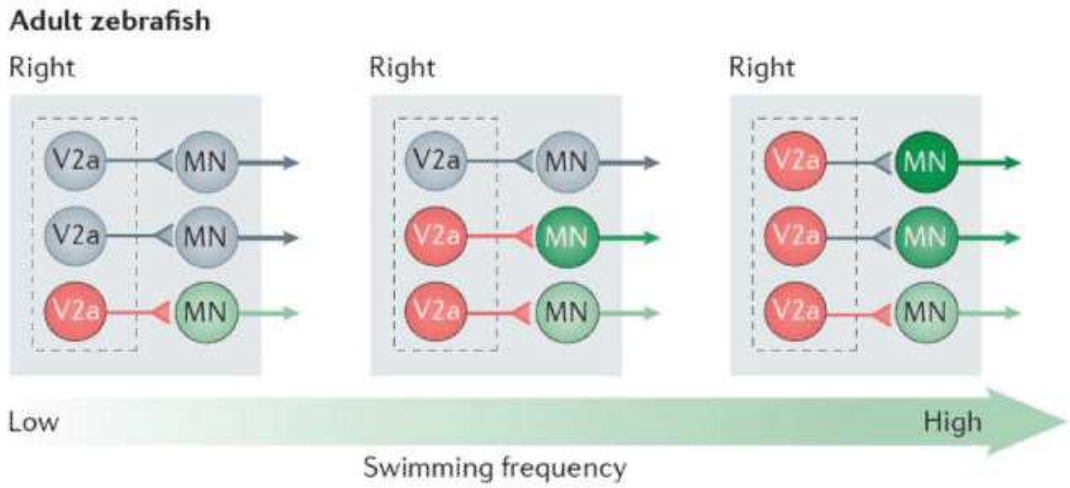

Fig 8: Schematic principle of the sequential recruitment of excitatory V_{2a} INs

V_{2a} population, just like V_{0V} population, is sequentially recruited depending on the speed of locomotion.

Zebrafish V_{2b} VeLDs population function has not been thoroughly characterized, but it is a GABAergic population that displays pacemaker-like activity and is recruited in early spontaneous activity in Zebrafish embryos (Batista et al., 2008; Saint-Amant and Drapeau, 2001). Additionally, a subpopulation of the V_{2b} has been attracting attention in the recent years: the CSF-cNs (Cerebro-Spinal Fluid contacting Neurons) population, also called Kolmer and Agduhr (KA) cells (Fig 7B). This small subpopulation expresses the markers of the V_{2b} (*Gata2a/3*, *Tal1*), as well as *Nkx6.1*, *Foxa2* and the channel *Pkd2L1* (Djenoune et al., 2014; Petracca et al., 2016). On top of this unique combinatorial molecular code, CSF-cNs display an atypical morphology, with a cilia extending into the cerebrospinal fluid-containing central canal of the spinal cord (Wyart et al., 2009). Functionally, CSF-cNs in Zebrafish seem to control the speed of locomotion (Fidelin et al., 2015; Wyart et al., 2009).

B - Genetic approaches for the study of locomotor CPG in model organisms

Two approaches are generally implemented to understand how CPGs function. The first one focuses on finding genes essential for CPG wiring and function. This is achieved most of the time through the study of loss of function alleles and allows for the identification of development-related genes (Lu et al., 2015; Zannino et al., 2014).

The second approach focuses on the CPG neuronal populations themselves, trying to identify groups of neurons that have similar function in the locomotor CPG (Björnfors and El Manira, 2016; Clark et al., 2016; Kohsaka et al., 2014). This approach relies on the use of genetic tools (like the UAS/Gal4 system in *Drosophila melanogaster*) to target neuronal populations as discrete and homogeneous as possible. CPG neuron populations characterization can be achieve through different (and often complementary) techniques. It can be done by ablation of the neuronal population of interest (Heckscher et al., 2015; Satou et al., 2009) or modulation of physiological activity, through either activation or inhibition (Clark et al., 2016; Fidelin et al., 2015; Kohsaka et al., 2014). Activation or inhibition can be achieved with different tools: thermosensitive tools like TrpA1 or shi^{ts} (Kitamoto, 2001; Pulver et al., 2009) or more recently optogenetic tools with the blue light-sensitive cation channel channelrhodopsin (Boyden et al., 2005; Nagel et al., 2002) and yellow light-sensitive chloride pump halorhodopsin (Han and Boyden, 2007; Zhang et al., 2007; Zhao et al., 2008).

III. *Drosophila melanogaster* as a model organism

A - Life cycle

Drosophila melanogaster is a holometabolous insect, which means it goes through a larval and pupa stage before becoming an adult fly. At 25°C, the *Drosophila* life cycle (from an adult to a new fertile adult) takes about 10 days (Fig 9). Eggs protected by the chorion and the vitelline membrane are laid by the fertilized female on a surface favourable to larval development. Embryogenesis lasts for 22 to 24h, finishing with the hatching of the first instar larva. This larva is at first 0,5 mm long and starts eating and growing. After 25h, the larva moult into a bigger larva, dubbed second instar. Twenty-four hours later, the larva moults once more into its final, third instar form. The third instar stage lasts for about two and a half days, during which the larva keeps eating. Towards the end of the third instar stage, the larva sets out to find a drier, cooler place to moult into a pupa. Three to four days later, the imago or adult fly emerges from the pupa, and becomes fertile after a couple of hours only. The adult fly can live for up to 10 weeks (Tyler, 2000).

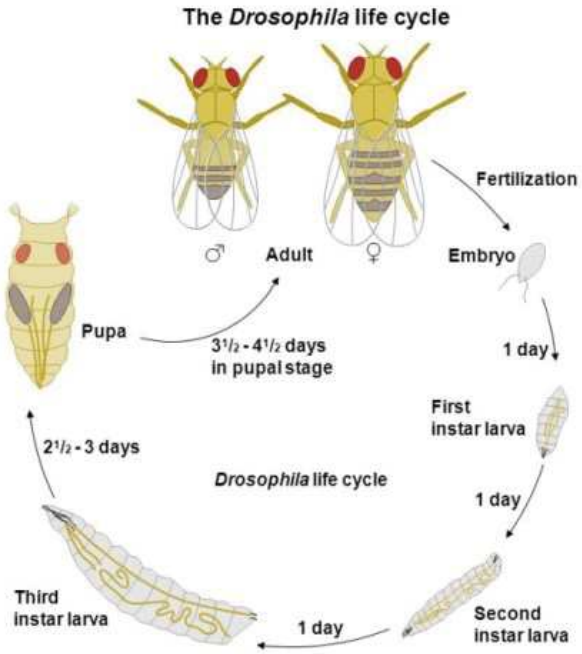

Fig.9: *Drosophila* life cycle.

Drosophila is a holometabolous insect that goes through embryonic, larval and pupal stages before reaching the adult, reproductive state. Complete life cycle of *Drosophila* lasts for about 10 days at 25°C.

B - *Drosophila* as a model for studying locomotor CPG

1. Nervous system and locomotion in *Drosophila* larva

Drosophila larval anatomy and locomotion are well characterized at the level of organism and segment. Locomotion itself includes a variety of behaviours: linear crawling (also called peristalsis), turns, head sweeping, rolling and other movements (Fig 10) (Heckscher et al., 2012).

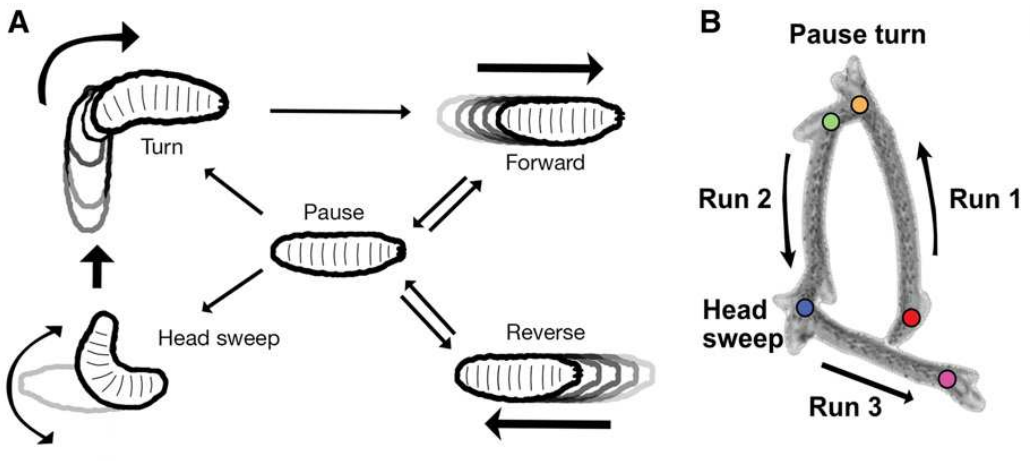

Fig.10: *Drosophila* larva locomotion.

A. Locomotor behaviours displayed by *Drosophila* larva: most of larval locomotion is comprised of forward peristalsis (called run), head sweeping, turns and pause. In case of danger, the larva also displays rolling behaviour. **B**. Example of a time-lapse typical locomotion pattern. From (Clark et al., 2016).

Drosophila larva nervous system harbours less than 10 000 neurons arranged in three main centres: the central brain or cerebellar lobes, the suboesophageal ganglion (SOG) and the ventral nerve cord (VNC) (Fig.11) (Riedl and Louis, 2012). The VNC is divided in segments: 3 thoracic segments, located just caudal to the SOG, 8 abdominal segments and a terminal plexus (Clark et al., 2018). While the CPG controlling turning resides in the thoracic segments only, the CPG controlling forward locomotion (peristalsis) lies in both thoracic and abdominal segments (Berni, 2015; Berni et al., 2012; Pulver et al., 2015). Therefore when studying the locomotor CPG, one usually focuses on the first 6 abdominal segments that have the same neuronal composition. More precisely, each abdominal hemisegment (meaning half a segment) contains 305 neurons in the late embryo: 35 MNs and 270 INs, each of them bearing a unique identity based on axonal pattern projection and cell body position (Rickert et al., 2011).

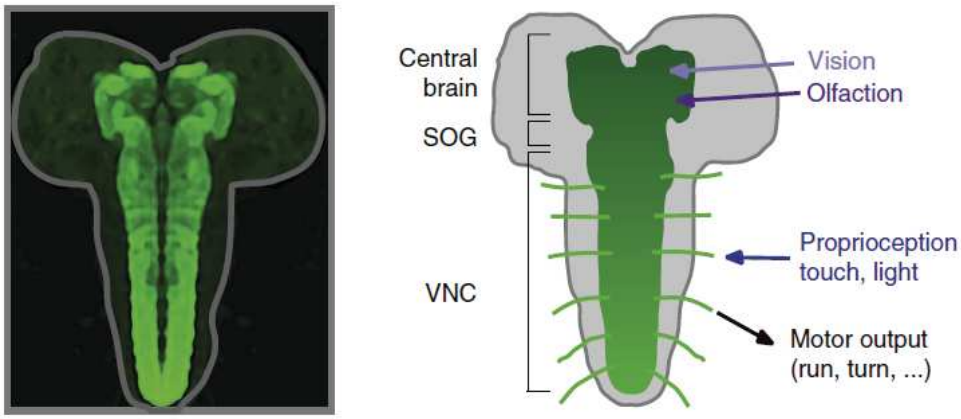

Fig.11: Gross anatomy of the CNS in a *Drosophila* larva.

The CNS is made of three centres: the central brain made of two cerebellar lobes, the suboesophageal ganglion (SOG) and the ventral nerve cord (VNC). Left image: the majority of neuronal connections in the VNC are made in the region highlighted in green: the neuropile. From (Riedl and Louis, 2012).

By the end of embryogenesis, neurons involved in the locomotor CPG start forming functional circuits that become active during a well described “critical period” occurring approximately 3.5h before hatching (Crisp et al., 2008). Interestingly, patterned neural activity is essential during this period for the proper wiring of the CPG and the development of an accurate motor output, namely coordinated peristaltic waves (Crisp et al., 2011; Kohsaka et al., 2012). It was later shown that specific sensory neurons activity manipulation during the critical period has lasting effects on the maturation of the motor circuits, emphasizing even more the importance of this critical period (Fushiki et al., 2013). The circuits controlling locomotion in the VNC are therefore in place and functional by the end of embryogenesis. The first instar larva once hatched is able to crawl immediately, albeit more slowly in the first 3-4 hours. Circuits controlling locomotion remain nearly identical during the three larval stages, with some consolidation of the existing connexions denoted by an increase in the number of synapses (Couton et al., 2015). During metamorphosis, the entirety of the nervous system is remodelled to innervate and coordinate a completely different anatomy and the majority of the functional larval neurons go through apoptosis. However some neurons (mainly MNs and sensory neurons) incredibly survive the highly traumatic pupal stage and are functional in adult fly just like they previously were in the larva (Banerjee et al., 2016;

Consoulas et al., 2000; Shimono et al., 2009; Tissot and Stocker, 2000; Williams and Shepherd, 1999; Williams and Shepherd, 2002).

2. Advantages of *Drosophila* larva as model for the study of locomotor CPG

Locomotion is highly stereotypic in *Drosophila* larva; therefore modifications of locomotion caused by modifications of CPG activity are often easy to visualize, even with limited magnification. *Drosophila* larvae possess a transparent cuticle, which makes the use of optogenetic techniques highly convenient on whole freely moving larvae, as the light easily reaches the cells that one wishes to target (Fushiki et al., 2016; Honjo et al., 2012; Kohsaka et al., 2014). This also makes possible the live-imaging of neurons activity by calcium imaging or two-photon microscopy during crawling behaviours, a particularly informative feat (Heckscher et al., 2015; Karagyozov et al., 2017). As a model, *Drosophila* presents the obvious advantages of being small and affordable, with a rapid life cycle. Numerous transgenes can be combined in an individual in a reasonable amount of time (compared to mice) and large cohorts of individuals can be used. Finally the *Drosophila* model is particularly attractive in terms of genetic tools availability. Ever since the generation of the first genetically modified *Drosophila* lines using the P transposon element, the number of genetic tools at one's disposal has expended and keeps expanding, with increasingly sophisticated options (Clark et al., 2018; Kohsaka et al., 2017; Venken et al., 2016).

Different techniques can be implemented for the study of locomotion in *Drosophila*. Preparations of "open-filet" can help dissect the function of presumed locomotor INs by monitoring their activity by electrophysiology or calcium imaging (Fig 12). Indeed, it is still possible in open-filet preparation to observe peristaltic waves travelling the length of the larva body and at the same time record or visualize neurons activity in the VNC (Pulver et al., 2015). The comparative small size of the larva VNC makes reconstruction of whole VNC segments using serial section Transmission Electron Microscopy (TEM) feasible, allowing for the mapping of the neurons, their cell bodies positions and neurite arbours as well as their synaptic partners (Clark et al., 2018). Synaptic connections between two populations can additionally be assessed by GRASP (GFP Reconstruction Across Synaptic Partners) (Feinberg et al., 2008; Macpherson et al., 2015) while search for new, unknown synaptic partners could be done by Tango Tracing (Talay et al., 2017). As a general

rule, *Drosophila* larva proves to be a powerful model for the study of the locomotor CPG.

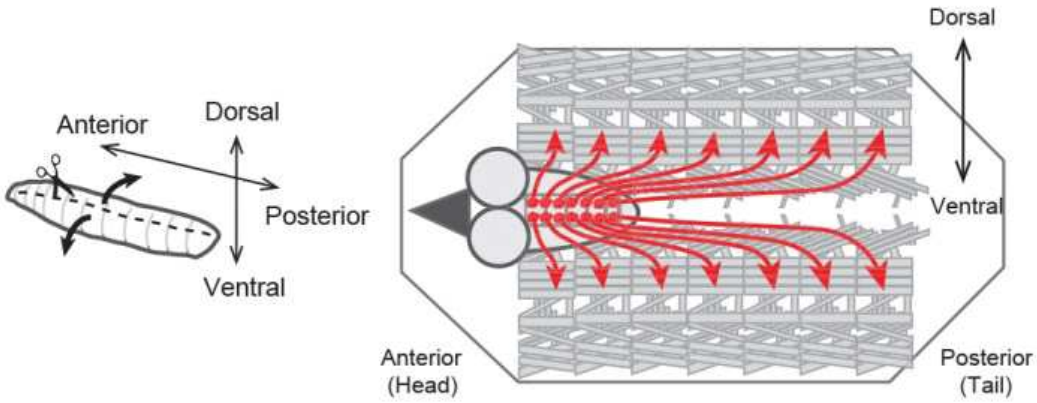

Fig 12: Schematics of an “open-filet” preparation

In “open-filet” preparation, the larva is dissected along the dorsal midline and flattened to expose the muscles and the VNC after the removal of the internal organs. If the dissection is properly performed, peristaltic waves can be seen travelling the length of the dissected larva body-wall, with a slower frequency compared to what is seen in live, freely moving larvae. In the open preparation drawing to the right, CNS of the larva is to the left and red arrows represent the motor nerves leaving the VNC to innervate muscles in the body-wall. From (Kohsaka et al., 2012)

3. Implication of MNs in the locomotor CPG

MNs are by far the most thoroughly characterized neurons of the locomotor CPG in *Drosophila*. Most of their characteristics, from their morphology to their development, muscle targeting, lineage, dependence on neurotrophic factors and molecular code are extensively documented (Kohsaka et al., 2012) (Fig 13). Unlike what is found in vertebrates, MNs in *Drosophila* are glutamatergic (Kohsaka et al., 2012).

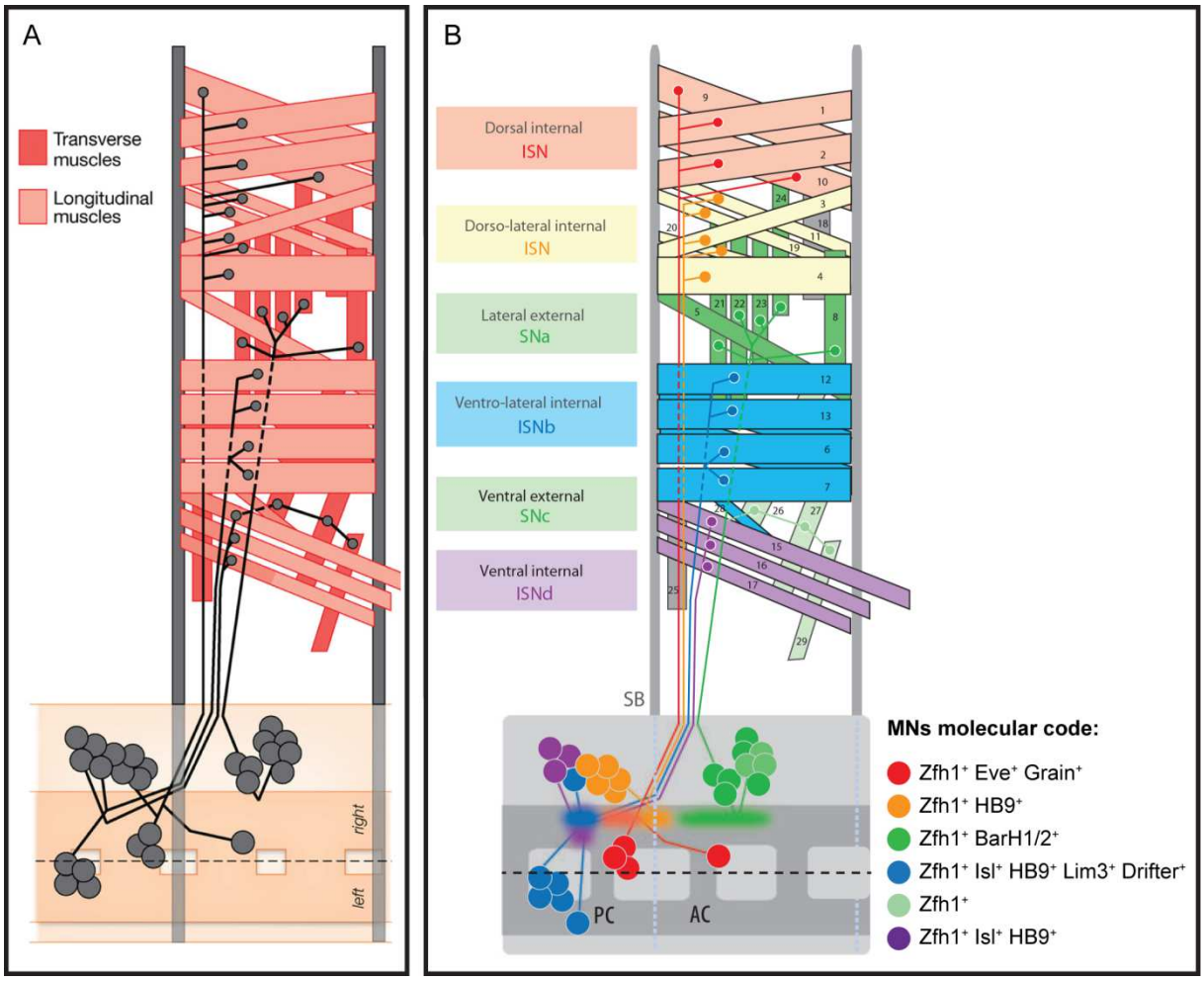

Fig 13: *Drosophila* larva myotopic maps and neuromuscular connectivity.

A. Myotopic map of one hemisegment highlighting the 30 muscles arranged in two groups of transverse muscles (dark red) and longitudinal muscles (pale red). The longitudinal muscles are aligned with the body axis while the transverse muscles are circumferential or orthogonal to the body axis. Transverse muscles are closest to the cuticle of the larva and therefore the outside environment whereas the longitudinal muscles are closer to the internal organs of the larva. Anterior of the larva is to the left, ventral midline is shown by the dashed line and dorsal midline at the top of the panel **B**. Myotopic map of one hemisegment where domains of muscles and their innervating MNs are shown in matched colours. In each hemisegment, 35 MNs (whose cell bodies are shown in the VNC at the bottom of the figure) innervate the 30 muscles present in every hemisegment through six peripheral nerves named to the left. The molecular code that allows for specific identification of MNs is listed on the right of the figure. The Transverse Nerve (TN) is not represented in this figure. Muscles are numbered according to (Bate, 1990). AC= anterior commissure; PC= posterior commissure; SB= segment boundary. Zfh1= Zinc Finger Homeodomain 1; Isl= Islet; Eve= Even-skipped; HB9= Homeobox 9; BarH1/2= BarH-like Homeobox 1/2; ISN= Intersegmental Nerve; SN= Segmental Nerve. From (Clark et al., 2018; Kohsaka et al., 2012)

In the CPG, MNs are the last effectors of the system, and as such one could naively think they are merely “executive” neurons that transmit whatever information is coming from the INs to the muscles. This arises also from the lack of connections formed by MNs on INs, with the exception of the famous Renshaw cells that receive excitatory input from intraspinal MN axon collaterals in the mouse (Eccles et al., 1954; Renshaw, 1946). MNs actually have a real role in the peristaltic wave in *Drosophila*, as their inhibition impairs its proper propagation (Inada et al., 2011). At the time it was still unknown by what connections and mechanisms MNs are able to impact on CPG activity. However recently it has been shown in Zebrafish that MNs influence directly motor pattern generation via gap-junctions with premotor V_{2a} INs. Indeed, propagation of voltage fluctuations from MNs to V_{2a} INs has impacts on the synaptic release and recruitment of the upstream V_{2a} INs that drive locomotion. Inhibiting MNs activity during ongoing locomotion de-recruits V_{2a} INs, strongly influencing locomotion (Song et al., 2016). Such a mechanism could also exist in *Drosophila*: in a *shaking-B* mutant *Drosophila* larva where gap-junctions are lost, manipulation of the MNs activity has no more effect on locomotion. This suggests that gap-junctions are actually required for MNs activity to have an impact on locomotion (Matsunaga et al., 2017).

4. Implication of sensory neurons in locomotor CPG

Although not strictly part of the locomotor CPG, sensory neurons nevertheless play an important role in modulating locomotion to attain the most favorable environment possible in terms of temperature, food source and safety from predators. *Drosophila* larva “sees” thanks to light detecting structures on its head called Bolwig’s organs (Sprecher and Desplan, 2008) and sensory neurons located in the bodywall and smells thanks to the dorsal organ located at the tip of the head (Vosshall and Stocker, 2007) (Fig 14A). Additionally, a variety of sensory neurons able to detect different stimuli line the *Drosophila* larval body wall (Fig 14A). Among them, the dorsal bipolar dendritic (dbd) and ventral bipolar dendritic (vbd) sensory neurons (Fig 14B) are muscle stretch receptors (Suslak et al., 2015) that influence locomotor activity via their connections with EL INs [discussed in the following paragraph - (Heckscher et al., 2015)]. The Class I md (multidendritic) sensory neurons are thought to be proprioceptors and their activity is required for normal locomotion;

indeed in all organisms discerning the position of the body and the status of the muscles is essential for the locomotion to be effective and coordinated (Hughes and Thomas, 2007). Class II and III md sensory neurons act likely as touch receptors (Tsubouchi et al., 2012). Class IV md sensory neurons are polymodal nociceptors that are sensitive to excessive thermal, mechanical and light stimuli (Kohsaka et al., 2017). Activation of Class IV md triggers rolling, a behaviour that allows the larva to quickly escape deleterious situations such as attacks by parasitoid wasps (Hwang et al., 2007). It was found recently that through IN intermediaries (in the VNC or the brain), Class IV md neurons activate a single pair command neurons for rolling, named Goro neurons (Ohyama et al., 2015). Simultaneous activation of the chordotonal sensory neurons actually enhances the Class IV md-evoked rolling behaviour. The combined action of Class IV md and chordotonal sensory neurons makes sense in the trigger of rolling behaviour, as the wasp's attack would be detected by the larva through sting pain (mediated by Class IV md) and vibrations in the air generated by the beating of the wasp's wings (detected by the chordotonal sensory neurons) (Ohyama et al., 2015) (Fig 14C). Rolling is also mediated by a second pathway independent of the Goro neurons. In this second pathway, Class IV md sensory neurons directly synapse onto medial clusters of C4 da second-order INs (or mCSIs) which indirectly contact SNa (BarH1/2^{+}) MNs as well as other non-defined MNs to trigger rolling (Yoshino et al., 2017).

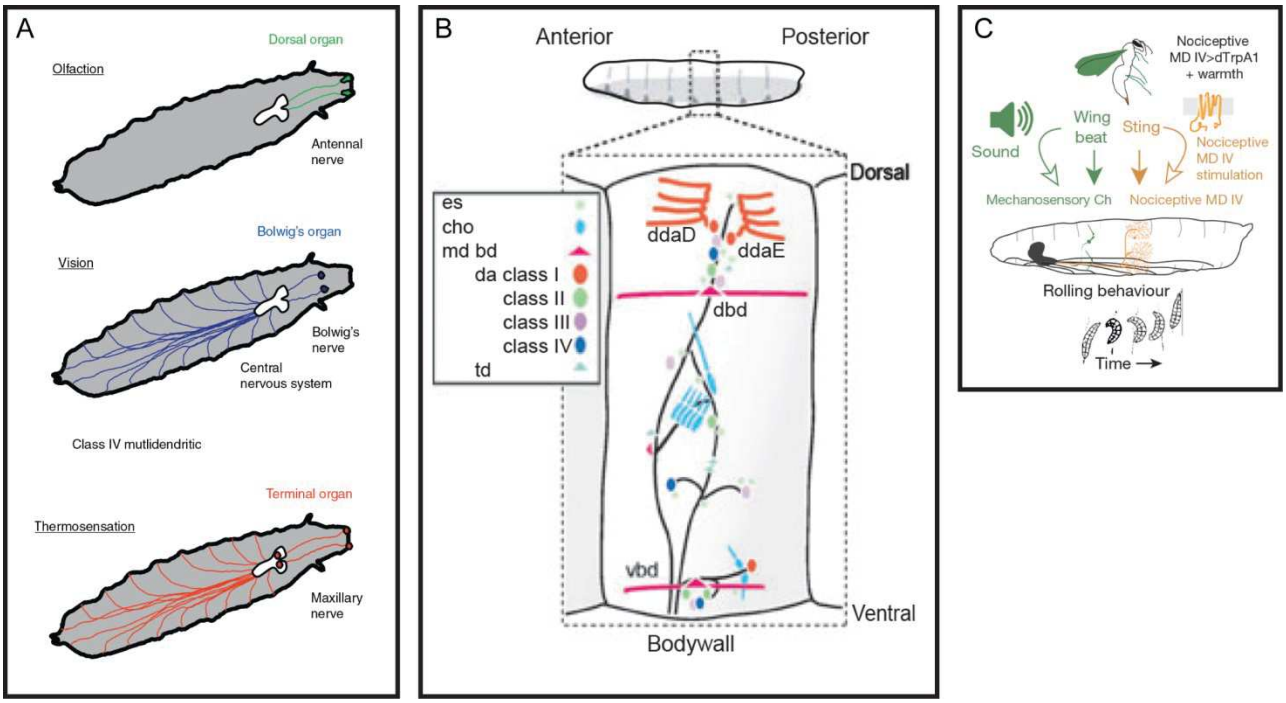

Fig 14: Sensory system in *Drosophila* larva

A. Schematic of peripheral sensory systems involved in olfaction, vision, and thermosensation. The two larval noses (dorsal organs) are located at the tip of the head. Each dorsal organ hosts 21 olfactory sensory neurons (OSNs) (Gerber and Stocker, 2007). The OSN axons form the antennal nerve which projects to the CNS (white). The larva is equipped with a visual system consisting of a pair of 12 photoreceptors forming Bolwig's organs (BOs). The photoreceptor neurons of the BOs project onto the larval optic neuropile of the central brain (Sprecher and Desplan, 2008). Response to light is also mediated by transient receptor potential (TRP) channels expressed in multidendritic class IV neurons covering the body wall (Xiang et al., 2010). Thermosensation is mediated by neurons located in the terminal organs of the head and chordotonal (ch) neurons found in the body wall (Kwon et al., 2008; Liu et al., 2003). Larval thermotaxis is also controlled by a set of TRP-expressing neurons in the central brain (Rosenzweig et al., 2005). **B**. Schematic diagram of the anatomy of sensory neurons present in a bodywall hemisegment. Cell bodies of the eight types of sensory neurons are shown in different colours and shapes. Dendritic morphology is detailed for two class I (da) neurons (ddaD and ddaE) and two bipolar dendritic (bd) neurons (dbd and vbd). es= external sensory **C**. Schematic example of one of the characterized sensory circuits: concomitant activation of chordotonal (Ch - green) sensory neurons by vibrations and the nociceptive multi-dendritic mIV (orange) by sting pain triggers rolling behaviour through activation of the command-neurons for rolling, the Goro neurons. Adapted from (Gomez-Marin and Louis, 2012; Kohsaka et al., 2012; Ohyama et al., 2015)

5. Implication of the descending inputs from the cerebellar lobes

The definition of a CPG goes by its ability to generate rhythmic activity and behaviour in the absence of central command and the locomotor CPG in *Drosophila* is no exception. Adult flies do not require their head to walk, groom or even jump

(Riedl and Louis, 2012). Regardless, brain centres receive information about the state of activity of the VNC-located locomotor CPG via ascending neurons (AN) and influence it via descending neurons (DN), for example in case of directed locomotion (phototaxis, chemotaxis) (Cardona et al., 2009). Functionally, it seems that most DNs constitute command neurons (Kupfermann and Weiss, 2010). The most striking examples of DNs are maybe the Giant Fibre that triggers the flight response (Mu et al., 2014) or the moonwalker descending neurons that prompt backward walking in flies (Bidaye et al., 2014). Apart from those and other sparse examples, virtually no information exists in regard to axonal pathways interconnecting the brain and ventral nerve cord of *Drosophila* adult fly (Hsu and Bhandawat, 2016). In *Drosophila* larva there seem to be even less characterization. One of the rare information available comes from first instar larva, where it is thought that out of the 1400 neurons residing in each cerebellar lobe, 50 have axons descending into the VNC (Cardona et al., 2009).

6. Different populations of IN characterized so far

Knowledge on the IN populations of the locomotor CPG in *Drosophila* is fairly recent, with most articles dating back less than 5 years (Hasegawa et al., 2016; Heckscher et al., 2015; Itakura et al., 2015; Kohsaka et al., 2014; Yoshikawa et al., 2016; Zwart et al., 2016). However, in this short time the wealth of information on IN populations, their function, morphology and connections has exponentially increased. We will attempt here to give a comprehensive view of the populations identified.

Some studies have focused on screening *Drosophila* lines using electrical inhibition (Iyengar et al., 2011; Yoshikawa et al., 2016) or electrical activation (Clark et al., 2016) in the search of locomotor phenotypes. These studies showed that modulation of relatively few INs within the CNS can alter locomotion, implying that discrete neuronal populations play a fundamental role in larval locomotion. Further characterization of the lines identified in these articles could broaden our knowledge on locomotor IN populations. VNC INs are known to be highly diverse. Studies show that an abdominal hemisegment contains a set of 270 INs that can be uniquely identified by their axonal projection pattern and their cell body position (Rickert et al., 2011). Those 270 INs can be furthermore subdivided into 80 different molecularly-defined IN subtypes, where a subtype is defined by a unique combination of markers

(Heckscher et al., 2014). This high molecular and morphological diversity might also hint at a high functional diversity.

Some studies have instead focused on a particular population, characterizing its function and connectivity in the VNC. Chronologically, the PMSI (for Period-positive Median Segmental INs) were among the first neuronal populations to be identified (Kohsaka et al., 2014). This population comprises 12 neurons per hemisegment, characterized as their name implies by their expression of the TF *period*. Their axons have distinct “lasso” morphology and they were found to be directly premotor, with identified connections with MNs using GRASP. PMSI are glutamatergic but despite the normal admitted property of this neurotransmitter (should be excitatory), they are thought to be inhibitory through hypothetic action on glutamate-gated inhibitory channels (Kohsaka et al., 2014). PMSIs are rhythmically active and their activation in each segment comes slightly after the MNs activation. Functionally PMSIs have a rather drastic effect on locomotion: upon activation by optogenetic techniques, they lead to paralysis of the larvae: all muscles of the larva become relaxed, which increases the length of the larva. Inhibition of the PMSI population causes a reduction in the speed of locomotion. The authors conclude that PMSIs are glutamatergic inhibitory premotor INs that control the duration of the burst of activity of MNs: their role would be to stop the burst of activity of the MN in the currently contracted segment to allow for the propagation of the contraction wave to the anterior segment (Fig 15). This role of PMSIs is reminiscent of that of V_1 INs population in the mouse.

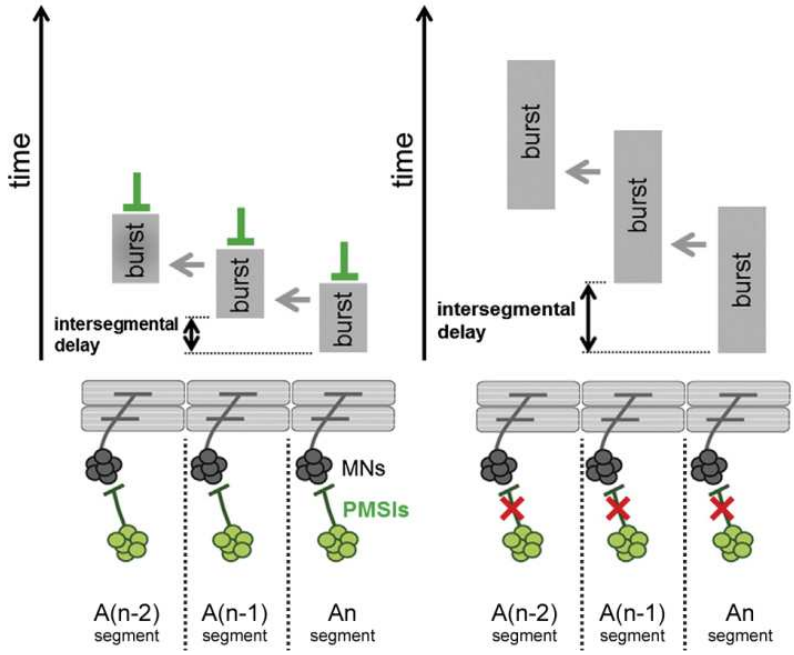

Fig 15: Schematics of the mode of action of PMSI neurons in abdominal segments

In physiological conditions, PMSI neurons are activated slightly after the beginning of the MN activity; when activated they finish the burst of activity of the MNs they innervate. When PMSIs are inhibited, the duration of the motor output is increased and therefore the contraction wave takes longer to travel the length of the larva. The behavioural consequence of such an inhibition is the slowed locomotion of the larvae. When activated, PMSIs completely inhibit MNs burst of activity, thus causing complete atonal relaxed paralysis of the larvae. Adapted from (Kohsaka et al., 2014).

The GVLIs (for Glutamatergic Ventro-Lateral INs) were identified the following year. They are glutamatergic, potentially premotor and rhythmically active during locomotion. Functionally they resemble the PMSIs but their activation seems to lag more after MNs activation (Fig 16). Furthermore, when activated in open preparation, they inhibit muscle contraction in the segment concerned. The authors surmise that GVLIs are part of a feedback inhibition system that closes the period of activation of MNs definitively after the contraction wave has passed and is already a few segment away (Itakura et al., 2015).

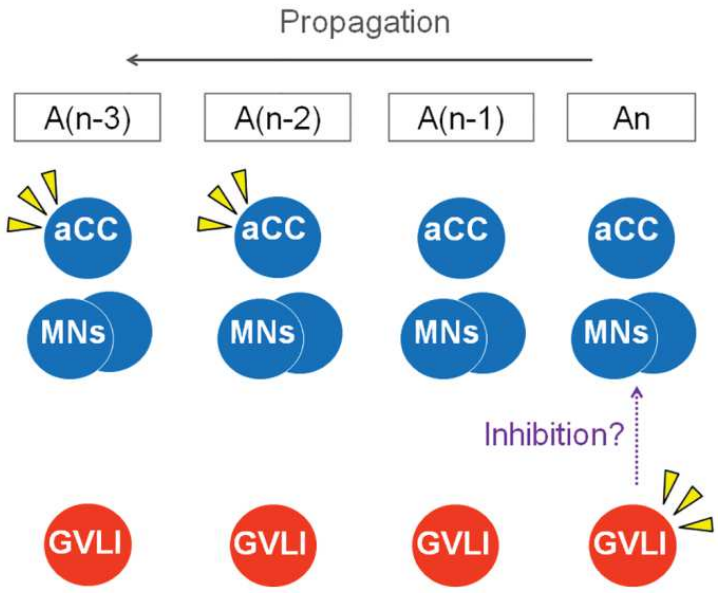

Fig 16: Schematic drawing of the hypothetical role of GVLIs in locomotor CPG in abdominal segments
Yellow arrowheads indicate active neurons. A forward wave develops from posterior to anterior, here An towards A(n-3). GVLIs are activated with a delay after the activation of the MNs in the same hemisegment: GVLI in An closes definitely the period of activation of the MNs in An when the MNs in anterior segments A(n-2) and A(n-3) are being active. Adapted from (Itakura et al., 2015).

EL (for Eve$^+$ lateral) INs are at the interphase between sensory system and locomotor system. In the absence of sensory intput, the EL INs fire spontaneously but do not display locomotor-like rhythmic activity: therefore they might not be strictly speaking part of the locomotor CPG. They are mainly cholinergic and symmetrically activated in the same segment in the VNC, which allows for symmetrical contraction of the segment when the contraction wave passes through. It was moreover shown that EL INs are contacted by Jaam1,3 neurons that are themselves contacted by proprioceptive sensory neurons dbd and vbd (dorsal and ventral bipolar dendritic multidendritic [md] neurons) able to sense the stretch of muscles. Therefore the role of Jaam could be to present proprioceptive information to EL INs, although more studies would be required to know their exact function. EL INs make few synapses on MNs but rather use an intermediary, the saaghi (SA) INs to communicate information to the MNs. EL IN-related network may serve to interpret sensory feedback of muscle contraction amplitudes and balance bilateral muscular contraction (Fig 17). From their expression of *eve*, their morphology as well as their role in left/right coordination, EL are thought to be the functional counterpart of the V_0 population in the mouse (Heckscher et al., 2015).

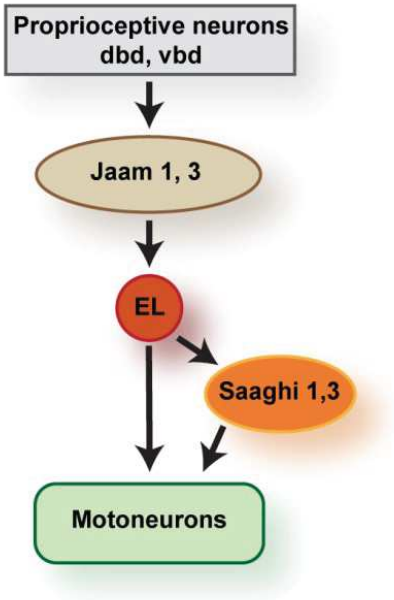

Fig 17: Schematics of the neural circuit related to EL neurons

EL INs are indirectly innervated by proprioceptive dorsal and ventral bipolar dendritic multidendritic neurons (dbd, vbd) via the Jaam neurons 1 and 3. EL INs then directly innervate MNs and also indirectly innervate them through the Saaghi neurons 1 and 3. Disruption of physiological activity of EL INs disrupts the amplitude of the bilateral symmetrical muscle contraction. Adapted from (Kohsaka et al., 2017)

LLN (for Lateral Locomotor Neurons) are a population of 25 IN per hemisegment without any known molecular marker. Both activation and inhibition of LLN INs lead to complete abolition of the locomotion. LLNs represent a heterogeneous population of both ipsi and contra-laterally projecting neurons, but it seems only the ipsilaterally-projecting neurons are indeed required for proper locomotion, as disruption of the contralateral projections has no effects on normal locomotion. It remains unknown whether LLNs are premotor INs, connecting muscles directly or via an intermediary (Fig 18). The LLN population studied is quite large and should be dissected, as the authors suggest (Yoshikawa et al., 2016).

During larval crawling two groups of muscles (transversal and longitudinal) display a sequential contraction pattern in the same segment (for groups of muscles in *drosophila* larva body-wall, see Fig 13). This is caused by the asynchronous activation period of the MN pools innervating these muscles. The differential in activation time is not related to excitatory output that is mediated in similar ways to the two pools of MNs by excitatory premotor INs eINs, but is rather regulated by a

single inhibitory GABAergic IN per hemisegment named iIN-1. iIN-1 selectively innervates the transversally-projecting MN pool, specifically delaying the inset of activation of this pool (Fig 18) (Zwart et al., 2016).

CLI 1 and 2 (for cholinergic lateral INs 1 and 2) are two segmental excitatory INs identified in 2016 (Hasegawa et al., 2016). They are rhythmically active and putatively cholinergic premotor INs (Fig 18). Moreover, they are activated in the segment just prior to MNs and in open preparation their activation induces contraction of the related segment. CLI1&2 would therefore be premotor excitatory INs that activate MNs sequentially from posterior to anterior segments during locomotion.

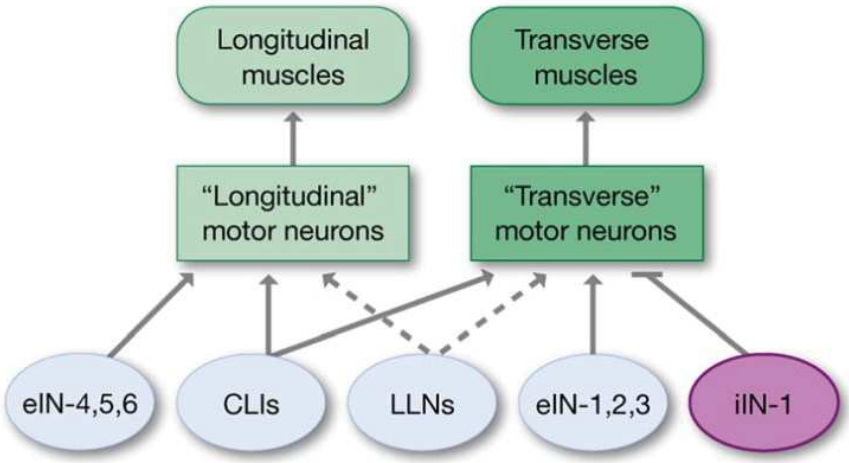

Fig 18: Schematics of eIN, iIN, CLI and LLN neurons in locomotor CPG in one hemisegment

In a same segment all MNs are contacted by several classes of excitatory INs including eINs and CLI1&2. MNs innervating transverse muscles are specifically contacted by an inhibitory IN iIN. iIN activity is responsible for the slight delay between activation of the "longitudinal" MNs and "transverse" MNs that reverberates on the delay of contraction between longitudinal muscles and transverse muscles. LLN neurons, identified as part of the locomotor CPG, might be directly premotor INs or contacting MNs via an intermediary. From (Clark et al., 2018).

An additional pair of INs named A27h, located in each segment and influencing the locomotion was identified. A27h is a premotor excitatory IN known to be cholinergic. In a fictive locomotion assay with a semi-intact preparation, A27h activation in a given segment is enough to contract the equivalent segment of the body of the larva. It was further found that A27h is part of a feed-forward system in coordination with another neuron, GDL (for GABAergic Dorso-Lateral IN). Using TEM, the authors showed that A27h contacts both MNs and GDL in the anterior segment

and propose the following functioning of A27h with GDL. The segment *n* is contracted thanks to the combined action of A27h and probably other yet non-identified excitatory premotor INs. At the same time A27h is giving a positive signal to the MN, it is also sending a positive signal to GDL in the *n-1* segment (the anterior segment to the one currently contracted). As GDL is GABAergic, it inhibits A27h as well as the above-mentioned other premotor excitatory INs in the *n-1* segment, thus allowing this segment to remain relaxed. When by a mechanism still unknown the motor activity of the *n* segment declines, A27h is less activated, thus GDL in *n-1* is less active, leading to the de-repression of A27h in the *n-1* segment which can then activate MNs in the *n-1* segment and GDL in the *n-2* segment (Fig 19) (Fushiki et al., 2016). GDL presynaptic partners (found with TEM) include some dendritic arborisation sensory neurons (vdaA and vdaC), which might mean that GDL receives information about the stretch condition of the muscles from the sensory system.

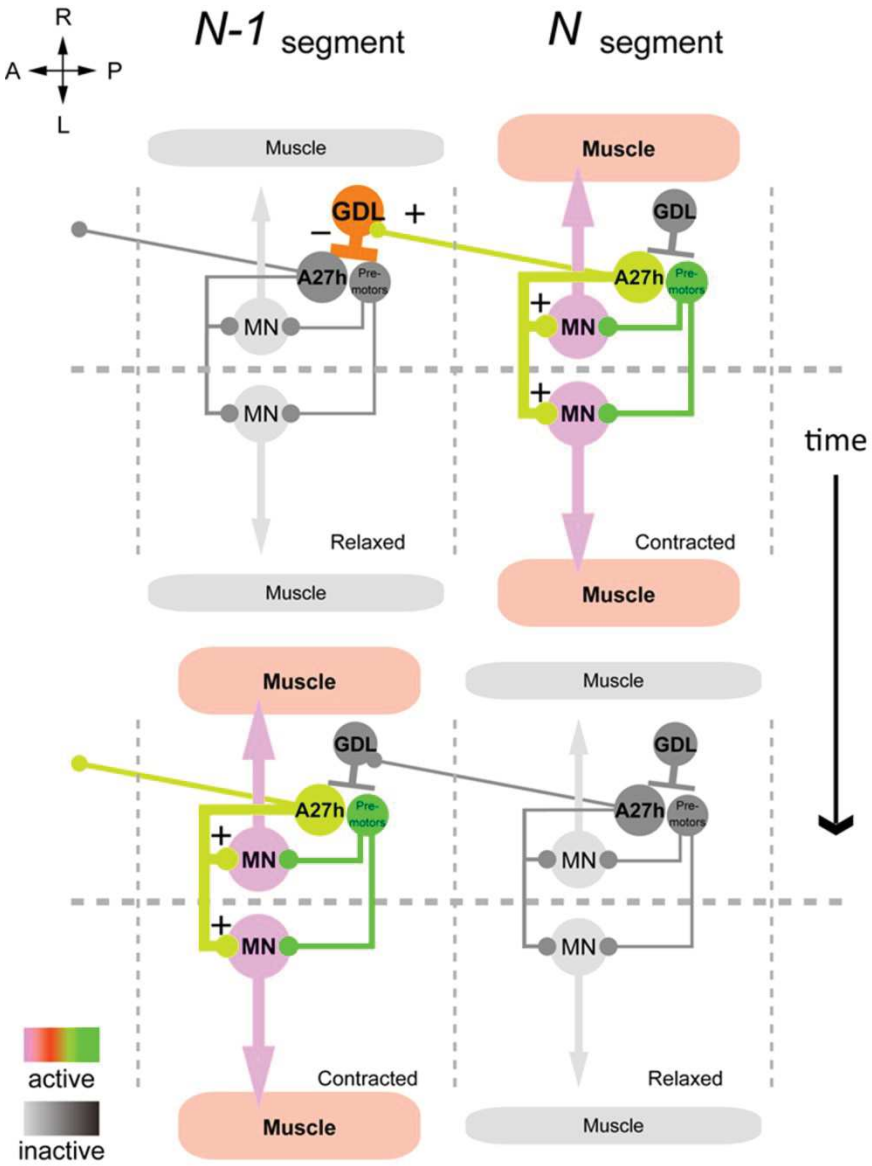

Fig 19: Summary schematics of the locomotor function of the circuit containing GDL and A27h.
During forward peristalsis, contraction wave propagation goes from N segment to anterior N-1 segment. N segment is contracted thanks to the combined action of A27h and probably other premotor excitatory INs on MNs. In the same time, A27h in N segment also contacts GDL in N-1 segment, activating it; GDL in N-1 fulfils its inhibiting role on A27h and other premotor INs in N-1, thus preventing the contraction of the N-1 segment prior to the arrival of the contraction wave. When the activity of A27h in N segment decreases, so does GDL activity in N-1 segment. This releases the inhibition on A27h and other premotor INs in N-1: they activate MNs in N-1, leading to the contraction of N-1 segment muscles. From (Fushiki et al., 2016).

Additionally to the identification of strictly locomotor CPG IN populations, a population of INs involved in the alternation of locomotor and feeding CPGs have been studied. They are called Hugin neurons from their expression of the neuropeptide hugin, a homolog of mammalian neuromedin U. Functionally speaking,

they seem to coordinate the activity of the locomotor and feeding CPGs so that the two programs are not active at the same time (Schoofs et al., 2014) (Fig 20).

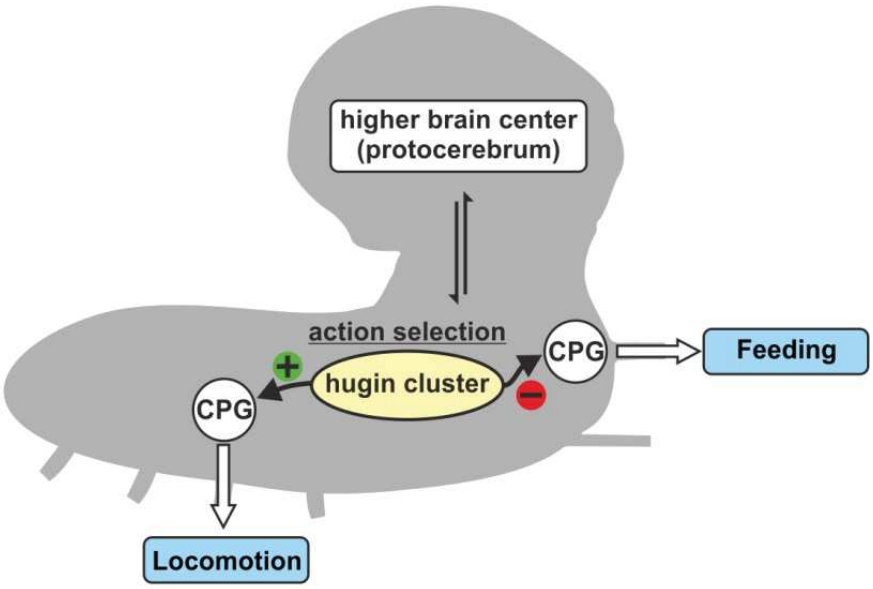

Fig 20: Schematics of the Hugin neurons function

Hugin neurons are located at the interphase between locomotor CPG and feeding CPG and coordinate their activity. Hugin neurons secrete the neuropeptide hugin, a homolog to the mammalian neuromedin U. From (Schoofs et al., 2014)

In *Drosophila* half the studies on IN locomotor populations focus on having a molecular characterization of the IN populations, while the other half almost exclusively studies the INs connectomics. Studies that associate both aspects, with full molecular and connectomics characterizations are scarce (Heckscher et al., 2015; Kohsaka et al., 2014). This truly is a shame, as it would allow us to make evolutionary comparisons and connections with Zebrafish and mouse models, and thus progress faster in the understanding of CPGs in general.

C - *Drosophila* as a model for understanding evolutionary conserved mechanisms

Over the last century *Drosophila* research has yielded results whose repercussions span beyond the invertebrate study circle. *Drosophila* has proved seminal in the discovery of essential genes and mechanisms that were thereafter shown to be conserved through evolution.

In the domain of development, *Drosophila* pioneering works are abundant. For example, embryo segmentation and establishment of segment polarity mechanisms were initially studied in *Drosophila*. More particularly, the homeotic genes were identified and characterized in *Drosophila* and it was subsequently shown that their function is conserved in all vertebrates including humans (Krumlauf, 1994; Lawrence and Morata, 1994). In the domain of sensory organ development, the initial discovery of *eyeless* and its targets in *Drosophila* led to the identification of its human and mouse ortholog *Pax6* with similar functions and targets (Halder et al., 1998; Hill et al., 1991; Kumar, 2009; Quiring et al., 1994). The proneuronal gene *atonal* was discovered in *Drosophila* where its crucial role in photoreceptor neurons and chordotonal organs development was assessed (Jarman et al., 1993; Jarman et al., 1994). The function of *atonal* orthologs is conserved through evolution, with *Math5* and *Math1* in mammals (Bermingham et al., 1999; Brown et al., 2001).

Numerous critical pathways were initially identified in *Drosophila*: Hedgehog ligand and its receptor Patched as well as the members of the Wnt pathway, to stay concise, were identified in *Drosophila* (Bhanot et al., 1996; Brunner et al., 1997; Hooper and Scott, 1989; Lee et al., 1992; Nüsslein-Volhard and Wieschaus, 1980; Siegfried et al., 1992; Tabata et al., 1992; Wehrli et al., 2000). Discovery and extensive study of the Notch pathway was first conducted in *Drosophila* (Artavanis-Tsakonas et al., 1995; Artavanis-Tsakonas et al., 1999; Wharton et al., 1985). All those pathways have major roles in human development and disease (Ejsmont and Hassan, 2014). *Drosophila* seems therefore to be a good model to understand evolutionary conserved mechanisms.

IV. The evolutionary conserved MafL transcription factor family

A - MafL genes in mammals

The Maf (for musculo-aponeurotic fibrosarcoma) proteins are part of the AP1 superfamily of basic leucine zipper (bZIP) TFs, just like JUN or FOS (Eychène et al., 2008) (Fig 21A). The Maf TF family is divided in two groups: large Maf (MafL) proteins (MafA, MafB, cMaf and nrl in the mouse) and small Maf proteins (MafK, MafF, MafG in the mouse) (Fig 21B). The small Maf proteins differ from the large

ones by the absence of a transactivation domain, making them unable to have a positive transcriptional activity (Kataoka, 2007). MafL factors activate transcription through the formation of homodimers and bind to a Maf recognition element (MARE) sequence (Kerppola and Curran, 1994).

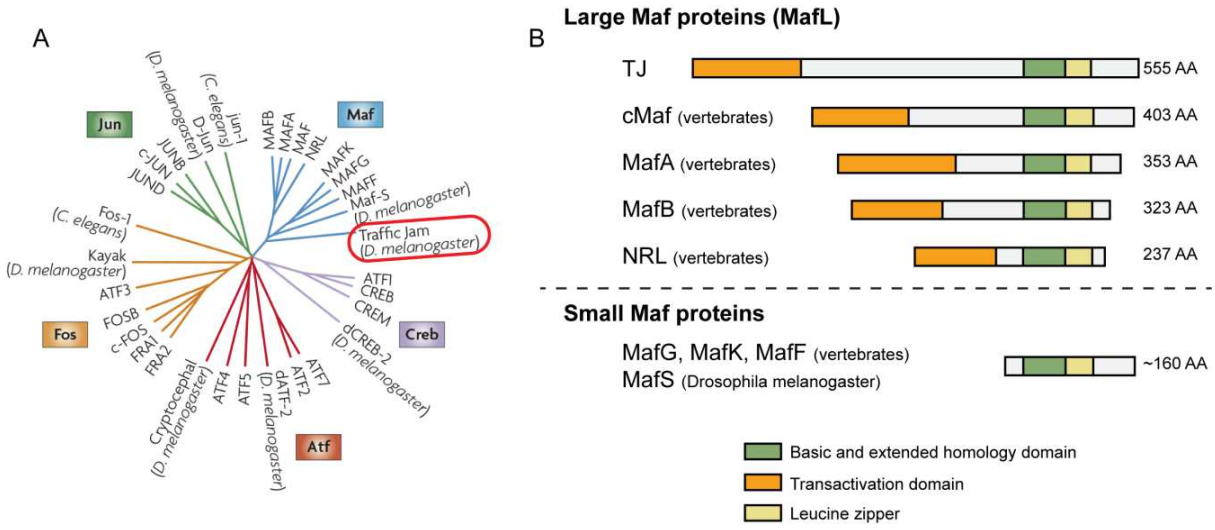

Fig 21: Maf proteins characteristics

A. Maf proteins belong to the AP1 superfamily of basic-leucine zipper (bZip) TFs, just like Jun, Fos, Creb and Atf. **B**. Maf TFs are divided in two subfamilies: small and large Maf TF. Large Maf TF possess a transactivation domain, a basic domain and leucine zipper that confer them full TF activity. In *Drosophila* a single ortholog TJ exists for the 4 vertebrates MafL. Small Maf TF are differentiated from large Maf TFs by the absence of transactivation domain. Adapted from (Eychène et al., 2008).

In physiological conditions, MafL genes are involved early in tissue specification and later in terminal differentiation (Eychène et al., 2008). It is therefore not surprising to find up-regulation of Maf TFs in some cancer types where they act as oncogenes (Eychène et al., 2008). MafA has been extensively studied in β pancreatic cells, where it plays an important part in insulin transcription and production (Eychène et al., 2008). MafB is exclusively expressed in α-cells in the pancreatic islets and regulates glucagon gene expression (Kataoka, 2007). In the nervous sytem, MafB is necessary for the proper segmentation of the developing hindbrain, especially in 5th and 6th rhombomeres (rh5-6). c-Maf is implicated in T helper (Th2) cells differentiation through induction of interleukin-4 expression in this cell type (Kataoka, 2007). Additionally, it is expressed in both α and β-cells of the islets of the pancreas (Kataoka, 2007) and in the liver, renal tubules, adipocytes, and

muscle (Tsuchiya et al., 2015). Both MafA and MafB are expressed in the gonads but their function seems to be dispensible for proper gametogenesis (Shawki et al., 2018). Nrl (for neural retina leucine zipper) is involved in the eye where it regulates the expression of rod photoreceptor specific genes including rhodopsin (Jayaram et al., 2012). Finally, expression of MafA, MafB and c-Maf delineates refined subpopulations of the central (Bikoff et al., 2016; Francius et al., 2013; Gabitto et al., 2016; Lu et al., 2015; Sweeney et al., 2018) and peripheric nervous systems in the dorsal root ganglia neurons (Bourane et al., 2009; Hu et al., 2012).

B - In other organisms

Apart from the mammals, members of the MafL can be found in fishes, invertebrates (Traffic Jam – TJ in *Drosophila*) and even Cnidarians, a phylum containing jellyfish and corals for example (Coolen et al., 2005; Seipel et al., 2004). The most important functional part of Maf TFs, the bZIP domain, is highly conserved between *Homo sapiens*, *Drosophila melanogaster* and the jellyfish *Podocoryne carnea* (Fig 22A). Amazingly, in jellyfish, MafL is expressed in the gonads, in differentiating neurons and in light sensing organs (Seipel et al., 2004), much in the same way MafL are expressed in vertebrates. MafL genes seem therefore to be evolutionarily conserved and pre-date the vertebrate/invertebrate split (Fig 22B). Moreover, as Cnidarians have a radial symmetry, Maf genes existed before bilateralism (Seipel et al., 2004).

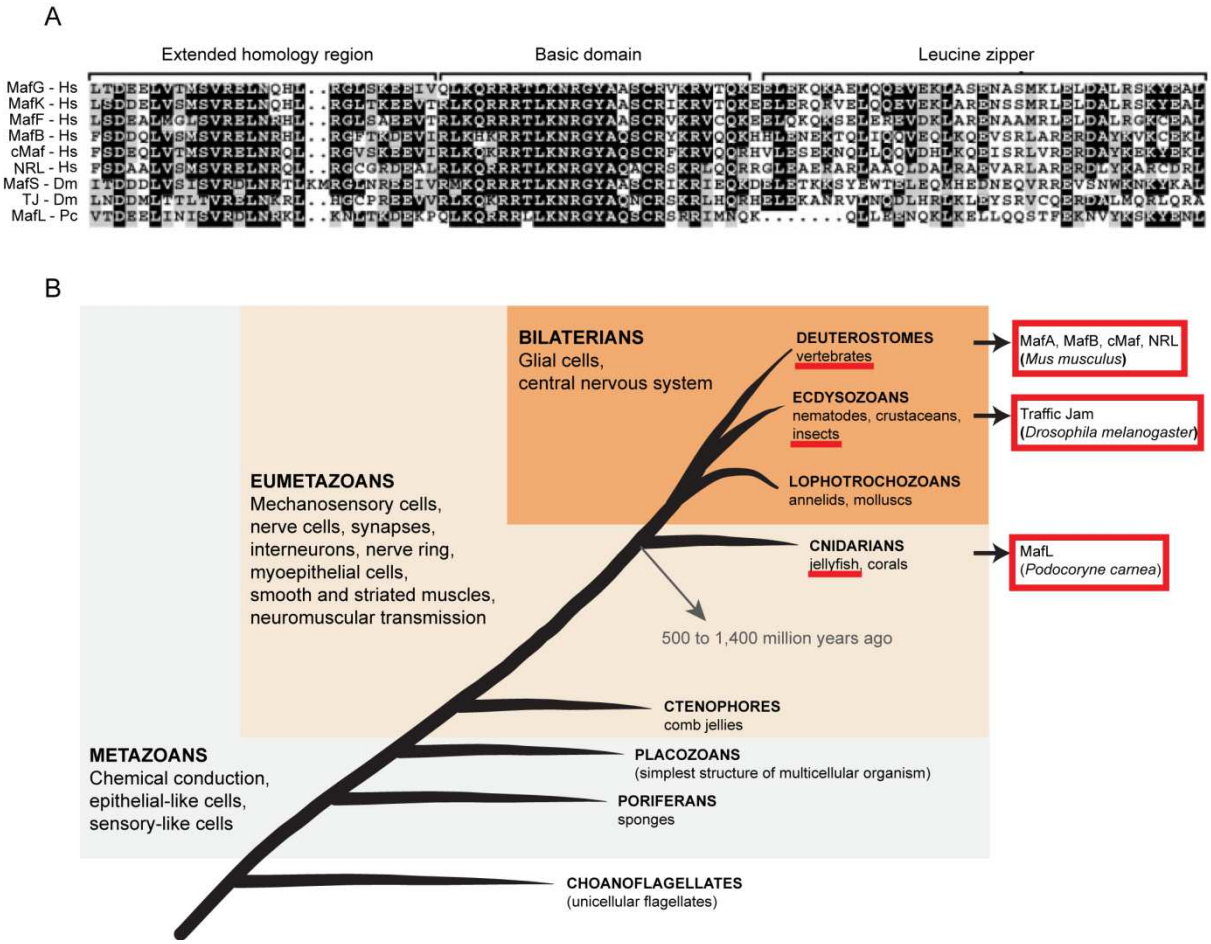

Fig 22: Conservation of large Maf TF across evolution

A. Alignment of extended homology region, basic domain and leucine zipper in large and small Maf proteins in *Homo sapiens* (Hs), *Drosophila melanogaster* (Dm) and the Cnidarians-belonging jellyfish *Podocoryne carnea* (Pc). Identical amino acids are boxed in black, and similar amino acids are boxed in gray. **B**. Simplified phylogenic representation of the origin of neurogenesis and progressive acquisition of a nervous system during evolution. Large Maf proteins have so far been identified in Deuterostomes (vertebrates including fishes, mouse and human), ecdysozoans (including *Drosophila*) and Cnidarians (in the jellyfish *Podocoryne carnea*). Maf TFs were probably already part of the genetic machinery of the common ancestor of Cnidarians and Bilaterians, some 500 to 1,400 million years ago. Adapted from (Galliot et al., 2009; Seipel et al., 2004).

C - MafL in *Drosophila*

The sole ortholog of the large Maf TF in *Drosophila* is Traffic Jam (TJ). *tj* gene is 3,2 kb long, possesses a single exon and encodes for a 555 amino acids protein (Fig 21B). It was initially characterized for its critical role in the gonads where it modulates adhesive properties of the somatic cells, allowing for germline-soma interactions that are essential for germ cell differentiation. Complete loss of function of *tj* leads therefore to total sterility of both males and females flies (Li et al., 2003). It

was moreover shown later that in the gonads *tj* 3'UTR is a substrate of Piwi to generate piRNAs targeting adhesion protein FasIII expression (Saito et al., 2009). Subsequently, it was revealed that TJ regulates opsin expression and plays a role in R8 photoreceptor fate in *Drosophila* eye via its association with Otd (Orthodenticle) (Jukam et al., 2013). This control of opsin expression is conserved across evolution, with Otd/TJ orthologs Crx/nrl playing the same part in the mouse (Jukam et al., 2013; Swaroop et al., 2010). In 2003, TJ expression in the CNS was noted by in-situ hybridization in embryos but this pattern of expression was subsequently never discussed in literature (Kawashima et al., 2003; Li et al., 2003).

V. Specific aims / Thesis outline

In this context the two main aims of my thesis are to:

- characterize TJ-expressing neurons in the *Drosophila* larva VNC in terms of i) cell body position and ii) molecular identity.

- study the implication of the TJ^{+} neurons population and subpopulations in *Drosophila* larva locomotion.

Chapter 2: Material and methods

I. Fly Stocks and fly maintenance

Fly stocks are kept on nutritious medium containing maize, sugar, yeast, glucose and agar as well as an anti-fungus agent in a room at 17°C with normal day-night light cycle. All genetic crosses were performed at 24°C unless otherwise specified.

***Drosophila* lines**	**Source**	**Characteristics**	**Identifier**
RapGAP1-lexA	Bloomington Stock Center	Expressed in MNs	BL # 66663
R70C01-lexA (noted *PMSI-lexA*)	Bloomington Stock Center	Expressed in a PMSI subpopulation	BL # 54927
R36G02-gal4 (noted *A27h-gal4*)	Bloomington Stock Center	Expressed in A27h neuron	BL # 49939
R26A08-gal4	Bloomington Stock Center	GVLI-gal4 – expresses gal4 under control of DNA sequences in or near *fur*	BL # 49153
R26F05-gal4	Bloomington Stock Center	GVLI-gal4 – expresses gal4 under control of DNA sequences in or near *fur*	BL # 49192
R78F11-gal4	Bloomington Stock Center	Ventral contraction - expresses gal4 under control of DNA sequences in or near *SPR*	BL # 40008
R79E03-gal4	Bloomington Stock Center	Ventral contraction - expresses gal4 under control of DNA sequences in or near *CG9650*	BL # 48353
R92C05-gal4	Bloomington Stock Center	Ventral contraction - expresses gal4 under control of DNA sequences in or near *beat-1c*	BL # 40609
GMR40H07-lexA driver (also called *TJjan-lexA*)	Bloomington Stock Center	Expresses lexA under the control of DNA sequences in or near *tj*	BL # 54786
UAS-lexA	Bloomington Stock Center	Expresses the LexA DNA binding domain fused to the transcriptional activator VP16 under the control of UAS.	BL # 29958
GMR47D01-gal4	Bloomington Stock Center	Drives in LLN neurons	BL # 48171

LMO-gal4 (or *PG137*)	Gift from Alain Vincent (Bourbon et al., 2002)	Drives in a restricted CNS neuronal population	NA
Abd-B-gal4	Gift from F. Karch (Gligorov et al., 2013)	Drives in all cells in abdominal segments A5 to A9.	NA
HB9-gal4	Bloomington Stock Center	Expressed in a subset of MNs and INs	BL # 32555
OK6-gal4	Bloomington Stock Center	Expresses Gal4 primarily in MNs	BL # 26160
TrpA1-gal4	Bloomington Stock Center	A GAL4 knock-in replacement of 178 nucleotides spanning the TrpA1-A and -B isoform translation initiation codon.	BL # 67131
UAS-βgal	Bloomington Stock Center	Expresses tau-tagged lacZ under the control of UAS. Beta-galactosidase is targeted to microtubules.	BL # 5148
GMR83H09-gal4	Bloomington Stock Center	Expressed in iIN	BL # 41311
9-20-gal4	Gift from JB Thomas (Hughes and Thomas, 2007)	Expressed in GDL (among other cells)	NA
GMR15C11-gal4	Bloomington Stock Center	Expressed in GDL (among other cells) - expresses GAL4 under the control of DNA sequences in or near *sc*	BL # 48684
HugS3-gal4 (also Hugin-gal4*)*	Gift from M. Pankratz (Melcher and Pankratz, 2005)	Expressed in Hugin neurons	NA
lexAop>>CsChrimson^{Venus}	Bloomington Stock Center	Expresses a red-shifted channel-rhodopsin under the control of the lexA operator.	BL # 55138
UAS>>CD8GFP	(Wong et al., 2002)	Expresses CD8-GFP under UAS control and upon FLP-mediated removal of a stop cassette	NA
GMR47G08-lexA	Bloomington Stock Center	Expressed some midline cells	BL # 52793
Cut-gal4	Bloomington Stock Center	Expressed in some midline cells	BL # 27327

OK6-lexA	Tokyo Stock Center	Supposedly expressed in MNs	DGRC # 116998
UAS-IVS-mCD8::RFP, lexAop2-mCD8::GFP	Bloomington Stock Center	Expresses mCD8-tagged RFP under the control of UAS and mCD8-tagged GFP under the control of LexAop	BL # 32229

Table 2: List of *Drosophila* lines used

II. Antibody list

Primary Antibodies	Species	Dilution	Source
Anti-Fd59a	Guinea pig	1:1000	Gift from Jim Skeath (Lacin et al., 2014)
Anti-β-gal	Chicken	1:2000	Abcam Ab9361
Anti-β-gal	Rabbit	1:2000	Cappel 559762
Anti-Islet-1/2 39.4D5 and 40.2D6	Mouse	1:20	Development Studies Hybridoma Bank, University of Iowa

Table 3: List of primary antibodies used

III. Larva locomotion assay (Optogenetics-based)

Second instar larvae of the right genotype were picked up and allowed to develop for 1 day at 24°C on agar plate supplemented with grape juice and spread with a yeast paste containing 1 mM of all-trans retinal. Yeast paste was prepared as follow: 5 µl of 100 mM all-trans retinal was added to 500 µl of deionized water and then thoroughly mixed with 0,7 g dried yeast. Handling of all products containing all-trans retinal was done under dim light. Agar plate containing larvae and all-trans retinal supplemented yeast paste were incubated at 24°C in a light-proof box. For the locomotion assay, a single larva at a time was retrieved from the yeast paste supplemented agar plate and placed on a regular, fresh agar plate supplemented with grape juice. Free moving larvae locomotion was assessed upon red light (660 nm) illumination.

IV. Adult phenotype assay

Eggs were left to be laid for a day and individuals went through normal development unperturbed at 24°C. Flies hatched for less than 24 hours were sorted

out for presence of all the transgenes and then transferred to fresh tubes containing standard feeding medium (used for the stocks and crossings). For the experiments, flies were placed in an incubator at 31°C for short activation period (1h) or long activation period (7h). Vials containing the flies were simply taken out to observe flies behaviours; when measuring the displacement of the wings, flies were anesthetized with ether for 15 seconds and placed under a binocular microscope for macroscopic observation and to take pictures.

V. 3D reconstruction (morphology analysis)

3D reconstruction of larva VNC to visualize morphology of TJ^{+} neurons was done with Imaris software (Bitplane).

Chapter 3: Characterization of TJ$^+$ neurons function in *Drosophila* larva locomotion

I. Introduction

TJ expression in the CNS was initially noted in the articles from Li and collaborators (2003) and Kawashima and collaborators (2003) but its precise pattern of expression was subsequently never discussed in literature. Initial observation in the laboratory reported that TJ is expressed in a restricted neuronal population in the VNC and cerebellar lobes. As the large Maf TFs are expressed in neuronal populations belonging to locomotor CPG in mouse (Bikoff et al., 2016; Francius et al., 2013; Lu et al., 2015), we were interested to know if the same could be said of TJ$^+$ population in *Drosophila*.

II. Results

A - *TJ-Flp* line

The emergence of intersectional genetics techniques has opened up new ways to target transgenes to highly restricted cellular populations. In such systems, the expression of the transgene is limited by the intersection of two (or more) overlapping gene expression patterns. In *Drosophila*, intersectional genetics relies on the combination of two binary systems such as UAS/Gal4, lexA/lexAop, Q-system or FRT/Flp or the use of split-gal4 technology (Alekseyenko et al., 2014; Luan et al., 2006; Sjulson et al., 2016). Prior to the work presented here, the only available genetic tool to delineate and target TJ$^+$ population was a *TJ-gal4* line that perfectly matches the normal TJ pattern of expression (as shown in the article - 3.2.C chapter). Although very convenient, this gal4 is not ideal to study the implication of TJ$^+$ neurons in locomotion, as it only allows simple, direct manipulation of the whole TJ$^+$ population. We therefore decided to generate a *TJ-Flippase* (*TJ-Flp*) line. As previous swapping attempts using a P element conversion approach (Sepp and Auld, 1999) to replace the gal4 of *TJ-Gal4* by a Flp failed, we switched approaches and chose to use instead a technique developed by Ejsmont et al (2009). This technique

relies on homologous recombination in bacteria to replace, in our case, a part of *tj* sequence by a Flp sequence. Briefly, a fosmid bank containing random sequences from *Drosophila* genome was generated and described by Ejsmont and collaborators (2009). We were lucky to find in this bank a 40kb fosmid containing the entire *tj* locus (coding sequence, 3'UTR as well as 5'UTR) thus foreseeing that this fosmid would contain all of *tj* regulatory elements. We also had access to a *TJ-GFP* tagged *Drosophila* line in which this fosmid was used to express a tagged version of TJ (generous gift from F. Schnorrer) (Sarov et al., 2016). Examination of this line revealed that the number and position of the GFP^+ neurons in the embryo and larva VNC were highly reminiscent of TJ^+ cells (data from the lab – not shown). With this information we thus decided to use this fosmid to precisely replace the coding sequence and 3'UTR of *tj* by a Flp. We chose to use a Flp optimized for codon use (or FlpO) that moreover contains a NLS sequence (nuclear localization signal) allowing for a more efficient translocation in the nucleus were it completes its function (generous gift from S. Bourane, Goulding's lab, Salk Institute for Biological Studies, USA).

First of all, I generated a cassette containing the sequence of the FlpO followed by a SV40 polyA signal to ensure the end of the Flp transcription; a kanamycin resistance gene, used as selection marker in the technique, was moreover added (Fig 23A). The cassette was amplified by PCR using a proofreading polymerase (Pfu – Promega) and oligonucleotides with 3' 50bp-long hanging sequences that are homologous to TJ sequence (Fig 23B and 23C). We thus obtained a PCR product containing the sequence of the optimized flippase with the SV40polyA and the kanamycin resistance gene flanked by TJ homologous sequences.

A

B TJrec s oligonucleotide:

5'ATGTGAGACCCGTAATCGACCCTCTCCGGTCCCTGGTCGATCCAATGAAAATGGCTCCTAAGAAGAAGAGG

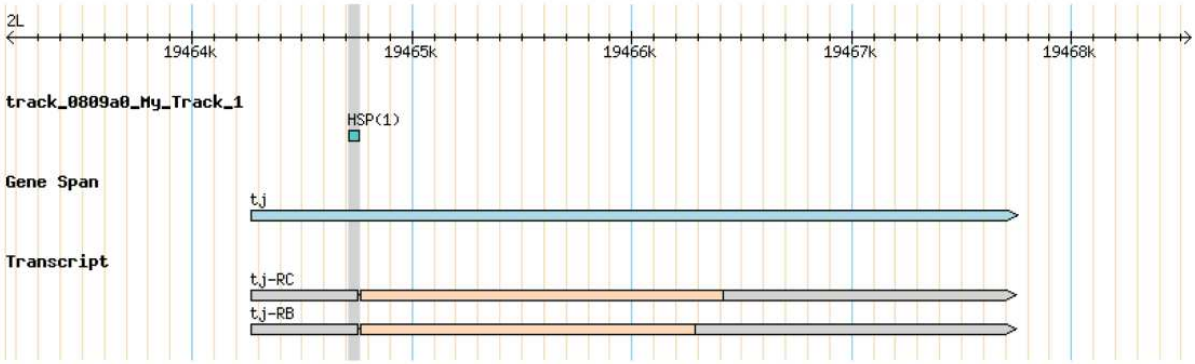

C TJrec as oligonucleotide:

5'ATTCATTAATTTAGATTTATTTATTACTAAATTGTTTTATGCACACTTATAACTCAGAAGAACTCGTCAAG

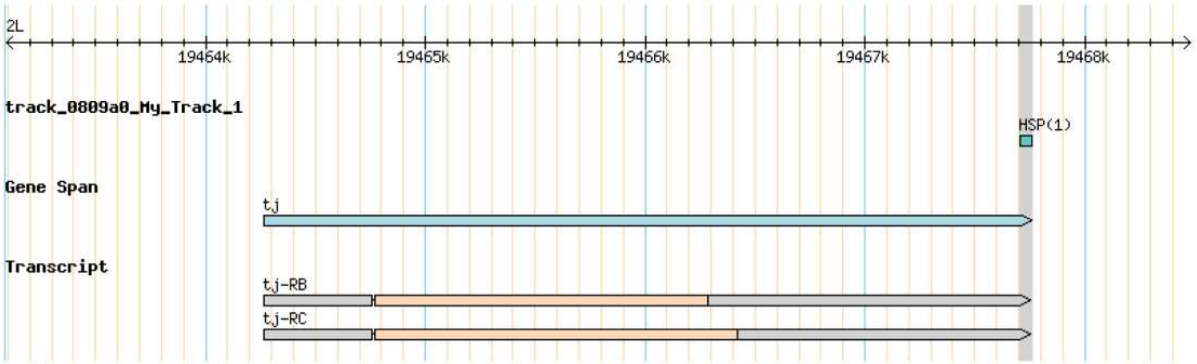

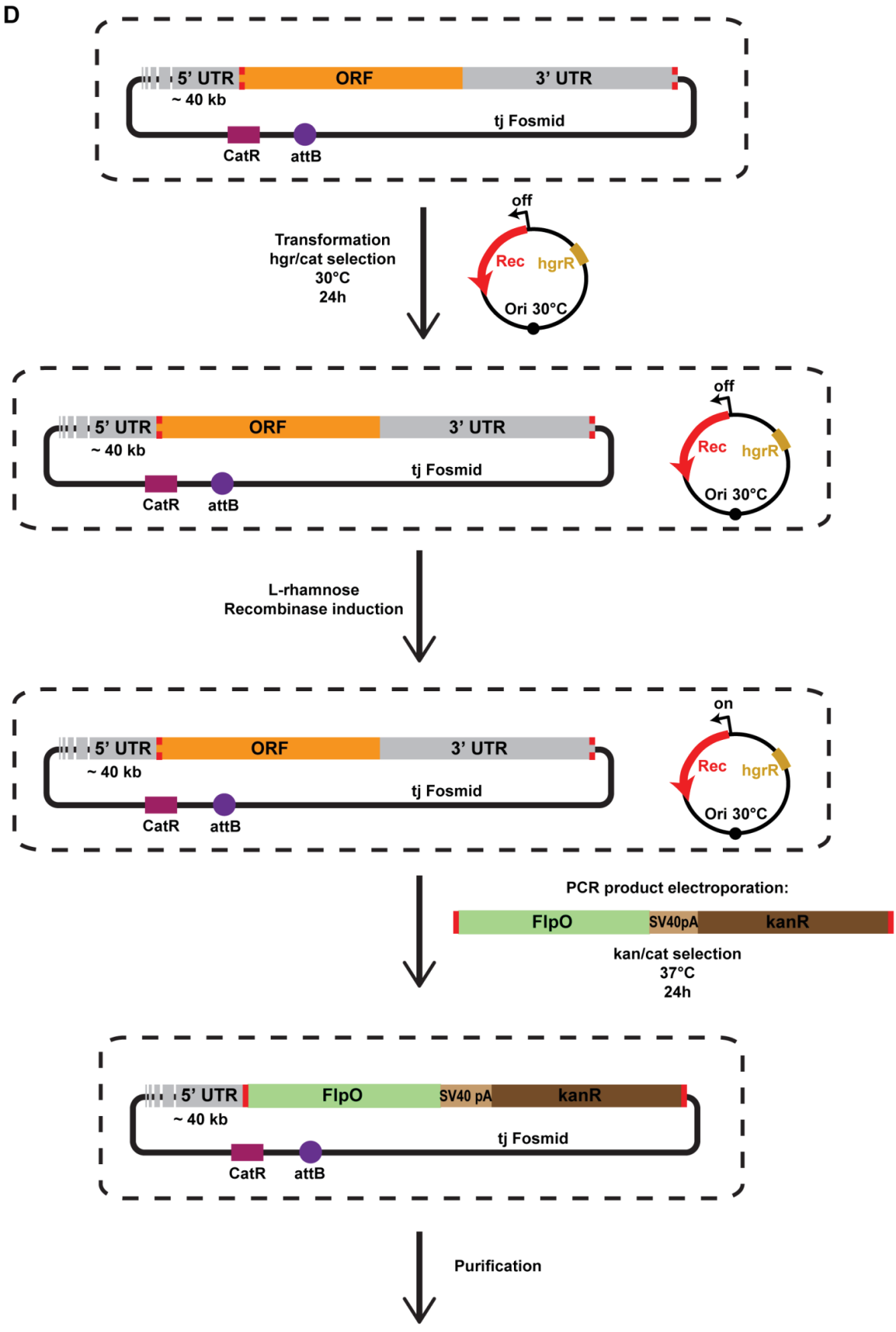
D
5' UTR
ORF
3' UTR
~ 40 kb
tj Fosmid
CatR
attB
Transformation
hgr/cat selection
30°C
24h
off
Rec
hgrR
Ori 30°C
L-rhamnose
Recombinase induction
on
PCR product electroporation:
FlpO
SV40pA
kanR
kan/cat selection
37°C
24h
FlpO
SV40 pA
kanR
Purification

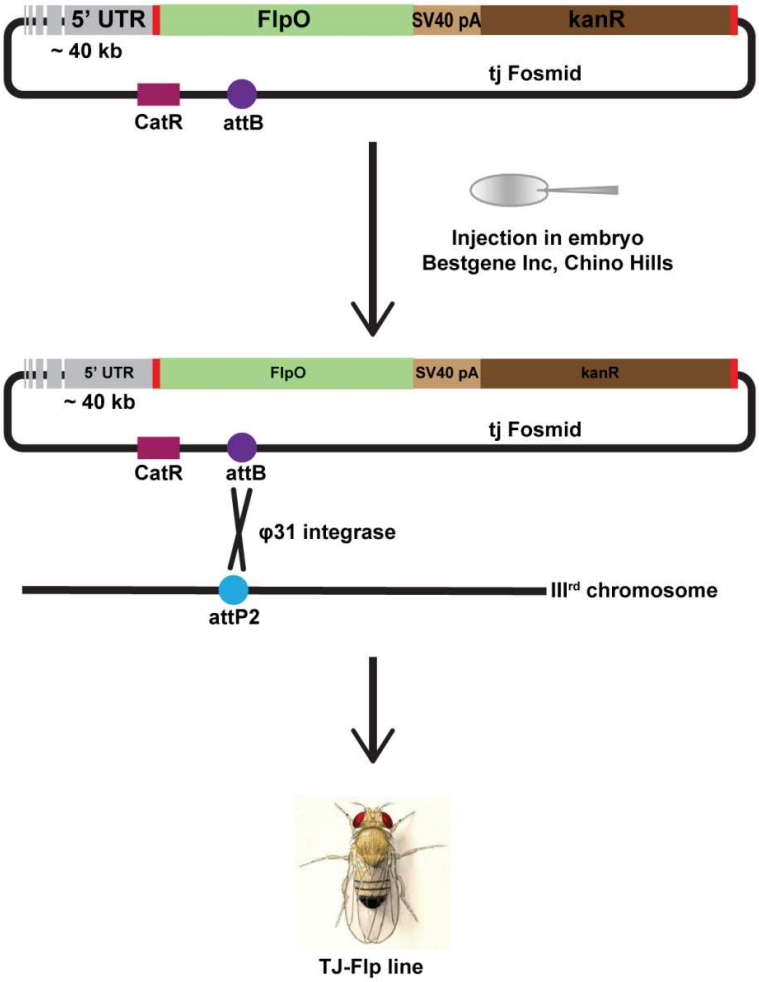

Fig 23: Stages of *TJ-Flp* line building

A. Cassette to be recombined: contains optimized Flp sequence (FlpO), a SV40pA transcription terminal sequence and a kanamycin resistance gene. **B**. Sequence of the sense oligonucleotide used to add homologous arms to the sequence to be recombined (presented in A) during PCR. Red sequence of the oligonucleotide is homologous to the 5' UTR just prior to the start codon of *tj* (blast of this sequence in Flybase shows the recombination zone targeted). Black sequence corresponds to the sense primer used to amplify FlpO-SV40-kanR cassette during PCR. **C**. Sequence of the antisense oligonucleotide used to add homologous arms to the sequence to be recombined (presented in A) during PCR. Red sequence of the oligonucleotide is homologous to the 3' UTR sequence of *tj* at the polyA signal (blast of this sequence in Flybase shows the recombination zone targeted). Black sequence corresponds to the antisense primer used to amplify FlpO-SV40-kanR cassette during PCR. **D**. Schematics of the recombination protocol in bacteria to obtain *TJ-Flp*. Briefly E.coli containing TJ-fosmid are transformed with a helper plasmid. The bacteria containing both fosmid and helper plasmid are selected on hygromycin and chloramphenicol resistances at 30°C. L-rhamnose is added in the culture medium to induce expression of the recombinase gene located on the helper plasmid. Then the PCR product consisting in the sequence of the FlpO, a SV40polyA and kanamycin resistance flanked by homologous sequences of TJ is electroporated in the bacteria. Bacteria containing the

recombined fosmid are selected on chloramphenicol and kanamycin resistance at 37°C. The fosmid is then purified. Targeted transgenesis, allowed by the presence of an attB site on the fosmid backbone, is done in an attp2 site (on the IIIrd chromosome) by Bestgene Inc, Chino Hills. Adapted from (Ejsmont et al., 2009).

Recombination was performed in bacteria following the protocol specified in Ejsmont et al (2009) (Fig 23D). The last stage of recombination with removal of the kanamycin resistance gene proposed in the initial protocol was skipped. The fosmid was integrated using targeted transgenesis in the genome in an attp2 landing site on the IIIrd chromosome (by Bestgene Inc, Chino Hills). Balancing of the *Drosophila* line obtained was carried out in the lab and the pattern of expression of the flippase assessed (results presented in the article supplemental figures (3.2.C chapter)).

As is shown in more details in the following manuscript, the expression of the FlpO recombinase in this *Drosophila* line faithfully recapitulates the expression of TJ in the larva. TJ-Flp line expression pattern is shown in the following manuscript.

B - Introduction to submitted Article

In the past five years or so the wealth of knowledge on locomotor INs populations in *Drosophila* larva has greatly increased. Regardless, much work will be required in the future to continue this characterization. In our article we report a new, discrete neuronal population implicated in the locomotor CPG and singled out by its expression of the Maf TF TJ. Despite its comparative small size (29 neurons out of 305 per hemisegment), TJ$^+$ population is highly diverse and comprises both MNs and INs that are divided in three glutamatergic, cholinergic and GABAergic subpopulations. Intersectional genetics approach combined with a new *TJ-Flp* line allowed us to functionally dissect the role of TJ$^+$ subpopulations in locomotion. We find that TJ$^+$ MNs only have a slight impact on locomotion while TJ$^+$ cholinergic INs induce ventral contraction of the larvae. More interestingly, upon activation of the TJ$^+$ GABAergic INs, we observe a normal though slowed locomotion: those cells seem to regulate the speed of locomotion. Using a triple intersection approach we identify 3 TJ$^+$ GABAergic neurons per segment that partially regulate the speed of locomotion. Molecular characterization of these 3 neurons identifies them as midline cells, and more particularly MNB progeny neurons.

C - Article

Traffic Jam-expressing MNB progeny neurons regulate the speed of locomotion in *Drosophila* larva

Babski, H[1]., Surel, C[1]., Yoshikawa, S[2]., Valmier, J[1]., Thomas, J.B[2]., Carroll, P[1]* and Garcès, A[1]*.

[1] Inserm U1051, Institute for Neurosciences of Montpellier, University of Montpellier, 34295 Montpellier, France

[2] Molecular Neurobiology Laboratory, The Salk Institute for Biological Studies, La Jolla, CA 92037, United States.

***These authors contributed equally to this work.**

Contact: alain.garces@inserm.fr

Key words: Central Pattern Generators; intersectional genetics; locomotion; Maf Transcription factor; interneurons; MNB progeny neurons; *Drosophila* larva

Abstract (156 words)

Interneurons (INs) coordinate the activity of motoneurons to generate adequate patterns of muscle contractions providing animals with the ability to adjust their body posture and to move over a range of speeds. In the *Drosophila* larvae several IN subtypes have been morphologically described and their function well documented. Yet, the combinatorial expression of transcription factors (TFs) within these subsets is scarcely known, limiting our understanding of the common principles underlying the logic of the locomotor circuitry among species. Here we characterize a highly restricted neuronal subset expressing the Maf TF Traffic Jam (TJ). We found that TJ^+ neurons are highly diverse and their activation using intersectional genetics disrupted larval body posture and locomotion speed. Our results also showed that a small subset of TJ^+ GABAergic INs, singled out by the unique expression of *Per*, *Fkh*, *Grain* and *Hlh3b*, a molecular signature highly reminiscent to V_{2b} INs in vertebrate, substantially impacted the crawling speed of the larvae.

Introduction

The wiring and functioning of the neuronal circuits that provides animals with the ability to move over a range of speeds have been extensively studied (Clark et al., 2018; Kiehn, 2016; Ziskind-Conhaim and Hochman, 2017). In mammals as in invertebrates the speed of locomotion is regulated by central pattern generator (CPG) neuronal circuits which coordinate, via motoneurons (MNs), the sequential activation of muscles (Andrzejczuk et al., 2018; Caldeira et al., 2017; Dougherty et al., 2013; Fidelin et al., 2015; Gosgnach et al., 2006; Kohsaka et al., 2014; Zhong et al., 2010). The rhythmic bursts of MNs activity are controlled by local excitatory and inhibitory interneurons (INs) and in vertebrates the major components of CPG circuits derive from four classes of INs (V_0, V_1, V_2, and V_3) located in the ventral part of the spinal cord (Kiehn, 2016; Ziskind-Conhaim and Hochman, 2017). These INs subtypes are categorized on the basis of their connectivity patterns, physiological properties such as neurotransmitter used, and by the set of specific transcription factors (TFs) they express (Jessell, 2000). The V_1 premotor inhibitory INs control the speed of locomotion as they mediate recurrent inhibition of MNs. Recently their tremendous diversity has been exemplified as V_1 INs fractionate into 50 highly diverse subsets on the basis of the expression of 19 TFs (Gabitto et al., 2016).

The combinatorial expression of TFs expression by subsets of INs thus provides a powerful and systematic tool for assessing genetically, when transgenic lines are available, the function of highly restricted subpopulations of INs, for example using intersectional genetics, through the controlled expression of ion channel proteins that regulate their activity (Borgius et al., 2014; Talpalar et al., 2013; Wyart et al., 2009). Such an approach used in mouse and in *Drosophila* has proved instrumental in dissecting the core logic of the CPG circuits that generate the rhythm and pattern of motor output (Clark et al., 2016; Fidelin et al., 2015; Kohsaka et al., 2014). Still, and in light of the remarkable diversity of INs in the vertebrate spinal cord (Bikoff et al., 2016; Gabitto et al., 2016) and in the *Drosophila* nerve cord (Heckscher et al., 2014; Rickert et al., 2011), a thorough description of the functioning of the CPG regulating the speed of locomotion in animals is far from complete.

In 2014, a class of segmentally arrayed local premotor inhibitory INs named PMSIs (for period-positive median segmental interneurons) was characterized in *Drosophila*. PMSIs control the speed of larval locomotion by limiting, via inhibition, the duration of MNs outputs and have been proposed to be the fly equivalent of the V_1 INs. Thus PMSIs in

Drosophila and V_1 INs in vertebrates represent a phylogenetically conserved IN population that shape motor outputs during locomotion (Kohsaka et al., 2014). During the following years specific IN subtypes contributing to the diversity of locomotor behaviours in the *Drosophila* larvae have been identified providing a wealth of information on each IN subpopulation, their function, morphology and connections established ((Hasegawa et al., 2016; Heckscher et al., 2015; Itakura et al., 2015; Kohsaka et al., 2014; Yoshikawa et al., 2016; Zwart et al., 2016). However only little is known about the combinatorial expression of TFs within these different IN subtypes identified so far and this lack of knowledge impedes cross species comparisons thus limiting our understanding of the common principles of CPG organization in vertebrates and invertebrates.

Here we investigate in the *Drosophila* larva the role of a small pool of highly diverse INs (23/hemisegment) expressing the evolutionary conserved TF Traffic Jam (TJ, the orthologue of MafA, Mafb, c-Maf and NRL in the mouse). Interestingly, MafA, MafB and c-Maf are expressed by restricted subpopulations of ventral premotor INs in the developing mouse spinal cord (Bikoff et al., 2016; Francius et al., 2013; Gabitto et al., 2016; Lu et al., 2015; Sweeney et al., 2018) but the function of these INs subtypes is to date unknown. To characterize TJ-expressing INs we generated a *TJ-Flippase* line and we used intersectional genetics to activate TJ^+ subpopulations depending on their neurotransmitter properties. We found that manipulation of these IN subsets modulate larval locomotor behaviours. Our results also show that activation of a restricted subpopulation of GABAergic/Per^+/TJ^+ (3 INs/segment), belonging to the PMSIs group of INs and known as MNB progeny neurons, considerably impacts the crawling speed of the larvae.

Results

Traffic Jam is expressed in a restricted subpopulation of neurons located in the VNC and involved in larval locomotion

We initiated a detailed analysis of the transcription factor (TF) Traffic Jam (TJ) expression in the embryonic and larval nervous systems, using a previously characterized TJ-specific antibody (Li et al., 2003) and an enhancer trap for *TJ* (*TJ-Gal4*) (Hayashi et al., 2002). During embryogenesis TJ expression is first detected in late stage 12 (st 12) in few cells in the brain and in 12 to 15 cells/hemisegment in the ventral nerve cord (VNC) (Fig.1A). Co-immunostaining with the glial marker Repo showed that TJ is exclusively expressed in neurons and excluded from glia cells (Fig.1B). Using *TJ-Gal4::UAS-GFP* we found that *TJ-Gal4* faithfully recapitulates TJ expression in all embryonic (Fig.1C) and larval stages analysed (Fig.2C-G). Closer analysis of TJ expression over time showed that TJ is consistently found in a subset of 29 neurons per hemisegment in the VNC abdominal region (A2-A6) from st17 to L3 larval stages (Fig.2A, A', B, B') and excluded from sensory neurons (data no shown). We used *TJ-Gal4::UAS-H2AGFP* in combination with anti-TJ immunostainings to establish a precise topographic map of TJ^+ neurons in second instar larvae, a stage representative of the continuous expression pattern of TJ (Fig.2 C-G, C1-G1).

Next, we decided to explore the function of TJ^+ neurons in larval locomotion using the *TJ-Gal4* driver as a tool to either inactivate or activate the entire TJ^+ neuronal population. We inactivated neurons by expressing thermosensitive shibire (shi^{ts}) (Kitamoto, 2001); neuronal activation was achieved by expressing *TrpA1* (Pulver et al., 2009). Inactivation of the entire TJ^+ population led to a slight decrease in the number of larval peristaltic waves (Fig.2H – second beige bar) accompanied by a general disorganization of the peristaltic waves (video 1). Electrical activation of the TJ^+ neurons had more drastic effects, with almost complete abolition of locomotion (Fig.2I – second red bar) and larvae displaying a complete paralysis which we named "spastic paralysis". This phenotype was characterized by immobility, tonic contraction of all body segments and a drastic shortening of the whole larval body length (video 2). When placed back at permissive temperature (23°C), the larvae resumed normal locomotion, proving that this spastic paralysis phenotype is fully reversible. TJ is expressed in a restricted number of neurons in the cerebellar lobes. To assess the role of these neurons in the spastic paralysis phenotype, we restricted the expression of *TrpA1* to

the TJ^+ cerebellar lobes neurons using *tsh-gal80* (Clyne and Miesenböck, 2008) in combination with *TJ-Gal4* and *UAS-TrpA1*. Under these conditions locomotion appeared normal (Fig.2I – second cream-coloured bar) arguing that TJ^+ neurons in the cerebellar lobes do not have a function in locomotion in *Drosophila* larva.

We thus conclude that TJ^+ neurons within the VNC are part of a neuronal circuit controlling *Drosophila* larval crawling and that normal function of TJ^+ neurons is to maintain proper muscle contraction and peristaltic wave propagation during locomotion.

Activation of TJ^+ neurons in the VNC using an intersectional genetic approach leads to spastic paralysis of the larvae

To further characterize the identity of TJ^+ neurons regulating crawling behaviour in the larva we developed an intersectional-based genetic approach, using candidate *LexA* drivers to express a *LexAop-FRT-stop-FRT-dTrpA1* transgene (generous gift from Y. Aso, Janelia Research Campus) in combination with a source of Flippase. To specifically target TJ^+ neurons we generated a *TJ-Flippase* line (see Materials and Methods). Within a ~40kb backbone fosmid carrying all the endogenous regulatory elements of *tj*, we substituted the full open reading frame and 3' UTR sequences of *tj* with an optimized *Flippase* (*FlpO*) by in *vivo* homologous recombination in *Escherichia coli* (Ejsmont et al., 2009). We first characterized in "flip-out" experiments the accuracy and efficiency of *TJ-Flp* using *Act>Stop>Gal4::UAS-CD8-GFP* and found from embryonic stage 15 onward that only TJ^+ cells are GFP-labelled (supplementary Fig.1A). We quantified the efficiency of "flip-out" events in TJ^+ neurons and found from hemisegment to hemisegment and within all specimen analyzed (n=4) that more than half the TJ^+ neurons (64%) are already recombined in L1 larva (Fig.3A-C) and 89% in young L2 stage (Fig.3D-F). These numbers demonstrate the accurate recombination triggered by *TJ-Flp*. An examination of developing egg chambers of the ovary, a structure in which TJ has been reported to be specifically expressed by somatic cells (Li et al., 2003), revealed that all TJ^+ follicular cells are GFP-labelled thus confirming the accuracy of *TJ-Flp* (supplementary Fig.1B-C). Finally, we used *Tsh-LexA* to express a *LexAop-FRT-STOP-FRT-dTrpA1* transgene in combination with *TJ-Flp,* anticipating that activation TJ^+ neurons only in the VNC should give rise to the drastic spastic paralysis phenotype described above. We found it was indeed the case in all L1 larvae tested (n=12) (Fig.3K, movie 3).

Collectively, these results show that the *TJ-Flp* line we generated is an accurate and powerful genetic tool to genetically manipulate TJ^+ neurons, thus validating our intersectional-based genetic approach.

TJ^+ motoneurons activation only partially impacts larval crawling

We next asked whether the spastic paralysis phenotype we observe upon activation of the whole TJ^+ population would actually be caused by *TJ-Gal4* driving in MNs. Using pMad and Eve as reliable molecular markers for MNs we found TJ expression from st13 onward in 3 CQ/Us' MNs namely U1, U2 and U5 (asterisks in Fig.4 A2, A3, B2, B3 and C2, C3) plus another putative MN located in the vicinity of the CQ MNs (full arrowhead in Fig. 4 C3). Co-labelling using *Isl-Tmyc* and pMad also revealed TJ expression in 2 MNs located laterally in the dorsal and intermediate regions of the VNC that are putatively part of the ISNd MNs pool (Fig.4 C2 - inset). We noticed that TJ was neither expressed in aCC nor in any RPs MNs (RP1-5) (Fig.4A1 and C1 – curly brackets) nor in SNa MNs (Supplementary Fig.3A1, A2) nor in type II, octopaminergic $Tdc2^+$ MNs (Supplementary Fig.3B).

To confirm and further delineate the identity of TJ^+ MNs we used *TJ-Gal4* and expressed a myristoylated targeted RFP reporter (*UAS-myr-RFP*) (generous gift from M. Landgraf). From late st16 to L3, *TJ-Gal4::UAS-myr-RFP* revealed the high reproducibility of these peripheral projections as well as their terminal processes onto muscles VO3-VO6 (Supplementary Fig.2A-C) and onto the dorsal-most muscles LL1, DO5, DO2 and DO1 (from lateral to dorsal-most, Supplementary Fig.2A'-C'). These results are in agreement with the above immunostaining results and we conclude that in each abdominal hemisegment there is a contingent of 2 TJ^+/$pMad^+$/$Islet\text{-}myc^+$ MNs (ISNd MNs that project on muscles VO3-VO6), 3 TJ^+/$pMad^+$/Eve^+ MNs (ISNdm MNs U1, U2 and U5, that respectively project on muscles DO1, D02 and LL1) and 1 TJ^+/$pMad^+$ MN that projects on muscle DO5.

To investigate the role of TJ^+ MN on locomotion we used *CQ2-lexA* (Heckscher et al., 2015) which allows specific activation of the three TJ^+ U MNs U1, U2 and U5. Detailed monitoring of *CQ2-lexA* expression also revealed that this line additionally drives from st17 to mid-L2 in 1 TJ^+ IN (arrow in Fig.4F) and 1 TJ^+ ISNd MN (arrowhead in Fig.4D), albeit inconsistently from hemisegment to hemisegment. Using *CQ2-lexA*, we therefore activated 3 to 4 of the 6 TJ^+ MNs per hemi-segment, and observed a moderate decrease in the number of peristaltic waves and no striking visible locomotor phenotype in the vast majority of the

larvae (Fig.4G – second black bar). However some larvae (in 27% of the specimen analysed) displayed a slight dorsal contraction that made them tilt on their side and crawl in large circles. Importantly, no spastic paralysis was ever observed upon activation of TJ^+ MNs using the *CQ2-lexA* driver (video 4).

From this experiment we conclude that activation of 50% of TJ^+ MNs does not trigger the spastic paralysis phenotype observed upon activation of the whole TJ^+ population but rather eventually caused a slight dorsal contraction of the larva, a predictable behaviour in regards to the dorsal muscle innervations provided by U1, U2 and U5.

TJ^+-cholinergic and TJ^+-GABAergic interneuron populations are distinctly involved in the locomotor behaviour of the larvae

Next we chose to use drivers allowing the targeting of specific interneuronal populations. We first investigated a possible expression of TJ in peptidergic, dopaminergic, serotonergic, and histaminergic INs and found no expression of TJ in these IN subclasses (Supplementary Fig.3 C1-E2). Further molecular characterization using highly specific lexA drivers (Diao et al., 2015) showed that 10 out of 29 TJ^+ neurons per hemisegment are cholinergic (Fig.5A-E'; Supplementary Fig.4D-F1). Activation of those TJ^+ cholinergic INs by intersectional genetics using *ChAT-lexA* in combination with *TJ-Flp* and the *LexAop-FRT-stop-FRT-dTrpA1* cassette caused disrupted locomotor behaviour. Larvae frequently adopted a characteristic "crescent shape", with head and tail regions brought close together by a tonic contraction of the ventral muscles (movie 5). This ventral contraction phenotype was heterogeneous in terms of severity, with some larvae being continually immobile with ventral contraction (movie 5), while some others displayed bouts of ventral contraction interrupting otherwise seemingly normal crawling. Counting the number of peristaltic waves produced by these larvae reflected the heterogeneity of this phenotype, but also revealed that the number of waves are significantly reduced in these animals compared to control specimen (Fig.5F – second orange bar). Interestingly, such a spectrum of severity has also been recently reported when different subsets of VNC neurons, upon activation with *TrpA1*, lead to a ventral contraction phenotype (Clark et al., 2016).

Among the remaining TJ^+ INs, 8 per hemisegment are GABAergic (Fig.5G-J'; Supplementary Fig.4A-C1). Examining *Gad1-lexA* co-localization with TJ, we noticed that among those 8 neurons, the 3 most ventral ones are located at the midline (neurons n°22,

28, 29 in Fig.5I-J') and do not appear to have counterparts in the adjoining hemisegment, indicating that those cells are unpaired, midline cells (Wheeler et al., 2006). When activated, the TJ^+-GABAergic IN subpopulation led to seemingly normal locomotion (video 6). However, counting the number of peristaltic waves actually revealed that locomotion was slowed, with a reduction of 37% of the number of waves compared to control specimen at 31°C. (Fig.5K - second green bar).

The remaining 5 TJ^+ INs per hemisegment are glutamatergic and differentiating them from TJ^+ MNs (also glutamatergic) is possible by counterstaining with pMad (Fig.5L-Q'; Supplementary Fig.4G-I1). We chose to use *vGlut-lexA* in combination with *TJ-Flp* to activate this IN population, keeping in mind that by using such genetic combination we are also activating TJ^+ MNs. We found upon activation of the whole TJ^+ glutamatergic contingent a complete paralysis of the larvae, with forward propagating waves largely absent (Fig.5R – second red bar). Another feature of this phenotype was the vertical lifting of the most anterior segments of the larvae (thoracic head region) off the substrate (Movie 7). As this phenotype is considerably different from the one observed upon activation of 50% of TJ^+ MNs (see section above), we can assume that TJ^+ glutamatergic INs play an important role in the normal locomotor behaviour of the larva.

Taken together these data show that activation of restricted subpopulations of TJ^+ neurons defined on the basis of their neurotransmitter identity impact the crawling of the larvae with distinct behavioural hallmarks.

A heterogeneous population of 6 TJ^+ glutamatergic and 3 TJ^+ GABAergic INs per segment regulate the speed of locomotion

While searching for more restricted lexA drivers that would allow us to subdivide more finely the TJ^+ population implicated in locomotion, we identified the *Per-lexA* driver (Kohsaka et al., 2014) whose expression co-localizes with 9 of the most ventral TJ^+ neurons per segment (Fig.6A-F; neurons n°22,24,25,26,28 and 29 on Fig.2F and 2G) . Activation of those 9 TJ^+/Per^+ neurons per segment led to a decrease in the number of peristaltic waves (fig.6G – second purple bar). Interestingly these larvae displayed relaxed, slightly atonic abdominal segments (Movie 8). Upon careful characterization of this TJ^+/Per^+ population, we discovered that 6 of them (3 per hemisegment) are glutamatergic (Fig.6D-F; neurons n°24, 25, 26 on Fig.2F and 2G) while the 3 remaining, located medially, are GABAergic (Fig.6A-C).

Indeed, these three TJ$^+$/*Per*$^+$/GABAergic neurons correspond to the three unpaired, midline GABAergic cells that we described above (see Fig.5G-J; neurons n°22, 28, 29) and that do not have counterparts in the adjoining hemisegment.

Together these results show that activation of a heterogeneous population of 6 glutamatergic and 3 GABAergic TJ$^+$/*Per*$^+$ neurons per segment significantly impacts larval locomotion.

3 TJ$^+$ GABAergic midline MNB progeny neurons per segment regulate the speed of locomotion in *Drosophila* larva

Given the median position of the 3 GABAergic TJ$^+$/*Per*$^+$ neurons and the fact they lack counterparts in the adjoining hemisegment, we hypothesized that those neurons are a subset of the midline cells. Midline cells belong to the *sim* domain (Wheeler et al., 2006) and we confirmed by quadruple immunostaining with TJ, Gad1, Prospero and *sim-Gal4* driving a nuclear GFP that TJ$^+$ median GABAergic neurons are *sim*$^+$ in embryonic stage 17 VNC (Fig.7A-B2, single and double empty arrowheads). We noticed weak *sim* expression in these neurons at this stage, an observation consistent with low *sim* expression in late embryonic stages as previously reported (Pearson and Crews, 2014). It is important to note that the TJ$^+$ non GABAergic (glutamatergic-positive) neurons located in the ventral part of the VNC are not *sim-Gal4*$^+$ (depicted by arrows in Fig.7C-C2). We then found that 2 of the 3 TJ$^+$ GABAergic midline cells belong to the Median Neuroblast (MNB) progeny subpopulation identified by nuclear Prospero expression (Prosp-nucl) (Wheeler et al., 2006) (Fig.7A, double empty arrowheads). We also found that all 3 TJ$^+$ GABAergic cells are *fkh*$^+$ and En$^+$ (Fig.7D-E, full arrowheads), two TFs known to be expressed in a subpopulation of MNB progeny but also iVUMs (Wheeler et al., 2006). To further delineate the exact identity of the third TJ$^+$ GABAergic midline neuron (GAD$^+$, *Per*$^+$, *fkh*$^+$, *En*$^+$, Prosp$^-$) we examined stage 16 embryo where midline cell identities can be determined accordingly to the highly stereotyped dorso-ventral and anterior-posterior location of the cells. Using these stereotyped positions along with *Per*, *fkh* and TJ immunostainings, we showed that TJ is not expressed in the iVUMs (Supplementary Fig.5C and 5F - asterisks), easily recognizable by their ventral-most position among midline cells, located close to the posterior boundary of the segment and posterior to H-sib (Supplementary Fig.5B and 5E - empty arrowhead). Instead we visualized TJ expression in cells located above the iVUMs in a position where the MNB progeny neurons

are normally located (Supplementary Fig.5B-C and 5E – circled cells and full arrowhead). We conclude that the 3 ventral TJ+ GABAergic INs are MNB progeny neurons and additionally show that they express the TFs *grain* (Fig.7G-J – full arrowheads) and *hlh3b* (Fig.7K-M – full arrowheads).

Although specification of midline cell identities in the embryo has been extensively documented over the years (Bossing and Brand, 2006; Kearney et al., 2004; Pearson and Crews, 2014; Wheeler et al., 2006; Wheeler et al., 2008) the implication of the different midline neuron subtypes in regard to *Drosophila* locomotor behaviour has so far been only partially addressed (Fox et al., 2006; Koon et al., 2011; Saraswati et al., 2003; Selcho et al., 2012), in part due to the lack of highly specific genetic tools. Using a sophisticated triple intersectional genetic approach based on the combinatorial expression of *TJ*, *Per* and *Gad1*, we specifically activated these 3 neurons. A large proportion of the manipulated larvae (~70%) displayed a marked reduction in their speed of locomotion compared to control larvae at 31°C (Fig.7O), while a minority appeared unaffected (~30%). The incomplete or low dTrpA1 expression in every pool of 3 neurons in all segments for a given larva could explain the heterogeneity within the experimental group. In agreement with such possibility we noticed rather weak *Per-Gal4* expression in these neurons, which would be predicted to reduce the expression levels of the $lexA^{DBD}$ component in this triple intersectional approach.

Altogether these results show that a GABAergic population of 3 MNB progeny neurons singled out by the combinatorial expression of *TJ*, En, *fkh*, *Period*, *hlh3b* and *grain* is involved in the regulation of speed of locomotion in *Drosophila* larva.

Discussion

In this study, we characterized from embryogenesis to larval stage L3 TJ-expressing neurons in the VNC and investigated their role in the crawling behaviour of freely moving *Drosophila* larvae. We generated a *TJ-Flp* line and developed an intersectional genetic approach based on the use of TrpA1 to specifically activate different TJ^+ subpopulations depending on their neurotransmitter properties.

Charting the VNC: TJ a reliable marker for a restricted subset of neurons in the embryo and larva

Our time course analysis revealed that TJ is expressed in the same restricted subset of neurons from the moment they are born in the embryo to the L3 larval stage. Our comprehensive mapping revealed that the number of TJ^+ neurons (29 neurons/hemisegment) remains constant from st 17 to L3 within the abdominal A2-A6 region of the VNC. Within one hemisegment we counted 10 TJ^+ cholinergic INs, 11 TJ^+ glutamatergic neurons and 8 TJ^+ GABAergic INs.

To our knowledge, such a detailed time course analysis of the expression profile of a TF within the VNC has been rarely described. One good example is the highly restricted expression pattern of the B-H1/H2 homeoproteins in the VNC and their continuous expression within a small subpopulation of MNs identifiable from embryogenesis to late larval stages (Garces et al., 2006). In fact it is often a challenging task to precisely apprehend the complete spatial and temporal expression pattern of a gene of interest. This is notably the case when genes under investigation display broad expression patterns because the labelling of many neurons renders difficult the characterization of each single neuron. Within the list of TFs expressed in restricted subpopulation of neurons in the VNC the bHLH gene *Dimmed* has been for example reported to be selectively expressed in central and peripheral neuroendocrine cells (Hewes et al., 2003). Substantial work aiming at identifying and characterizing DIMM-expressing cells have generated a comprehensive map of nearly all 306 DIMM-positive cells in the central nervous system but the exact time course and minor changes of expression within these cells, although noticed, have not been systematically examined (Park et al., 2008).

To date the TF that probably displays the most restricted and constant expression in the same group of VNC neurons is Eve (Even skipped). Eve is expressed from st13 onward in 16 cells per abdominal hemisegment: medially in the aCC, U1 and RP2 MNs and in the pCC IN; mediolaterally, in four U/CQ MNs (U2-U5); and laterally in eight to ten EL INs (Doe et al., 1988; Heckscher et al., 2015; Landgraf et al., 1999). The identification of such cell type-specific TF and the characterisation of genetic tools such as Gal4 or LexA lines capturing the expression patterns of these "markers" have recently proved instrumental for characterizing neuronal circuits in the larval VNC. For example the recently elucidated neuronal circuit that promotes escape behaviour upon noxious stimuli in Drosophila larvae (Yoshino et al., 2017) involves the contribution of SNa MNs that were genetically amenable thanks to the highly specific *BarH1-gal4* line (Garces et al., 2006). Similarly, the very restricted *EL-Gal4* driver active in Eve-expressing lateral (EL) INs (Fujioka et al., 1999) has allowed deciphering the implication of EL INs within a sensorimotor circuit that maintains left-right symmetry of muscle contraction amplitude in the *Drosophila* larva (Heckscher et al., 2015). We thus foresee that our exhaustive mapping of TJ-expressing neurons together with the reliable *TJ-Flp* line we generated will facilitate future studies aiming at identifying and investigating neuronal circuit formation and functioning in embryonic or larval VNC.

TJ$^+$ cholinergic neurons control body posture in *Drosophila* larva

Activation of the TJ$^+$ cholinergic subpopulation gave rise to a ventral contraction phenotype, with larvae frequently adopting a "crescent shape" position. We noticed that the ventral contraction phenotype was heterogeneous between specimens. The larvae with the most dramatic features were persistently immobile and ventrally curved but peristaltic waves could still be observed emerging from the posterior part of the body (movie 5). Another group of larvae displayed bouts of ventral contraction interrupting otherwise seemingly normal crawling phases that were characterized by regular propagation of peristaltic waves along the body. In light of these observations we currently favour the hypothesis that TJ$^+$ cholinergic INs are part of a neuronal circuit controlling the body posture of the larva rather than being intrinsically involved in the control of the speed of locomotion.

Recently, Clark and collaborators (2016), while surveying Janelia Gal4 lines (Jenett et al., 2012) crossed to *UAS-TrpA1*, identified from their screen several lines that gave rise to similar ventral contraction phenotypes. Interestingly, they also reported a spectrum of

severity with some larvae continually blocked with tonically contracted ventral muscles, while others would go through periods of ventral contraction followed by attempts to crawl. From this screen three different lines specifically expressed in subsets of INs were identified and in the future it will be interesting to determine to what extent these INs are indeed TJ^+ cholinergic INs. Alternatively, an appealing possibility would be that these INs subsets and TJ^+ cholinergic INs are different components of the same circuit regulating ventral bending of the larva. In such a scenario we can foresee two major alternatives: 1) either these different IN subsets are linearly and sub sequentially activated converging all toward the contraction of the whole ventral muscle field via the activation of ISNb, ISNd and SNc MNs or 2) each IN subset is selectively and independently used as a premotor excitatory command allowing specific ventral group of muscles to be activated via only one MN subpopulation (ISNb or ISNd or SNc). To date such a precise coordination of muscles contraction within a same muscle field has been exemplified by the activity of an inhibitory IN denoted iIN. iIN specifically innervates "transverse" MNs and not "longitudinal" MNs, thus allowing for the sequential contraction of transverse and longitudinal muscles for an efficient contraction of the larval body segment (Zwart et al., 2016).

TJ^+ glutamatergic neurons are components of a circuit controlling locomotion

The TJ^+ glutamatergic population comprises, within one hemisegment, 6 MNs (U1, U2, U5, DO5 MN and 2 lateral $Islet^+$ ISNd MNs), 3 ventral PMSI INs and 2 dorso-lateral INs. Our study on the functional role of TJ^+ glutamatergic INs is hindered by the fact that when using *vGlut-lexA* both TJ^+ MNs and TJ^+ INs are targeted; to our knowledge no genetic tools exist that would allow us to specifically activate TJ^+ glutamatergic INs. We nevertheless investigated the implication of TJ^+ MNs using two non-optimal drivers (*CQ2-lexA and RapGAP1-lexA* (data not shown)) and found that TJ^+ MNs activation leads to a defect in locomotion, i.e reduction of the number of peristaltic waves. Similarly, when we used *Per-lexA* to activate the whole TJ^+ PMSI population (6 TJ^+ glutamatergic INs and 3 TJ^+ GABAergic INs per segment) we noticed a reduction of the speed of locomotion and a partial relaxed paralysis of the posterior segments of the larvae. Interestingly, in both cases these genetic manipulations did not give rise to the severe spastic paralysis phenotype we observed while activating the whole TJ^+ glutamatergic population. Because it could be argued, when using *Per-lexA,* that activation of TJ^+ PMSI GABAergic INs is in some ways "dominant" over the

activation of TJ^+ PMSI glutamatergic INs, it will be informative to only activate TJ^+ PMSI glutamatergic INs. Unfortunately a *vGlut*^{AD} driver, an equivalent of the *GAD1*^{AD} line, has not been generated, thus precluding at the moment the implementation of this paradigm. Nevertheless, it would be interesting to solely activate all *Per*$^+$ glutamatergic INs (and thus not the *Per*$^+$ TJ^+ GABAergic INs) and this could theoretically be achieved using the following transgenes: *lexAop>>dTrpA1*, *vGlutLexA*, *Per-Gal4* and an *UAS-FLP* (Duffy et al., 1998). Since we reported strong expression of *Per-Gal4* in the vast majority of *Per*$^+$ glutamatergic neurons we expect recombination events in the targeted neurons to be efficient and we thus assume that this experiment will be conclusive.

TJ^+ GABAergic neurons regulate the speed of locomotion

Activation of TJ^+ GABAergic neurons gave rise to an apparently normal, though slowed locomotion, with a number of peristaltic waves accomplished by larvae placed at 31°C similar to the number at 23°C. Since larvae tend to crawl faster when the temperature exceeds their 24°C comfort temperature (in young L3) (Sokabe et al., 2016), we wondered if TJ^+ GABAergic neurons could be modulator component(s) of the temperature sensing system that detects uncomfortable temperatures and induces acceleration as a way to escape. $TrpA1^+$ neurons located in the larval brain have been recently reported to be sensitive to the speed of the temperature increase (Luo et al., 2017) and we have found that these neurons do not express TJ (data not shown). The possibility that TJ^+ GABAergic neurons are nonetheless part of this temperature sensing neuronal circuit awaits future experimental analysis.

Further subdivision within the TJ^+ GABAergic INs pool, using a triple intersectional genetics approach, revealed that 3 *Per*$^+$/TJ^+ GABAergic INs located at the midline and known as MNB progeny neurons substantially impact the crawling speed of the larvae. It thus appears that this *Per*$^+$ GABAergic population was overlooked in the previous characterization of PMSIs and this might be due to the fact that within one segment only 3 *Per*$^+$ (over a contingent of 20 *Per*$^+$ INs) are indeed GABAergic and because of low *period* expression in these INs, especially in third instar larvae, a stage in which the characterization PMSIs was originally carried out (Kohsaka et al., 2014).

Molecular characterization of the *Per*$^+$/TJ$^+$ GABAergic (MNB progeny neurons); searching for equivalents throughout evolution

Cell body position and molecular characterization of the *Per*$^+$ TJ$^+$ GABAergic neurons allowed us to identify them as part of the MNB progeny among the midline cells. Although development of the midline cells has been meticulously described (Fontana and Crews, 2012; Kearney et al., 2004; Manning et al., 2012; Pearson and Crews, 2014; Tio et al., 2011; Watson and Crews, 2012; Wheeler et al., 2006; Wheeler et al., 2008), the functional implication of those cells in locomotion or other behaviours is comparatively poor (Fox et al., 2006; Koon et al., 2011; Saraswati et al., 2003; Selcho et al., 2012). In this respect the present study is pioneering, as it shows that MNB progeny neurons have a relevant function in the locomotor behaviour of the larva. It additionally adds a new marker (TJ) offering the possibility to identify and genetically manipulate these neurons (with *TJ-Gal4* or *TJ-Flp*).

Our molecular characterization of the *Per*$^+$ TJ$^+$ GABAergic MNB progeny INs is thorough and thus allowed us to survey for hypothetical counterparts in other model species. As reported here *Per*$^+$ TJ$^+$ GABAergic INs are characterized by their expression of *hlh3b* and *grain*. In the mouse, the respective ortholog genes are *Tal1/Tal2/Scl* and *Gata2/3*, a transcription code specifically found in V_{2b} GABAergic INs (Lu et al., 2015). Interestingly, the V_{2b} IN subpopulation is known to regulate, in cooperation with V_1 Ia INs, the limb central pattern generator that coordinate in mouse the flexor-extensor motor activity (Zhang et al., 2014). We have also described that *Per*$^+$ TJ$^+$ GABAergic MNB progeny INs expressed *Fkh* and are midline cells derived from *Sim*-expressing precursor cells. Intriguingly a subset of V_{2b} INs in the mouse and known as cerebrospinal fluid-contacting neurons (CSF-cNs, or KA, Kolmer-Agduhr neurons in Zebrafish) express *Foxa2*, the vertebrate orthologue gene of *Fkh* and arise from the *Sim1*$^+$ progenitor domain p3 bordering the floor plate. This subset denoted CSF-cN" is characterized by their very ventral location in the spinal cord abutting the floor plate (Petracca et al., 2016). Since CSF-cN have been reported to modulate slow locomotion and body posture in Zebrafish (Fidelin et al., 2015; Wyart et al., 2009) it is thus tempting to speculate that *sim*-derived *Per*$^+$/TJ$^+$/*Fkh*$^+$ MNB progeny neurons would indeed be the *Drosophila* counterpart of CSF-cN in vertebrates and more particularly of the *Sim1*-derived CSF-cN". In the annelid *Platynereis dumerilii*, a recent study focusing on the molecular characterization of neuron types brought to light a group of neurons specifically co-expressing the TFs *Gata1/2/3* and *Tal* that may be related to CSF-cN (Vergara et al., 2017)

indicating that the molecular nature and physiological function of this neuronal type may have been conserved during evolution. The remarkable similarities of combinatorial expression of TFs within this IN class further exemplifies that the molecular mechanisms used during the wiring of the locomotor system are conserved and evolutionarily ancient.

Materials and methods

Antibody list

Primary Antibodies	**Species**	**Dilution**	**Source**
Anti-TJ	Guinea Pig	1:4000	Gift from D. Godt
Anti-Engrailed 4D9	Mouse	1:50	Development Studies Hybridoma Bank, University of Iowa
Anti-p-Mad	Rabbit	1:500	(Tanimoto et al., 2000)
Anti-GFP	Chicken	1:2000	Abcam Ab13970
Anti-GFP	Rabbit	1:4000	Invitrogen A6455
Anti-RFP	Rabbit	1:8000	Gift from S. Heidmann (Herzog et al., 2013)
Anti-myc 9E10	Mouse	1:40	Development Studies Hybridoma Bank, University of Iowa
Anti-eve 3C10	Mouse	1:40	Development Studies Hybridoma Bank, University of Iowa
Anti-eve	Rabbit	1:200	Gift from M. Frasch (Frasch et al., 1987)
Anti-dv-glut C-ter	Rabbit	1:1000	Gift from H. Aberle (Mahr and Aberle, 2006)
Anti-dGad 818	Rabbit	1:500	Gift from F.R. Jackson (Featherstone et al., 2000)
Anti-repo 8D12	Mouse	1:40	Development Studies Hybridoma Bank, University of Iowa
Anti-prospero	Mouse	1:40	Development Studies Hybridoma Bank, University of Iowa
Anti-FasII 1D4	Mouse	1:80	Development Studies Hybridoma Bank, University of Iowa
Anti-5-HT	Rabbit	1:2000	Immunotech ref. 0601
Secondary antibodies	**Species**	**Dilution**	**Source**
Anti-guinea pig A488	Goat	1:1000	Alexa Fluor™ (Invitrogen)
Anti-guinea pig A555	Goat	1:2000	
Anti-guinea pig A647	Donkey	1:1000	
Anti-chicken A488	Goat	1:1000	
Anti-mouse A488	Donkey	1:1000	
Anti-mouse A405	Goat	1:1000	

Anti-mouse A555	Donkey	1:2000	
Anti-mouse A647	Donkey	1:1000	
Anti-rabbit A488	Donkey	1:1000	
Anti-rabbit A555	Donkey	1:2000	
Anti-rabbit A647	Donkey	1:1000	
Other reagents			
Phalloïdin-FluoProbes 647	NA	1:25	FP-BA0320, Interchim

Drosophila stocks

Drosophila lines	**Source**	**Identifier**
TJ-gal4	Tokyo Stock Center	DGRC # 104055
TJ-Flp	generated by the lab	N/A
Gad1-lexA	Bloomington Stock Center	BL # 60324
Vglut-lexA	Bloomington Stock Center	BL # 60314
ChAT-lexA	Bloomington Stock Center	BL # 60319
UAS-trpA1	Bloomington Stock Center	BL # 4308
UAS-shi^{ts}	(Kitamoto, 2001)	NA
lexAop>stop>dTrpA1 (2 lines on II^{d} and III^{d} chromosomes)	Gift from Aso Y., Janelia Research Campus/HHMI	N/A
per-lexA	Tokyo Stock Center	DGRC # 116999
per-gal4	Bloomington Stock Center	BL # 7127
FkhGFP	Bloomington Stock Center	BL # 43951
Tsh-lexA	Gift from J. Simpson (Ohyama et al., 2015)	NA
Tsh-gal80	Gift from G. Miesenböck (Clyne and Miesenböck, 2008)	NA
lexAop-IVS-tdTomato.nls	Bloomington Stock Center	BL # 66680
UAS-H2AGFP	(Tan et al., 2015)	NA
Act>>gal4	Bloomington Stock Center	BL # 4779
UAS-CD8GFP	Bloomington Stock Center	BL # 5137
CQ2-lexA	Gift from C. Doe (Heckscher et al., 2015)	NA
sim-gal4 (or *sim3.7-gal4*)	Bloomington Stock Center	BL # 9150

Hlh3bGFP	Gift from P. Tomancak (unpublished)	NA
Grain-lacZ	(Spradling et al., 1999)	NA
Gad^{AD}	Bloomington Stock Center	BL # 60322
UAS-lexA^{DBD}	Bloomington Stock Center	BL # 56528
UAS-myrGFP	Bloomington Stock Center	BL # 32198
B-H1-gal4	(Sato et al., 1999)	NA
Tdc2-gal4	Bloomington Stock Center	BL # 9313
Dimm-gal4	Bloomington Stock Center	BL # 25373
TH-gal4 (also called *ple-gal4*)	Bloomington Stock Center	BL # 8848
vmatGFP	Bloomington Stock Center	BL # 60263
UAS>>TrpA1^{myc}	Bloomington Stock Center	BL # 66871
lexAop-Flp	Bloomington Stock Center	BL # 55820

Generation of the TJ flippase

Reagents

Components	**Plasmid of origin**	**Source**
kanR	2xTY1-kanR	Gift from P. Tomancak
Late SV40 pA	pCAGGS-Ires2-eGFP-linkerPacI-sv40pA	Gift from J.F. Brunet Adapted from(Koshiba-Takeuchi et al., 2000)
nlsFlpO	pPGK FlpO bpA	Gift from S. BOurane, Goulding's lab
pBluescript-II-KS(+)	NA	Addgene
pFly-fosmid-TJ	NA	Gift from P. Tomancak
pRed-Flp4	NA	Gift from P. Tomancak

Oligonucleotide name	**Sequence**	**Use**
recTJsens	5'ATGTGAGACCCGTAATCGACCCTC TCCGGTCCCTGGTCGATCCAATGAA	Amplification of FlpO-lateSV40pA-kanR cassette

	A**ATGGCTCCTAAGAAGAAGAGG** (TJ 5' homologous sequence) **(FlpO 5' sequence)** ATG: start codons in *tj*	to add homologous recombination arms to it
recTJantisens	5'ATTCATTAATTTAGATTTATTTAT TACTAAATTGTTTTATGCACACTTA T**AACTCAGAAGAACTCGTCAAG** (TJ 3' homologous sequence) **(KanR 3' sequence)**	Amplification of FlpO-lateSV40pA-kanR sequence to add homologous recombination arms to it

Oligonucleotides were ordered from Eurofins Genomics.

Protocol

We chose to use pFly-Fos technology (Ejsmont et al., 2009) to generate *TJ-Flp* line after several trials at "transposon swap" strategies to replace gal4 transposon in *TJ-gal4* line by a flippase failed.

Ejsmont *et al* (2009) generated among their fosmid library a pFly-TJ-fosmid that contains the full *tj* sequence and probably all of *tj* regulatory elements; indeed expression of pFly-tj-Fos tagged with GFP perfectly recapitulates *tj* endogenous expression (data not shown). Briefly, in this fosmid and following Ejsmont and collaborators (2009) protocol, we replaced *tj* open reading frame and 3' UTR by an optimized flippase sequence followed by a late SV40 polyadenylation sequence and a kanamycine resistance gene using the recombination oligonucleotides recTJsens and recTJantisens listed in the above table. Recombination oligonucleotides were chosen in order to: i) conserve the two endogenous *tj* transcription start signals (ATG) upstream of the flippase sequence in the *TJ-Flp* line and ii) conserve *tj* polyA signal sequence. Following recombination and contrary to Ejsmont protocol, we did not remove the kanamycine resistance sequence from the final fosmid used for transgenesis. Final fosmid was sent for targeted transgenesis in attp2 landing site (III^{rd} chromosome) (Bestgene Inc.).

Immunohistochemistry

On larvae

Briefly, larvae of the right genotype were sorted out in Phosphate Buffered Saline-0,1% triton (DPBS 1X $CaCl2^{+}$ $MagCl2^{+}$ Gibco Invitrogen, Sigma-Aldrich; Triton X-100, Sigma Life

Science) (PBS-T), rinsed in DPBS and transferred with tweezers to the DPBS-filled dissection chamber. Dissection chamber consists of a silicone-delineated well on poly-lysine coated glass slides; a double-sided piece of adhesive tape covers part of the dissection chamber floor. Dissection takes place on the adhesive tape. Head of the larvae were cut with scissors and posterior part of the body removed. Central Nervous Systems (CNS) were delicately dissected with tweezers (second and third instar larvae) or tungsten wires (first instar larvae) and all other tissues removed. CNS were then transferred to the non-adhesive covered part of the chamber and left to adhere to the slide, ventral part of the VNC against the slide (apart for period-observing dissections: CNS were placed dorsal part of the VNC against the slide). Further incubation steps were completed in the silicone chamber. CNS were fixed for 12 minutes with 3,7% formaldehyde diluted in DPBS (37% Formaldehyde solution, ref 252549, Sigma-Aldrich), then washed 3x5 minutes with PBS-T. At this point the double-sided piece of tape was removed. Blocking step was performed with PBS-T supplemented with 4% donkey serum (normal donkey serum S30-100 ml, Millipore) and 0.02% azide (Sodium azine NaN_3, ref S2002, Sigma-Aldrich) for 30 minutes. CNS were then incubated with primary antibodies for 1h at room temperature (RT) in a humid chamber, washed 3x5 minutes with PBS-T and then incubated with secondary antibodies 1h at RT in humid chamber in darkness. After 4x5 minutes of washing with PBS-T, silicone walls of the chamber were scraped off and Mowiol and a coverslip placed over stained CNS for imaging.

On embryos

Immunolabeling of embryos was carried out as previously described (Thor et al., 1999).

Image acquisition and processing

Images were acquired on a Zeiss LSM700 confocal with 40x or 63x objectives, treated and cropped in Photoshop (Adobe) and assembled in Illustrator (Adobe). For the benefit of colour-blind readers, double-labelled images were falsely coloured in Photoshop. 3D projection of whole VNC was implemented using Zen software (Zeiss).

Locomotion assay

Larvae sorting

For first instar larvae testing, decorionated late stage 17 embryos of the right genotype were sorted out and placed on an agar/grape juice plate supplemented with some feeding

medium (maize, sucrose and yeast). Hatching time was monitored and larvae locomotion assessed 6 hours after hatching.

For third instar larvae testing, eggs were laid for 5 hours on basic maize feeding medium. Approximately 72 hours later burrowing third instar larvae were picked up and assessed for locomotion.

Assay

Larvae clean of food were gently picked up with tweezers (in the case of the third instar larvae) or the back of tweezers (for first instar larvae) and placed on a 56 mm-agar plate supplemented with grape juice. After a 30-seconds acclimation period, the number of peristaltic waves done by the larvae was manually counted (by that time plate surface temperature was 23°C). The plate was transferred on a hot plate to heat for 2 minutes and 30 seconds or until it reached 31°C. The plate was quickly removed from the heat and the number of peristaltic waves done by the larvae manually assessed for 30 seconds more. Plate was left to rest for 4 minutes until temperature reached 23°C. Number of peristaltic waves in 30 sec was assessed once more.

Statistical analysis

Statistical tests were carried out using Graphpad Prism (Graphpad software, Inc). We used one-way ANOVA with a Tukey post-hoc test to analyse more than two groups of data. When comparing only two groups we used unpaired Student t-test.

Acknowledgments

We thank the Developmental Studies Hybridoma Bank at the University of Iowa, the Bloomington Stock Center and the Drosophila Genetic Resource Center in Kyoto Institute of Technology for monoclonal antibodies and fly stocks. We would also like to thank D. Godt, S. Heidmann, M. Frasch, H. Aberle, F.R. Jackson, M. Landgraf, Y. Aso, J. Simpson, G. Miesenböck, C. Doe, P. Tomancak, S. Bourane for generously sharing fly lines, antibodies and vectors. This work was funded by grants from INSERM and a 3-year PhD funding from Association Française contre les Myopathies (AFM) for H.B. Imaging analysis was carried out on the regional reference core facility (RIO) supported by the French Ministry of Scientific Research. The authors have declared that no competing interests exist.

References

Andrzejczuk LA, Banerjee S, England SJ, et al. (2018) Tal1, Gata2a, and Gata3 Have Distinct Functions in the Development of V2b and Cerebrospinal Fluid-Contacting KA Spinal Neurons. *Frontiers in Neuroscience* 12.

Bikoff JB, Gabitto MI, Rivard AF, et al. (2016) Spinal Inhibitory Interneuron Diversity Delineates Variant Motor Microcircuits. *Cell* 165: 207-219.

Borgius L, Nishimaru H, Caldeira V, et al. (2014) Spinal Glutamatergic Neurons Defined by EphA4 Signaling Are Essential Components of Normal Locomotor Circuits. *The Journal of Neuroscience* 34: 3841-3853.

Bossing T and Brand AH. (2006) Determination of cell fate along the anteroposterior axis of the Drosophila ventral midline. *Development* 133: 1001-1012.

Caldeira V, Dougherty KJ, Borgius L, et al. (2017) Spinal Hb9::Cre-derived excitatory interneurons contribute to rhythm generation in the mouse. *Scientific Reports* 7: 41369.

Clark MQ, McCumsey SJ, Lopez-Darwin S, et al. (2016) Functional Genetic Screen to Identify Interneurons Governing Behaviorally Distinct Aspects of Drosophila Larval Motor Programs. *G3 (Bethesda)* 6: 2023-2031.

Clark MQ, Zarin AA, Carreira-Rosario A, et al. (2018) Neural circuits driving larval locomotion in Drosophila. *Neural Dev* 13: 6.

Clyne JD and Miesenböck G. (2008) Sex-Specific Control and Tuning of the Pattern Generator for Courtship Song in Drosophila. *Cell* 133: 354-363.

Diao F, Ironfield H, Luan H, et al. (2015) Plug-and-Play Genetic Access to Drosophila Cell Types Using Exchangeable Exon Cassettes. *Cell Rep* 10: 1410-1421.

Doe CQ, Smouse D and Goodman CS. (1988) Control of neuronal fate by the Drosophila segmentation gene even-skipped. *Nature* 333: 376.

Dougherty Kimberly J, Zagoraiou L, Satoh D, et al. (2013) Locomotor Rhythm Generation Linked to the Output of Spinal Shox2 Excitatory Interneurons. *Neuron* 80: 920-933.

Duffy JB, Harrison DA and Perrimon N. (1998) Identifying loci required for follicular patterning using directed mosaics. *Development* 125: 2263-2271.

Ejsmont RK, Sarov M, Winkler S, et al. (2009) A toolkit for high-throughput, cross-species gene engineering in Drosophila. *Nature Methods* 6: 435.

Featherstone DE, Rushton EM, Hilderbrand-Chae M, et al. (2000) Presynaptic Glutamic Acid Decarboxylase Is Required for Induction of the Postsynaptic Receptor Field at a Glutamatergic Synapse. *Neuron* 27: 71-84.

Fidelin K, Djenoune L, Stokes C, et al. (2015) State-Dependent Modulation of Locomotion by GABAergic Spinal Sensory Neurons. *Current Biology* 25: 3035-3047.

Fontana JR and Crews ST. (2012) Transcriptome analysis of Drosophila CNS midline cells reveals diverse peptidergic properties and a role for castor in neuronal differentiation. *Dev Biol* 372: 131-142.

Fox LE, Soll DR and Wu C-F. (2006) Coordination and Modulation of Locomotion Pattern Generators in Drosophila Larvae: Effects of Altered Biogenic Amine Levels by the Tyramine β Hydroxlyase Mutation. *J Neurosci* 26: 1486-1498.

Francius C, Harris A, Rucchin V, et al. (2013) Identification of Multiple Subsets of Ventral Interneurons and Differential Distribution along the Rostrocaudal Axis of the Developing Spinal Cord. *Plos One* 8: e70325.

Frasch M, Hoey T, Rushlow C, et al. (1987) Characterization and localization of the even-skipped protein of Drosophila. *The EMBO Journal* 6: 749-759.

Fujioka M, Emi-Sarker Y, Yusibova GL, et al. (1999) Analysis of an even-skipped rescue transgene reveals both composite and discrete neuronal and early blastoderm enhancers, and multi-stripe positioning by gap gene repressor gradients. *Development (Cambridge, England)* 126: 2527-2538.

Gabitto MI, Pakman A, Bikoff JB, et al. (2016) Bayesian Sparse Regression Analysis Documents the Diversity of Spinal Inhibitory Interneurons. *Cell* 165: 220-233.

Garces A, Bogdanik L, Thor S, et al. (2006) Expression of Drosophila BarH1-H2 homeoproteins in developing dopaminergic cells and segmental nerve a (SNa) motoneurons. *European Journal of Neuroscience* 24: 37-44.

Gosgnach S, Lanuza GM, Butt SJB, et al. (2006) V1 spinal neurons regulate the speed of vertebrate locomotor outputs. *Nature* 440: 215.

Hasegawa E, Truman JW and Nose A. (2016) Identification of excitatory premotor interneurons which regulate local muscle contraction during Drosophila larval locomotion. *Scientific Reports* 6.

Hayashi S, Ito K, Sado Y, et al. (2002) GETDB, a database compiling expression patterns and molecular locations of a collection of gal4 enhancer traps. *genesis* 34: 58-61.

Heckscher ES, Long F, Layden MJ, et al. (2014) Atlas-builder software and the eNeuro atlas: resources for developmental biology and neuroscience. *Development (Cambridge, England)* 141: 2524-2532.

Heckscher ES, Zarin AA, Faumont S, et al. (2015) Even-Skipped(+) Interneurons Are Core Components of a Sensorimotor Circuit that Maintains Left-Right Symmetric Muscle Contraction Amplitude. *Neuron* 88: 314-329.

Herzog S, Nagarkar Jaiswal S, Urban E, et al. (2013) Functional Dissection of the Drosophila melanogaster Condensin Subunit Cap-G Reveals Its Exclusive Association with Condensin I. *PLoS Genet* 9: e1003463.

Hewes RS, Park D, Gauthier SA, et al. (2003) The bHLH protein Dimmed controls neuroendocrine cell differentiation in Drosophila. *Development* 130: 1771-1781.

Itakura Y, Kohsaka H, Ohyama T, et al. (2015) Identification of Inhibitory Premotor Interneurons Activated at a Late Phase in a Motor Cycle during Drosophila Larval Locomotion. *Plos One* 10: e0136660.

Jenett A, Rubin GM, Ngo T-TB, et al. (2012) A GAL4-Driver Line Resource for Drosophila Neurobiology. *Cell Rep* 2: 991-1001.

Jessell TM. (2000) Neuronal specification in the spinal cord: inductive signals and transcriptional codes. *Nature Reviews Genetics* 1: 20.

Kearney JB, Wheeler SR, Estes P, et al. (2004) Gene expression profiling of the developing Drosophila CNS midline cells. *Dev Biol* 275: 473-492.

Kiehn O. (2016) Decoding the organization of spinal circuits that control locomotion. *Nature reviews. Neuroscience* 17: 224-238.

Kitamoto T. (2001) Conditional modification of behavior in Drosophila by targeted expression of a temperature-sensitive shibire allele in defined neurons. *J Neurobiol* 47: 81-92.

Kohsaka H, Takasu E, Morimoto T, et al. (2014) A Group of Segmental Premotor Interneurons Regulates the Speed of Axial Locomotion in Drosophila Larvae. *Current Biology* 24: 2632-2642.

Koon AC, Ashley J, Barria R, et al. (2011) Autoregulatory and paracrine control of synaptic and behavioral plasticity by octopaminergic signaling. *Nat Neurosci* 14: 190-199.

Koshiba-Takeuchi K, Takeuchi JK, Matsumoto K, et al. (2000) Tbx5 and the Retinotectum Projection. *Science* 287: 134-137.

Landgraf M, Roy S, Prokop A, et al. (1999) even-skipped Determines the Dorsal Growth of Motor Axons in Drosophila. *Neuron* 22: 43-52.

Li MA, Alls JD, Avancini RM, et al. (2003) The large Maf factor Traffic Jam controls gonad morphogenesis in Drosophila. *Nat Cell Biol* 5: 994.

Lu DC, Niu T and Alaynick WA. (2015) Molecular and cellular development of spinal cord locomotor circuitry. *Frontiers in Molecular Neuroscience* 8.

Luo J, Shen WL and Montell C. (2017) TRPA1 mediates sensation of the rate of temperature change in Drosophila larvae. *Nat Neurosci* 20: 34-41.

Mahr A and Aberle H. (2006) The expression pattern of the Drosophila vesicular glutamate transporter: A marker protein for motoneurons and glutamatergic centers in the brain. *Gene Expression Patterns* 6: 299-309.

Manning L, Heckscher ES, Purice MD, et al. (2012) A resource for manipulating gene expression and analyzing cis-regulatory modules in the Drosophila CNS. *Cell Rep* 2: 1002-1013.

Ohyama T, Schneider-Mizell CM, Fetter RD, et al. (2015) A multilevel multimodal circuit enhances action selection in Drosophila. *Nature Reviews Cancer* 520: 633-639.

Park D, Shafer OT, Shepherd SP, et al. (2008) The Drosophila Basic Helix-Loop-Helix Protein DIMMED Directly Activates PHM, a Gene Encoding a Neuropeptide-Amidating Enzyme. *Molecular and Cellular Biology* 28: 410-421.

Pearson JC and Crews ST. (2014) Enhancer diversity and the control of a simple pattern of Drosophila CNS midline cell expression. *Dev Biol* 392: 466-482.

Petracca YL, Sartoretti MM, Di Bella DJ, et al. (2016) The late and dual origin of cerebrospinal fluid-contacting neurons in the mouse spinal cord. *Development* 143: 880-891.

Pulver SR, Pashkovski SL, Hornstein NJ, et al. (2009) Temporal Dynamics of Neuronal Activation by Channelrhodopsin-2 and TRPA1 Determine Behavioral Output in Drosophila Larvae. *Journal of Neurophysiology* 101: 3075-3088.

Rickert C, Kunz T, Harris K-L, et al. (2011) Morphological Characterization of the Entire Interneuron Population Reveals Principles of Neuromere Organization in the Ventral Nerve Cord of Drosophila. *The Journal of Neuroscience* 31: 15870-15883.

Saraswati S, Fox Lyle E, Soll David R, et al. (2003) Tyramine and octopamine have opposite effects on the locomotion of Drosophila larvae. *J Neurobiol* 58: 425-441.

Sato M, Kojima T, Michiue T, et al. (1999) Bar homeobox genes are latitudinal prepattern genes in the developing Drosophila notum whose expression is regulated by the concerted functions of decapentaplegic and wingless. *Development* 126: 1457-1466.

Selcho M, Pauls D, el Jundi B, et al. (2012) The Role of octopamine and tyramine in Drosophila larval locomotion. *Journal of Comparative Neurology* 520: 3764-3785.

Sokabe T, Chen H-C, Luo J, et al. (2016) A Switch in Thermal Preference in Drosophila Larvae Depends on Multiple Rhodopsins. *Cell Rep* 17: 336-344.

Spradling AC, Stern D, Beaton A, et al. (1999) The Berkeley Drosophila Genome Project Gene Disruption Project: Single P-Element Insertions Mutating 25% of Vital Drosophila Genes. *Genetics* 153: 135-177.

Sweeney LB, Bikoff JB, Gabitto MI, et al. (2018) Origin and Segmental Diversity of Spinal Inhibitory Interneurons. *Neuron* 97: 341-355.e343.

Talpalar AE, Bouvier J, Borgius L, et al. (2013) Dual-mode operation of neuronal networks involved in left–right alternation. *Nature* 500: 85.

Tan L, Zhang KX, Pecot MY, et al. (2015) Ig Superfamily Ligand and Receptor Pairs Expressed in Synaptic Partners in Drosophila. *Cell* 163: 1756-1769.

Tanimoto H, Itoh S, ten Dijke P, et al. (2000) Hedgehog Creates a Gradient of DPP Activity in Drosophila Wing Imaginal Discs. *Molecular Cell* 5: 59-71.

Thor S, Andersson SGE, Tomlinson A, et al. (1999) A LIM-homeodomain combinatorial code for motor-neuron pathway selection. *Nature* 397: 76.

Tio M, Toh J, Fang W, et al. (2011) Asymmetric cell division and Notch signaling specify dopaminergic neurons in Drosophila. *Plos One* 6: e26879.

Vergara HM, Bertucci PY, Hantz P, et al. (2017) Whole-organism cellular gene-expression atlas reveals conserved cell types in the ventral nerve cord of Platynereis dumerilii. *Proc Natl Acad Sci U S A* 114: 5878-5885.

Watson JD and Crews ST. (2012) Formation and specification of a Drosophila dopaminergic precursor cell. *Development* 139: 3316-3325.

Wheeler SR, Kearney JB, Guardiola AR, et al. (2006) Single-cell mapping of neural and glial gene expression in the developing Drosophila CNS midline cells. *Dev Biol* 294: 509-524.

Wheeler SR, Stagg SB and Crews ST. (2008) Multiple Notch signaling events control Drosophila CNS midline neurogenesis, gliogenesis and neuronal identity. *Development* 135: 3071-3079.

Wyart C, Bene FD, Warp E, et al. (2009) Optogenetic dissection of a behavioural module in the vertebrate spinal cord. *Nature* 461: 407.

Yoshikawa S, Long H and Thomas JB. (2016) A subset of interneurons required for Drosophila larval locomotion. *Mol Cell Neurosci* 70: 22-29.

Yoshino J, Morikawa RK, Hasegawa E, et al. (2017) Neural Circuitry that Evokes Escape Behavior upon Activation of Nociceptive Sensory Neurons in Drosophila Larvae. *Current Biology* 27: 2499-2504.e2493.

Zhang J, Lanuza Guillermo M, Britz O, et al. (2014) V1 and V2b Interneurons Secure the Alternating Flexor-Extensor Motor Activity Mice Require for Limbed Locomotion. *Neuron* 82: 138-150.

Zhong G, Droho S, Crone S, et al. (2010) Electrophysiological characterization of the V2a interneurons and their locomotor-related activity in the neonatal mouse spinal cord. *J Neurosci* 30: 170-182.

Ziskind-Conhaim L and Hochman S. (2017) Diversity of molecularly defined spinal interneurons engaged in mammalian locomotor pattern generation. *Journal of Neurophysiology* 118: 2956-2974.

Zwart MF, Pulver SR, Truman JW, et al. (2016) Selective Inhibition Mediates the Sequential Recruitment of Motor Pools. *Neuron* 91: 615-628.

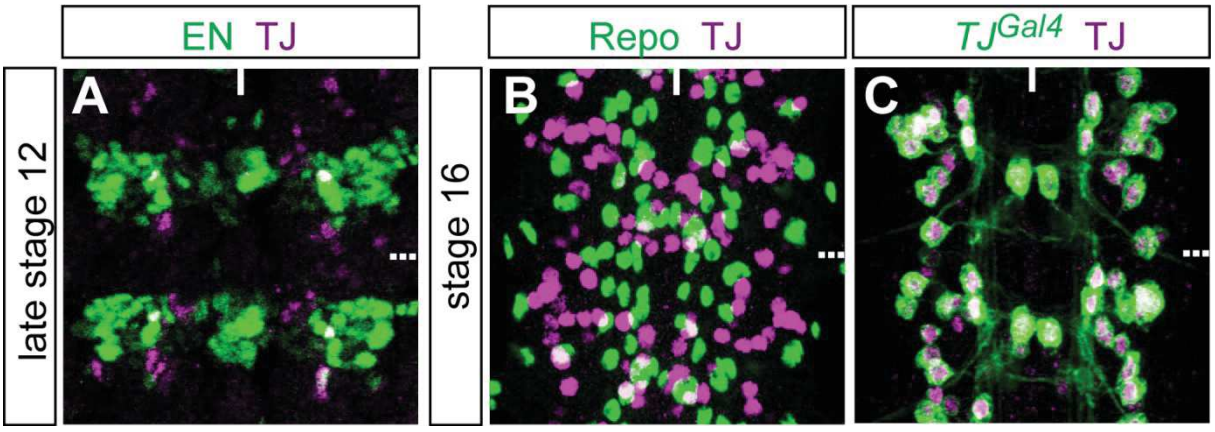

Figure 1

Fig. 1: TJ is specifically expressed in post-mitotic neurons in *Drosophila* embryo CNS

A Staining of stage 12 embryo VNC for TJ (magenta) and Engrailed (EN) (green). TJ starts to be expressed at stage 12 in *Drosophila* larva VNC.

B Staining of stage 16 embryo VNC for TJ (magenta) and glial marker Repo (green). TJ is only expressed in neurons and excluded from glial cells.

C Staining of stage 16 embryo VNC for TJ (magenta) and GFP driven by *TJ-gal4* (green). In embryonic stages *TJ-gal4* faithfully reports the expression of TJ (as seen with the antibody).

For all A, B and C panels: Dashed lines on the right-hand side of the panels indicate segment boundaries and the full line the midline. Two segments are shown in each panel. Anterior of the VNC is up.

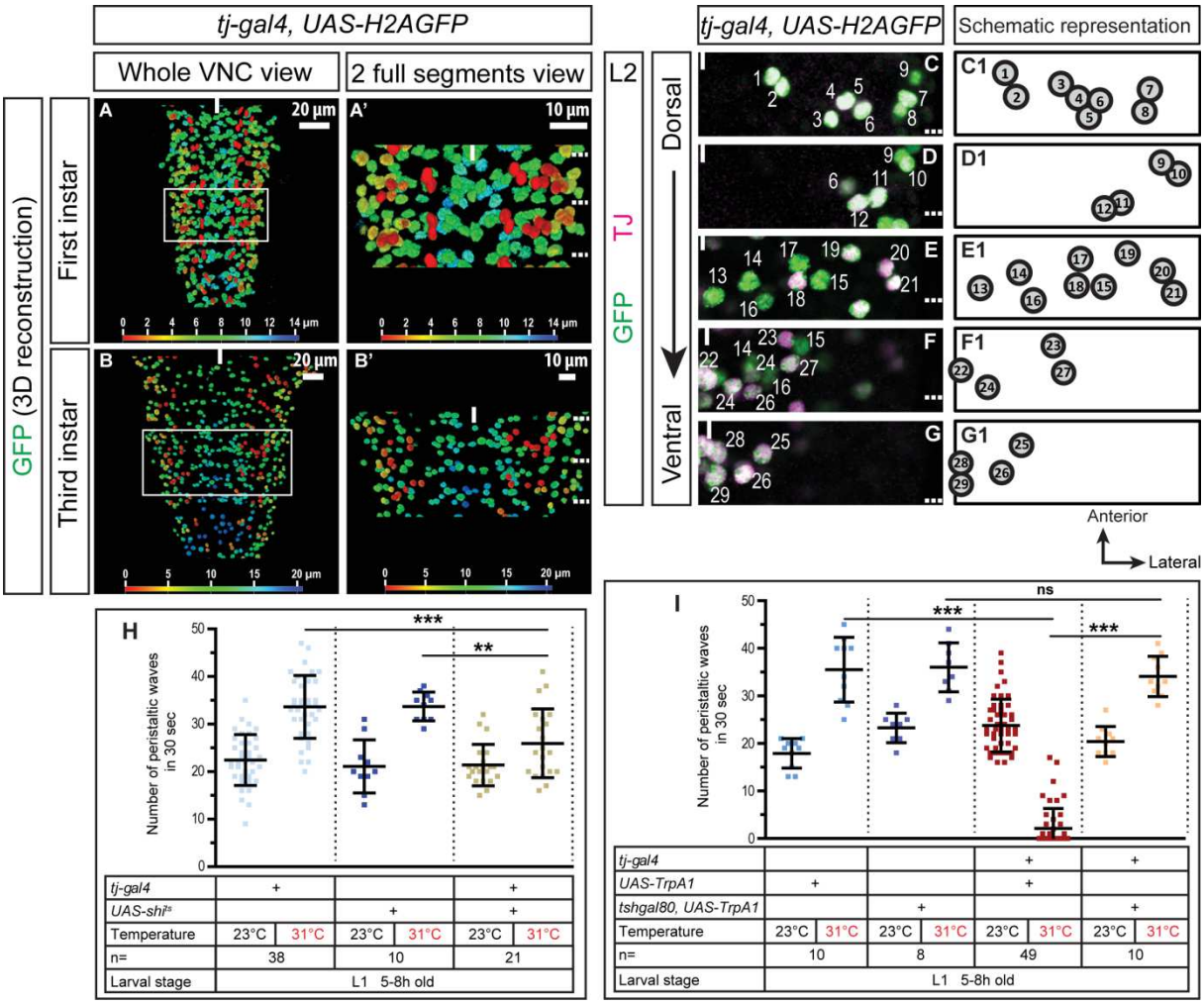
tj-gal4, UAS-H2AGFP
Whole VNC view
2 full segments view
GFP (3D reconstruction)
First instar
Third instar
A
A'
B
B'
20 µm
10 µm
0 2 4 6 8 10 12 14 µm
0 5 10 15 20 µm
tj-gal4, UAS-H2AGFP
Schematic representation
L2
GFP TJ
Dorsal
Ventral
C
D
E
F
G
C1
D1
E1
F1
G1
Anterior
Lateral
H
Number of peristaltic waves in 30 sec
***
**
tj-gal4 + + +
UAS-shits + + +
Temperature 23°C 31°C 23°C 31°C 23°C 31°C
n= 38 10 21
Larval stage L1 5-8h old
I
ns
***
***
tj-gal4 + + +
UAS-TrpA1 + + +
tshgal80, UAS-TrpA1 + + +
Temperature 23°C 31°C 23°C 31°C 23°C 31°C 23°C 31°C
n= 10 8 49 10
Larval stage L1 5-8h old

Figure 2

Fig. 2: TJ is expressed in a restricted population of 29 neurons per hemi-segment in the larva VNC

A, A', B, B' 3D reconstruction of whole VNC (**A, B**) and 2 full segments (**A', B'**) of first (**A, A'**) and third (**B, B'**) instar larvae expressing nuclear GFP under the control *TJ-gal4*. Colour scale is the z-axis scale; most dorsal cells are red, most ventral are blue. White scale is the x/y-axis scale.

C-G Staining of second instar larva VNC for TJ (magenta) and *TJ-gal4* expression reported by nuclear H2AGFP (green). Totality of TJ^+ cells are shown in dorsal (**C**) to ventral (**G**) panels. Dashed lines on the right-hand side of the panels indicate segment boundaries and the full line the midline. A unique hemi-segment is shown in each panel. Anterior of the VNC is up.

C1-G1 Schematic representation of one hemisegment showing stereotyped ventral-dorsal and medial-lateral cell position in first and second instar larvae (cell positions may slightly change in third instar).

H Number of peristaltic waves per 30 seconds at permissive (23°C) and restrictive temperature (31°C). Upon electrical inhibition of the whole TJ^+ population (second beige bar), we observe a slight decrease in the number of peristaltic waves. Each single point represents recording of a single first instar larva.

I Number of peristaltic waves per 30 seconds at permissive (23°C) and restrictive temperature (31°C). Upon electrical activation of the whole TJ^+ population (second red bar), we observe a drastic decrease in the number of peristaltic waves. This drastic decrease is no longer visible upon electrical activation of the TJ^+ neurons in the brain (second salmon pink bar). Each single point represents recording of a single first instar larva. Error bars indicate the SD and n denotes the number of larvae tested. Statistical analysis: One way ANOVA. ***$p<0.001$, ns=not significantly different

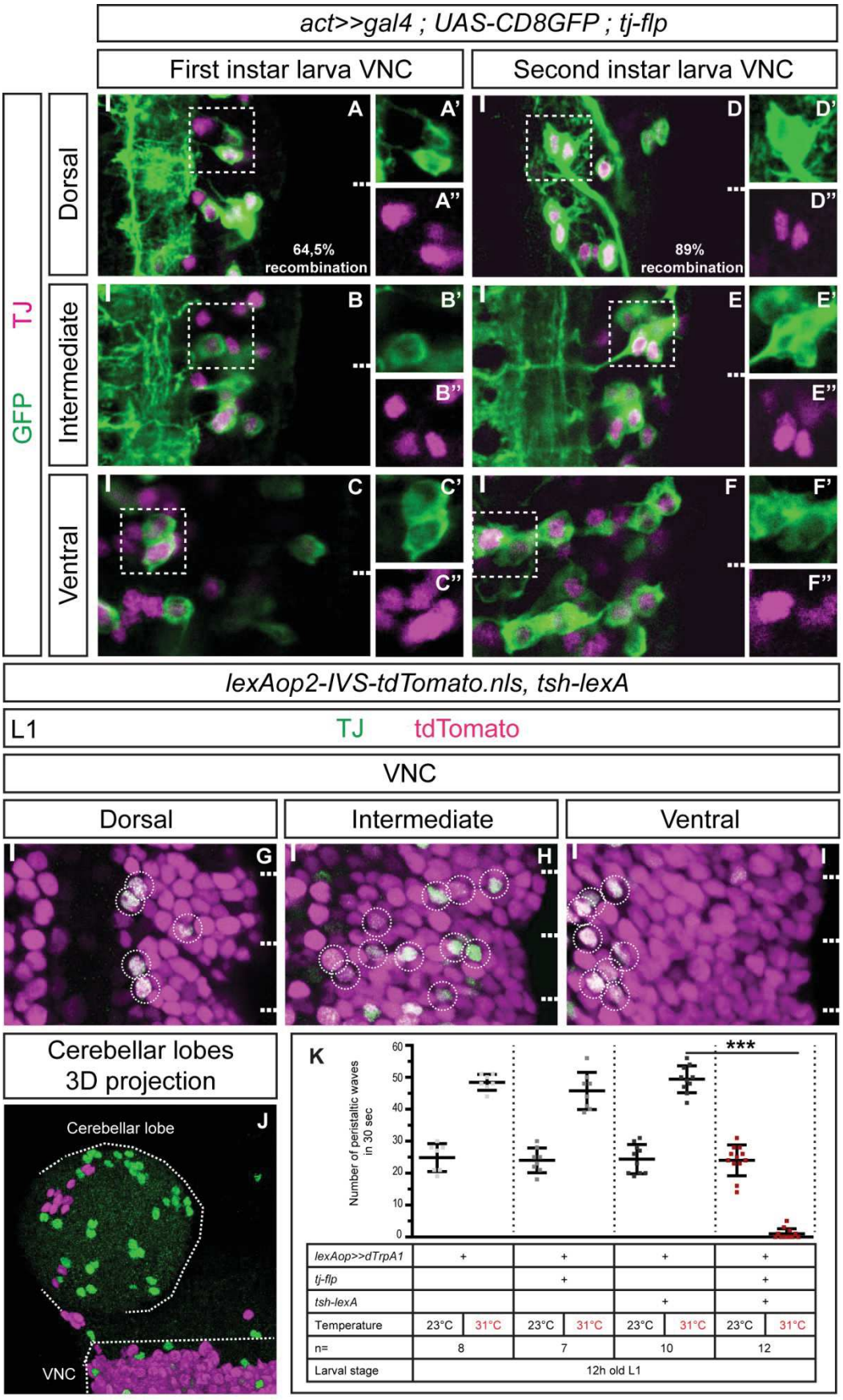
act>>gal4 ; UAS-CD8GFP ; tj-flp
First instar larva VNC
Second instar larva VNC
GFP TJ
Dorsal
Intermediate
Ventral
A
A'
A''
64,5% recombination
D
D'
D''
89% recombination
B
B'
B''
E
E'
E''
C
C'
C''
F
F'
F''
lexAop2-IVS-tdTomato.nls, tsh-lexA
L1
TJ tdTomato
VNC
Dorsal
Intermediate
Ventral
G
H
I
Cerebellar lobes 3D projection
Cerebellar lobe
VNC
J
K
Number of peristaltic waves in 30 sec
***
lexAop>>dTrpA1
tj-flp
tsh-lexA
Temperature
n=
Larval stage
12h old L1

Figure 3

Fig. 3: TrpA1 activation of the TJ^+ cells in the VNC using novel *TJ-Flp* tool leads to rigid paralysis of the larvae

A-F Staining for TJ (magenta) and recombined cells (expressing *TJ-Flp* –green) in first (**A to C**) and second (**D to F**) instar larva VNC. Percentages of recombination (calculated as follow: $TJ\text{-}Flp^+$ cells/total TJ^+ cells*100) are indicated in respective first panels.

G-J Staining for TJ (green) and *Tsh-lexA* driving an *nls-tdTomato* (magenta) in first instar larva VNC (**G-I**) and in first instar larva cerebellar lobe (**J**). All TJ^+ cells in the VNC are $Tsh\text{-}lexA^+$ while no co-localisation is found in the brain.

K Number of peristaltic waves per 30 seconds at permissive (23°C) and restrictive (31°C) temperatures. Upon activation of the TJ^+ of the VNC only (second red bar), we recapitulate the whole TJ^+ population activation behaviour presented in Fig.2I. Each single point represents a single 12h-old first instar larva. Error bars indicate the SD and n denotes the number of larvae tested. Statistical analysis: One way ANOVA. ***$p<0.001$.

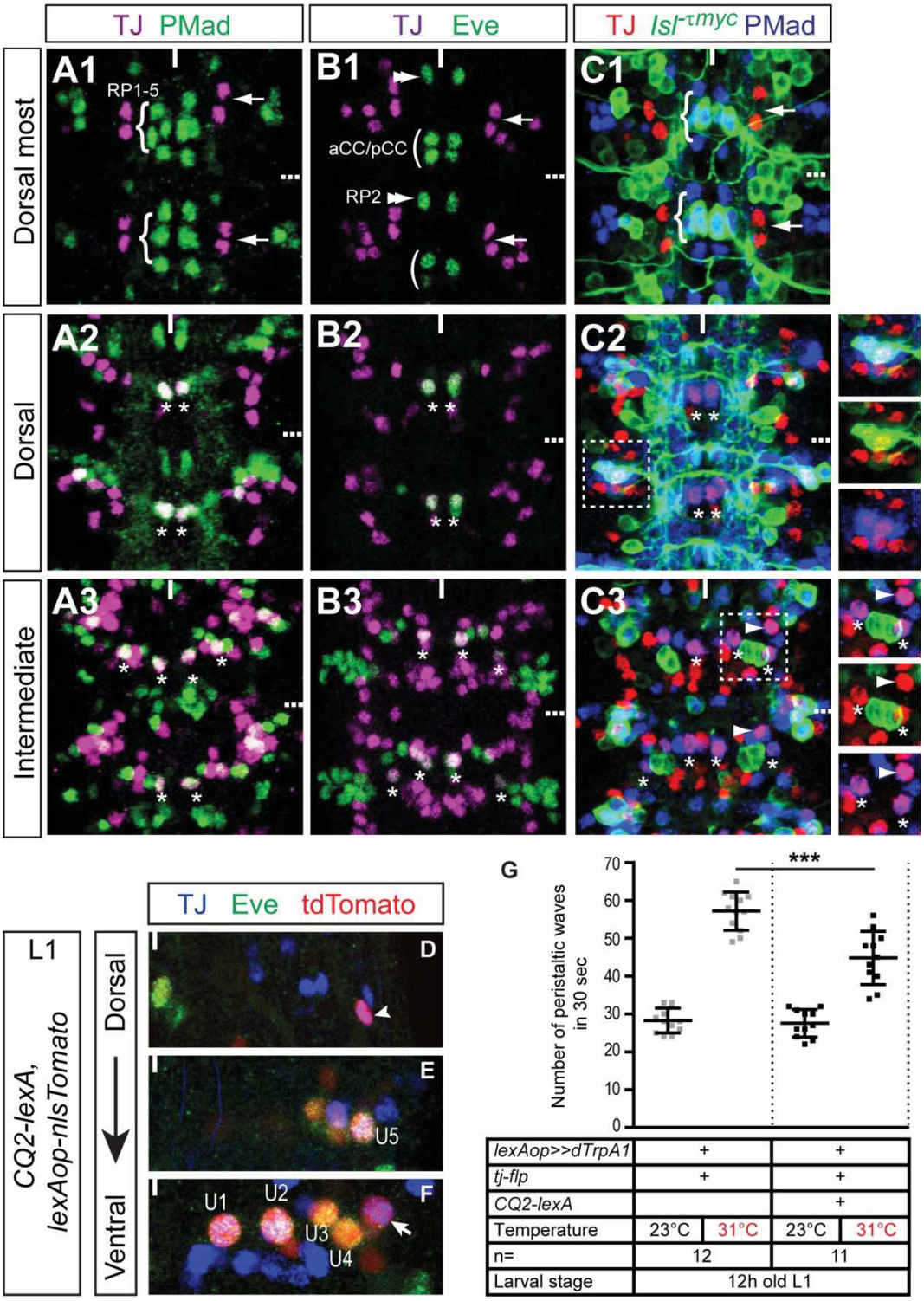
TJ PMad
TJ Eve
TJ Isl-τmyc PMad
Dorsal most
Dorsal
Intermediate
A1
B1
C1
A2
B2
C2
A3
B3
C3
RP1-5
aCC/pCC
RP2
TJ Eve tdTomato
L1
CQ2-lexA,
lexAop-nlsTomato
Dorsal
Ventral
D
E
F
U1
U2
U3
U4
U5
G
Number of peristaltic waves in 30 sec
***
lexAop>>dTrpA1
tj-flp
CQ2-lexA
Temperature
23°C
31°C
n=
12
11
Larval stage
12h old L1

Figure 4

Fig. 4: Activation of TJ^+ MN belonging to ISNd and ISNdm only slightly impairs locomotion.

A1-A3 Representative views of two segments of stage 16 embryo VNC stained for TJ (magenta) and motoneuron marker pMad (green). Cells are shown from dorsal-most (**A1**) to intermediate (**A3**) positions. TJ is excluded from RP1-5 (**A1**, curly brackets) and expressed in U MN (**A2** and **A3**, asterisks). Arrows in **A1** highlight the dorsal-most pair of TJ^+ neurons.

B1-B3 Representative views of two segments of stage 16 embryo VNC stained for TJ (magenta) and Eve (green). Cells are shown from dorsal-most (**B1**) to intermediate (**B3**) positions. TJ is excluded from aCC/pCC (**B1**, curly brackets) and RP2 (**B1**, double arrowhead) and expressed in U MNs (**B2** and **B3**, asterisks). Arrows in **B1** highlight the dorsal-most pair of TJ^+ neurons.

C1-C3 Representative views of two segments of stage 16 embryo VNC stained for TJ (red), pMad (blue) and Isl^{-Tmyc} (green). Cells are shown from dorsal-most (**C1**) to intermediate (**C3**) positions. TJ is expressed in 2 dorsal lateral Isl^+ motoneurons (**C2**, inset), in the Isl^- U MNs (**C2** and **C3**, asterisks) and in 1 TJ^+ $pMad^+$ MN that innervates DO5 (**C3**, full arrowhead). Arrows in **C1** highlight the dorsal-most pair of TJ^+ neurons and asterisks in **C2** and **C3** show U MNs.

D-F Representative views of a single hemisegment of L1 larva VNC stained for TJ (blue), Eve (green) and endogenous nls-tdTomato driven *CQ2-lexA*. Cells are shown from dorsal-most (**D**) to ventral (**F**) positions. *CQ2-lexA* drives in TJ^+ U MNs U1, U2 and U5 as well as one of the dorsal ISNd TJ^+ MN (**D,** full arrowhead) and 1 non-identified TJ^+ IN (**F**, arrow).

G Number of peristaltic waves per 30 seconds at permissive (23°C) and restrictive (31°C) temperatures. Upon activation of 3 to 4 of the 6 TJ^+ MNs, we observe a slight decrease in the number of peristaltic waves. Each single point represents a single 12h-old first instar larva. Error bars indicate the SD and n denotes the number of larvae tested. Statistical analysis: One way ANOVA. ***$p<0.001$.

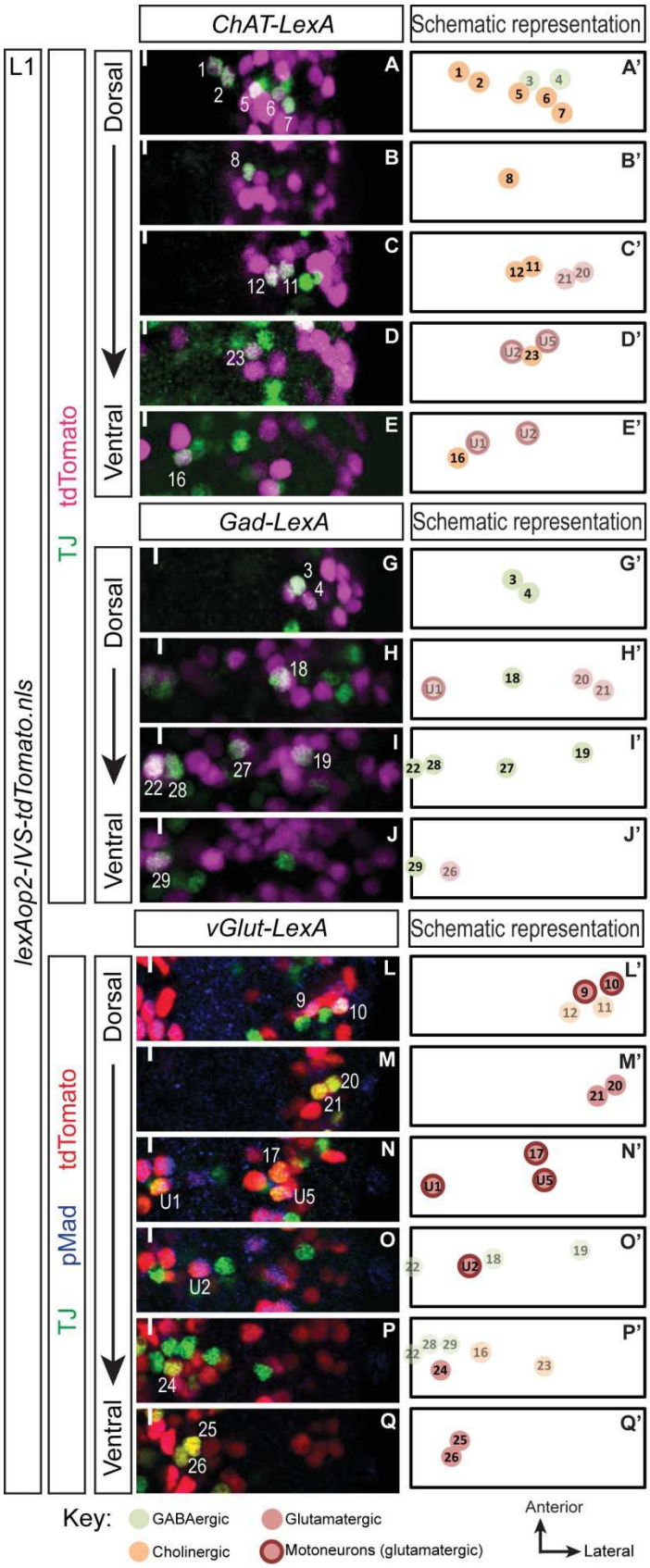

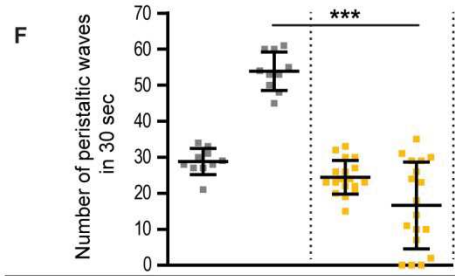

lexAop>>dTrpA1	+		+	
TJ-Flp			+	
ChAT-LexA	+		+	
Temperature	23°C	31°C	23°C	31°C
n=	10		18	
Larval stage	L3			

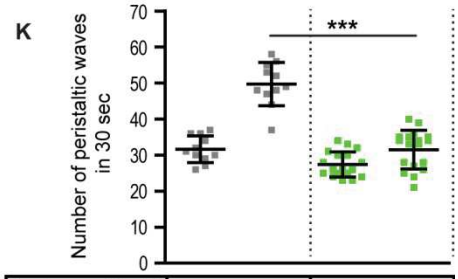

lexAop>>dTrpA1	+		+	
TJ-Flp			+	
Gad1-LexA	+		+	
Temperature	23°C	31°C	23°C	31°C
n=	11		18	
Larval stage	L3			

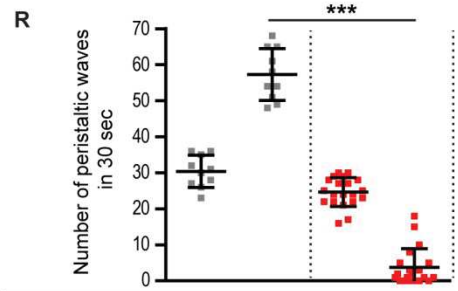

lexAop>>dTrpA1	+		+	
TJ-Flp			+	
vGlut -LexA	+		+	
Temperature	23°C	31°C	23°C	31°C
n=	10		20	
Larval stage	L3			

Figure 5

Fig. 5: Activation of TJ^+ sub-populations defined by neurotransmitter properties gave rise to distinct locomotor behaviours

A-E Representative views of one hemisegment of first instar larva VNC stained for TJ (green) and cholinergic cells (magenta – using *ChAT-LexA* driving *lexAop-nlsTomato*). Cells are shown from dorsal (**A**) to ventral (**E**) positions. The full line indicates the midline and anterior of the VNC is up. **A'-E'** Schematic representation of the adjacent immunostaining panels. TJ^+ cholinergic neurons are represented in block orange colour while other non-cholinergic neurons are shown with paler colours. The identity of TJ^+ non-cholinergic neurons is inferred from their position compared to TJ^+ cholinergic neurons. **F** Number of peristaltic waves per 30 seconds at permissive (23°C) and restrictive (31°C) temperatures done by larvae expressing TrpA1 in TJ^+ cholinergic neurons (orange bars) versus controls that do not express TrpA1 (grey bars). **G-J** Representative views of one hemisegment of first instar larva VNC stained for TJ (green) and GABAergic cells (magenta – using *Gad1-LexA* driving *lexAop-nlsTomato*). Cells are shown from dorsal (**G**) to ventral (**J**) positions. The full line indicates the midline and anterior of the VNC is up. **G'-J'** Schematic representation of the adjacent immunostaining panels. TJ^+ GABAergic neurons are represented in block green colour while other non-GABAergic neurons are shown with paler colours. The identity of TJ^+ non-GABAergic neurons is inferred from their position compared to TJ^+ GABAergic neurons. **K** Number of peristaltic waves per 30 seconds at permissive (23°C) and restrictive (31°C) temperatures done by larvae expressing TrpA1 in TJ^+ GABAergic neurons (green bars) versus controls that do not express TrpA1 (grey bars). **L-Q** Representative views of one hemisegment of first instar larva VNC stained for TJ (green), glutamatergic cells (red – using *vGlut-LexA* driving a *lexAop-nlsTomato*) and the motoneuron marker pMad (blue). Cells are shown from dorsal (**L**) to ventral (**Q**) positions. **L'-Q'** Schematic representation of the adjacent immunostaining panels. TJ^+ glutamatergic neurons are represented in block red colour while other non-glutamatergic neurons are shown with paler colours. The identity of TJ^+ non-glutamatergic neurons is inferred from their position compared to TJ^+ glutamatergic neurons. **R** Number of peristaltic waves per 30 seconds at permissive (23°C) and restrictive (31°C) temperatures done by larvae expressing TrpA1 in TJ^+ glutamatergic neurons (red bars) versus controls that do not express TrpA1 (grey bars).

In **F**, **K** and **R**: each single point represents a single third instar larva. Error bars indicate the SD and n denotes the number of larvae tested. Statistical analysis: One way ANOVA. ***p<0.001.

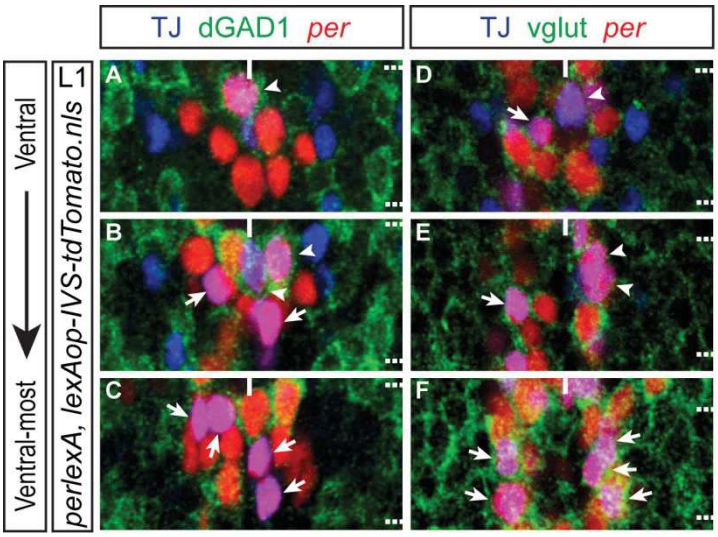

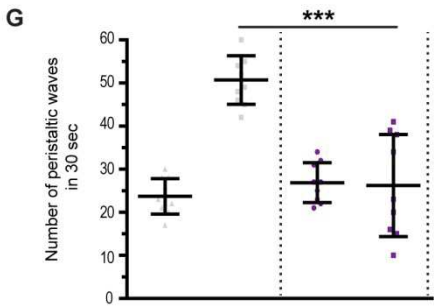

lexAop>>dTrpA1	+		+	
tj-flp			+	
per-lexA	+		+	
Temperature	23°C	31°C	23°C	31°C
n=	10		9	
Larval stage	12h old L1			

Figure 6

Fig. 6: Activation of heterogeneous TJ^+ glutamatergic and GABAergic population lead to a decrease in the speed of locomotion

A-C Staining for TJ (blue), GAD1 (green) and nls-tdTomato (red) expressed under *per-lexA* driver in freshly hatched first instar larva VNC. Staining reveals 9 TJ^+ Per^+ cells per segment, located in the ventral part of the VNC. The 3 most dorsal cells, located at the midline, are GABAergic (full arrowheads), while the 6 other cells are not (arrows). Notice how one of the TJ^+ Per^+ GABAergic neurons (often the most dorsal) is Per^+ weak.

D-F Staining for TJ (blue), vglut (green) and nls-tdTomato (red) expressed under *Per-lexA* driver in freshly hatched first instar VNC. The remaining 6 non-GABAergic cells are glutamatergic (arrows).

G Number of peristaltic waves per 30 seconds at permissive (23°C) and restrictive (31°C) temperatures done by larvae expressing TrpA1 in TJ^+ Per^+ neurons (purple bars) versus controls that do not express TrpA1 (grey bars). Activation of the TJ^+ Per^+ population (9 cells per segments) lead to a drastic decrease in the speed of locomotion of 12h old larvae (second violet column). Phenotype is characterized by partial relaxed paralysis of the most-posterior segments of the larvae. One way ANOVA. ***$p<0.001$.

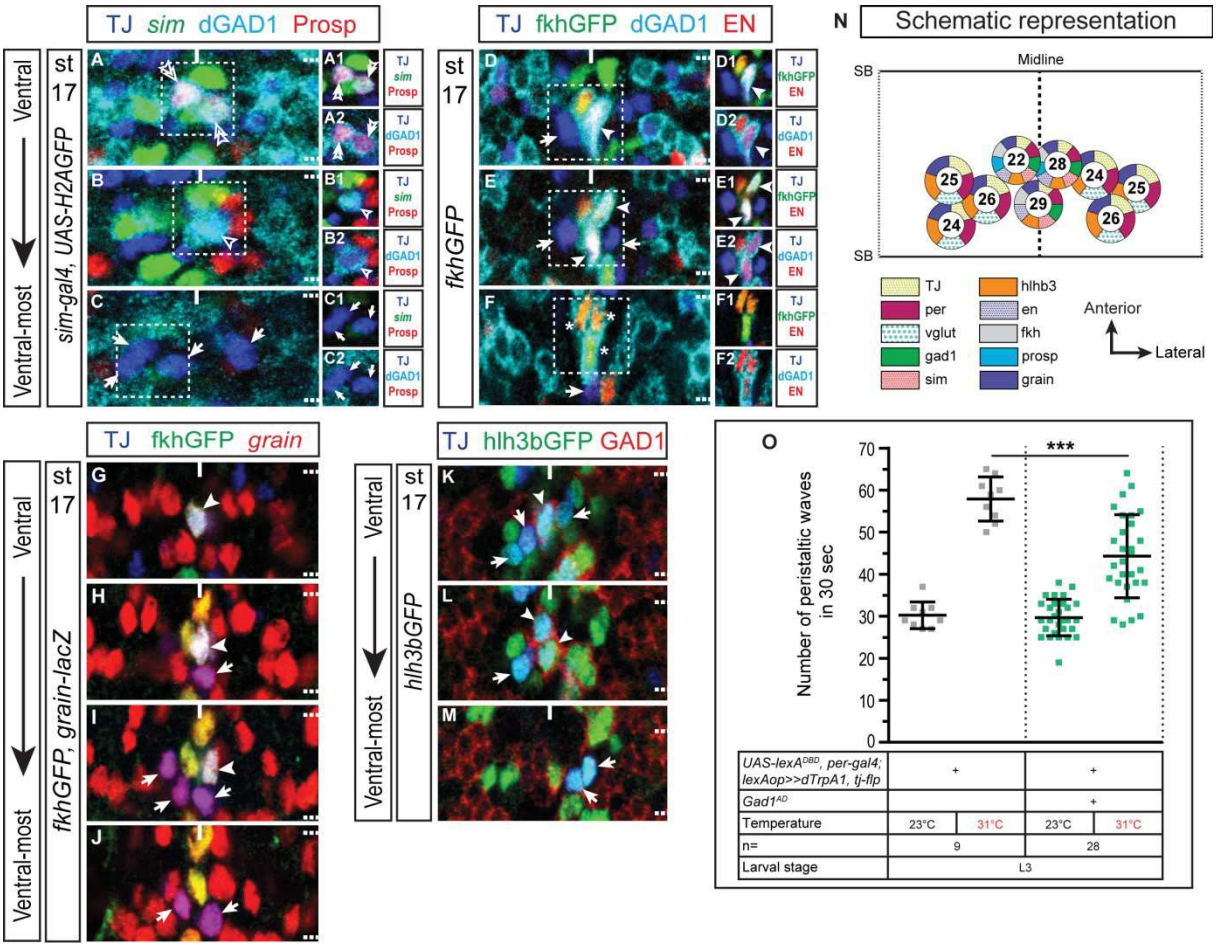
TJ sim dGAD1 Prosp
st 17
Ventral
Ventral-most
sim-gal4, UAS-H2AGFP
TJ fkhGFP dGAD1 EN
fkhGFP
N
Schematic representation
Midline
SB
TJ
per
vglut
gad1
sim
hlhb3
en
fkh
prosp
grain
Anterior
Lateral
TJ fkhGFP grain
fkhGFP, grain-lacZ
TJ hlh3bGFP GAD1
hlh3bGFP
O
Number of peristaltic waves in 30 sec
***
UAS-lexA^DBD, per-gal4; lexAop>>dTrpA1, tj-flp
Gad1^AD
Temperature
23°C
31°C
n=
9
28
Larval stage
L3

Figure 7

Fig. 7: Activation of 3 TJ^+ *Per*$^+$ GABAergic neurons lead to a decrease in the speed of locomotion

A-C Staining for TJ (blue), GAD1 (cyan), Prospero (red) and GFP (green) driven by *sim-gal4* in late stage 17 embryo VNC. *Sim-gal4* (green) is weakly expressed in GABAergic TJ^+ ventral neurons only, identifying them as midline cells (simple and double empty arrowheads) in **A** and **B** panels. Remaining TJ^+ ventral population (TJ^+ glutamatergic neurons – arrows – full contingent not shown) are *sim-gal4*$^-$, hence not part of the midline cells. Among the 3 TJ^+ *sim*$^{+weak}$ GABAergic located at the midline, two are positive for the MNB progeny neuron marker Prospero (double empty arrowheads) and one negative (simple empty arrowhead).

D-F Staining for TJ (blue), GAD1 (cyan), Engrailed (red) and fkhGFP fusion protein (green) in late stage 17 embryo VNC. TJ^+ ventral GABAergic neurons (full arrowheads) are EN^+ and Fkh^+, two markers of MNB progeny subpopulation. Notice in the ventral-most part of the VNC, located ventrally to TJ^+ neurons, three EN^+ Fkh^+ Gad^+ TJ^- cells: the iVUMs (asterisks in panel **F**).

G-J Staining for TJ (blue), fkhGFP fusion protein (green) and βgal (red) from *Grain-lacZ* in late stage 17 embryo VNC. Both ventral GABAergic (full arrowhead) and glutamatergic (arrows) TJ^+ neurons are *Grain*$^+$.

K-M Staining for TJ (blue), GAD1 (red) and hlh3bGFP fusion protein (green) in late stage 17 embryo VNC. Both ventral GABAergic (full arrowhead) and glutamatergic (arrows) TJ^+ neurons are $hlh3b^+$.

N Recapitulative schematic representation of the TJ^+ most ventral neurons molecular code. Schematic represents a full segment.

O Number of peristaltic waves per 30 seconds at permissive (23°C) and restrictive (31°C) temperatures done by larvae expressing TrpA1 in TJ^+ *per*$^+$ GABAergic neurons (light blue bars) versus controls that do not express TrpA1 (grey bars). Activation of the 3 TJ^+ *Per*$^+$ GABAergic population per segment leads to a decrease in the speed of locomotion (second light blue bar) in third instar larvae. One way ANOVA. ***$p<0.001$.

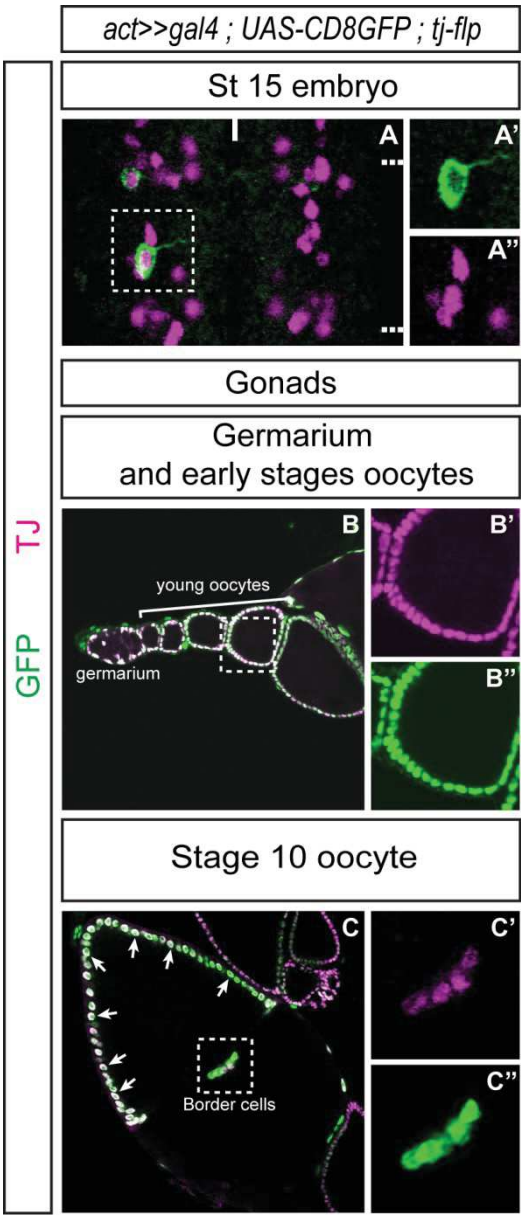

Supplementary Figure 1

Supp Fig. 1: *TJ-Flp* expression starts in stage 15 embryo VNC and matches TJ expression detected by antibody in adult gonads.

A Staining for TJ (magenta) and recombined neurons (*TJ-Flp* expressing cells – green) in stage 15 embryo VNC. First recombined cells expressing GFP can be detected by embryonic stage 15.

B-C Staining for TJ^{+} neurons (magenta) and recombined cells (*TJ-Flp* expressing cells – green) in female flies gonads: germarium and early stages oocytes (**B**) and stage 10 oocyte (**C**). Cell types well characterised for their expression of TJ (follicular cells, arrows; border cells, circled) express the flippase.

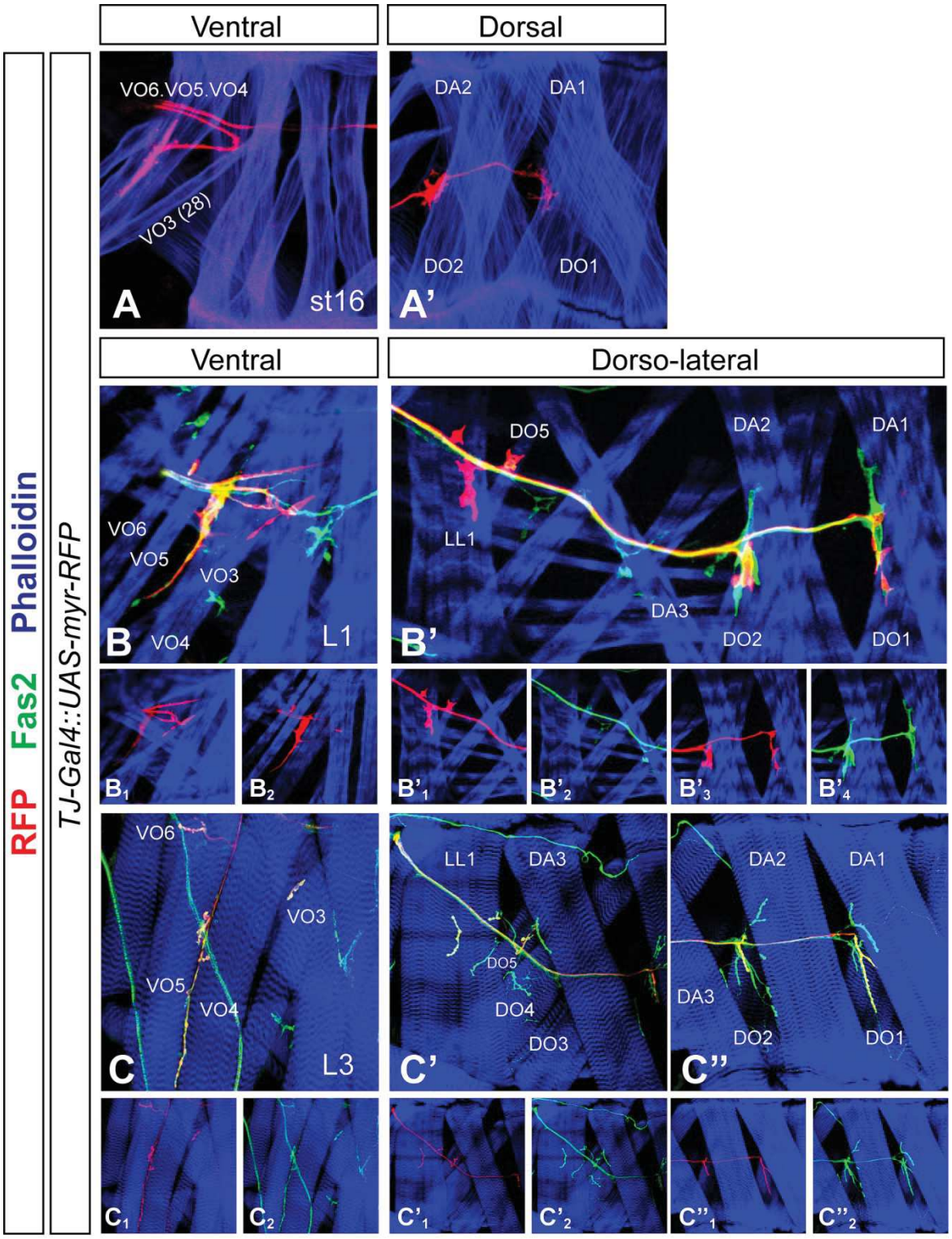

Supplementary Figure 2

Supp Fig. 2: TJ^+ MNs projections remain constant from embryonic stage 16 to L3 larval stage

Stage 16 embryo and first and third larval stages stained with FasII (green), *TJ-gal4* driving a *UAS-myrRFP* (red) and Phalloidin-TX (blue). FasII labels all MNs axons projections while Phalloidin-TX stains muscles fibres.

A-A' TJ^+ MNs project through ISNd on muscles VO3, VO4, VO5 and VO6 (**A**) and through ISNdm on muscles DO1 and DO2 (**A'**) in stage 16 embryo.

B-B' TJ^+ MNs project through ISNd on muscles VO3, VO4, VO5 and VO6 (**B**) and through ISNdm on muscles DO1, DO2, DO5 and LL1 (**B'**) in first instar larva. Two focus plans are shown below **B** and **B'** to better visualize TJ^+ projections on VO3, VO4, VO5 and VO6 ($\mathbf{B_1}$, $\mathbf{B_2}$), DO5 and LL1 ($\mathbf{B'_1}$, $\mathbf{B'_2}$) and DO1 and DO2 ($\mathbf{B'_3}$, $\mathbf{B'_4}$).

C-C'' TJ^+ MNs project through ISNd on muscles VO3, VO4, VO5 and VO6 (**C**) and through ISNdm on muscles DO5, LL1 (**C'**), DO1and DO2 (**C''**) in third instar larva. Two focus plans are shown below **C, C'** and **C''** to better visualize TJ^+ projections on VO3, VO4, VO5 and VO6 ($\mathbf{C_1}$, $\mathbf{C_2}$), DO5 and LL1 ($\mathbf{C'_1}$, $\mathbf{C'_2}$) and DO1 and DO2 ($\mathbf{C''_1}$, $\mathbf{C''_2}$).

TJ^+ MNs projections remain unchanged through late embryonic and larval life.

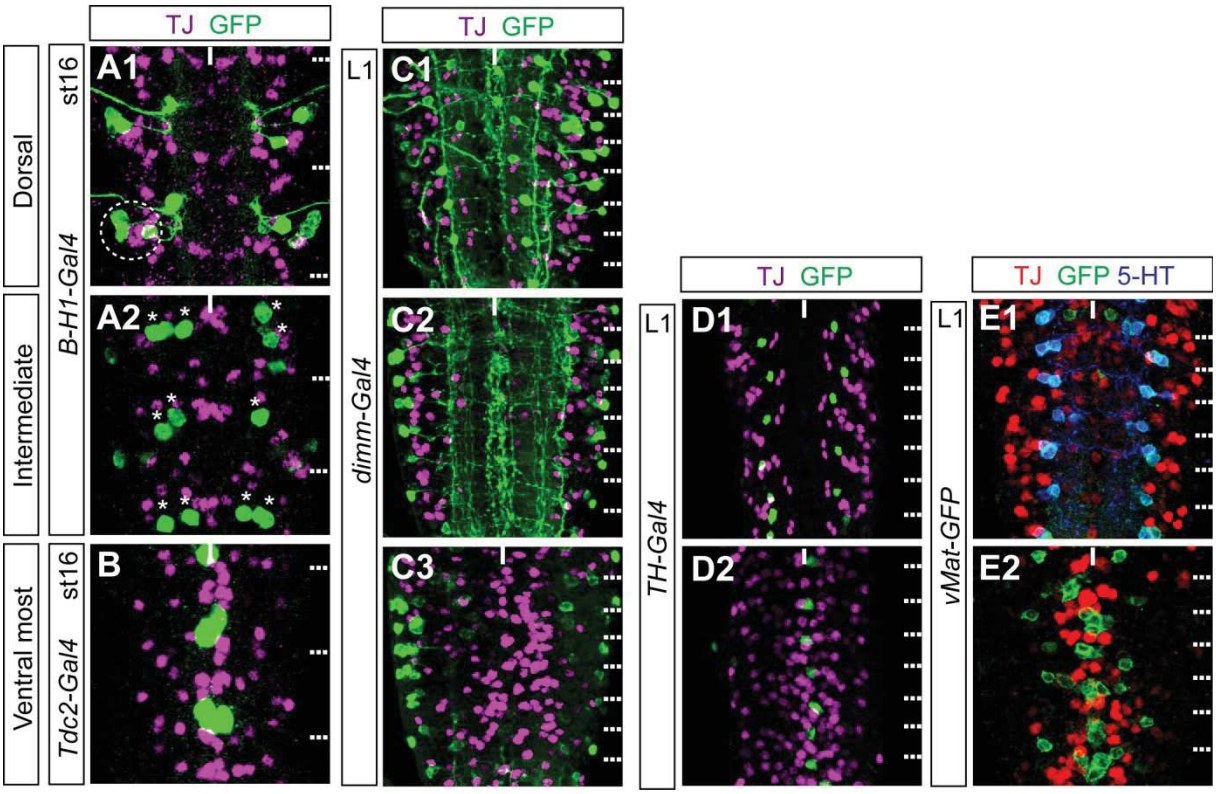

Supplementary Figure 3

Supp Fig. 3: TJ is excluded from monoaminergic and peptidergic neuronal populations

A1-A2 Representative views of two segments of stage 16 embryo VNC stained for TJ (magenta) and GFP labelling SNa MNs (thanks to *B-H1-gal4* driver). TJ is excluded from SNa MNs (**A1**, circle).

B Representative views of two segments of stage 16 embryo VNC stained for TJ (magenta) and GFP labelling the ventral median octopaminergic mVUM (ventral Median Unpaired MNs) (thanks to *tdc2-gal4* driver). TJ is excluded from mVUM MNs.

C1-C3 Representative views of first instar larva VNC stained for TJ (magenta) and GFP labelling the peptidergic cells (thanks to *dimm-gal4* driver). TJ is completely excluded from the larve peptidergic population.

D1-D2 Representative views of first instar larva VNC stained for TJ (magenta) and GFP labelling the dopaminergic neurons (thanks to *TH-gal4* driver). TJ is excluded from dopaminergic neurons.

E1-E2 Representative views of first instar larva VNC stained for TJ (red), 5-HT (blue) and GFP labelling the monoaminergic neurons (visualized thanks to the *vMat-GFP* fusion protein). TJ is excluded from monoaminergic neurons.

In all panels, anterior of the VNC is up, midline denoted by the full line on top of the panels and the segment boundaries by the dashed lines on the right side of the panels.

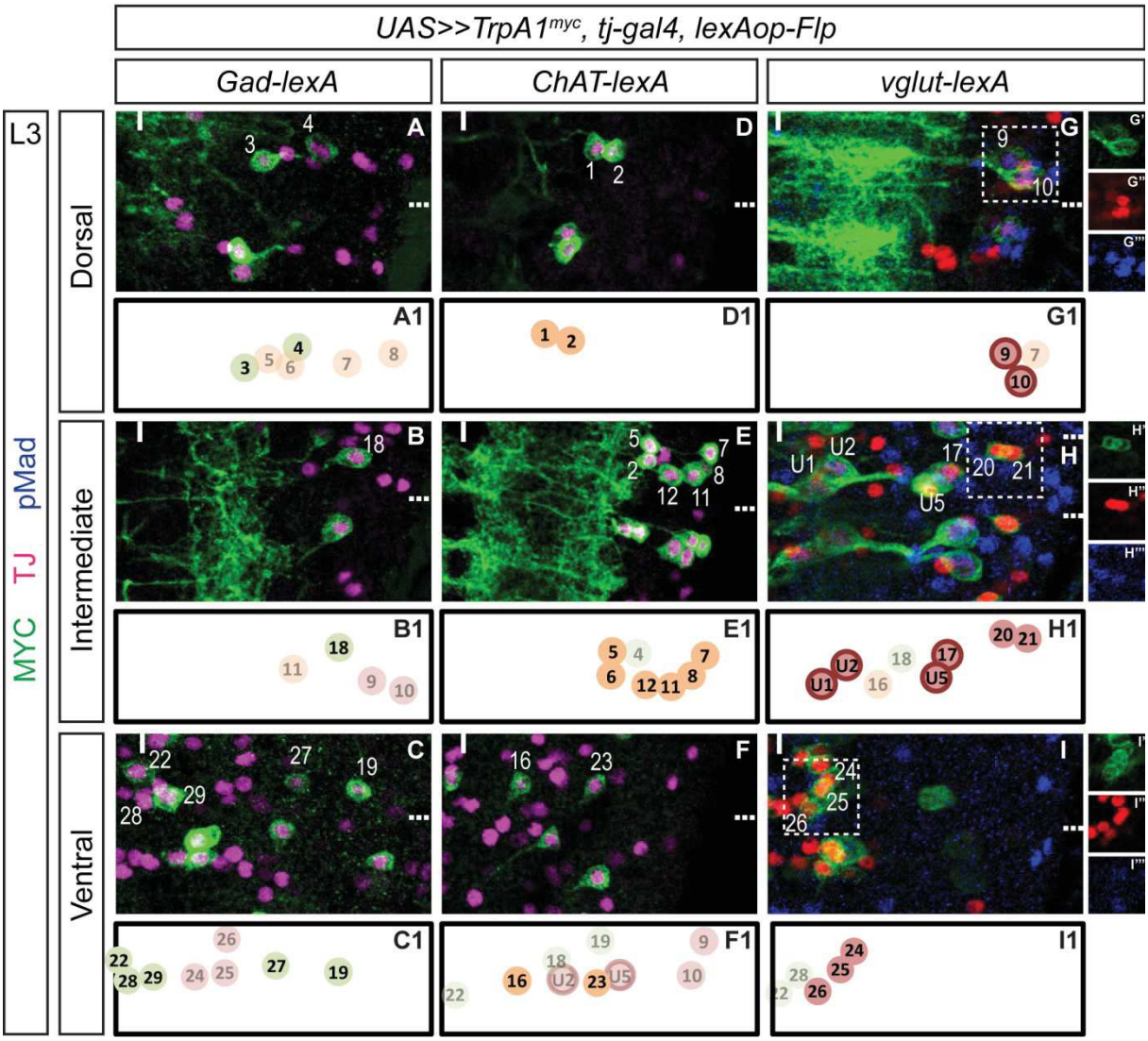

Supplementary Figure 4

Supp Fig 4: TJ is expressed in highly diverse populations of interneurons in third instar larva

Using an alternative genetic approach in third instar larva, we confirm the number of TJ^+ cells expressing the neurotransmitters GABA, acetylcholine and glutamate.

A-C Representative views of third instar larva VNC stained for TJ (magenta) and CD8GFP (green - expressed upon combined expression of *Gad1-lexA* driver and *TJ-gal4*). Cells are shown from dorsal (**A**) to ventral (**C**) positions. **A1-C1** Schematic of the first hemisegment of each panel. GABAergic TJ^+ cells are represented in block colours while other TJ^+ cells are represented in faded colours. Numbering in the schematic matches Fig.2 C1-G1 schematic. Please be aware that number labels of the TJ^+ Gad^- cells is inferred from cell position in the anterior-posterior and medial-lateral axis compared to TJ^+ Gad^+ cells and might not be fully accurate.

D-F Representative views of third instar larva VNC stained for TJ (magenta) and CD8GFP (green - expressed upon combined expression of *ChAT-lexA* driver and *TJ-gal4*). Cells are shown from dorsal (**D**) to ventral (**F**) positions. **D1-F1** Same as A1-C1 but considering TJ^+ cholinergic cells.

G-I Representative views of third instar larva VNC stained for TJ (magenta), CD8GFP (green - expressed upon combined expression of *vglut-lexA* driver and *TJ-gal4*) and pMad (blue – motoneuron marker). Cells are shown from dorsal (**G**) to ventral (**I**) positions. **G1-I1** Same as A1-C1 but considering TJ^+ glutamatergic cells.

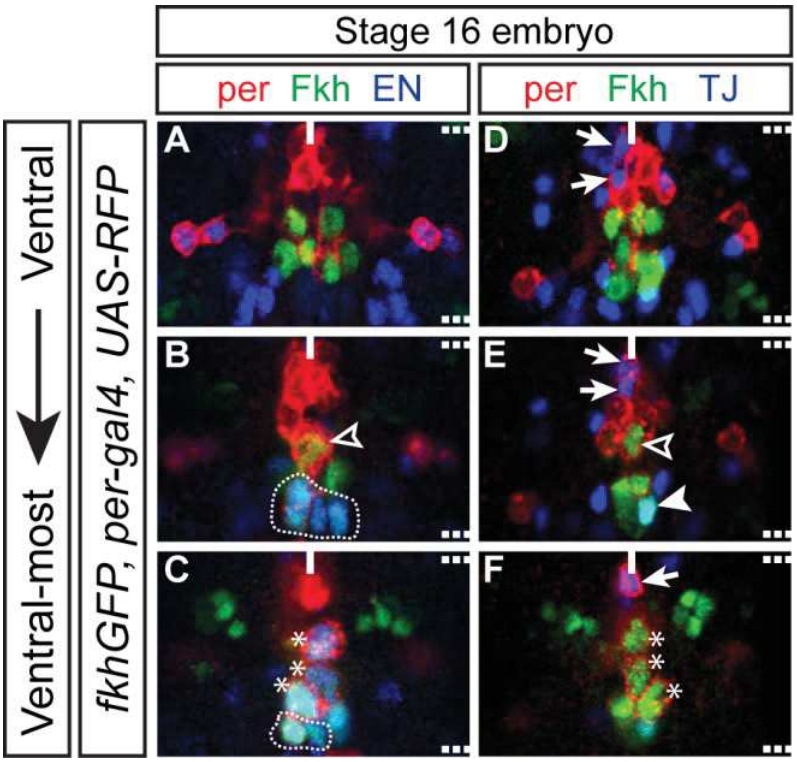

Supplementary Figure 5

Supp Fig. 5: In stage 16 embryo, TJ is expressed in midline MNB progeny neurons but not iVUMs

A-C Staining for EN (blue), *Per* (red) and FkhGFP fusion protein (green) in stage 16 embryo VNC. Using highly stereotyped midline cells positions and *Period*, Forkhead and Engrailed stainings, it is possible to precisely identify the midline cells. H-cell sib (empty arrowhead) is a big Per^+ Fkh^+ EN^- cell (**B**) located in the middle of the segment and dorsally to the remaining Per^+ neurons. The 3 iVUMs (asterisks) are Per^+ Fkh^+ and EN^+ and located most ventrally (**C**). A group of cells located posteriorly to H-cell sib and above and posterior to the iVUMs and characterized by their expression of Fkh and EN (and sometimes *Per*) are the MNB progeny neurons (circled cells in **B** and **C**).

Each panel represent a single segment. Segment boundaries are noted by dotted lines on the right-hand side of the panels and midline by the full line. Anterior of the VNC is up.

D-F Using stereotyped positions and *Period* and Forkhead stainings, we affirm that neither H-cell sib (empty arrowhead in **E**) nor the 3 iVUMs (asterisks in **F**) express TJ. Instead, at stage 16, TJ seems to be expressed in 1 MNB progeny neuron (full arrowhead in **E**). It is also expressed in 5 Per^+ only cells located in the anterior part of the segment (arrows in **D** and **E**). Those Per^+ cells (as seen in fig.7A-C) are not part of the *sim* domain, hence not part of the midline cells.

D - Additional results

1. Further functional characterization of the TJ$^+$ subpopulations

a- Initial approach using UAS>>TrpA1^{myc} cassette

Initial attempts at intersectional genetics had me using *TJ-gal4* alongside a published *UAS>>TrpA1^{myc}* cassette (von Philipsborn et al., 2011), a *lexAop-Flp* (Ohyama et al., 2015) and various lexA drivers (Diao et al., 2015). Such an approach was required at the time, while the *TJ-Flp* line was under construction. For the different genetic combinations I used (see section 5.I., table 5), I performed locomotor experiments in third instar larvae to give time for the recombination to occur in all targeted neurons. Larvae tested for behaviour were immuno-stained for myc which reported accurate expression of TrpA1 protein in the entire TJ$^+$ subpopulations considered (presented in the supplementary figure 4 in our article). Although recombination seemed complete and TrpA1 expression was detected, behavioural experiments did not yield any locomotor phenotype or only slight phenotypes at high temperatures (34°C) (data not shown). Subsequent experiments done using another cassette (*lexAop>>dTrpA1*) (unpublished – gift from Y. Aso, Janelia Research Campus) with *TJ-Flp* and the same lexA drivers did yield locomotor phenotypes (results presented in the article), proving that the modulation of the activity of the subpopulations does have an impact on locomotion; in this particular case we were rather facing a technical problem when using the *UAS>>TrpA1^{myc}* cassette.

b- Additional results using lexAop>>dTrpA1 and lexA drivers (follow up of the article results)

Based on the lexA drivers availability, I chose to activate TJ$^+$ subpopulations using the efficient *TJ-Flp, lexAop>>dTrpA1* genetic approach. As mentioned in the draft article, TJ is expressed in U1, U2 and U5 MNs as well as DO5 MN and two lateral ISNd MNs. To understand the implication of TJ$^+$ MNs in locomotion, I decided to use the non-characterized *RapGAP1-lexA* driver (Kockel et al., 2016) since the *OK6-lexA* [supposedly an enhancer trap insertion in the *RapGAP1* gene (Kohsaka et al., 2014)] gave rise to low or no expression in MNs when crossed to a lexAop

reporter (data not shown). In L3 larvae, activation of the TJ$^+$ *RapGAP1-lexA*$^+$ neurons led to a decrease in the number of peristaltic waves and a slight contraction of the body of the larvae (Fig 24G – second brown bar), that cannot be solely imputed to TJ$^+$ MNs. Indeed I found that *RapGAP1-lexA* driver is far from being ideal, as it does not allow for the targeting of all TJ$^+$ MNs in every hemisegment in L1 larvae (full arrowheads in Fig 24C). Moreover, *RapGAP1-lexA* drives in a median ventral TJ$^+$ IN (asterisk in Fig 24D). Inferring from its position, this IN is most probably one of the TJ$^+$ *per*$^+$ neurons we described in our article. Activation of the TJ$^+$ *per*$^+$ neurons has an impact on locomotion (see results of the article). Therefore we are not able to affirm that the locomotor phenotypes obtained upon activation of the TJ$^+$ *RapGAP1-lexA*$^+$ neurons is exclusively due to the TJ$^+$ MNs.

Next, I tested *GMR70C01-lexA* driver (or *PMSI-lexA* driver) described in Kohsaka et al. (2014). This driver is expressed in a subpopulation of the *period*$^+$ neurons. As TJ co-localizes with 9 *per*$^+$ neurons per segment, I wondered if TJ co-localizes with *PMSI-lexA* driver. I found in L1 larvae 1 TJ$^+$ *PMSI-lexA*$^+$ neuron per hemisegment (Fig 24E – co-localization done with gal4 – enhancer used for gal4 and lexA lines is the same). In L3 larvae, activation of this single neuron per hemisegment had no effect on the number of waves and general locomotor behaviour of the larvae (Fig 24G, second pink bar).

Next we tested the implication in locomotion of a single TJ$^+$ GABAergic neuron per hemisegment that co-localizes with a *GMR40H07-lexA* driver (also called *TJjan-lexA*) (Fig 24F). Activation of this neuron had no effect on locomotion, number of waves or general body posture of the larvae (Fig 24G, second light blue bar).

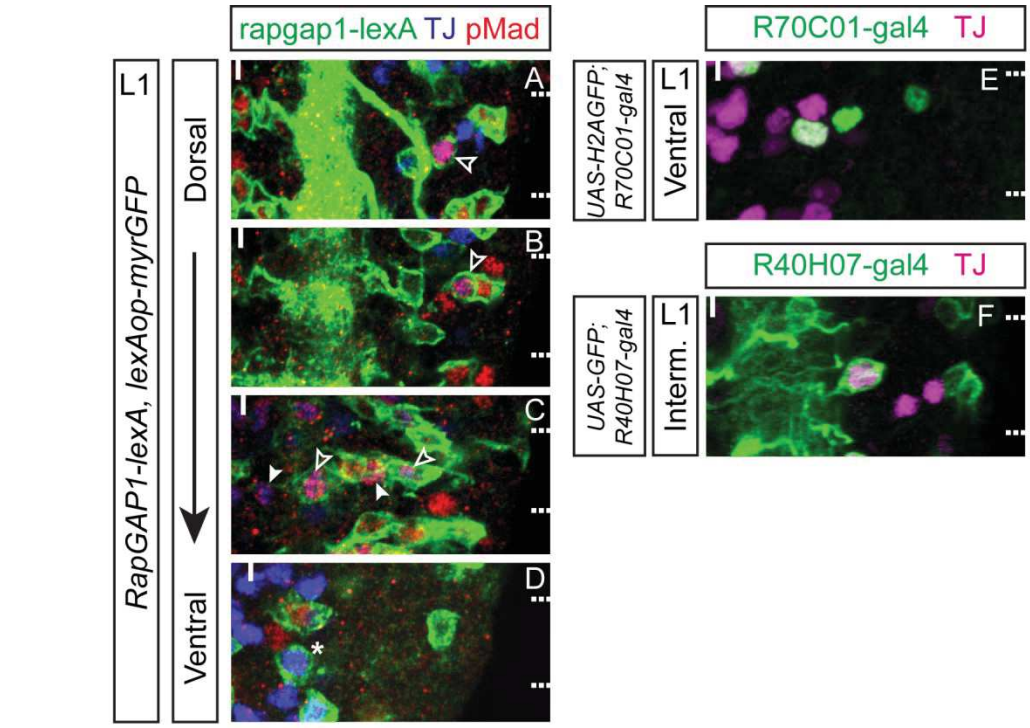

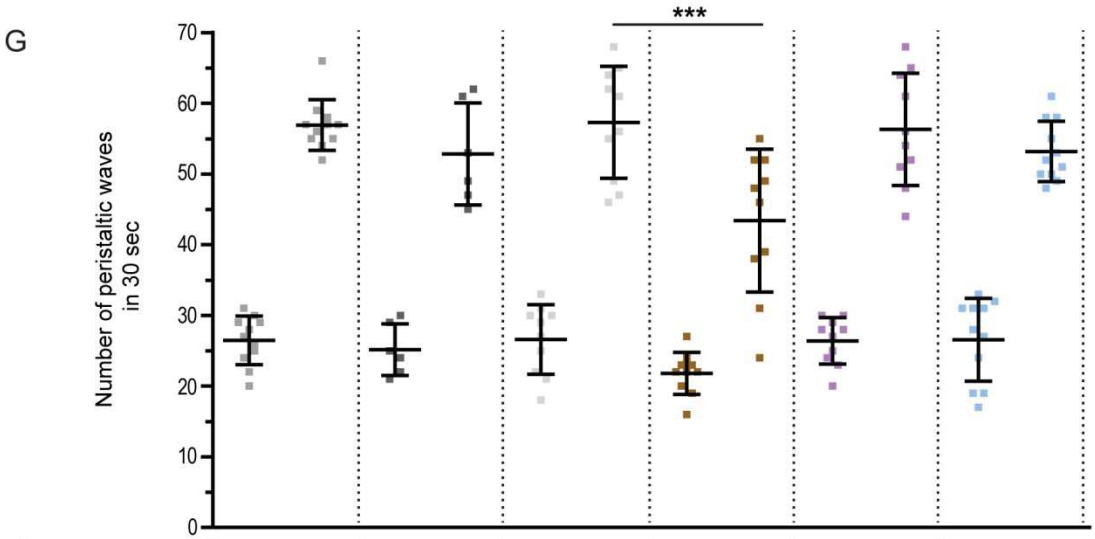

lexAop>>dTrpA1	+		+		+		+		+		+	
TJ-Flp			+				+		+		+	
RapGAP1-lexA					+		+					
GMR70C01-lexA									+			
GMR40H07-lexA											+	
Temperature	23°C	31°C	23°C	31°C	23°C	31°C	23°C	31°C	23°C	31°C	23°C	31°C
n=	11		6		10		10		10		11	
Larval stage	L3											

Fig 24: Pattern of expression and effects of the activation of different lexA lines that drive in TJ^+ neurons.

A-D. Immunostaining of first instar larva VNC for TJ (blue), the MN marker pMad (red) and myristoylated GFP driven by *RapGAP1-lexA*. TJ^+ MNs that co-localize with *RapGAP1-lexA* are pointed out by empty arrowheads while those that do not co-localize with *RapGAP1-lexA* are pointed by full

arrowheads. *RapGAP1-lexA* also drives in a ventral median IN shown with an asterisk on panel D. **E**. Immunostaining of first instar larva VNC for TJ (magenta) and nuclear GFP driven by *GMR70C01-lexA* (also called *PMSI-lexA*) (green). **F**. Immunostaining of first instar larva VNC for TJ (magenta) and GFP driven by *GMR40H07-lexA* (also called *TJjan-lexA*) (green). A single hemisegment is shown in each panel, with segments boundaries on the right (dashed lines) and midline location indicated on top left of the panel. Statistical analysis: One way ANOVA. ***p<0.001 Error bars represent the SD.

c- Additional approach using lexAop>>dTrpA1 cassette with gal4 drivers

Using the *lexAop>>dTrpA1* cassette that we know is functional, I implemented another approach with *TJ-Flp* and a *UAS-lexA* to "convert" gal4 drivers of interest into lexA. The positive control of this experiment, consisting in crossing *TJ-gal4* with *UAS-lexA* and *lexAop>>dTrpA1* did not give rise to the full spastic contracted paralysis that I expected (data not shown). Some larvae however displayed defaults in locomotion that might arise from the expression of dTrpA1 in only a portion of the TJ^+ neurons. I am unable to verify this hypothesis, as dTrpA1 is not tagged. In this genetic approach, I hypothesize that *TJ-gal4* and *UAS-lexA* are the limiting transgenes, as *TJ-Flp* and *lexAop>>dTrpA1* showed their efficiency when subdividing TJ^+ population depending on neurotransmitter properties (results presented in the article). I nevertheless tested this approach with several other lines: *LMO-gal4*, *Abd-gal4*, *HB9-gal4*, *OK6-gal4* and *GMR47D01-gal4* (expressed in LLN INs (Yoshikawa et al., 2016). *LMO-gal4* drives in 7 TJ^+ neurons per segment or 3 TJ^+ neurons per hemisegment plus a midline neuron (arrows in Fig 25A-C). More particularly, it is highly expressed in the most anterior neuron of the TJ^+ dorsal pair of neurons, and in two lateral INs located close to the pair of ISNd TJ^+ MNs labelled by *Islet* (empty arrowheads in Fig 25B). Additionally, *LMO-gal4* drives occasionally in a neuron located at the midline that does not have a counterpart in the adjacent hemisegment; it most probably is one of the TJ^+ MNB progeny neurons. *Abd-B-gal4* is expressed in all cells from the posterior segments A5 to A9 (Estacio-Gómez et al., 2013). Therefore, by using it in an intersectional genetic approach with *TJ-Flp*, I am targeting all TJ^+ neurons located in the A5 to A9 abdominal segments. *HB9-gal4* drives in 6 TJ^+ neurons per hemisegment: strongly in 2 dorsal INs (arrows in Fig 25D) and the 2 lateral ISNd MNs (arrowheads in Fig 25D and 25E) and weakly in 2 ventral

INs (arrows in Fig 25F). *GMR47D01-gal4* [expressed in LLN INs (Yoshikawa et al., 2016)] drives in two TJ$^+$ ventral INs per hemisegment (arrows in Fig 25G).

Even though the genetic technique implemented here is not optimal, I nevertheless observed consistent locomotor defects upon activation of the TJ$^+$ *LMO-gal4*$^+$ neurons. Locomotor defects were also detected in some larvae upon activation of the posterior-most TJ$^+$ *Abd-B-gal4*$^+$ neurons. No phenotype was observed upon activation of the TJ$^+$ MNs using *OK6-gal4* using this approach.

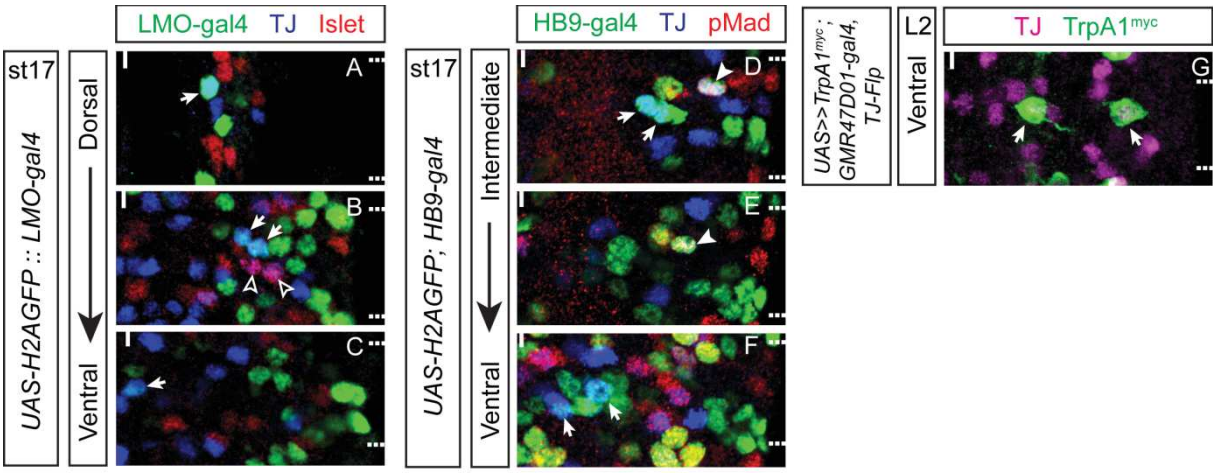

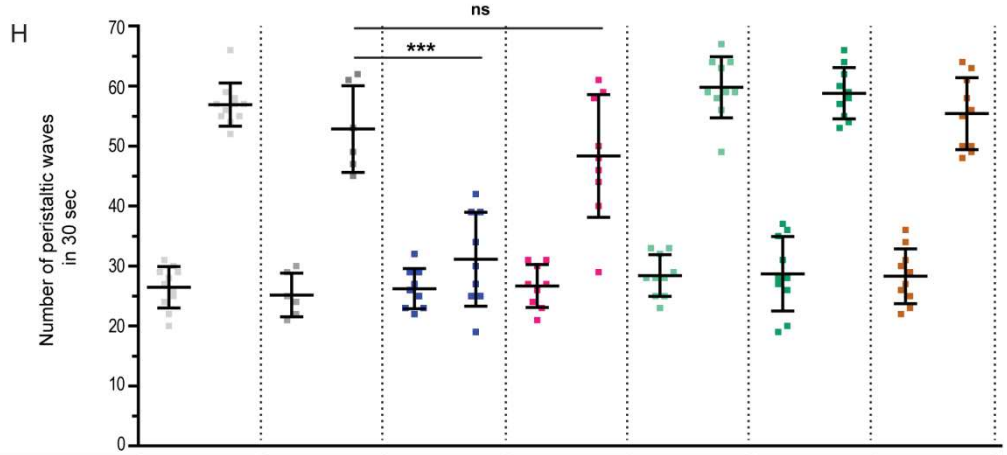

lexAop>>dTrpA1	+		+		+		+		+		+		+
TJ-Flp			+		+		+		+		+		+
UAS-lexA					+		+		+		+		+
LMO-gal4					+								
Abd-gal4							+						
HB9-gal4									+				
GMR47D01-gal4 (LLN)											+		
OK6-gal4													+
Temperature	23°C	31°C	23°C	31°C	23°C	31°C	23°C	31°C	23°C	31°C	23°C	31°C	23°C	31°C
n=	11		6		9		9		10		10		10	
Larval stage	L3													

Fig 25: Pattern of expression and effects of the activation of different gal4 lines that drive in discrete subpopulations of TJ$^+$ neurons.

A-C. Immunostaining of late stage 17 embryo VNC for TJ (blue), the MN subpopulation marker Islet (red) and nuclear GFP driven by *LMO-gal4* (green). *LMO-gal4* drives in the anterior neuron of the most dorsal TJ^+ pair (arrow in A), in two intermediate lateral INs (arrows in B) located close to the ISNd TJ^+ MNs (empty arrowheads in B) and in one midline TJ^+ MNB progeny neuron (arrow in C). **D-F**. Immunostaining of first instar larva VNC for TJ (blue), the MN marker pMad (red) and nuclear GFP driven by *HB9-gal4* (green). *HB9-gal4* drives strongly in two intermediate TJ^+ INs (arrows in D) and in the two lateral ISNd TJ^+ MNs (arrowheads in D and E) and weakly in two ventral INs (arrows in F). **G**. Immunostaining of second instar larva VNC for TJ (magenta) and TrpA1 myc-tagged driven in neurons expressing both *GMR47D01-gal4* and TJ-Flp (green). *GMR47D01-gal4* co-localize with TJ in two ventral INs per hemisegment. A single hemisegment is shown in each panel, with segments boundaries on the right (dashed lines) and midline location indicated on top left of the panel Statistical analysis: One way ANOVA. ***p<0.001 Error bars represent the SD.

d- The A27h interneurons

GMR36G02-gal4 (*A27h-gal4*) pattern of expression and involvement in the locomotion was initially reported in Fushiki et al, 2016. In this work the authors focused on the most anterior of the two most dorsal neurons reported by this gal4 driver and named it A27h. I performed co-immunostaining with this gal4 line and TJ and found that a reproducible pattern of expression of *A27h-gal4* includes 4 neurons per hemisegment: 2 most dorsal, strongly expressing the gal4 (arrows in Fig 26A) and 2 ventral with weak gal4 expression (full and empty arrowheads in Fig 26B). In some hemisegments, an additional neuron can be found, either in ventral or lateral position (not shown). TJ consistently co-localizes with the four $A27h^+$ neurons. I found that the 2 TJ^+ *A27h-gal4*$^+$ dorsal neurons are always $ChAT^+$ (arrows, Fig 26A). Among the 2 ventral TJ^+ *A27h-gal4*$^+$ neurons, one is $ChAT^+$ (in 88% of hemisegments) (full arrowhead in Fig 26B) and one $ChAT^-$ (in 85% of hemisegments) (empty arrowhead in Fig 26B).

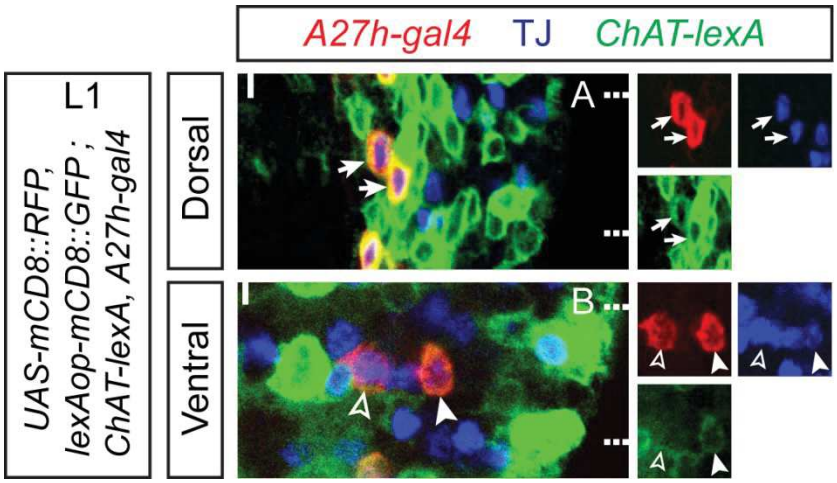

Fig 26: *GMR36G02-gal4* (*A27h-gal4*) pattern of expression and neurotransmitter properties

A-B. . Immuno-staining of first instar larva VNC for TJ (blue), myristoylated RFP driven by *A27h-gal4* (red) and myristoylated GFP driven by *ChAT-lexA* (green). *A27h-gal4* drives strongly in the 2 dorsal-most TJ$^+$ neurons (arrows in A) and more faintly in 2 ventral INs (empty and full arrowheads in B). The 2 dorsal-most *A27h-gal4*$^+$ neurons as well as one of the ventral ones are cholinergic (arrows in A and full arrowhead on B).

In their article, Fushiki et al (2016) characterized the A27h neuron as a cholinergic excitatory neuron whose activation in L3 semi-intact filet preparation leads to contraction of the equivalent innervated segment. As all *A27h-gal4*$^+$ neurons are TJ$^+$, I did not use intersectional genetics here but directly used the line; additionally the equivalent *A27h-lexA* line has not been generated, preventing the use of intersectional genetics approach in this case. We find that activation of all four *A27h-gal4*$^+$ neurons leads to a spastic contraction of the larva very reminiscent of that observed when activating the whole TJ$^+$ population (Graph 1 - Second orange bar). Surprisingly though, this phenotype is age-dependent and only visible in young L1 larvae aged less than 5 hours. Larvae aged 6 h old or more do not display this spastic contraction phenotype anymore, although 18h old L1 larvae still have a reduced number of waves compared to control (Graph 1 - Fourth and sixth orange bar).

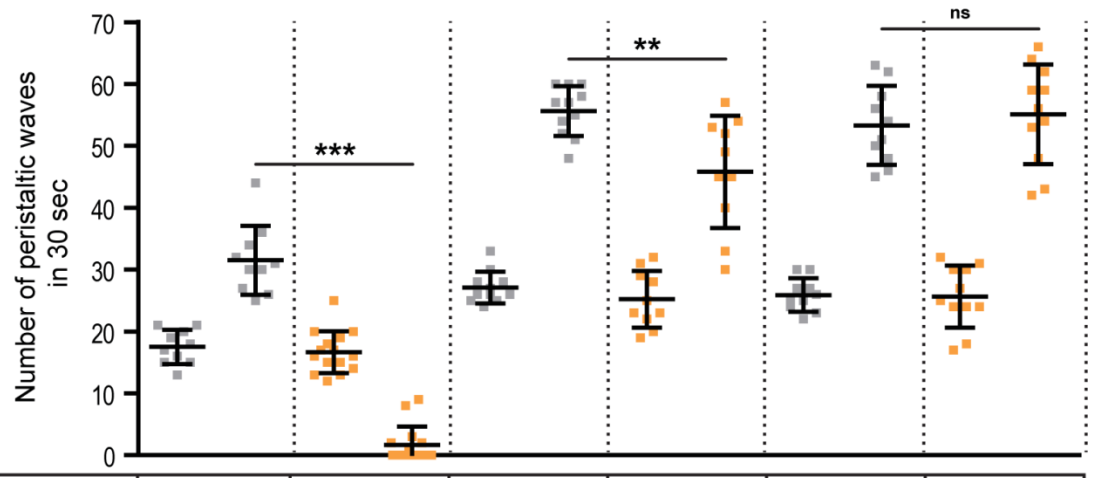

A27h-gal4	+		+		+		+		+		+	
UAS-TrpA1			+				+				+	
Temperature	23°C	31°C	23°C	31°C	23°C	31°C	23°C	31°C	23°C	31°C	23°C	31°C
n=	10		15		11		10		10		11	
Larval stage	< 5h old L1				18h old L1				L3			

Graph 1: Evolution of the number of peristaltic waves done by the larvae upon activation of the *A27h-gal4*$^{+}$ neurons depending on larval stage.

Genotypes, temperatures, number of larvae tested (n) and age of the larvae tested are specified in the table below the graph. Statistical analysis: One way ANOVA. ***p<0.001, **p<0.005 Error bars represent the SD.

We initially thought this difference in the behaviour of the larvae depending on their age might come from a variation in the pattern of expression of *A27h-gal4*. I therefore performed a time course of the expression of the *A27h-gal4* driver and found that the number and position of the *A27h-gal4*$^{+}$ neurons remain constant throughout larval stages (Graph 2).

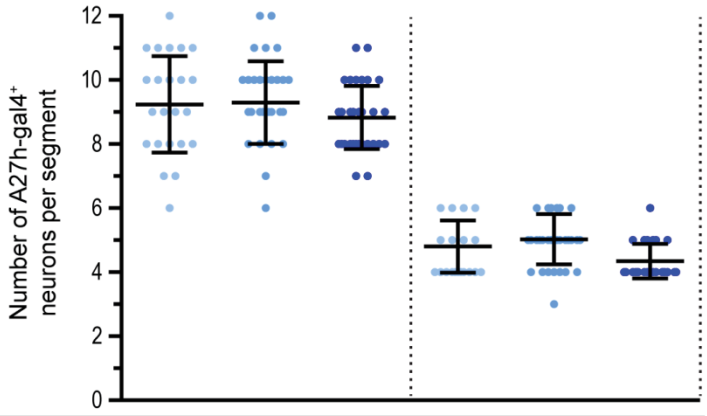

Population considered	Total population			Dorsal population		
Larval stage	<2h old L1	10h old L1	L3	<2h old L1	10h old L1	L3
n° of larvae; n° of segments	5; 25	7; 35	8; 35	5; 25	7; 35	8; 35
Mean value +/- SD	9 +/- 2	9 +/- 2	9 +/- 1	5 +/- 1	5 +/- 1	4 +/- 1

Graph 2: Total number of *A27h-gal4*$^{+}$ neurons per segment and number of *A27h-gal4*$^{+}$ dorsal neurons per segment.

The number of neurons expressing *A27h-gal4* does not vary between 2h old and 10h old L1 larvae and only slightly varies in L3. Error bars represent the SD.

It seems therefore that *A27h-gal4*$^{+}$ (TJ^{+}) neurons activation causes a spastic paralysis phenotype in young larvae that disappears when they age. This also implies that among the TJ^{+} population, neurons distinct from those 4 neurons must be implicated in the spastic paralysis phenotype observed upon activation of the whole TJ^{+} population in all larval stages.

e- Implementation of optogenetics intersectional genetics

To confirm results I obtained with TrpA1-based activation experiments, I decided to implement an optogenetics-based intersectional genetics approach. This approach relies on the use of a *lexAop>>CsChrimson*^{Venus} cassette (Hoopfer et al., 2015) used alongside *TJ-Flp* and different lexA drivers (Diao 2015). Preliminary results that consist in simple observation of the phenotypes without quantification are summarized in the following table.

Genetics	Neuronal population activated	Behaviour observed	Consistency with TrpA1-based intersectional genetics approach?
tsh-lexA:: lexAop>>CsChrimson^{Venus}; TJ-Flp	All TJ^{+} neurons in the VNC	Full tonic contraction of the larva body	Yes
lexAop>>CsChrimson^{Venus}; TJ-Flp, Gad1-lexA	TJ^{+} GABAergic neurons	Apparently normal, though slowed locomotion	Yes
per-lexA, lexAop>>CsChrimson^{Venus}; TJ-Flp	TJ^{+} *per*$^{+}$ neurons (TJ^{+} PMSI neurons)	Relaxed posterior segments causing a slowed locomotion	Yes

Table 4: Summary of the preliminary results obtained with an optogenetic-based intersectional genetics approach.

Preliminary results, using an optogenetics-based intersectional method to activate TJ^{+} subpopulation, seem to confirm the results obtained with the TrpA1-based intersectional genetics approach used until now (see article results). More experiments will be performed to bring strong arguments to support those preliminary results.

2. Further molecular characterization of the TJ^{+} population

a- Already characterized neuronal populations

As TJ^{+} neurons are implicated in locomotion, I checked if TJ is expressed in already identified locomotor neuronal populations. TJ does not co-localize with iIN (Zwart et al., 2016) (Fig 27A), the GVLI population (Itakura et al., 2015) (Fig 27F-G), Eve and therefore the EL population (Heckscher et al., 2015) (Fig 27H-J) or lines (*R78F11-gal4*, *R79E03-gal4* and *R92C05-gal4*) characterized by Clark and collaborators (2016) and known, when used with *UAS-TrpA1*, to give rise to a ventral contraction of the larvae, a behaviour highly reminiscent to the one we observe upon activation of the TJ^{+} cholinergic subpopulation (Fig 27K-P). However, TJ partially co-localizes with two drivers used to delineate GDL population (Fushiki et al., 2016) (Fig 27B-E). More precisely, TJ co-localizes with two dorsal neurons per hemisegment with the *9-20-gal4* line (Fig 27B) and with three or more neurons per hemisegment

with the *R15C11-gal4* line (Fig 27C-E) but pinpointing GDL was impossible since these drivers are expressed in numerous other neurons.

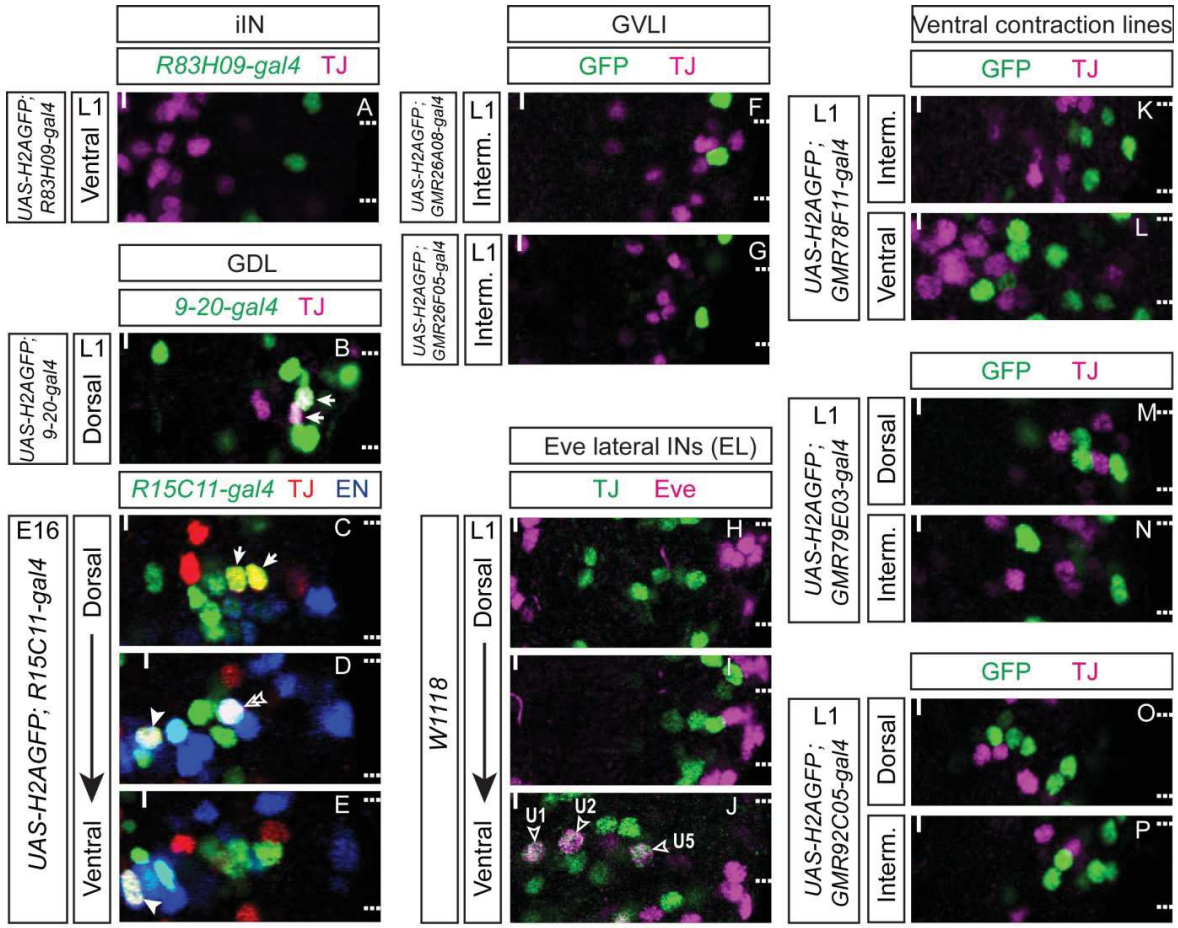

Fig 27: Co-localization of TJ$^+$ neurons with other previously characterized IN populations implicated in locomotion

A. Immuno-staining of first instar larva VNC for TJ (magenta) and nuclear GFP driven by *R83H09-gal4* driver that delineates iIN (green). No co-localization was found. **B.** Immuno-staining of first instar larva VNC for TJ (magenta) and nuclear GFP driven by *9-20-gal4* (green) that delineates GDL population. Co-localization was found in two dorsal neurons (arrows). **C-E.** Immuno-staining of stage 16 embryo VNC for TJ (red), Engrailed (blue) and nuclear GFP driven by *R15C11-gal4* (green) that delineates GDL population. Co-localization was found in two dorsal neurons (arrows in C), an intermediary ventral En$^+$ neuron (double empty arrowheads in D) and occasionally in midline TJ$^+$ MNB progeny neurons (full arrowheads in D and E). **F-G.** Immuno-staining of first instar larva VNC for TJ (magenta) and nuclear GFP driven by *R26A08-gal4* (green in F) and *R26F05-gal4* (green in G), two drivers that delineate GVLI population. No co-localization was found with TJ$^+$ neurons. **H-J.** Immuno-staining of first instar larva VNC for TJ (green) and Eve (magenta). Ventral TJ$^+$ U MNs U1, U2 and U5 co-localize with Eve (empty arrowheads in J). No other co-localizations were found. **K-P.** Immuno-staining of first instar larva VNC for TJ (magenta) and nuclear GFP driven by *R78F11-gal4* (green in K-L) or *R79E03-gal4* (green in M-N) or *R92C05-gal4* (green in O-P), three gal4 lines that, when used with *UAS-TrpA1,*

give rise to a ventral contraction phenotype (Clark et al., 2016). TJ did not co-localize with any of the three drivers. A single hemisegment is shown in each panel, with segments boundaries on the right (dashed lines) and midline location indicated on top left of the panel.

Last, I checked for the expression of TJ in Hugin neurons involved in the alternation between crawling and feeding CPGs (Schoofs et al., 2014). TJ is completely excluded from Hugin population located in the joining region between VNC and cerebellar lobe, the subesophageal zone (SEZ) in first and third instar larvae (Fig 28).

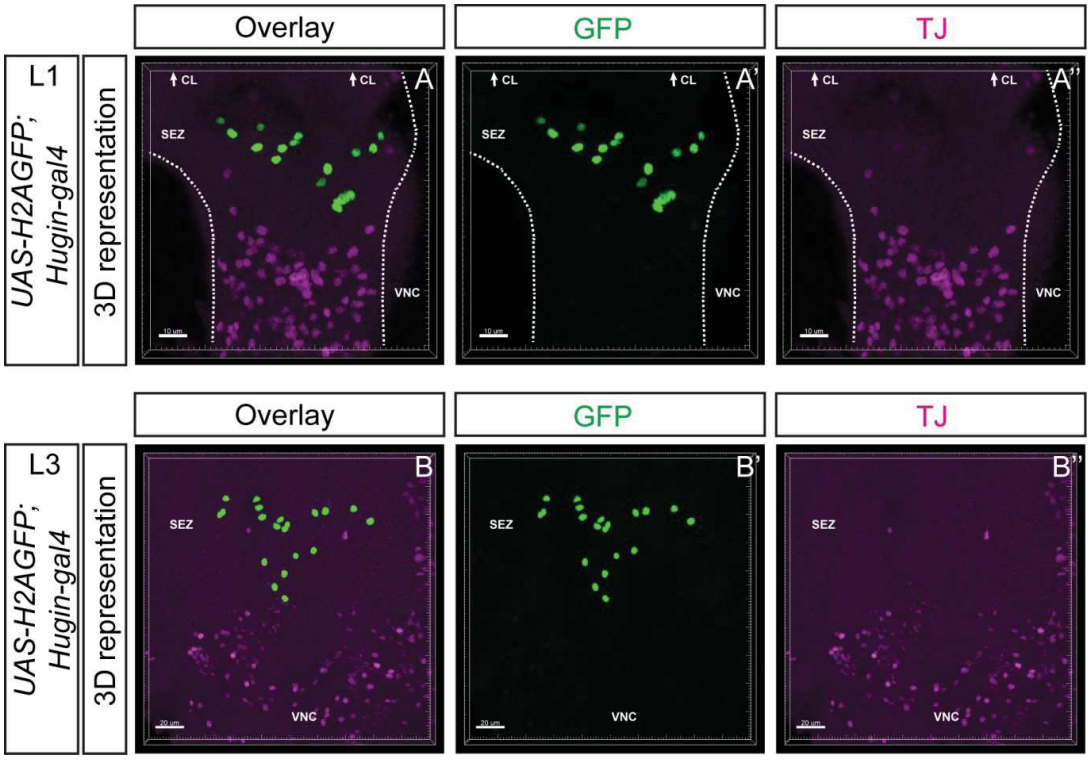

Fig 28: Absence of co-localization of TJ in Hugin neurons

A-A''. 3D reconstruction of first instar larva CNS immuno-stained for TJ (magenta) and nuclear GFP driven by *Hugin-gal4* (green). TJ is not expressed in the Hugin neurons in first instar larva. **B-B''**. 3D reconstruction of third instar larva CNS immuno-stained for TJ (magenta) and nuclear GFP driven by *Hugin-gal4* (green). TJ is not expressed in the Hugin neurons in third instar larva. All panels are reconstruction of the SEZ located between the VNC and the cerebellar lobes. CL= cerebellar lobes; SEZ= subesophageal zone ; VNC= ventral nerve cord

b- Molecular characterization

In parallel to the functional characterization of TJ^+ population, additional immunostainings were carried out to extend the molecular characterization of the TJ^+

population. First I confirmed that TJ is not expressed in TrpA1-expressing neurons (Kim et al., 2010) in the CNS (Fig 29A-D). Additionally, I found that TJ co-localizes with Fd59a in two dorsal and one ventral neurons per hemisegment (Fig 29E-F).

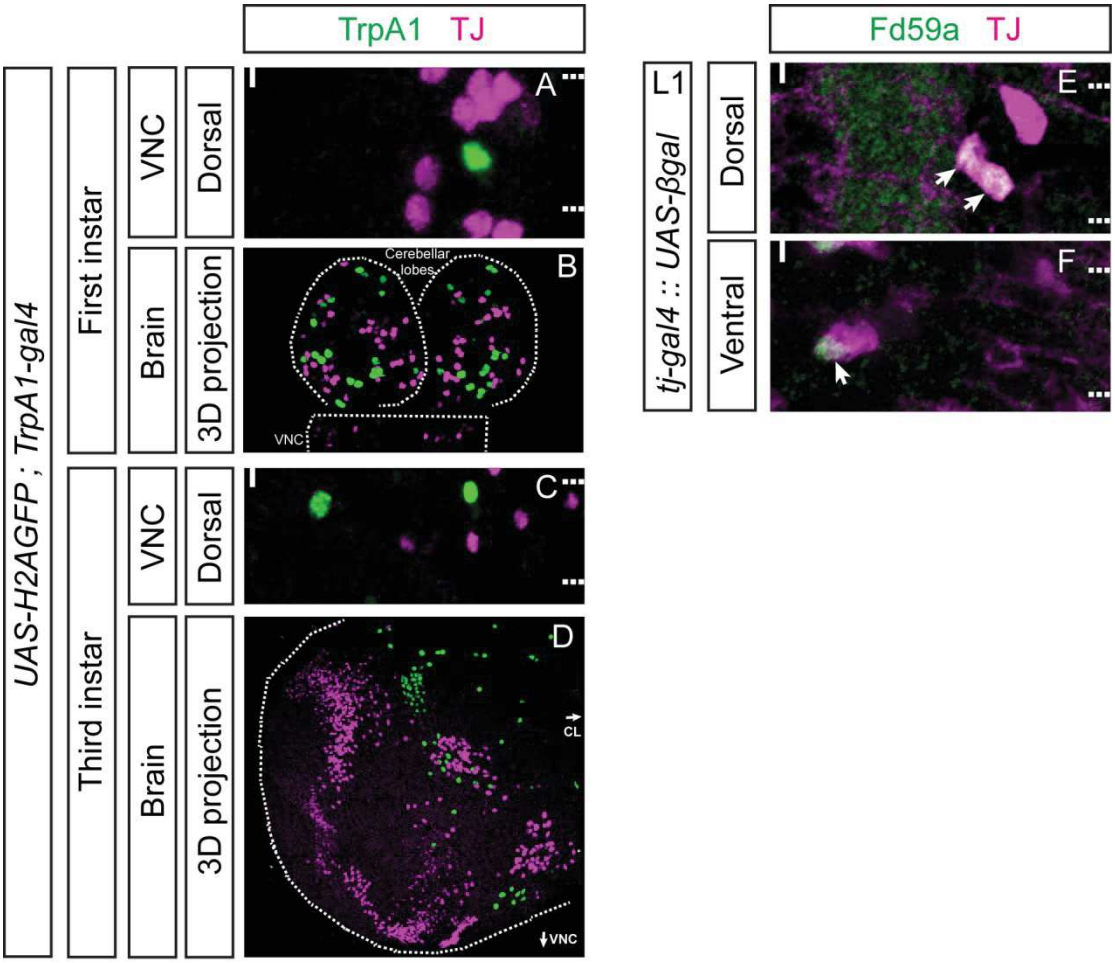

Fig 29: TJ is excluded from *TrpA1-gal4*-expressing neurons and co-localizes with 3 Fd59a^{+} neurons per hemisegment.

A-B. Immuno-staining of first instar larva VNC and brain lobes for TJ (magenta) and nuclear GFP driven by *TrpA1-gal4* (green). There is no co-localization between TJ^{+} neurons and TrpA1-expressing neurons in the VNC or the cerebellar lobes in first instar larva. **C-D.** Immuno-staining of third instar larva VNC and brain lobe for TJ (magenta) and nuclear GFP driven by *TrpA1-gal4* (green). There is no co-localization between TJ^{+} neurons and TrpA1-expressing neurons in the VNC or the cerebellar lobes in third instar larva. **E-F.** Immuno-staining of first instar larva VNC for β-gal driven by *TJ-gal4* (magenta) and Fd59a (green). TJ co-localizes with Fd59a in two dorsal neurons and one ventral neuron (arrows in E and F). For A,C,E and F, a single hemisegment is shown in each panel, with segment boundaries on the right (dashed lines) and midline location indicated on top left of the panel.
B and D are 3D reconstruction of respectively 2 and 1 cerebellar lobes of first and third instar larvae.
CL= cerebellar lobe, VNC= Ventral Nerve Cord

3. Morphological characterization of the TJ$^+$ MNB progeny neuron population

During this PhD, three TJ$^+$ MNB progeny neurons per segment were found to control of the speed of locomotion in *Drosophila* larva. I did a thorough molecular characterization the TJ$^+$ MNB progeny neurons and went a step further to look at their morphology.

TJ$^+$ MNB progeny neurons morphology was observed by two means: first it was observed using an intersectional genetics approach with *TJ-gal4*, *Gad1-lexA*, *lexAop-Flp* and *UAS>>CD8GFP*. This genetic approach is inefficient, therefore only a limited number of TJ$^+$ GABAergic neurons per VNC express CD8GFP, which allows to track their morphology (Fig 30A, B, C). A TJ$^+$ MNB progeny neuron labelled with CD8GFP was identified easily thanks to its position at the midline in the most-ventral part of the VNC and its expression of Engrailed (Fig 30A and 30D, full arrowhead). The TJ$^+$ MNB progeny neuron seems to send a single neurite straight up dorsally, that then divides in two to follow both sides of the neuropile, spanning several segments anteriorly and posteriorly to the segment where the cell body is located (Fig 30A). Other TJ$^+$ GABAergic are expressing GFP close to the arborescence of the TJ$^+$ GABAergic neuron, therefore we cannot affirm that the neurites visualized are strictly TJ$^+$ MNB progeny neuron's. Second, we used the *GMR47G08-lexA* line. Indeed, we found that this line drives in one to two TJ$^+$ MNB progeny neurons per segment. To visualize the TJ$^+$ *GMR47G08-lexA*$^+$ cells, I used the intersectional genetics approach with *TJ-Flp* and l*exAop>>CsChrimson*^{Venus}. Morphology of the labelled TJ$^+$ MNB progeny neuron can be seen thanks to the endogenous signal of the Venus-tag attached to CsChrimson. In the VNC presented in Fig 30E, endogenous Venus signal was detectable with different intensities in three MNB progeny neurons located in three adjoining segments (asterisks, Fig 30E). One of the TJ$^+$ MNB progeny neuron located in segment A5 was particularly strongly labelled, with its neurites fully visible. Its morphology is highly reminiscent of the one observed with the first approach; a single neurite going upward and then dividing to follow both sides of the neuropile, in both anterior and posterior directions (Fig 30E, close-ups in Fig 30F, G, H). The TJ$^+$ MNB progeny neuron morphology we find is radically different from the morphology of the PMSI population that was characterized by Kohsaka and collaborators (2014). Indeed, PMSIs (including TJ$^+$ *per*$^+$ glutamatergic

neurons) have a “lasso” morphology, with axons extending to the dorsal neuropile region after having gone through a lateral “loop” (Fig 30I, J and K).

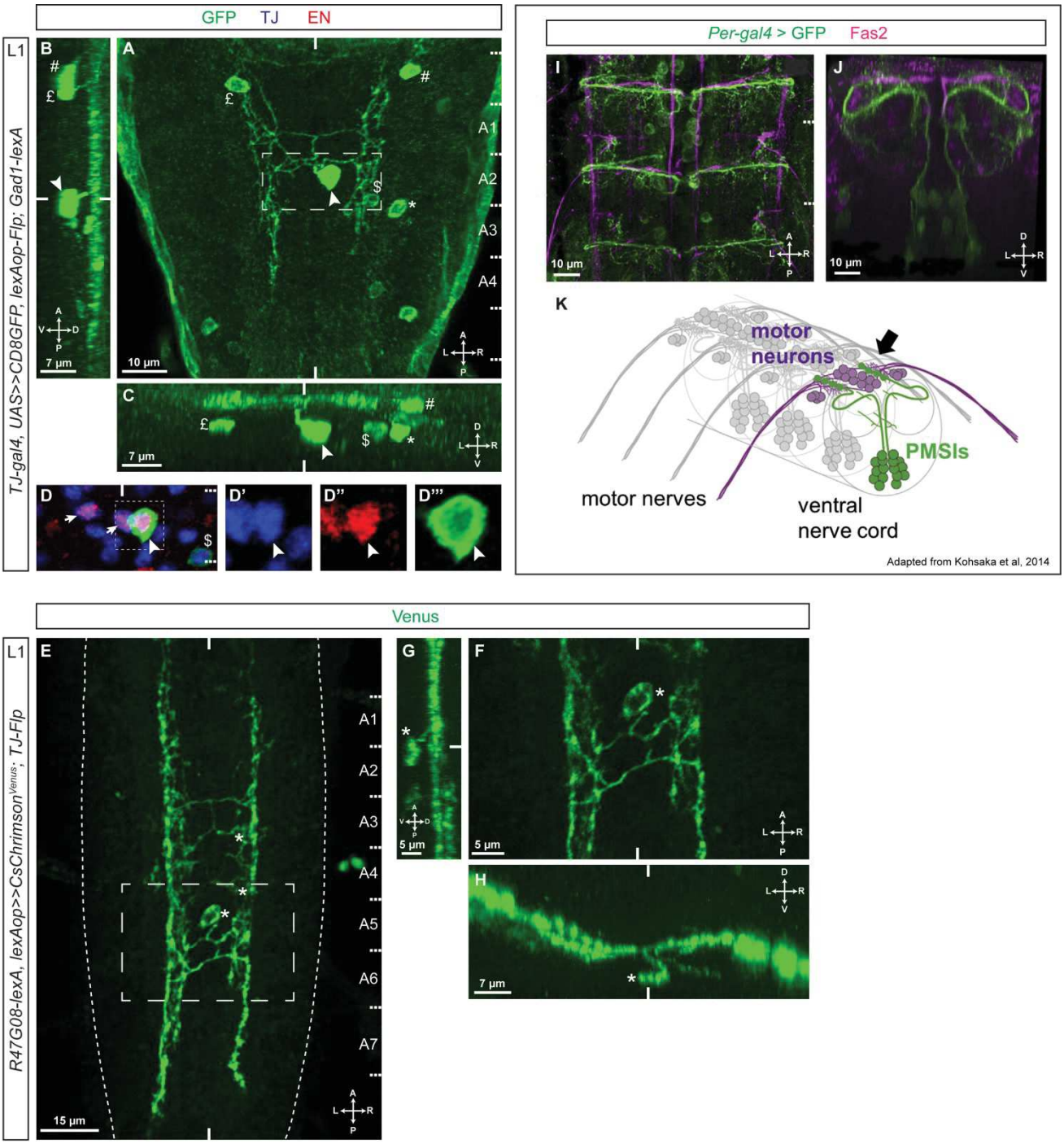

Fig 30: TJ$^+$ MNB progeny neuron morphology (preliminary data)

A, B, C, D. Immuno-staining of a first instar larva VNC for TJ (blue), engrailed (red) and CD8GFP (green) driven by the coordinated expression of *TJ-gal4* and *Gad1-lexA* – GFP$^+$ cells are necessarily TJ$^+$ GABAergic neurons. **A**. Dorsal view of the 3D projection of the VNC. To clearly visualize the projections of the cells, the engrailed and TJ stainings have been removed. TJ$^+$ MNB progeny neuron is recognizable by the position of its cell body at the midline (full arrowhead). Its projections go to both

sides of the VNC and span several segments posteriorly and anteriorly. Anterior of the VNC is up, midline denoted by full line and segment boundaries by dashed lines to the right. **B**. Lateral view of the 3D projection of the VNC. GFP-labelled TJ^+ MNB progeny cell body is located ventrally (arrowhead). From there the MNB progeny neuron sends a neurite upward which then runs anteriorly and posteriorly. Midline is denoted by the full lines on the right and left of the panel. **C** .Posterior view of the 3D projection of the VNC. The upward neurite sent by the TJ^+ MNB progeny neuron then divides and goes to both sides of the VNC midline. The midline is denoted by the full lines at the top and bottom of the panel. GFP^+ TJ^+ GABAergic non-MNB progeny neurons cell bodies are labelled with #, $, £ and * in **A**, **B** and **C**. **D**. Inset of the cell body of the MNB progeny neuron showing its expression of TJ and en (arrowhead). The two other TJ^+ MNB progeny neurons located in the segments and that do not express GFP are visible (arrows). **E-H**. First instar larva VNC with endogenous Venus signal driven by coordinated expression of *TJ-Flp* and *GMR47G08-lexA* driver. **E**. Dorsal view of the 3D projection of the VNC. Neurites arbours of 3 MNB progeny neurons located in three adjacent segments are visible (cell bodies position signalled by asterisks). Midline position is denoted by the full lines at the top and bottom of the panel and the segment boundaries are signalled to the right. **F-H**. Close-up of the 3D reconstruction shown in E. **F**. Dorsal view of the most strongly labelled MNB progeny neuron (located in A5 abdominal segment). The MNB progeny neuron sends projections to both sides of the VNC, anteriorly and posteriorly. **G**. Lateral view of the 3D projection of the VNC. The MNB progeny neuron cell body is located ventrally and sends a projection dorsally that then runs anteriorly and posteriorly. Midline is denoted by the full lines on the right of the panel. **H**. Posterior view of the 3D projection of the VNC. The upward neurite sent by the TJ^+ MNB progeny neuron then divides and goes to both sides of the VNC midline. The midline is denoted by the full lines at the top and bottom of the panel. Projections are wavy because the VNC was slightly twisted during dissection. **I-J**. Anatomy of *Per-Gal4*-expressing cells (PMSIs) in third instar larva seen dorsally (**I**) and from a posterior view (**J**). These neurons project dorsally, then turn laterally and make a loop to finally terminate in the dorsal neuropile region. **K**. Schematic drawing of the PMSI morphology. **I-K** are adapted from Kohsaka et al, 2014.

My preliminary results require confirmation, but I can already say that TJ^+ MNB progeny neurons have a particular morphology, distinct from that of other per^+ glutamatergic neurons.

Chapter 4: Effects of the activation of TJ^+ neurons in adult flies

I. Introduction

Modulation of TJ^+ neurons activity in *Drosophila* larva gives rise to an alteration in locomotion, proving that those neurons are part of the locomotor CPG in the larval life stage. I wondered if this also applied to the fly imago, namely if activating TJ^+ neurons in the adult fly would modify its locomotor behaviour.

II. Results

1. Whole TJ^+ population activation

I first decided to study the effects of the whole TJ^+ population activation using *TJ-gal4* and *UAS-TrpA1* (the same genetic approach as used in larvae). Flies were placed in an incubator at 31°C for variable times and then observed directly in their containers or under anaesthesia for gross anatomical defects.

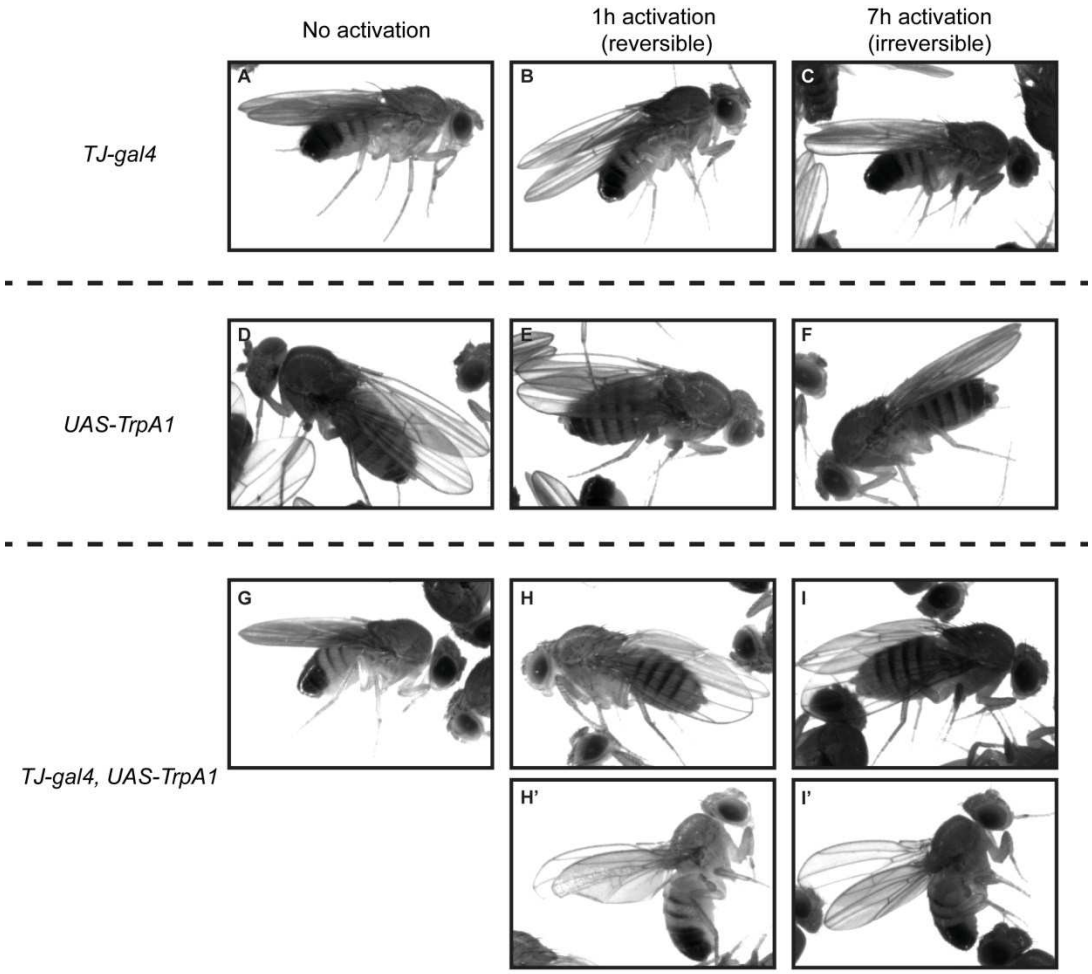

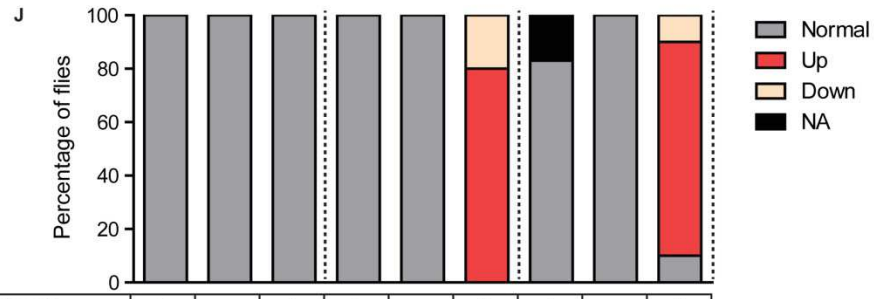

TJ-gal4	+		+	+		+	+		+
UAS-TrpA1		+	+		+	+		+	+
Length of activation	None			1h (reversible)			7h (irreversible)		
Number of flies tested	9	10	10	6	9	10	6	9	10

Fig 31: Effect of the activation of TJ$^+$ neurons on adult flies wing position.

A-I'. Pictures of flies of different genotypes with no activation, short activation or long activation of TJ$^+$ neurons. **J**. Percentage of flies with different wing positions (normal, up or down) depending on genotype and duration of the activation. NA= non applicable: in this case it denotes fly death.

Upon activation of the whole TJ$^+$ population in adult flies, the most striking phenotype was a displacement of the wings, either up (wings raised straight above the fly back Fig 31H') or down (wings drooping on either side of the fly body – Fig

31H). Those wing phenotypes are indeed caused by the whole TJ^+ population activation, as all control flies carrying either one of the two transgenes had normal wings position after short (1h – Fig 31B and 31E) or long period of time spent at 31°C (7h – Fig 31C and 30F). Displacement of wings was visible after only 10 minutes of 31°C "treatment" and was reversible when the flies were returned to room temperature (about 21°C). However after a long period of activation (>2h), the displacement of the wings was irreversible (Fig 31I and 31I'). I also noticed that upon activation of the whole TJ^+ population, the flies were mainly non-active, staying immobile at the bottom of the tube.

2. Activation of TJ^+ subpopulations

Next I decided to activate TJ^+ cholinergic, glutamatergic or GABAergic subpopulations using the same intersectional genetics approach as used in larvae (see results in the article). Control flies that do not carry all the transgenes required for TJ^+ neurons activation showed no obvious phenotype and normal wing positions (Fig 32B and 32C). When TJ^+ cholinergic neurons were activated, the majority of flies (80%) had down-turned wings after both short and long-term activation (Fig 32E and 32F). Moreover, the flies displayed excessive grooming activity, with both fore and hind limbs used to groom the head and wings. When activating TJ^+ glutamatergic population, a majority of flies (69%) had their wings up (Fig 32H' and 32I'). Activation of TJ^+ GABAergic did not give rise to any obvious phenotype at short or long-term, including no wing phenotype (Fig 32K and 32L). Just as I observed upon activation of the whole TJ^+ population, wing phenotypes were reversible when length of activation was short (1h) but became irreversible after 7h of activation (Fig 32F, 32I and 32I'). Grooming phenotype observed when activating TJ^+ cholinergic neurons remained reversible even after a long activation period.

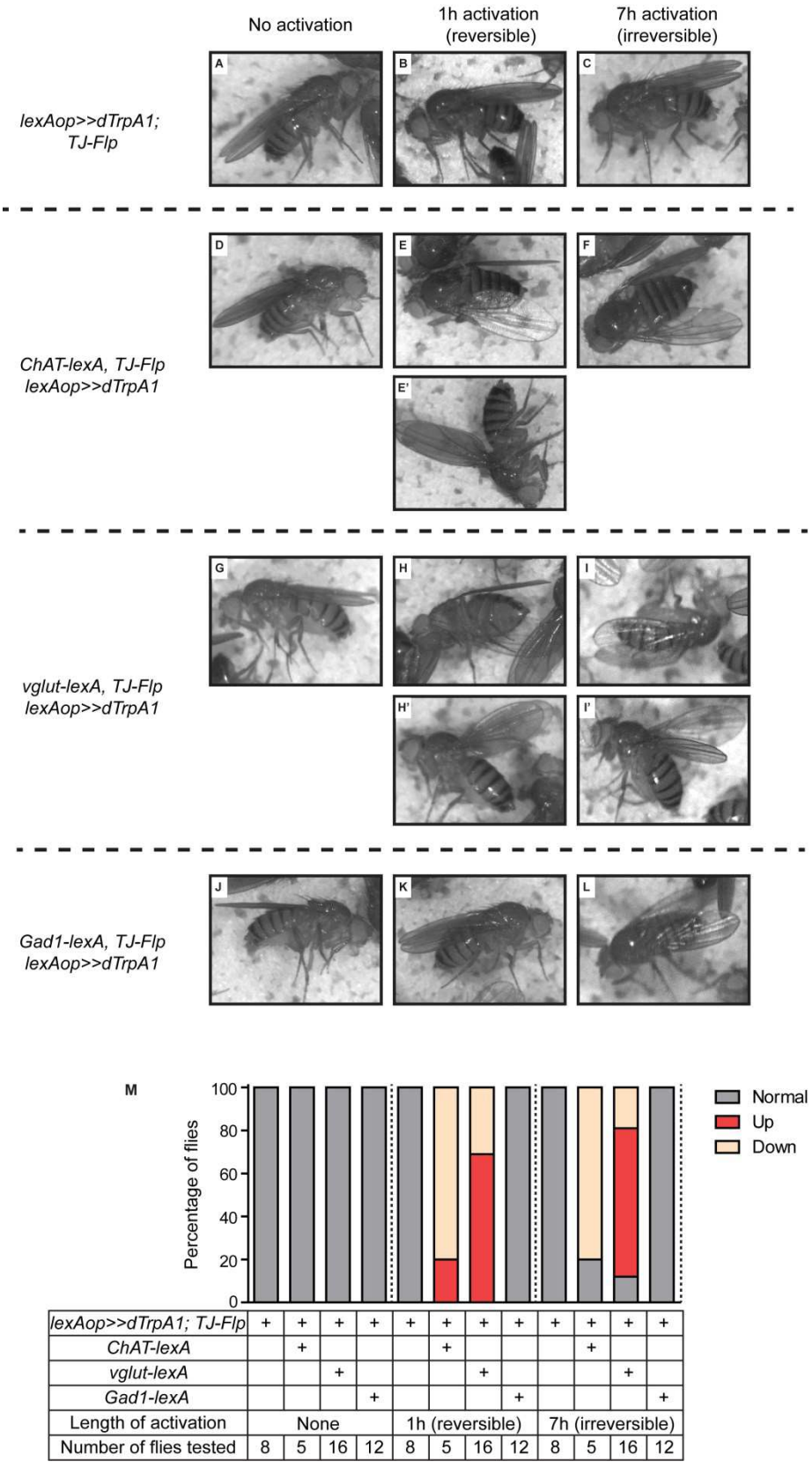

Fig 32: Effect of the activation of TJ^+ neuron subpopulations on adult flies wing position.

A-L . Pictures of flies of different genotypes with no activation, short activation or long activation of TJ^+ neuron subpopulations. **M**. Percentage of flies with different wing positions (normal, up or down) depending on genotype and duration of the activation.

Chapter 5: Discussion

I. Comparison of the different genetic approaches used

In the course of my PhD, intersectional genetics technique was applied through five different genetic approaches that have been variously successful. Table 5 recapitulates the genetic tools used for each of the intersectional genetics approaches.

	Approach 1	Approach 2	Approach 3	Approach 4	Approach 5
TJ-gal4	×				
TJ-Flp		×	×	×	×
UAS>>TrpA1^{myc}	×				
lexAop>>dTrpA1		×	×	×	×
lexAop-Flp	×				
UAS-lexA			×		
lexA drivers : *vglut-lexA* *ChAT-lexA* *Gad1-lexA* *Per-lexA* *tsh-lexA* *CQ2-lexA* *RapGAP1-lexA*	×	×			
gal4 drivers : *LMO-gal4* *HB9-gal4* *OK6-gal4* *Abd-gal4* *Dac-gal4*			×		
UAS-lexA^{DBD}				×	
Per-gal4				×	
Gad1^{AD}				×	
lexAop>>CsChrimson^{Venus}					×
Readout of the expression	YES (myc-tag)	NO	NO	NO	YES (Venus tag)
Outcome	Not efficient	Efficient	Not efficient	Partially efficient?	Efficient (preliminary)

Table 5: Recapitulative table of the transgenes used for each of the intersectional genetics approaches used in this work.

Approach 1 results are described in Chapter 3, section II.D.1.a. Approach 2 is the most efficient approach we used and results are presented mainly in the article and chapter 3, section II.D.1.b. Third approach results are presented in chapter 3, section II.D.1.c. Approach 4 (or triple intersection) is

probably only partially efficient and results are presented in the article. Finally approach 5 is currently being implemented (chapter 3, section II.D.1.e); from the preliminary results obtained it seems that this approach is efficient.

The sole efficient approach I used is approach 2, with the *TJ-Flp*, a *lexAop>>dTrpA1* cassette and various lexA drivers. The success of this approach might lie in the limited number of transgenes used. It might also function properly because the lexA drivers used are strong drivers, as could be expected of drivers placed under the control of neurotransmitter genes for example in the case of *ChAT-lexA*, *Gad1-lexA* and *vglut-lexA*. A downside of this approach lies in the absence of readout of the proper expression of the TrpA1 protein in the targeted cells.

The approach I initially used (Approach 1 in the table) relies on the use of *TJ-gal4*, *UAS>>TrpA1^{myc}* cassette and different lexA drivers whose expression is "converted" in Flp by a *lexAop-Flp*. As TrpA1 is myc-tagged, I was able to monitor for its proper expression in the targeted cells (see complementary figure 4 in article). Despite clear expression of TrpA1, I failed to observe clear phenotypes upon activation of TJ^{+} subpopulations. Does it mean that function of TrpA1^{myc} is impaired? *UAS>>TrpA1^{myc}* cassette has been mostly used in the adult fly to study courtship singing and aggression in male flies (Hoopfer et al., 2015; von Philipsborn et al., 2011). Von Philipsborn and collaborators (2011) reported that use of the stop cassette TrpA1 requires higher temperature – an increase of 2 to 3°C - to illicit the same song behaviour in flies as with direct TrpA1 expression. The authors hypothesize that because TrpA1 expression relies on the combined expression of two transgenes, it might consequently be low. In Hoopfer et al. (2015) it was reported that TrpA1^{myc} transgene was expressed at low levels and in a variable pattern in the targeted cell population. In larvae, *UAS>>TrpA1^{myc}* cassette was used in one report for the study of the rolling-command neurons Goro (Ohyama et al., 2015). Their genetic approach is similar to ours; using a *lexAop-Flp* with a lexA driver, a gal4 driver and the *UAS>>TrpA1^{myc}* cassette. They reported that expression of TrpA1 in the appropriate neurons (Goro) triggered the awaited behaviour (rolling) in only 76% of cases, showing that the technique is only partially effective. They highlighted the fact that the gal4 driver driving the expression of TrpA1 once the recombination had occurred was a strong driver.

In those articles the use of the *UAS>>TrpA1*^{myc} cassette gave results, albeit variable in efficiency. In our case why is this genetic approach failing? First of all, it is worth noting that the cassette has been mainly used in adult flies; the biological system considered is therefore different. Second, although we know from our immunostaining that TrpA1^{myc} is correctly expressed in the targeted cells, levels of expression might be too low to efficiently activate TJ^{+} neurons upon reaching 31°C. Indeed the levels of expression of TrpA1^{myc} are a subject of concern in all three articles cited above (Hoopfer et al., 2015; Ohyama et al., 2015; von Philipsborn et al., 2011); moreover as mentioned above, Ohyama et al. (2015) emphasize the fact that the gal4 driver used is strongly expressed. *TJ-gal4* driver expression levels vary among cells, thus some cells might express low levels of TrpA1^{myc}. Lastly, let us not forget that TrpA1 is tagged with myc. Addition of a tag on a protein may have negative effects, including changes in protein folding and alterations in their function (Arnau et al., 2006). TrpA1^{myc} protein conformation might be slightly changed and its activity as an ion channel might be decreased. From the negative results obtained using this genetic approach we draw a conclusion to be shared with the scientific community: results of intersectional genetics experiments obtained in larvae with this cassette should be treated with caution, as the risk of false negatives is high.

The third approach I used relies on *TJ-Flp* and *lexAop>>dTrpA1* cassette as well as different gal4 driver that are converted to lexA by a *UAS-lexA* transgene. Yet again I have no way of monitoring the proper expression of TrpA1. However the functional positive control I used (utilising *TJ-gal4* as the driver) was meant to give rise to the fully contracted, characteristic phenotype observed upon activation of the whole TJ^{+} population. This was not the case. Implementation of this approach with other gal4 drivers to activate other TJ^{+} subpopulations mostly gave no locomotor phenotype, apart from the *LMO-gal4* driver. We may hypothesize that *LMO-gal4* is a stronger gal4 driver compared to the other drivers we used, which might explain why we do have a phenotype when we use it.

The final approach I used (Approach 4 in the table) was a triple intersectional genetics approach; I combined yet again the *TJ-Flp* and *lexAop>>dTrpA1* cassette and a full functional lexA rebuilt from a lexA^{DBD} expressed under the control of *Per-gal4* driver and *Gad1*^{AD}. Here again I cannot visualize the expression of TrpA1. This approach gives rise to heterogeneous phenotypes. Is it due to a technical problem with the genetic approach, where all TJ^{+} MNB progeny

neurons are not properly expressing TrpA1 and are therefore not all activated during the experiment? Presently we are unable to conclude.

I am currently working on a last approach (Approach 5 in the table) using *TJ-Flp* and various lexA drivers along with a *lexAop>>CsChrimson* cassette (Hoopfer et al., 2015). In this approach I am no longer using temperature-activated proteins like TrpA1 but light activated proteins (CsChrimson) to activate the neuronal populations of interest. This last approach is compelling for three reasons: first it will allow me to confirm the results obtained with the second approach (*TJ-Flp, lexAop>>dTrpA1*, various lexA drivers). Second, CsChrimson is venus-tagged, which allows me to follow its expression in the neuronal population of interest. Finally the use of such an optogenetic technique allows for activation of neurons independently of the temperature, a parameter which by itself impacts the larvae locomotion speed (Iyengar et al., 2011). Additionally CsChrimson can be used in the context of approach 4 to confirm if indeed all TJ^+ MNB progeny neurons are being targeted in this genetic approach.

II. TJ delineates a new neuronal population implicated in locomotion

TJ expression in the CNS of *Drosophila* larva has never been studied before. Results obtained during the course of my PhD show that TJ is expressed in a restricted neuronal population of 29 neurons per hemisegment in the VNC and that TJ^+ neurons have a functional implication in locomotion. The majority of TJ^+ neurons do not co-localize with known markers of already characterized locomotor neuronal populations. However, TJ does co-localize with a subpopulation of previously characterized PMSI neurons (Kohsaka et al., 2014) and we show that this TJ^+ PMSI subpopulation has a functional role in locomotion. TJ also co-localizes with drivers expressed in GDL neurons (Fushiki et al., 2016); however in our hands those drivers are expressed in large neuronal populations and it is not yet possible to affirm that the co-localization is indeed occurring in the GDL IN. We hypothesize that TJ is not expressed in GDL, as the phenotype obtained in freely moving larvae upon activation of the GDL is characterized by a contracted paralysis of the posterior segments of the larva (Fushiki et al., 2016), which is quite different from our own TJ^+ GABAergic

activation phenotype with its apparent normal, though slowed locomotion. Regardless, further characterization would be required to answer this question.

III. Role of TJ$^+$ cholinergic neurons in *Drosophila* larva locomotion

Electrical activation of the TJ$^+$ cholinergic subpopulation gives rise to a ventral contraction phenotype, with larvae adopting a “crescent shape” position. This phenotype was previously reported once by Clark and collaborators (2016). In two of the lines they tested, this phenotype arose from the activation of ventral acute, ventral oblique and ventral longitudinal muscle groups. Those muscle groups are innervated by MNs who project their axons through ISNb, ISNd (namely *Islet*$^+$ MNs) and SNc nerves (Fig 13B). Therefore we can hypothesize that at least some of the TJ$^+$ cholinergic INs innervate ISNb, ISNd and/or SNc MNs, either directly or through excitatory relays. How many ventrally-projecting MNs are being contacted by TJ$^+$ cholinergic INs? Activating *HB9*$^+$ MNs (which belong to the ISNb and ISNd nerves and innervate the acute and longitudinal ventral muscles – Fig 13B) as well as other HB9$^+$ INs using a *HB9-gal4>UAS-TrpA1* approach does not produce a “crescent” shape phenotype in the larvae (preliminary data not shown). Therefore, as our phenotype is more drastic, it is tempting to say that TJ$^+$ cholinergic INs innervate all of the ventrally-projecting MNs, but at this time I cannot bring any solid proof in this direction. What could be the role in locomotion of an IN population solely innervating ventrally-projecting MNs? In the literature, the closest example that I could find with such a dichotomy in the innervations of different muscle groups is the example of the inhibitory iIN (Zwart et al., 2016). iIN specifically innervates “transverse” MNs and not “longitudinal” MNs, thus allowing for the sequential contraction of transverse and longitudinal muscles for an efficient contraction of the larval body segment. An interesting observation I made while activating TJ$^+$ cholinergic INs is that some larvae (3 out of 18 larvae, or 16% of the larvae tested) would roll on themselves, a behaviour I never saw with any other genotype. The command neurons for rolling behaviour, called Goro neurons, are instrumental in protecting *Drosophila* larva against parasitoid wasps attacks (Ohyama et al., 2015). Rolling is also triggered in larvae in a desperate attempt to escape fast rising temperatures in the environment (Luo et al., 2017), a behaviour yet again mediated by the Goro neurons (Burgos et al.,

2018). Although the “sensory side” that gets rolling-command Goro neurons activated is being actively studied and getting well characterized by this point (Burgos et al., 2018; Ohyama et al., 2015), the locomotor effectors (INs and MNs) that are then innervated by Goro neurons are presently not known. Nor is the exact muscles contraction sequence that allows for the larva to roll. Resolving this question might be made easier by the optimization of tracking tools to detect and quantify rolling behaviours (Risse et al., 2015). In the meantime, knowing if TJ^+ cholinergic INs are involved in the Goro-related circuit might prove tricky; two scenarios are possible. Either TJ^+ cholinergic INs are direct synaptic partners of Goro neurons, or they are part of their downstream circuit in the midst of other neuronal relays. If TJ^+ cholinergic neurons and Goro neurons are direct synaptic partners, it would be possible to prove it by implementing a GRASP (GFP Reconstruction Across Synaptic Partners) approach (Feinberg et al., 2008; Macpherson et al., 2015). Briefly, in GRASP technique, two neuronal populations are made to express split parts of the GFP. Those GFP subunits are targeted to the outer membrane of the synapse. When the GFP subunits are brought close enough to one another (ie, when the neurons that express the two parts of the GFP are forming synapses), the GFP is reconstructed and emits fluorescence. In our case, we would have part of the split GFP expressed in Goro neurons thanks to a specific driver, *R69F06-gal4* (Ohyama et al., 2015), and the other part of the split GFP expressed in TJ^+ cholinergic neurons thanks to a published flip-out GRASP cassette (Fig 33) (Karuppudurai et al., 2014).

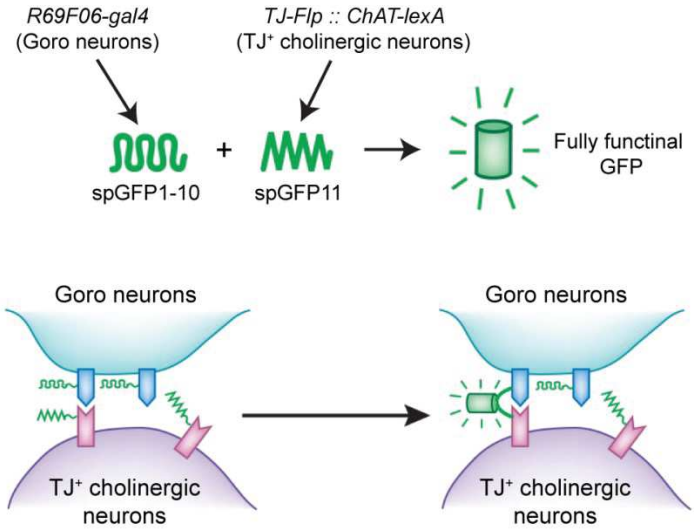

Fig 33: GRASP experiment proposed to test for Goro neurons and TJ^+ cholinergic putative synapses

The GRASP method is based on a protein complementation assay using a split GFP. If the split parts of the GFP (spGFP1-10 and spGFP11) are brought close enough to one another as is the case when a synapse is formed, the GFP is "rebuilt" and functional, emitting fluorescence. To know if Goro neurons directly form synapses onto TJ^+ cholinergic neurons, we propose to have the Goro neurons expressing the spGFP1-10 split part of the GFP (thanks to the *R69F06-gal4* specific driver and a *UAS-spGFP1-10* transgene) and the TJ^+ cholinergic neurons expressing spGFP11 subunit (thanks to the combination of the transgenes *TJ-Flp*, *ChAT-lexA* and *lexAop>stop>spGFP11*). Adapted from (Miyawaki, 2010).

If TJ^+ cholinergic INs are placed in the downstream circuit of Goro neurons amidst other neuronal relays, it may be more complicated to prove it. We might in this case rely on TEM technique to find the Goro neurons synaptic partners and try to rebuild the whole neuronal circuit down to the TJ^+ cholinergic neurons; however this would be hard, time-consuming work (Schneider-Mizell et al., 2016). A functional way of proving that TJ^+ cholinergic INs are part of the downstream circuit of Goro neurons would be to inhibit TJ^+ cholinergic INs activity while activating Goro neurons; if TJ^+ cholinergic neurons are indeed part of the Goro effecting circuit, we would expect the rolling induced by Goro neurons to be reduced. To inhibit TJ^+ cholinergic neurons we may use a *UAS>>shi^{ts}* cassette or if this approach fails, we could alternatively remove TJ^+ cholinergic population by killing it. We already tried to use a *UAS>>ricin* cassette [Gift from C. O'Kane (Allen et al., 2002)] that was not efficient in our hands; we will be soon testing a *UAS>>hid* cassette (Gift from Jonathan Enriquez) (Shang et al., 2008) that might prove more effective. An additional pathway independent of Goro neurons and involved in the control of rolling also exists, and is mediated by

mCSIs and SNa (*BarH1/2*$^{+}$) MNs. It is known that activation of mCSIs induces SNa MNs activation, but GRASP experiments showed that mCSIs do not directly synapse on SNa MNs (Yoshino et al., 2017). Could TJ^{+} cholinergic INs be the missing link between mCSIs and SNa MNs? To test this hypothesis, we could, as suggested above in the study of the Goro neurons pathway, use GRASP to see if TJ^{+} cholinergic neurons are presynaptic to SNa MNs [that can be targeted with the *BarH1/2-gal4* driver (Yoshino et al., 2017)], or if they are post-synaptic to mCSIs [than can be targeted with the *R94B10-gal4* driver (Yoshino et al., 2017)].

IV. Role of TJ^{+} glutamatergic neurons in locomotion

My results on the functional role of TJ^{+} glutamatergic INs are hindered by the fact that when using *vglut-lexA* as a driver to activate this population, I am targeting both TJ^{+} MNs and TJ^{+} INs. Therefore I cannot really know the locomotor effects generated by the activation of TJ^{+} glutamatergic INs alone. TJ^{+} glutamatergic population comprises 6 MNs (U1, U2, U5, DO5 MN and 2 lateral *Islet*$^{+}$ ISNd MNs), 3 ventral PMSI INs and 2 dorso-lateral INs. We have hints of the implication of TJ^{+} MNs on locomotion thanks to two experiments that use non-optimal drivers (*RapGAP1-lexA*, *CQ2-lexA*) and that give us only half-conclusions. Although TJ^{+} MNs activation leads to a defect in locomotion, it seems unlikely it would cause by itself the immobility phenotype generated by the activation of the whole TJ^{+} glutamatergic population. Activation of the TJ^{+} PMSIs reduces the speed of locomotion through a partial relaxed paralysis of the posterior segments of the larvae; yet again, these neurons do not cause by themselves the immobility phenotype observed. It might be possible that the dorso-lateral glutamatergic TJ^{+} INs activation also has an effect on locomotion and that simultaneous activation of the MNs, the TJ^{+} PMSIs and the dorso-lateral INs eventually leads to the immobility phenotype observed. Alas, yet again what we are missing are specific, strong drivers to manipulate those different TJ^{+} subpopulations. It would be informative to activate specifically the TJ^{+} *per*$^{+}$ glutamatergic neurons (3 ventral cells per hemisegment) using a triple intersectional genetics approach similar to the one I used to activate the TJ^{+} *per*$^{+}$ GABAergic neurons; I would then be using *TJ-Flp* in combination with *Per-gal4*, *UAS-lexA*^{DBD} and *vglut*^{AD}. Unfortunately I am lacking the *vglut*^{AD} transgene to implement this approach. It seems that with the current technologies available I will

hardly be able to go any further in the characterization of the TJ^+ glutamatergic population.

V. Role of TJ^+ GABAergic neurons in locomotion

Activation of 9 TJ^+ GABAergic neurons by TrpA1 temperature-dependent experiments gives rise to an apparently normal, though slowed locomotion, with a number of waves close to the numbers done by the larvae at 23°C. Larvae tend to crawl faster when the temperature exceeds their 24°C comfort temperature (in young L3) (Sokabe et al., 2016). This made us wonder if TJ^+ GABAergic neurons could be part of the temperature sensing system that detects uncomfortable temperatures and induces acceleration in larvae. I therefore used *TrpA1-gal4* to show that TJ^+ neurons do not express TrpA1, one of the ion channels responsible for the detection of uncomfortable temperatures (Kwon et al., 2008). I then decided to use optogenetics experiments to activate TJ^+ GABAergic neurons, allowing me to activate these neurons in a temperature independent manner. Preliminary results show that upon activation of TJ^+ GABAergic neurons with optogenetics, larvae display a decrease in the speed of locomotion of similar magnitude to the one observed when using TrpA1-based assay. This result therefore suggests that TJ^+ GABAergic neurons are not part of a temperature sensing neuronal circuit that allows the larva to adapt its speed in response to temperature variations.

To further study the TJ^+ GABAergic population, I used a triple intersectional genetics approach to subdivide it, targeting 3 TJ^+ per^+ GABAergic neurons per segment. Activation of the 3 TJ^+ GABAergic neurons gave rise to a somehow slowed locomotion phenotype as well, but less drastic than the one observed upon activation of the whole TJ^+ GABAergic population. The 3 TJ^+ per^+ GABAergic neurons might therefore be only partially responsible for the slowed locomotion phenotype observed upon activation of the whole TJ^+ GABAergic population. It is paramount to note that the per^+ GABAergic population was overlooked in the previous characterization of the per^+ population (PMSI population). It might be due to low *period* expression in TJ^+ per^+ GABAergic neurons, especially in third instar larvae in which the characterization was done (Kohsaka et al., 2014). PMSI population functional characterization showed that they are premotor INs that limit the burst of activity of MNs; inhibition of PMSI neurons leads to a decrease in the speed of locomotion

(Kohsaka et al., 2014). This functional characterization rested on the fact that all *per*$^+$ neurons are glutamatergic; to really know the impact of *per*$^+$ glutamatergic neurons on locomotion while excluding the role of *per*$^+$ GABAergic neurons, it would be necessary to specifically activate *per*$^+$ glutamatergic neurons using an intersectional genetics approach.

What can we infer from our characterization of the TJ$^+$ *per*$^+$ GABAergic neurons on their function in locomotion? In Kohsaka and collaborators (2014) article, functional characterization was done on the whole per$^+$ population, GABAergic and glutamatergic. Most of the *per*$^+$ population is glutamatergic, and seem to express *Per-gal4* at higher levels, as we just discussed in the previous paragraph. Therefore we can suppose that their functional characterization was actually performed on *per*$^+$ glutamatergic neurons. Thus TJ$^+$ *per*$^+$ GABAergic might have a different mode of action to regulate speed. Preliminary data suggest that TJ$^+$ *per*$^+$ GABAergic neurons have a particular morphology, different from that of TJ$^+$ glutamatergic neurons. As TJ$^+$ *per*$^+$ GABAergic neurons neurite arbours display bilateral innervations of the VNC, it is tempting to say that whatever information they relay needs to go to both sides of the VNC in a similar fashion, maybe synchronizing the two sides of the VNC. Furthermore, as the neurites of TJ$^+$ *per*$^+$ GABAergic neurons seem to unfurl in a ventral part of the neuropile and not in the dorsal part of the neuropile where the dendrites of MNs are located, I suppose that TJ$^+$ *per*$^+$ GABAergic neurons would not be premotor INs. Additional experiments are of course required to confirm the above-mentioned hypotheses.

My functional characterization of TJ$^+$ *per*$^+$ GABAergic population relies exclusively on observations made upon ectopic activation of this population. I wish to examine the effects of the genetic ablation of this population using a *UAS>>hid* transgene [Gift from J. Enriquez (Shang et al., 2008)] in combination with *TJ-Flp* and a *cut-gal4* line that we recently found and that constantly co-localizes exclusively with the TJ$^+$ *per*$^+$ GABAergic neurons (data not shown).

VI. Morphological characterization of TJ$^+$ MNB progeny neurons.

In *Drosophila*, midline cells development has been extensively studied and characterized (Fontana and Crews, 2012; Kearney et al., 2004; Manning et al., 2012;

Pearson and Crews, 2014; Tio et al., 2011; Watson and Crews, 2012; Wheeler et al., 2006; Wheeler et al., 2008; Heckscher et al., 2014). They arise from a *sim*$^{+}$ domain and form a heterogeneous population made of glial cells, INs and MNs. Midline cells, as their name indicates, lie at the ventral midline; they are for the most part unpaired, meaning they are unique in a segment and do not occur in bilaterally symmetrical pairs. Comparatively to the wealth of knowledge on the molecular code of midline cells, their morphology has been only sparsely reported, and only at embryonic stages (Bossing and Brand, 2006; Ruiz et al., 2010; Wheeler et al., 2006; Wheeler et al., 2008). Probably because they are unpaired cells located at the midline, most of them extend projections to both sides of the midline; this was reported for INs such as the H-cell, H-cell sib, the iVUMs (Ventral Unpaired Median INs) and mVUMs (Ventral Unpaired Median MNs) (Bossing and Brand, 2006; Ruiz et al., 2010; Wheeler et al., 2006; Wheeler et al., 2008). Published morphological characterization of H-cell, H-cell sib, iVUMs and mVUMs are presented in a recapitulative figure below (Fig 34A, B, C, D).

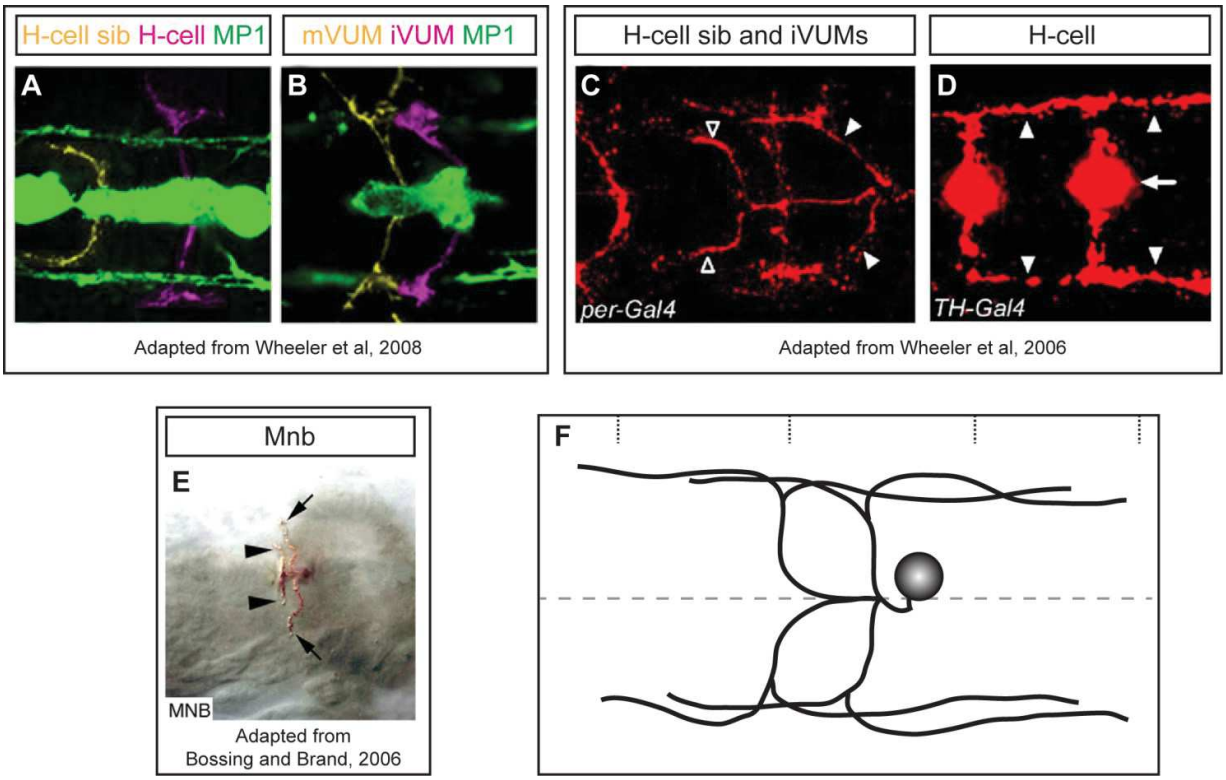

Fig 34: Midline cells morphology

A. Ventral view of a single segment from stage 15 *sim-Gal4 UAS-tau-GFP* embryo allowing visualization of all midline cells. Midline axons are discerned based on their characteristic position along the antero-posterior and dorso-lateral axes: here axons from the H-cell sib (yellow), H-cell (magenta) and MP1 (green) have been falsely coloured and the axons of other midline cells have been subtracted for an clearer observation. H-cell sib axon (yellow) sends projections on both sides of the midline in an anterior direction. The H-cell axon (magenta) sends projections laterally. **B**. Ventral view of a single segment from stage 15 *sim-Gal4 UAS-tau-GFP* embryo allowing visualization of all midline cells. Midline axons are discerned based on their characteristic position along the antero-posterior and dorso-lateral axes: here axons from the mVUM (yellow), iVUMs (magenta) and MP1 (green) have been falsely coloured and the axons of other midline cells have been subtracted for an clearer observation. The mVUM axons (yellow) project along the segmental and intersegmental nerves into the muscle fields while the iVUM axons (magenta) extend projections anteriorly. **C**.Ventral view of 1 segment of stage 15-17 *Per-gal4>UAS-tau-lacZ* embryo allowing visualization of the axons of H-cell sib (empty arrowheads) and iVUMs (filled arrowheads). The cell bodies are not visible as they are out of focus. **D**. Ventral view of 2 segments of stage 15-17 *TH-gal4>UAS-tau-lacZ* embryo allowing visualization of H-cell cell-body (arrow) and projections (arrowheads). **E**. Ventral view of supposed stage 17 embryo showing MNB progeny neurons cell bodies and projections. Projections of MNB progeny MNs (arrows) and MNB progeny INs (arrowheads) are supposedly visible. **F**. Schematic representation of TJ^{+} MNB progeny neuron morphology as we observed it in dorsal view in larval stages. Projections of the MNB progeny neuron span several segments anteriorly and posteriorly to the segment where the cell body is located. Anterior is to the left, midline is materialized by dashed-line and segment boundaries by short dashed lines on the top of the schematic drawing.

MNB progeny neurons morphology was described in an article from Bossing and Brand in 2006. Characterization was done by fluorescent dye DiI injection in the midline cells progenitors and observation of their progeny in embryos; although the exact stage of development is not mentioned, it is probably close to embryonic stage 17 (Bossing and Brand, 2006). The authors say that the neurites belong to two groups of MNB progeny neurons: the MNB progeny MNs (arrows) and the MNB progeny INs (full arrowheads) (Fig 34E). Among the midline cells, there seems to be a discrepancy in the characterization of the MNB progeny neurons. In the DiI characterization done in 1994 (Bossing and Technau, 1994), there is reference to MNB progeny projections in the intersegmental nerve, which would imply that some of the MNB progeny neurons are MNs. However, in subsequent, more recent articles, no more mention is made of a MNB progeny neuron subpopulation being MNs. The current stand-point seems to be that the three mVUMs are the only MN population among the midline cells (Fontana and Crews, 2012; Manning et al., 2012; Pearson and Crews, 2014; Watson and Crews, 2012), and these mVUMs are not supposed to be derived from the MNB neuroblast that gives rise to the MNB progeny neurons. It might have been that at the time of Bossing and Technau study, and due to the lack of resolution of the DiI technique, a mVUM was labelled at the same time as a MNB progeny neuron, thus misleading the authors. The morphology they present in their study and that is shown in Fig 34E looks similar to the morphology of a single MNB progeny neuron in our preliminary results (Fig 34F); it might be therefore that the growing projections that we visualize in Fig 34E are actually the projections of a single MNB progeny IN. Additional stainings will be required to confirm those results.

VII. Molecular characterization of the TJ$^+$ *per*$^+$ GABAergic (MNB progeny) neurons; searching for equivalents throughout evolution

Cell body position and molecular characterization of the TJ$^+$ *per*$^+$ GABAergic allowed us to identify them as part of the MNB progeny neurons among the midline cells. Although development of the midline cells has been meticulously described (Fontana and Crews, 2012; Kearney et al., 2004; Manning et al., 2012; Pearson and Crews, 2014; Tio et al., 2011; Watson and Crews, 2012; Wheeler et al., 2006;

Wheeler et al., 2008), the functional implication of those cells in locomotion or other behaviours is comparatively poor. In this aspect the work done during this PhD on MNB progeny neurons is pioneering, as it shows that they have a relevant function in the locomotor CPG. It additionally adds a new marker (TJ) to identify a MNB progeny neuron subpopulation. Indeed, MNB progeny neurons are the least characterized of all midline cells and specific markers to delineate them are hard to come by (S. Crews, personal communication).

As our molecular characterization of the TJ^+ per^+ GABAergic neurons is thorough, we tried to look for hypothetical counterparts in other model species. TJ^+ per^+ GABAergic neurons are characterized by their expression of *fkh*, *hlh3b* and *grain*. In the mouse, the equivalent combinatorial code would be *Foxa2*, *Tal1*/*Tal2*/*Scl*, *Gata2/3*, which is reminiscent of the one found in V_{2b} population. One of the V_{2b} subpopulations is known to regulate, in cooperation with V_1 Ia INs, the flexor-extensor coordination (Zhang et al., 2014). This population is ipsilaterally-projecting, which does not fit with the morphology we expect from the TJ^+ MNB progeny neurons. In Zebrafish, a characterized V_{2b} subpopulation are the CSF-cNs or KA cells. CSF-cNs/KA cells are located at the spinal cord midline, close to the central canal (Wyart et al., 2009) and appear to regulate the speed of locomotion in Zebrafish (Fidelin et al., 2015; Wyart et al., 2009). An appealing hypothesis would be that TJ^+ MNB progeny neurons are the counterpart of CSF-cNs neurons in invertebrates. Such a hypothesis has been previously formulated in regard to another invertebrate, the annelid *Platynereis dumerilii*. In this animal model, a study focusing on the molecular characterization of neuron types brought to light a group of neurons specifically co-expressing *Gata1/2/3* and *Tal* TFs. This population may relate to the V_{2b} IN population and KA cells/CSF-cNs in vertebrates. The authors of this study hypothesize that *Gata1/2/3-Tal*-expressing neurons in annelids and CSF-cN / KA cells in vertebrates might originate from the same ancestor (Vergara et al., 2017). This is encouraging for us, because if such a CSF-cN-like population is found in annelids, it might as well be found in *Drosophila*.

However we cannot affirm that TJ^+ per^+ GABAergic neurons are CSF-cNs counterpart by solely comparing their function in locomotion and their TF molecular code. More morphological and functional evidences are required to support this hypothesis. CSF-cNs strong characteristics distinguishing them from all other neurons include expression of the channel *Pkd2L1* and presence of a unique cilium

extending from a brush of microvilli into the cerebrospinal fluid-containing central canal (Böhm et al., 2016; Djenoune et al., 2014; Petracca et al., 2016). To this day we could not detect expression of *Amo*, the *Pkd2L1* ortholog in *Drosophila*, in the larva VNC (data not shown). Because *Amo* is a channel, its staining might take the shape of tiny dots and might be delicate to visualize; we actually may have missed it in our stainings. Further stainings might be required to clear this aspect. In regard to the CSF-cNs cilia, additional dichotomy with *Drosophila* is emerging. Indeed there is no anterio-posterior canal spanning *Drosophila* CNS that would be the equivalent of the cerebrospinal fluid-containing central canal. There is however in each hemisegment of *Drosophila* VNC a duct-like structure penetrating the nervous system vertically on the midline and piercing it from dorsal to ventral: the dorsoventral channel (DV channel). These channels are lined by a specific subset of glia and their inner surface is contiguous with the outer VNC surface (Beckervordersandforth et al., 2008; Evans et al., 2010; Ito et al., 1995). The precise function of these channels is currently unknown, but it would be interesting to see in the future if homologies in function can be found between DV channels and Cerebrospinal fluid-containing central canal. Next, would CSF-cNs equivalents in *Drosophila* be expected to have cilia? In metazoans, TFs belonging to the family of regulatory factor X (rfx) are master regulators of ciliogenesis (Chu et al., 2010). As CSF-cNs in the mouse and KA cells in Zebrafish are ciliated cells, it would make sense for them to express rfx proteins. If our hypothesis is true and MNB progeny neurons indeed are ciliated cells and CSF-cN equivalents, then it is likely they will express rfx. In *Drosophila*, rfx is expressed in the peripheral nervous system, and most particularly in the es and ch sensory neurons, where it is essential for ciliogenesis (Dubruille et al., 2002; Durand et al., 2000; Laurençon et al., 2007). Additionally, its expression can be detected in the brain throughout the developmental stages (embryo, larva and adult fly) and in the spermatids in the adult fly (Vandaele et al., 2001). No expression was ever reported in the VNC, but as most of the expression pattern characterization was done using wholemount in situ hybridization, extremely discrete expression in the VNC might have been missed. Therefore it would be informative to do an immunostaining for rfx directly on the VNC to answer this question.

VIII. A27h: the mystery of the disappearing phenotype

My experiments with *A27h-gal4* line in free moving larva show that *A27h-gal4*$^+$ (TJ$^+$) neurons activation causes a spastic paralysis phenotype in young larvae that disappears with the aging of the larva. This result is in contradiction with those already published (Fushiki et al., 2016). Indeed, in L3 semi-intact filet preparations, activation of A27h in a particular VNC segment causes the contraction of the equivalent segment of the larva. In freely moving larvae, my results show that activation of A27h as well as 3 other neurons per hemisegment causes full spastic paralysis in young larvae (less than 5h old) and has no effect on the locomotion of older larvae, including L3 larvae. This discordance could come from the absence of sensory signals in open preparation. It is known that in open preparation the spontaneous peristaltic waves observed are less frequent and travel slower than in living freely moving individuals; this means that sensory feedback has a real implication in locomotion (Fox et al., 2006; Hughes and Thomas, 2007). Sensory feedback might play a role in opposing A27h-mediated segment contraction in intact larva that would therefore not be present in open filet preparation. This implies that A27h has to be contacted directly or indirectly by sensory neurons; and A27h is indeed connected indirectly by sensory neurons through GDL (Fushiki et al., 2016), as it has been shown using TEM. Moreover, as we describe a phenotype in young larvae that disappears in older larvae, we might hypothesize that in young larvae, the mechanism that prevents full contraction upon activation of A27h is not yet fully mature and functional. It is indeed known that locomotor circuits in *Drosophila* larva are functional as soon as the larva hatches (Crisp et al., 2011). However it is also known that the circuits continue to mature, with more synapses being generated over time for example (Couton et al., 2015). Additionally, even though the pattern of expression of *A27h-gal4* does not evolve in the VNC during the course of the larval developmental stages, it might change in the sensory system or in the cerebellar lobes. This change in expression might be responsible for the alteration of phenotype depending on the larval stage. To rule out this hypothesis, I would have to activate specifically TJ$^+$ *A27h-gal4*$^+$ neurons by using intersectional genetics; as we know that TJ is not expressed in the periphery, we would thus be sure to exclude sensory neurons implication in the disappearance of the phenotype.

On a more general note, it makes sense that fictive locomotion models would not always yield the same results as intact freely-moving animals as in one case we are looking at the whole organism and in the other at an isolated model; the best approach would be of course to use both models for the study of a neuronal population.

IX. Function of TJ^+ neurons in the adult fly

While looking for a locomotor phenotype caused by the activation of TJ^+ neurons in adult flies, my attention was caught by a striking and highly-penetrant wing displacement phenotype. First, it is interesting to note that activation of both TJ^+ glutamatergic and cholinergic neurons has effects on the wing position of flies. This means that TJ^+ cholinergic INs and potentially TJ^+ glutamatergic INs are connecting MNs that innervate wing muscles. Additionally, non-published preliminary results from the lab show that some TJ^+ MNs innervate direct wing muscles (Fig 35). As no phenotype was observed upon activation of the TJ^+ GABAergic neurons in adult fly, we cannot know if there still are TJ^+ GABAergic neurons in the adult fly CNS.

Wing displacement in the adult *Drosophila* fly has been previously reported in a number of articles focusing mainly on neurodegenerative processes (Clark et al., 2006; Fernandes and Rao, 2011; Füger et al., 2012; Sanhueza et al., 2014; Zhang et al., 2001). Interestingly the two phenotypes we observe - wings “raised” or “drooping” - are seen concomitantly in most of the articles above cited. While some phenotypes seem to be associated with muscular degeneration of the indirect flight muscles involved in the positioning of the wing (Fig 35) (Clark et al., 2006), some other are not associated with muscle damage but are rather due to impaired MNs function (Füger et al., 2012). It would be necessary in our case to have staining of indirect flight muscles to know if muscle defect is implicated; however taking into consideration that the phenotype become irreversible after only 2 hours of recurrent activation of TJ^+ neurons, it seems unlikely that muscle degeneration is involved. Rather, I would hypothesize that recurrent activity of TJ^+ MNs or TJ^+ INs innervating MNs could lead to denervation of the neuromuscular junction and potentially even death of MNs by excitotoxicity.

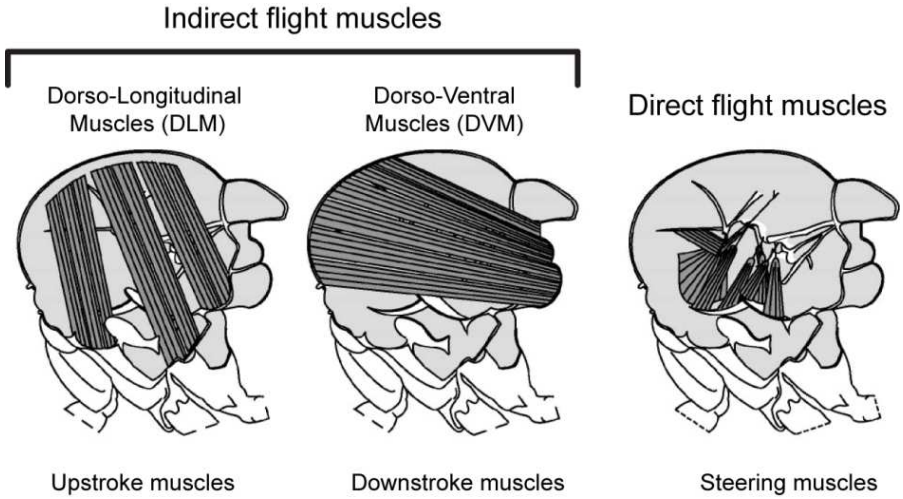

Fig 35: Overview of flight muscles in *Drosophila* fruit fly

Lateral view of thorax of a *Drosophila* fruit fly with the different flight muscles shown in darker grays. Indirect flight muscles are power muscles involved in the generation of the beat of the wings: dorso-longitudinal muscles more particularly generate upstroke motion of the wing while dorso-ventral muscles generate downstroke motion of the wing. Direct flight muscles in comparison are tiny; their role is to steer the wing to allow for fine flight manoeuvres. Adapted from (Dickinson, 2005)

Apart from the striking wing displacement phenotype, activation of TJ^+ cholinergic INs also induced what seemed like excessive grooming. TJ^+ cholinergic neurons implicated in this behaviour could be located in the cerebellar lobes and have a command-role in this behaviour. They could also be VNC relays in the circuit involved in grooming. For example, they could be part of the nociceptive circuit that relay information coming from sensory receptors to trigger grooming behaviour, even in decapitated flies (Yanagawa et al., 2014).

Finally, in the preliminary results for the activation of the TJ^+ population presented here I focused on wing phenotype as it is a strong, easily visible phenotype. Some other more discrete phenotypes might have been missed when looking at the flies; therefore videotaping and analysing the behaviour of flies with the appropriate settings might bring to light other worthwhile phenotypes. Overall, although preliminary, these results open up exciting prospects for studying the implication of TJ^+ neurons and the physiological mechanisms underlying wing position control and even flight in adult flies.

References

Al-Mosawie A, Wilson JM and Brownstone RM. (2007) Heterogeneity of V2-derived interneurons in the adult mouse spinal cord. *European Journal of Neuroscience* 26: 3003-3015.

Alekseyenko OV, Chan Y-B, de la Paz Fernandez M, et al. (2014) Single serotonergic neurons that modulate aggression in Drosophila. *Curr Biol* 24: 2700-2707.

Allen MJ, O'Kane C and Moffat K. (2002) *Cell ablation using wild-type and cold-sensitive Ricin-A chain in Drosophila embryonic mesoderm*.

Alvarez FJ, Jonas PC, Sapir T, et al. (2005) Postnatal phenotype and localization of spinal cord V1 derived interneurons. *Journal of Comparative Neurology* 493: 177-192.

Ampatzis K, Song J, Ausborn J, et al. (2014) Separate Microcircuit Modules of Distinct V2a Interneurons and Motoneurons Control the Speed of Locomotion. *Neuron* 83: 934-943.

Andrzejczuk LA, Banerjee S, England SJ, et al. (2018) Tal1, Gata2a, and Gata3 Have Distinct Functions in the Development of V2b and Cerebrospinal Fluid-Contacting KA Spinal Neurons. *Frontiers in Neuroscience* 12.

Arnau J, Lauritzen C, Petersen GE, et al. (2006) Current strategies for the use of affinity tags and tag removal for the purification of recombinant proteins. *Protein Expression and Purification* 48: 1-13.

Artavanis-Tsakonas S, Matsuno K and Fortini M. (1995) Notch signaling. *Science* 268: 225-232.

Artavanis-Tsakonas S, Rand MD and Lake RJ. (1999) Notch Signaling: Cell Fate Control and Signal Integration in Development. *Science* 284: 770-776.

Ausborn J, Mahmood R and El Manira A. (2012) Decoding the rules of recruitment of excitatory interneurons in the adult zebrafish locomotor network. *Proceedings of the National Academy of Sciences* 109: E3631-E3639.

Aydogdu I, Tanriverdi Z and Ertekin C. (2011) Dysfunction of bulbar central pattern generator in ALS patients with dysphagia during sequential deglutition. *Clinical Neurophysiology* 122: 1219-1228.

Banerjee S, Toral M, Siefert M, et al. (2016) dHb9 expressing larval motor neurons persist through metamorphosis to innervate adult-specific muscle targets and function in Drosophila eclosion. *Dev Neurobiol* 76: 1387-1416.

Bate M. (1990) The embryonic development of larval muscles in Drosophila. *Development* 110: 791-804.

Batista MF, Jacobstein J and Lewis KE. (2008) Zebrafish V2 cells develop into excitatory CiD and Notch signalling dependent inhibitory VeLD interneurons. *Dev Biol* 322: 263-275.

Beckervordersandforth RM, Rickert C, Altenhein B, et al. (2008) Subtypes of glial cells in the Drosophila embryonic ventral nerve cord as related to lineage and gene expression. *Mech Dev* 125: 542-557.

Bermingham NA, Hassan BA, Price SD, et al. (1999) Math1: An Essential Gene for the Generation of Inner Ear Hair Cells. *Science* 284: 1837-1841.

Berni J. (2015) Genetic dissection of a regionally differentiated network for exploratory behavior in Drosophila larvae. *Curr Biol* 25: 1319-1326.

Berni J, Pulver Stefan R, Griffith Leslie C, et al. (2012) Autonomous Circuitry for Substrate Exploration in Freely Moving Drosophila Larvae. *Current Biology* 22: 1861-1870.

Bhanot P, Brink M, Samos CH, et al. (1996) A new member of the frizzled family from Drosophila functions as a Wingless receptor. *Nature* 382: 225.

Bidaye SS, Machacek C, Wu Y, et al. (2014) Neuronal Control of Drosophila Walking Direction. *Science* 344: 97-101.

Bikoff JB, Gabitto MI, Rivard AF, et al. (2016) Spinal Inhibitory Interneuron Diversity Delineates Variant Motor Microcircuits. *Cell* 165: 207-219.

Björnfors ER and El Manira A. (2016) Functional diversity of excitatory commissural interneurons in adult zebrafish. *Elife* 5: e18579.

Böhm UL, Prendergast A, Djenoune L, et al. (2016) CSF-contacting neurons regulate locomotion by relaying mechanical stimuli to spinal circuits. *Nat Commun* 7: 10866.

Borowska J, Jones CT, Zhang H, et al. (2013) Functional Subpopulations of V3 Interneurons in the Mature Mouse Spinal Cord. *The Journal of Neuroscience* 33: 18553-18565.

Bossing T and Brand AH. (2006) Determination of cell fate along the anteroposterior axis of the Drosophila ventral midline. *Development* 133: 1001-1012.

Bossing T and Technau GM. (1994) The fate of the CNS midline progenitors in Drosophila as revealed by a new method for single cell labelling. *Development* 120: 1895-1906.

Bourane S, Garces A, Venteo S, et al. (2009) Low-Threshold Mechanoreceptor Subtypes Selectively Express MafA and Are Specified by Ret Signaling. *Neuron* 64: 857-870.

Bourbon H-M, Gonzy-Treboul G, Peronnet F, et al. (2002) A P-insertion screen identifying novel X-linked essential genes in Drosophila. *Mech Dev* 110: 71-83.

Boyden ES, Zhang F, Bamberg E, et al. (2005) Millisecond-timescale, genetically targeted optical control of neural activity. *Nat Neurosci* 8: 1263.

Briscoe J, Sussel L, Serup P, et al. (1999) Homeobox gene Nkx2.2 and specification of neuronal identity by graded Sonic hedgehog signalling. *Nature* 398: 622.

Brocard F, Tazerart S and Vinay L. (2010) Do Pacemakers Drive the Central Pattern Generator for Locomotion in Mammals? *The Neuroscientist* 16: 139-155.

Brown NL, Patel S, Brzezinski J, et al. (2001) Math5 is required for retinal ganglion cell and optic nerve formation. *Development (Cambridge, England)* 128: 2497-2508.

Brunner E, Peter O, Schweizer L, et al. (1997) pangolinencodes a Lef-1 homologue that acts downstream of Armadillo to transduce the Wingless signal in Drosophila. *Nature* 385: 829.

Buchanan J and Grillner S. (1987) Newly identified 'glutamate interneurons' and their role in locomotion in the lamprey spinal cord. *Science* 236: 312-314.

Bucher D. (2009) *Encyclopedia of Neuroscience*: Academic Press (June 26, 2009).

Burgos A, Honjo K, Ohyama T, et al. (2018) Nociceptive interneurons control modular motor pathways to promote escape behavior in Drosophila. *Elife* 7: e26016.

Caldeira V, Dougherty KJ, Borgius L, et al. (2017) Spinal Hb9::Cre-derived excitatory interneurons contribute to rhythm generation in the mouse. *Scientific Reports* 7: 41369.

Cardona A, Larsen C and Hartenstein V. (2009) Neuronal fiber tracts connecting the brain and ventral nerve cord of the early Drosophila larva. *J Comp Neurol* 515: 427-440.

Chervin RD, Consens FB and Kutluay E. (2003) Alternating leg muscle activation during sleep and arousals: A new sleep-related motor phenomenon? *Movement Disorders* 18: 551-559.

Chu JSC, Baillie DL and Chen N. (2010) Convergent evolution of RFX transcription factors and ciliary genes predated the origin of metazoans. *BMC Evolutionary Biology* 10: 130-130.

Clark IE, Dodson MW, Jiang C, et al. (2006) Drosophila pink1 is required for mitochondrial function and interacts genetically with parkin. *Nature* 441: 1162.

Clark MQ, McCumsey SJ, Lopez-Darwin S, et al. (2016) Functional Genetic Screen to Identify Interneurons Governing Behaviorally Distinct Aspects of Drosophila Larval Motor Programs. *G3 (Bethesda)* 6: 2023-2031.

Clark MQ, Zarin AA, Carreira-Rosario A, et al. (2018) Neural circuits driving larval locomotion in Drosophila. *Neural Dev* 13: 6.

Consoulas C, Duch C, Bayline RJ, et al. (2000) Behavioral transformations during metamorphosis: remodeling of neural and motor systems. *Brain Research Bulletin* 53: 571-583.

Coolen M, Sii-Felice K, Bronchain O, et al. (2005) Phylogenomic analysis and expression patterns of large Maf genes in Xenopus tropicalis provide new insights into the functional evolution of the gene family in osteichthyans. *Development Genes and Evolution* 215: 327-339.

Cosentino FII, Iero I, Lanuzza B, et al. (2006) The neurophysiology of the alternating leg muscle activation (ALMA) during sleep: Study of one patient before and after treatment with pramipexole. *Sleep Medicine* 7: 63-71.

Couton L, Mauss Alex S, Yunusov T, et al. (2015) Development of Connectivity in a Motoneuronal Network in Drosophila Larvae. *Current Biology* 25: 568-576.

Crisp S, Evers JF, Fiala A, et al. (2008) The Development of Motor Coordination in Drosophila Embryos. *Development (Cambridge, England)* 135: 3707-3717.

Crisp SJ, Evers JF and Bate M. (2011) Endogenous patterns of activity are required for the maturation of a motor network. *J Neurosci* 31: 10445-10450.

Crone SA, Quinlan KA, Zagoraiou L, et al. (2008) Genetic Ablation of V2a Ipsilateral Interneurons Disrupts Left-Right Locomotor Coordination in Mammalian Spinal Cord. *Neuron* 60: 70-83.

Crone SA, Zhong G, Harris-Warrick R, et al. (2009) In Mice Lacking V2a Interneurons, Gait Depends on Speed of Locomotion. *The Journal of Neuroscience* 29: 7098-7109.

Diao F, Ironfield H, Luan H, et al. (2015) Plug-and-Play Genetic Access to Drosophila Cell Types Using Exchangeable Exon Cassettes. *Cell Rep* 10: 1410-1421.

Dickinson MH. (2005) The Initiation and Control of Rapid Flight Maneuvers in Fruit Flies1. *Integrative and Comparative Biology* 45: 274-281.

Djenoune L, Khabou H, Joubert F, et al. (2014) Investigation of spinal cerebrospinal fluid-contacting neurons expressing PKD2L1: evidence for a conserved system from fish to primates. *Frontiers in Neuroanatomy* 8: 26.

Dougherty Kimberly J, Zagoraiou L, Satoh D, et al. (2013) Locomotor Rhythm Generation Linked to the Output of Spinal Shox2 Excitatory Interneurons. *Neuron* 80: 920-933.

Dubruille R, Laurençon A, Vandaele C, et al. (2002) Drosophila Regulatory factor X is necessary for ciliated sensory neuron differentiation. *Development* 129: 5487-5498.

Dubuc R, Brocard F, Antri M, et al. (2008) Initiation of locomotion in lampreys. *Brain Research Reviews* 57: 172-182.

Durand B, Vandaele C, Spencer D, et al. (2000) Cloning and characterization of dRFX, the Drosophila member of the RFX family of transcription factors. *Gene* 246: 285-293.

Eccles JC, Eccles RM and Lundberg A. (1957) Synaptic actions on motoneurones in relation to the two components of the group i muscle afferent volley. *The Journal of Physiology* 136: 527-546.

Eccles JC, Fatt P and Koketsu K. (1954) Cholinergic and inhibitory synapses in a pathway from motor-axon collaterals to motoneurones. *The Journal of Physiology* 126: 524-562.

Eccles JC, Fatt P and Landgren S. (1956) Central pathway for direct inhibitory action of impulses in largest afferent nerve fibres to muscle. *Journal of Neurophysiology* 19: 75-98.

Ejsmont R and Hassan B. (2014) The Little Fly that Could: Wizardry and Artistry of Drosophila Genomics. *Genes* 5: 385.

Ejsmont RK, Sarov M, Winkler S, et al. (2009) A toolkit for high-throughput, cross-species gene engineering in Drosophila. *Nature Methods* 6: 435.

Erdem NS, Karaali K, Ünal A, et al. (2016) The interaction between breathing and swallowing in amyotrophic lateral sclerosis. *Acta Neurologica Belgica* 116: 549-556.

Estacio-Gómez A, Moris-Sanz M, Schäfer A-K, et al. (2013) Bithorax-complex genes sculpt the pattern of leucokinergic neurons in the *Drosophila* central nervous system. *Development* 140: 2139-2148.

Evans IR, Hu N, Skaer H, et al. (2010) Interdependence of macrophage migration and ventral nerve cord development in Drosophila embryos. *Development* 137: 1625-1633.

Eychène A, Rocques N and Pouponnot C. (2008) A new MAFia in cancer. *Nature Reviews Cancer* 8: 683.

Feinberg EH, Vanhoven MK, Bendesky A, et al. (2008) GFP Reconstitution Across Synaptic Partners (GRASP) defines cell contacts and synapses in living nervous systems. *Neuron* 57: 353-363.

Feldman AG and Orlovsky GN. (1975) Activity of interneurons mediating reciprocal 1a inhibition during locomotion. *Brain Research* 84: 181-194.

Fernandes C and Rao Y. (2011) Genome-wide screen for modifiers of Parkinson's disease genes in Drosophila. *Molecular Brain* 4: 17.

Fidelin K, Djenoune L, Stokes C, et al. (2015) State-Dependent Modulation of Locomotion by GABAergic Spinal Sensory Neurons. *Current Biology* 25: 3035-3047.

Fidelin K and Wyart C. (2014) Inhibition and motor control in the developing zebrafish spinal cord. *Current Opinion in Neurobiology* 26: 103-109.

Fontana JR and Crews ST. (2012) Transcriptome analysis of Drosophila CNS midline cells reveals diverse peptidergic properties and a role for castor in neuronal differentiation. *Dev Biol* 372: 131-142.

Fox LE, Soll DR and Wu C-F. (2006) Coordination and Modulation of Locomotion Pattern Generators in Drosophila Larvae: Effects of Altered Biogenic Amine Levels by the Tyramine β Hydroxlyase Mutation. *J Neurosci* 26: 1486-1498.

Francius C, Harris A, Rucchin V, et al. (2013) Identification of Multiple Subsets of Ventral Interneurons and Differential Distribution along the Rostrocaudal Axis of the Developing Spinal Cord. *Plos One* 8: e70325.

Füger P, Sreekumar V, Schüle R, et al. (2012) Spastic Paraplegia Mutation N256S in the Neuronal Microtubule Motor KIF5A Disrupts Axonal Transport in a Drosophila HSP Model. *PLoS Genet* 8: e1003066.

Fushiki A, Kohsaka H and Nose A. (2013) Role of Sensory Experience in Functional Development of Drosophila Motor Circuits. *Plos One* 8: e62199.

Fushiki A, Zwart MF, Kohsaka H, et al. (2016) A circuit mechanism for the propagation of waves of muscle contraction in Drosophila. *Elife* 5.

Gabitto MI, Pakman A, Bikoff JB, et al. (2016) Bayesian Sparse Regression Analysis Documents the Diversity of Spinal Inhibitory Interneurons. *Cell* 165: 220-233.

Gabriel JP, Ausborn J, Ampatzis K, et al. (2010) Principles governing recruitment of motoneurons during swimming in zebrafish. *Nat Neurosci* 14: 93.

Galliot B, Quiquand M, Ghila L, et al. (2009) Origins of neurogenesis, a cnidarian view. *Dev Biol* 332: 2-24.

Gerber B and Stocker RF. (2007) The Drosophila Larva as a Model for Studying Chemosensation and Chemosensory Learning: A Review. *Chemical Senses* 32: 65-89.

Gligorov D, Sitnik JL, Maeda RK, et al. (2013) A Novel Function for the Hox Gene Abd-B in the Male Accessory Gland Regulates the Long-Term Female Post-Mating Response in Drosophila. *PLoS Genet* 9: e1003395.

Gomez-Marin A and Louis M. (2012) Active sensation during orientation behavior in the Drosophila larva: more sense than luck. *Current Opinion in Neurobiology* 22: 208-215.

Gosgnach S, Lanuza GM, Butt SJB, et al. (2006) V1 spinal neurons regulate the speed of vertebrate locomotor outputs. *Nature* 440: 215.

Goulding M, Lanuza G, Sapir T, et al. (2002) The formation of sensorimotor circuits. *Current Opinion in Neurobiology* 12: 508-515.

Griener A, Zhang W, Kao H, et al. (2015) Probing diversity within subpopulations of locomotor-related V0 interneurons. *Dev Neurobiol* 75: 1189-1203.

Grillner S, Deliagina T, El Manira A, et al. (1995) Neural networks that co-ordinate locomotion and body orientation in lamprey. *Trends Neurosci* 18: 270-279.

Grillner S, Parker D and El Manira A. (1998) Vertebrate Locomotion-A Lamprey Perspectivea. *Ann N Y Acad Sci* 860: 1-18.

Grillner S, Walle P, Brodin L, et al. (1991) Neuronal Network Generating Locomotor Behavior in Lamprey: Circuitry, Transmitters, Membrane Properties, and Simulation. *Annual Review of Neuroscience* 14: 169-199.

Grossmann KS, Giraudin A, Britz O, et al. (2010) Chapter 2 - Genetic dissection of rhythmic motor networks in mice. In: Gossard J-P, Dubuc R and Kolta A (eds) *Progress in Brain Research.* Elsevier, 19-37.

Guertin P. (2013) Central Pattern Generator for Locomotion: Anatomical, Physiological, and Pathophysiological Considerations. *Frontiers in Neurology* 3.

Halder G, Callaerts P, Flister S, et al. (1998) Eyeless initiates the expression of both sine oculis and eyes absent during Drosophila compound eye development. *Development* 125: 2181-2191.

Hale ME, Ritter DA and Fetcho JR. (2001) A confocal study of spinal interneurons in living larval zebrafish. *Journal of Comparative Neurology* 437: 1-16.

Han X and Boyden ES. (2007) Multiple-Color Optical Activation, Silencing, and Desynchronization of Neural Activity, with Single-Spike Temporal Resolution. *Plos One* 2: e299.

Hasegawa E, Truman JW and Nose A. (2016) Identification of excitatory premotor interneurons which regulate local muscle contraction during Drosophila larval locomotion. *Scientific Reports* 6.

Heckscher ES, Lockery SR and Doe CQ. (2012) Characterization of Drosophila Larval Crawling at the Level of Organism, Segment, and Somatic Body Wall Musculature. *Journal of Neuroscience* 32: 12460-12471.

Heckscher ES, Long F, Layden MJ, et al. (2014) Atlas-builder software and the eNeuro atlas: resources for developmental biology and neuroscience. *Development (Cambridge, England)* 141: 2524-2532.

Heckscher ES, Zarin AA, Faumont S, et al. (2015) Even-Skipped(+) Interneurons Are Core Components of a Sensorimotor Circuit that Maintains Left-Right Symmetric Muscle Contraction Amplitude. *Neuron* 88: 314-329.

Higashijima S-i, Masino MA, Mandel G, et al. (2004) Engrailed-1 Expression Marks a Primitive Class of Inhibitory Spinal Interneuron. *The Journal of Neuroscience* 24: 5827-5839.

Hill RE, Favor J, Hogan BLM, et al. (1991) Mouse Small eye results from mutations in a paired-like homeobox-containing gene. *Nature* 354: 522.

Hinckley CA, Hartley R, Wu L, et al. (2005) Locomotor-Like Rhythms in a Genetically Distinct Cluster of Interneurons in the Mammalian Spinal Cord. *Journal of Neurophysiology* 93: 1439-1449.

Hinckley CA and Ziskind-Conhaim L. (2006) Electrical Coupling between Locomotor-Related Excitatory Interneurons in the Mammalian Spinal Cord. *The Journal of Neuroscience* 26: 8477-8483.

Holz A, Kollmus H, Ryge J, et al. (2010) The transcription factors Nkx2.2 and Nkx2.9 play a novel role in floor plate development and commissural axon guidance. *Development* 137: 4249-4260.

Honjo K, Hwang RY and Tracey WD. (2012) Optogenetic manipulation of neural circuits and behavior in Drosophila larvae. *Nat Protoc* 7: 1470-1478.

Hooper JE and Scott MP. (1989) The Drosophila patched gene encodes a putative membrane protein required for segmental patterning. *Cell* 59: 751-765.

Hoopfer ED, Jung Y, Inagaki HK, et al. (2015) P1 interneurons promote a persistent internal state that enhances inter-male aggression in Drosophila. *Elife* 4: e11346.

Hsu CT and Bhandawat V. (2016) Organization of descending neurons in Drosophila melanogaster. *Scientific Reports* 6: 20259.

Hu J, Huang T, Li T, et al. (2012) c-Maf Is Required for the Development of Dorsal Horn Laminae III/IV Neurons and Mechanoreceptive DRG Axon Projections. *The Journal of Neuroscience* 32: 5362-5373.

Hughes CL and Thomas JB. (2007) A Sensory Feedback Circuit Coordinates Muscle Activity in Drosophila. *Mol Cell Neurosci* 35: 383-396.

Hultborn H. (2006) Spinal reflexes, mechanisms and concepts: From Eccles to Lundberg and beyond. *Progress in Neurobiology* 78: 215-232.

Hwang RY, Zhong L, Xu Y, et al. (2007) Nociceptive neurons protect Drosophila larvae from parasitoid wasps. *Curr Biol* 17: 2105-2116.

Inada K, Kohsaka H, Takasu E, et al. (2011) Optical Dissection of Neural Circuits Responsible for Drosophila Larval Locomotion with Halorhodopsin. *Plos One* 6: e29019.

Itakura Y, Kohsaka H, Ohyama T, et al. (2015) Identification of Inhibitory Premotor Interneurons Activated at a Late Phase in a Motor Cycle during Drosophila Larval Locomotion. *Plos One* 10: e0136660.

Ito K, Urban J and Technau G. (1995) *Distribution, classification, and development of Drosophila glial cells in the late embryonic and early larval ventral nerve cord*.

Iyengar BG, Chou CJ, Vandamme KM, et al. (2011) Silencing synaptic communication between random interneurons during Drosophila larval locomotion. *Genes, Brain and Behavior* 10: 883-900.

Jarman AP, Grau Y, Jan LY, et al. (1993) atonal is a proneural gene that directs chordotonal organ formation in the Drosophila peripheral nervous system. *Cell* 73: 1307-1321.

Jarman AP, Grell EH, Ackerman L, et al. (1994) atonal is the proneural gene for Drosophila photoreceptors. *Nature* 369: 398.

Jayaram H, Khaw P-T, MacLaren RE, et al. (2012) Focus on Molecules: Neural retina leucine zipper (NRL). *Experimental Eye Research* 104: 99-100.

Jukam D, Xie B, Rister J, et al. (2013) Opposite Feedbacks in the Hippo Pathway for Growth Control and Neural Fate. *Science* 342.

Karagyozov D, Mihovilovic Skanata M, Lesar A, et al. (2017) Recording neural activity in unrestrained animals with 3D tracking two photon microscopy. *bioRxiv*.

Karuppudurai T, Lin T-Y, Ting C-Y, et al. (2014) A Hard-wired Glutamatergic Circuit Pools and Relays UV Signals to Mediate Spectral Preference in Drosophila. *Neuron* 81: 603-615.

Kataoka K. (2007) Multiple Mechanisms and Functions of Maf Transcription Factors in the Regulation of Tissue-Specific Genes. *The Journal of Biochemistry* 141: 775-781.

Kawashima T, Nakamura A, Yasuda K, et al. (2003) Dmaf, a novel member of Maf transcription factor family is expressed in somatic gonadal cells during embryonic development and gametogenesis in Drosophila. *Gene Expression Patterns* 3: 663-667.

Kearney JB, Wheeler SR, Estes P, et al. (2004) Gene expression profiling of the developing Drosophila CNS midline cells. *Dev Biol* 275: 473-492.

Kerppola T and Curran T. (1994) *A conserved region adjacent to the basic domain is required for recognition of an extended DNA binding site by Maf/Nrl family proteins*.

Kiehn O. (2016) Decoding the organization of spinal circuits that control locomotion. *Nature reviews. Neuroscience* 17: 224-238.

Kim SH, Lee Y, Akitake B, et al. (2010) Drosophila TRPA1 channel mediates chemical avoidance in gustatory receptor neurons. *Proc Natl Acad Sci U S A* 107: 8440-8445.

Kimura Y, Okamura Y and Higashijima S-i. (2006) alx, a Zebrafish Homolog of Chx10, Marks Ipsilateral Descending Excitatory Interneurons That Participate in the Regulation of Spinal Locomotor Circuits. *The Journal of Neuroscience* 26: 5684-5697.

Kitamoto T. (2001) Conditional modification of behavior in Drosophila by targeted expression of a temperature-sensitive shibire allele in defined neurons. *J Neurobiol* 47: 81-92.

Kockel L, Huq LM, Ayyar A, et al. (2016) A Drosophila LexA Enhancer-Trap Resource for Developmental Biology and Neuroendocrine Research. *G3: Genes|Genomes|Genetics* 6: 3017-3026.

Kohsaka H, Guertin PA and Nose A. (2017) Neural Circuits Underlying Fly Larval Locomotion. *Curr Pharm Des* 23: 1722-1733.

Kohsaka H, Okusawa S, Itakura Y, et al. (2012) Development of larval motor circuits in Drosophila. *Development, Growth & Differentiation* 54: 408-419.

Kohsaka H, Takasu E, Morimoto T, et al. (2014) A Group of Segmental Premotor Interneurons Regulates the Speed of Axial Locomotion in Drosophila Larvae. *Current Biology* 24: 2632-2642.

Krumlauf R. (1994) Hox genes in vertebrate development. *Cell* 78: 191-201.

Kumar JP. (2009) The sine oculis homeobox (SIX) family of transcription factors as regulators of development and disease. *Cellular and molecular life sciences : CMLS* 66: 565-583.

Kupfermann I and Weiss KR. (2010) The command neuron concept. *Behavioral and Brain Sciences* 1: 3-10.

Kwon Y, Shim H-S, Wang X, et al. (2008) *Control of thermotactic behavior via coupling of a TRP channel to a phospholipase C signaling cascade*.

Lacin H, Rusch J, Yeh RT, et al. (2014) Genome-wide identification of Drosophila Hb9 targets reveals a pivotal role in directing the transcriptome within eight neuronal lineages, including activation of Nitric Oxide Synthase and Fd59a/Fox-D. *Dev Biol* 388: 117-133.

Lanuza GM, Gosgnach S, Pierani A, et al. (2004) Genetic Identification of Spinal Interneurons that Coordinate Left-Right Locomotor Activity Necessary for Walking Movements. *Neuron* 42: 375-386.

Laurençon A, Dubruille R, Efimenko E, et al. (2007) Identification of novel regulatory factor X (RFX) target genes by comparative genomics in Drosophila species. *Genome Biology* 8: R195-R195.

Lawrence PA and Morata G. (1994) Homeobox genes: Their function in Drosophila segmentation and pattern formation. *Cell* 78: 181-189.

Lee JJ, von Kessler DP, Parks S, et al. (1992) Secretion and localized transcription suggest a role in positional signaling for products of the segmentation gene hedgehog. *Cell* 71: 33-50.

Li MA, Alls JD, Avancini RM, et al. (2003) The large Maf factor Traffic Jam controls gonad morphogenesis in Drosophila. *Nat Cell Biol* 5: 994.

Liao JC and Fetcho JR. (2008) Shared versus Specialized Glycinergic Spinal Interneurons in Axial Motor Circuits of Larval Zebrafish. *The Journal of Neuroscience* 28: 12982-12992.

Liu L, Yermolaieva O, Johnson WA, et al. (2003) Identification and function of thermosensory neurons in Drosophila larvae. *Nat Neurosci* 6: 267.

Lu DC, Niu T and Alaynick WA. (2015) Molecular and cellular development of spinal cord locomotor circuitry. *Frontiers in Molecular Neuroscience* 8.

Luan H, Peabody NC, Vinson CR, et al. (2006) Refined Spatial Manipulation of Neuronal Function by Combinatorial Restriction of Transgene Expression. *Neuron* 52: 425-436.

Lundfald L, Restrepo CE, Butt SJB, et al. (2007) Phenotype of V2-derived interneurons and their relationship to the axon guidance molecule EphA4 in the developing mouse spinal cord. *European Journal of Neuroscience* 26: 2989-3002.

Luo J, Shen WL and Montell C. (2017) TRPA1 mediates sensation of the rate of temperature change in Drosophila larvae. *Nat Neurosci* 20: 34-41.

Machaalani R and Waters KA. (2008) Neuronal cell death in the Sudden Infant Death Syndrome brainstem and associations with risk factors. *Brain* 131: 218-228.

Machaalani R and Waters KA. (2014) Neurochemical abnormalities in the brainstem of the Sudden Infant Death Syndrome (SIDS). *Paediatric Respiratory Reviews* 15: 293-300.

Macpherson LJ, Zaharieva EE, Kearney PJ, et al. (2015) Dynamic labelling of neural connections in multiple colours by trans-synaptic fluorescence complementation. *Nat Commun* 6: 10024.

Manning L, Heckscher ES, Purice MD, et al. (2012) A resource for manipulating gene expression and analyzing cis-regulatory modules in the Drosophila CNS. *Cell Rep* 2: 1002-1013.

Marder E and Bucher D. (2001) Central pattern generators and the control of rhythmic movements. *Current Biology* 11: R986-R996.

Matsunaga T, Kohsaka H and Nose A. (2017) Gap Junction–Mediated Signaling from Motor Neurons Regulates Motor Generation in the Central Circuits of Larval Drosophila. *The Journal of Neuroscience* 37: 2045-2060.

Melcher C and Pankratz MJ. (2005) Candidate Gustatory Interneurons Modulating Feeding Behavior in the Drosophila Brain. *PLoS Biol* 3: e305.

Miyawaki A. (2010) Visualizing a neuronal handshake. *Nature Chemical Biology* 6: 885.

Moran-Rivard L, Kagawa T, Saueressig H, et al. (2001) Evx1 Is a Postmitotic Determinant of V0 Interneuron Identity in the Spinal Cord. *Neuron* 29: 385-399.

Mu L, Bacon JP, Ito K, et al. (2014) Responses of Drosophila giant descending neurons to visual and mechanical stimuli. *The Journal of Experimental Biology* 217: 2121-2129.

Nagel G, Ollig D, Fuhrmann M, et al. (2002) Channelrhodopsin-1: A Light-Gated Proton Channel in Green Algae. *Science* 296: 2395-2398.

Neul JL, Kaufmann WE, Glaze DG, et al. (2010) Rett Syndrome: Revised Diagnostic Criteria and Nomenclature. *Annals of neurology* 68: 944-950.

Nüsslein-Volhard C and Wieschaus E. (1980) Mutations affecting segment number and polarity in Drosophila. *Nature* 287: 795.

Ohyama T, Schneider-Mizell CM, Fetter RD, et al. (2015) A multilevel multimodal circuit enhances action selection in Drosophila. *Nature Reviews Cancer* 520: 633-639.

Pearson JC and Crews ST. (2014) Enhancer diversity and the control of a simple pattern of Drosophila CNS midline cell expression. *Dev Biol* 392: 466-482.

Petracca YL, Sartoretti MM, Di Bella DJ, et al. (2016) The late and dual origin of cerebrospinal fluid-contacting neurons in the mouse spinal cord. *Development* 143: 880-891.

Pierani A, Brenner-Morton S, Chiang C, et al. (1999) A Sonic Hedgehog–Independent, Retinoid-Activated Pathway of Neurogenesis in the Ventral Spinal Cord. *Cell* 97: 903-915.

Pierani A, Moran-Rivard L, Sunshine MJ, et al. (2001) Control of Interneuron Fate in the Developing Spinal Cord by the Progenitor Homeodomain Protein Dbx1. *Neuron* 29: 367-384.

Pombal MA and Megías M. (2018) Development and Functional Organization of the Cranial Nerves in Lampreys. *The Anatomical Record* 0.

Pulver SR, Bayley TG, Taylor AL, et al. (2015) Imaging fictive locomotor patterns in larval Drosophila. *Journal of Neurophysiology* 114: 2564-2577.

Pulver SR, Pashkovski SL, Hornstein NJ, et al. (2009) Temporal Dynamics of Neuronal Activation by Channelrhodopsin-2 and TRPA1 Determine Behavioral Output in Drosophila Larvae. *Journal of Neurophysiology* 101: 3075-3088.

Quiring R, Walldorf U, Kloter U, et al. (1994) Homology of the eyeless gene of Drosophila to the Small eye gene in mice and Aniridia in humans. *Science* 265: 785-789.

Ramírez-Jarquín UN, Lazo-Gómez R, Tovar-y-Romo LB, et al. (2014) Spinal inhibitory circuits and their role in motor neuron degeneration. *Neuropharmacology* 82: 101-107.

Renshaw B. (1946) Central effects of centripetal impulses in axons of spinal ventral roots. *Journal of Neurophysiology* 9: 191-204.

Rickert C, Kunz T, Harris K-L, et al. (2011) Morphological Characterization of the Entire Interneuron Population Reveals Principles of Neuromere Organization in the Ventral Nerve Cord of Drosophila. *The Journal of Neuroscience* 31: 15870-15883.

Riedl J and Louis M. (2012) Behavioral neuroscience: Crawling is a no-brainer for fruit fly larvae. *Curr Biol* 22: R867-869.

Risse B, Berh D, Otto N, et al. (2015) Quantifying subtle locomotion phenotypes of Drosophila larvae using internal structures based on FIM images. *Computers in Biology and Medicine* 63: 269-276.

Rosenzweig M, Brennan KM, Tayler TD, et al. (2005) The Drosophila ortholog of vertebrate TRPA1 regulates thermotaxis. *Genes Dev* 19: 419-424.

Ruiz S, Rickert C, Berger C, et al. (2010) Spatio-temporal pattern of cells expressing the clock genes period and timeless and the lineages of period expressing neurons in the embryonic CNS of Drosophilamelanogaster. *Gene Expression Patterns* 10: 274-282.

Saint-Amant L and Drapeau P. (2001) Synchronization of an Embryonic Network of Identified Spinal Interneurons Solely by Electrical Coupling. *Neuron* 31: 1035-1046.

Saito K, Inagaki S, Mituyama T, et al. (2009) A regulatory circuit for piwi by the large Maf gene traffic jam in Drosophila. *Nature* 461: 1296.

Sanhueza M, Zechini L, Gillespie T, et al. (2014) Gain-of-function mutations in the ALS8 causative gene VAPB have detrimental effects on neurons and muscles. *Biology Open* 3: 59-71.

Sapir T, Geiman EJ, Wang Z, et al. (2004) Pax6 and Engrailed 1 Regulate Two Distinct Aspects of Renshaw Cell Development. *J Neurosci* 24: 1255-1264.

Sarov M, Barz C, Jambor H, et al. (2016) A genome-wide resource for the analysis of protein localisation in Drosophila. *Elife* 5: e12068.

Satou C, Kimura Y, Kohashi T, et al. (2009) Functional Role of a Specialized Class of Spinal Commissural Inhibitory Neurons during Fast Escapes in Zebrafish. *The Journal of Neuroscience* 29: 6780-6793.

Schneider-Mizell CM, Gerhard S, Longair M, et al. (2016) Quantitative neuroanatomy for connectomics in Drosophila. *Elife* 5: e12059.

Schoofs A, Huckesfeld S, Schlegel P, et al. (2014) Selection of motor programs for suppressing food intake and inducing locomotion in the Drosophila brain. *PLoS Biol* 12: e1001893.

Seipel K, Yanze N, Müller P, et al. (2004) Basic leucine zipper transcription factors C/EBP and MafL in the hydrozoan jellyfish Podocoryne carnea. *Developmental Dynamics* 230: 392-402.

Sepp KJ and Auld VJ. (1999) Conversion of lacZ enhancer trap lines to GAL4 lines using targeted transposition in Drosophila melanogaster. *Genetics* 151: 1093-1101.

Shang Y, Griffith LC and Rosbash M. (2008) Light-arousal and circadian photoreception circuits intersect at the large PDF cells of the Drosophila brain. *Proc Natl Acad Sci U S A* 105: 19587-19594.

Shawki HH, Oishi H, Usui T, et al. (2018) MAFB is dispensable for the fetal testis morphogenesis and the maintenance of spermatogenesis in adult mice. *Plos One* 13: e0190800.

Shevtsova NA, Talpalar AE, Markin SN, et al. (2015) Organization of left–right coordination of neuronal activity in the mammalian spinal cord: Insights from computational modelling. *The Journal of Physiology* 593: 2403-2426.

Shimono K, Fujimoto A, Tsuyama T, et al. (2009) Multidendritic sensory neurons in the adult Drosophila abdomen: origins, dendritic morphology, and segment- and age-dependent programmed cell death. *Neural Dev* 4: 37.

Siegfried E, Chou T-B and Perrimon N. (1992) wingless signaling acts through zeste-white 3, the drosophila homolog of glycogen synthase kinase-3, to regulate engrailed and establish cell fate. *Cell* 71: 1167-1179.

Sjulson L, Cassataro D, DasGupta S, et al. (2016) Cell-Specific Targeting of Genetically Encoded Tools for Neuroscience. *Annual review of genetics* 50: 571-594.

Smoker WR. (1994) Craniovertebral junction: normal anatomy, craniometry, and congenital anomalies. *RadioGraphics* 14: 255-277.

Sokabe T, Chen H-C, Luo J, et al. (2016) A Switch in Thermal Preference in Drosophila Larvae Depends on Multiple Rhodopsins. *Cell Rep* 17: 336-344.

Song J, Ampatzis K, Björnfors ER, et al. (2016) Motor neurons control locomotor circuit function retrogradely via gap junctions. *Nature* 529: 399.

Spinelli J, Collins-Praino L, Van Den Heuvel C, et al. (2017) Evolution and significance of the triple risk model in sudden infant death syndrome. *Journal of Paediatrics and Child Health* 53: 112-115.

Sprecher SG and Desplan C. (2008) Switch of rhodopsin expression in terminally differentiated Drosophila sensory neurons. *Nature* 454: 533-537.

Sugimori M, Nagao M, Bertrand N, et al. (2007) Combinatorial actions of patterning and HLH transcription factors in the spatiotemporal control of neurogenesis and gliogenesis in the developing spinal cord. *Development* 134: 1617-1629.

Suslak TJ, Watson S, Thompson KJ, et al. (2015) Piezo Is Essential for Amiloride-Sensitive Stretch-Activated Mechanotransduction in Larval Drosophila Dorsal Bipolar Dendritic Sensory Neurons. *Plos One* 10: e0130969.

Suster ML, Kania A, Liao M, et al. (2009) A novel conserved evx1 enhancer links spinal interneuron morphology and cis-regulation from fish to mammals. *Dev Biol* 325: 422-433.

Swaroop A, Kim D and Forrest D. (2010) Transcriptional regulation of photoreceptor development and homeostasis in the mammalian retina. *Nature Reviews Neuroscience* 11: 563.

Sweeney LB, Bikoff JB, Gabitto MI, et al. (2018) Origin and Segmental Diversity of Spinal Inhibitory Interneurons. *Neuron* 97: 341-355.e343.

Tabata T, Eaton S and Kornberg TB. (1992) The Drosophila hedgehog gene is expressed specifically in posterior compartment cells and is a target of engrailed regulation. *Genes Dev* 6: 2635-2645.

Talay M, Richman EB, Snell NJ, et al. (2017) Transsynaptic Mapping of Second-Order Taste Neurons in Flies by trans-Tango. *Neuron* 96: 783-795.e784.

Talpalar AE, Bouvier J, Borgius L, et al. (2013) Dual-mode operation of neuronal networks involved in left–right alternation. *Nature* 500: 85.

Tassinari CA, Cantalupo G, Högl B, et al. (2009) Neuroethological approach to frontolimbic epileptic seizures and parasomnias: The same central pattern generators for the same behaviours. *Revue Neurologique* 165: 762-768.

Tassinari CA, Rubboli G, Gardella E, et al. (2005) Central pattern generators for a common semiology in fronto-limbic seizures and in parasomnias. A neuroethologic approach. *Neurological Sciences* 26: s225-s232.

Tazerart S, Vinay L and Brocard F. (2008) The Persistent Sodium Current Generates Pacemaker Activities in the Central Pattern Generator for Locomotion and Regulates the Locomotor Rhythm. *The Journal of Neuroscience* 28: 8577-8589.

Thaler J, Harrison K, Sharma K, et al. (1999) Active Suppression of Interneuron Programs within Developing Motor Neurons Revealed by Analysis of Homeodomain Factor HB9. *Neuron* 23: 675-687.

Tio M, Toh J, Fang W, et al. (2011) Asymmetric cell division and Notch signaling specify dopaminergic neurons in Drosophila. *Plos One* 6: e26879.

Tissot M and Stocker RF. (2000) Metamorphosis in Drosophila and other insects: the fate of neurons throughout the stages. *Progress in Neurobiology* 62: 89-111.

Tsubouchi A, Caldwell Jason C and Tracey WD. (2012) Dendritic Filopodia, Ripped Pocket, NOMPC, and NMDARs Contribute to the Sense of Touch in Drosophila Larvae. *Current Biology* 22: 2124-2134.

Tsuchiya M, Misaka R, Nitta K, et al. (2015) Transcriptional factors, Mafs and their biological roles. *World Journal of Diabetes* 6: 175-183.

Tyler MS. (2000) *Developmental biology : a guide for experimental study*: Sunderland, Mass. : Sinauer Associates, Publishers, 2000.

Vandaele C, Coulon-Bublex M, Couble P, et al. (2001) Drosophila regulatory factor X is an embryonic type I sensory neuron marker also expressed in spermatids and in the brain of Drosophila. *Mech Dev* 103: 159-162.

Venken KJT, Sarrion-Perdigones A, Vandeventer PJ, et al. (2016) Genome engineering: Drosophila melanogaster and beyond. *Wiley Interdisciplinary Reviews: Developmental Biology* 5: 233-267.

Vergara HM, Bertucci PY, Hantz P, et al. (2017) Whole-organism cellular gene-expression atlas reveals conserved cell types in the ventral nerve cord of Platynereis dumerilii. *Proc Natl Acad Sci U S A* 114: 5878-5885.

Visocchi M, Mehdorn HM, Katayama Y, et al. (2017) *Trends in Reconstructive Neurosurgery: Neurorehabilitation, Restoration and Reconstruction*: Springer International Publishing AG.

von Philipsborn AC, Liu T, Yu JY, et al. (2011) Neuronal Control of Drosophila Courtship Song. *Neuron* 69: 509-522.

Vosshall LB and Stocker RF. (2007) Molecular Architecture of Smell and Taste in Drosophila. *Annual Review of Neuroscience* 30: 505-533.

Wang C-M, Shieh W-Y, Weng Y-H, et al. (2017) Non-invasive assessment determine the swallowing and respiration dysfunction in early Parkinson's disease. *Parkinsonism & Related Disorders* 42: 22-27.

Watson JD and Crews ST. (2012) Formation and specification of a Drosophila dopaminergic precursor cell. *Development* 139: 3316-3325.

Wehrli M, Dougan ST, Caldwell K, et al. (2000) arrow encodes an LDL-receptor-related protein essential for Wingless signalling. *Nature* 407: 527.

Wharton KA, Johansen KM, Xu T, et al. (1985) Nucleotide sequence from the neurogenic locus Notch implies a gene product that shares homology with proteins containing EGF-like repeats. *Cell* 43: 567-581.

Wheeler SR, Kearney JB, Guardiola AR, et al. (2006) Single-cell mapping of neural and glial gene expression in the developing Drosophila CNS midline cells. *Dev Biol* 294: 509-524.

Wheeler SR, Stagg SB and Crews ST. (2008) Multiple Notch signaling events control Drosophila CNS midline neurogenesis, gliogenesis and neuronal identity. *Development* 135: 3071-3079.

Whelan PJ. (1996) Control of locomotion in the decerebrate cat *Progress in Neurobiology* 49: 481-515.

Wichterle H, Lieberam I, Porter JA, et al. (2002) Directed Differentiation of Embryonic Stem Cells into Motor Neurons. *Cell* 110: 385-397.

Williams DW and Shepherd D. (1999) *Persistent larval sensory neurons in adult Drosophila melanogaster*.

Williams DW and Shepherd D. (2002) Persistent larval sensory neurones are required for the normal development of the adult sensory afferent projections in Drosophila. *Development* 129: 617-624.

Wilson JM, Hartley R, Maxwell DJ, et al. (2005) Conditional Rhythmicity of Ventral Spinal Interneurons Defined by Expression of the Hb9 Homeodomain Protein. *The Journal of Neuroscience* 25: 5710-5719.

Wong AM, Wang JW and Axel R. (2002) Spatial Representation of the Glomerular Map in the Drosophila Protocerebrum. *Cell* 109: 229-241.

Wyart C, Bene FD, Warp E, et al. (2009) Optogenetic dissection of a behavioural module in the vertebrate spinal cord. *Nature* 461: 407.

Wyatt C, Bartoszek EM and Yaksi E. (2015) Methods for studying the zebrafish brain: past, present and future. *European Journal of Neuroscience* 42: 1746-1763.

Xiang Y, Yuan Q, Vogt N, et al. (2010) Light-avoidance-mediating photoreceptors tile the Drosophila larval body wall. *Nature* 468: 921-926.

Yanagawa A, Guigue AMA and Marion-Poll F. (2014) Hygienic grooming is induced by contact chemicals in Drosophila melanogaster. *Frontiers in Behavioral Neuroscience* 8: 254.

Yoshikawa S, Long H and Thomas JB. (2016) A subset of interneurons required for Drosophila larval locomotion. *Mol Cell Neurosci* 70: 22-29.

Yoshino J, Morikawa RK, Hasegawa E, et al. (2017) Neural Circuitry that Evokes Escape Behavior upon Activation of Nociceptive Sensory Neurons in Drosophila Larvae. *Current Biology* 27: 2499-2504.e2493.

Zagoraiou L, Akay T, Martin JF, et al. (2009) A Cluster of Cholinergic Premotor Interneurons Modulates Mouse Locomotor Activity. *Neuron* 64: 645-662.

Zannino DA, Downes GB and Sagerström CG. (2014) prdm12b specifies the p1 progenitor domain and reveals a role for V1 interneurons in swim movements. *Dev Biol* 390: 247-260.

Zhang F, Wang L-P, Brauner M, et al. (2007) Multimodal fast optical interrogation of neural circuitry. *Nature* 446: 633.

Zhang J, Lanuza Guillermo M, Britz O, et al. (2014) V1 and V2b Interneurons Secure the Alternating Flexor-Extensor Motor Activity Mice Require for Limbed Locomotion. *Neuron* 82: 138-150.

Zhang Y, Narayan S, Geiman E, et al. (2008) V3 Spinal Neurons Establish a Robust and Balanced Locomotor Rhythm during Walking. *Neuron* 60: 84-96.

Zhang YQ, Bailey AM, Matthies HJG, et al. (2001) Drosophila Fragile X-Related Gene Regulates the MAP1B Homolog Futsch to Control Synaptic Structure and Function. *Cell* 107: 591-603.

Zhao S, Cunha C, Zhang F, et al. (2008) Improved expression of halorhodopsin for light-induced silencing of neuronal activity. *Brain cell biology* 36: 141-154.

Zhong G, Droho S, Crone S, et al. (2010) Electrophysiological characterization of the V2a interneurons and their locomotor-related activity in the neonatal mouse spinal cord. *J Neurosci* 30: 170-182.

Ziskind-Conhaim L and Hochman S. (2017) Diversity of molecularly defined spinal interneurons engaged in mammalian locomotor pattern generation. *Journal of Neurophysiology* 118: 2956-2974.

Ziskind-Conhaim L, Mentis GZ, Wiesner EP, et al. (2010) Synaptic integration of rhythmogenic neurons in the locomotor circuitry: the case of Hb9 interneurons. *Ann N Y Acad Sci* 1198: 72-84.

Ziskind-Conhaim L, Wu L and Wiesner EP. (2008) Persistent Sodium Current Contributes to Induced Voltage Oscillations in Locomotor-Related Hb9 Interneurons in the Mouse Spinal Cord. *Journal of Neurophysiology* 100: 2254-2264.

Zwart MF, Pulver SR, Truman JW, et al. (2016) Selective Inhibition Mediates the Sequential Recruitment of Motor Pools. *Neuron* 91: 615-628.

Annexe: Thesis synthesis in French

Central Pattern Generators : des circuits neuronaux pas comme les autres

Les Central Pattern Generators (CPGs) sont des circuits neuronaux impliqués dans la génèse de comportements autonomes rythmiques essentiels à la vie, tels que la respiration, la locomotion (qu'elle soit sous la forme de marche, nage ou reptation par exemple) ou la mastication pour ne citer que les exemples les plus évidents. Ces circuits neuronaux sont capables de générer une activité « tous seuls », c'est-à-dire de façon indépendante vis-à-vis des centres nerveux supérieurs ou du système sensoriel. Toutefois des signaux provenant de ces deux centres jouent un rôle dans la modulation de l'activité des CPGs pour répondre à des changements environnementaux ou physiologiques. Chez les vertébrés, les CPGs sont localisés dans la moelle épinière (ou son équivalent chez les invertébrés) en ce qui concerne le CPG de la locomotion, ou dans le tronc cérébral en ce qui concerne les CPGs de la respiration et de la mastication. Cellulairement parlant, les CPGs sont composés bien évidemment de motoneurones (MNs), qui sont les derniers effecteurs du CPG, innervent les muscles et leur donnent l' « ordre » de contraction, et d'une grande diversité d'interneurones (INs) qui se connectent les uns les autres et/ou innervent les MNs. Certains INs sont par ailleurs chargés de relayer les informations provenant des centres nerveux supérieurs et du système sensoriel. Les CPGs sont des circuits neuronaux hautement complexes et les bases moléculaires et cellulaires à l'origine de leur activité rythmique restent inconnues (Bucher, 2009).

L'étude des CPGs présente deux intérêts majeurs : tout d'abord, comprendre le fonctionnement des CPGs serait un premier pas vers le traitement de patients souffrant de pathologies probablement liées au dysfonctionnement de CPGs, comme les traumas médullaires, la mort subite du nourrisson ou l'apnée centrale du sommeil entre autres (Marder and Bucher, 2001 ; Spinelli et al., 2017 ; Visocchi et al., 2017). Le deuxième intérêt est plus fondamental : la caractérisation de CPG permettrait de comprendre comment un circuit neuronal parvient à générer un comportement. Etant donné que les CPGs génèrent des comportements « simples », qui sont rythmiques et « facilement » visualisables et quantifiables, il semble possible, avec un tel modèle, de faire le lien entre le fonctionnement du circuit et le comportement observé. Les principes établis lors de la caractérisation des CPGs pourraient ensuite être

appliqués pour comprendre la façon dont d'autres circuits, qui génèrent des comportements plus complexes ou moins facilement étudiables, fonctionnent (Bucher, 2009).

Quelles approches pour l'étude du CPG locomoteur ?

Historiquement, l'étude des CPGs a débuté chez des modèles animaux tels que le chat ou la lamproie. La preuve scientifique de l'existence d'un CPG locomoteur a été faite chez ces modèles. Bien qu'historiquement très importants, ces modèles sont de nos jours délaissés au profit d'autres plus faciles à manier, et surtout génétiquement modifiables tels que la souris, le poisson Zebrafish (*Danio rerio*) ou encore la Drosophile. De façon générale, deux approches différentes sont utilisées pour caractériser le CPG locomoteur. La première se focalise sur l'identification de gènes essentiels au développement du CPG et passe souvent par le biais de l'étude d'allèles perte de fonction (Lu et al., 2015; Zannino et al., 2014). La deuxième approche consiste à caractériser les neurones eux-même, et essayer de les séparer en groupes homogènes ayant des fonctions similaires dans le CPG locomoteur. Pour cela, on utilise des outils génétiques (tels que le système UAS/Gal4) pour cibler des populations neuronales restreintes. L'étude de la fonction de neurones dans le CPG se fait en observant les effets de la modulation de l'activité de ces neurones sur le comportement locomoteur lui-même. Cette modulation d'activité peut se faire par ablation de la population d'intérêt (Heckscher et al., 2015; Satou et al., 2009) ou modulation de l'activité physiologique (activation ou inhibition) grâce des outils comme TrpA1, shi^{ts} ou channel-rhodopsine (Clark et al., 2016; Fidelin et al., 2015; Kohsaka et al., 2014).

La Drosophile comme modèle pour l'étude des CPG

La locomotion chez la larve de Drosophile est hautement stéréotypée et faite majoritairement de vagues péristaltiques. Une vague péristaltique consiste en la contraction séquentielle des segments de la larve, en commençant par le postérieur de la larve pour atteindre la tête. Cette contraction séquentielle parfaitement coordonnée permet à la larve de se propulser vers l'avant. A une même température les larves d'un même âge ont une locomotion quasi identique et effectuent le même nombre de vagues péristaltiques sur un temps fixe. La larve est également en

mesure de tourner et de réaliser des vagues péristaltiques arrière par exemple (Clark et al., 2016).

Dans les cinq dernières années, les connaissances sur les populations neuronales qui contrôlent la locomotion chez la larve de Drosophile ont considérablement augmentées. Des populations neuronales inhibitrices ont été identifiées, tels que les PMSIs (Period Median Segmental INs) qui sont des neurones pré-moteurs et contrôlent la vitesse de locomotion en arrêtant la phase d'activation des MNs (Kohsaka et al., 2014). Des populations excitatrices ont également été identifiées, comme les neurones CLI1/2 qui induisent la contraction des MNs du postérieur vers l'antérieur de la larve au cours du développement de la vague péristaltique (Hasegawa et al., 2016). Par ailleurs, des neurones impliqués dans le relais des informations provenant des systèmes sensoriels ont été également identifiés, tels que les neurones EL (pour Eve^{+} Lateral). Les EL reçoivent des informations provenant des neurones propriocepteurs et les font parvenir aux MNs par le biais de plusieurs intermédiaires, permettant ainsi d'adapter l'amplitude et la balance bilatérale de contraction des muscles (Heckscher et al., 2015).

Origine du projet de doctorat et objectifs

Comme il a été mentionné précédemment, la caractérisation des neurones qui font partie du CPG locomoteur chez la larve de Drosophile repose sur l'existence d'outils génétiques qui permettent de cibler des populations de neurones restreintes. Le driver *TJ-ga4* (*Traffic Jam-gal4*) est un tel outil car il permet de cibler une population de 29 neurones sur les 305 qui sont présents dans chaque hémi-segment de la Corde Nerveuse Ventrale (CNV) - l'hémi-segment est considéré comme l'unité fonctionnelle du système nerveux de la Drosophile (Rickert et al., 2011 ; Riedl and Louis, 2012). De façon intéressante, TJ fait partie de la famille des facteurs de transcription (FT) Maf (pour musculo-aponeurotic fibrosarcoma), et il est connu que des neurones exprimant des FTs de la famille des Mafs font partie du CPG locomoteur chez la souris (Bikoff et al., 2016; Francius et al., 2013; Gabitto et al., 2016; Lu et al., 2015; Sweeney et al., 2018). Serait-il possible que de façon identique les neurones TJ^{+} soient impliqués dans le CPG locomoteur de la larve de Drosophile ?

Dans ce contexte, le but de ma thèse a été de :

- caractériser les neurones TJ^+ en terme de i) position dans la CNV et ii) d'identité moléculaire
- d'étudier l'implication fonctionnelle des neurones TJ^+ dans le CPG locomoteur de la larve de Drosophile.

Résultats majeurs

Dans un premier temps, j'ai montré que les neurones TJ^+ peuvent être divisés en trois grandes catégories en fonction de leurs propriétés en neurotransmetteurs. Parmi les 29 neurones TJ^+ présents dans chaque hémi-segment, 10 sont cholinergiques, 8 sont GABAergiques et 11 glutamatergiques. De plus, la population TJ^+ comprend 6 MNs (U1, U2, U5, DO5 MN et 2 MNs latéraux dorsaux qui projettent leurs axones dans le nerf ISNd). Le reste des neurones TJ^+ sont des INs. Les neurones TJ^+ sont majoritairement exclus des populations neuronales déjà caractérisées comme faisant partie du CPG locomoteur chez la larve de Drosophile. Toutefois, TJ est exprimé dans 3 neurones par hémi-segment qui appartiennent à la classe des PMSI cités plus haut dans cette synthèse, ainsi que dans le neurone précédemment caractérisé A27h (Fushiki et al., 2013 ; Kohsaka et al., 2014).

Pour étudier le rôle des neurones TJ^+ dans la locomotion de la larve, j'ai décidé de les activer ou les inhiber spécifiquement en utilisant *TJ-gal4* en combinaison avec *UAS-TrpA1* ou *UAS-shi^{ts}* (Kitamoto, 2001; Pulver et al., 2009). L'inhibition de la totalité de la population TJ^+ conduit à un défaut léger de la locomotion : les larves effectuent un nombre de vagues péristaltiques légèrement inférieur à celui réalisé par les contrôles. Lorsque la totalité de la population TJ^+ est activée, l'effet sur la locomotion est bien plus drastique : les larves sont immobiles et tous leurs muscles semblent contractés, ce qui provoque une diminution de la longueur de la larve. Lors de cette activation, la propagation des vagues péristaltiques est complètement abolie. Ce premier résultat indique bien que les neurones TJ^+ présents dans la CNV font partie du CPG de la locomotion.

La population TJ^+ a une diversité élevée, elle est composée de MNs et de plusieures classes d'INs ; en activant la totalité de la population TJ^+, il n'est pas possible de conclure sur la fonction de ces différentes sous-populations de neurones. Pour résoudre ce problème, j'ai décidé d'utiliser une technique d'intersection génétique : grâce à celle-ci, il est possible de cibler une population neuronale en fonction de deux caractéristiques. Par exemple, l'intersection génétique permet de

cibler spécifiquement les neurones à la fois TJ^+ et glutamatergiques ou les neurones à la fois TJ^+ et cholinergiques. Pour effectuer des expériences d'intersection génétique, nous avions besoin d'une lignée *TJ-Flippase (TJ-Flp)* que j'ai généré au cours de la première année de thèse en suivant un protocol développé par Ejsmont et ses collaborateurs (2009). J'ai testé l'expression de cette Flp qui en effet récapitule parfaitement le patron d'expression de TJ ; il est donc possible d'utiliser cette lignée pour conduire des expériences d'intersection génétique pour étudier la population TJ^+.

Etant donné que lorsque l'on active tous les neurones TJ^+ les larves sont complètement contractées, je me suis demandé quel était le rôle des MNs TJ^+ dans ce phenotype. En effet, on pourrait imaginer qu'activer 6 MNs par hémi-segment est suffisant pour provoquer la contraction totale des larves. Avec les outils génétiques disponibles actuellement, il n'est pas possible d'activer tous les MNs TJ^+ à la fois. Je me suis donc contentée d'activer 3 des 6 MNs TJ^+ par hémi-segment: les larves ont un défaut de locomotion avec une diminution du nombre de vagues péristaltiques par rapport aux contrôles, mais qui n'est en rien comparable à celui obtenu lorsque l'on active la totalité de la population TJ^+. Bien que l'on ne puisse pas savoir l'effet de l'activation de tous les MNs TJ^+ sur la locomotion, il semble que les MNs aient en réalité un rôle limité dans le phénotype observé lors de l'activation de la totalité de la population TJ^+.

J'ai ensuite décidé d'observer les effets de l'activation des neurones TJ^+ glutamatergiques. Lorsqu'on les active, ces neurones provoquent une immobilité des larves, qui par ailleurs lèvent souvent la tête. Les MNs chez la larve de Drosophile sont glutamatergiques ; par conséquent lorsque l'on active les neurones TJ^+ glutamatergiques, on active à la fois les MNs et les INs glutamatergiques. Le phénotype observé est beaucoup plus drastique que celui observé lorsque l'on active les MNs TJ^+. Il semble donc que les INs glutamatergiques TJ^+ aient également un rôle dans la locomotion.

En continuant la caractérisation du rôle des sous-populations TJ^+ dans la locomotion de la larve, j'ai ensuite observé l'effet de l'activation des neurones TJ^+ cholinergiques. Lorsque les neurones TJ^+ cholinergiques sont activés, ils provoquent chez les larves une contraction ventrale. Cela nous fait supposer que les INs cholinergiques TJ^+ contactent des MNs qui projettent sur des muscles ventraux. Parmi la population cholinergique TJ^+ (10 INs par hémi-segment), il n'est pas

possible de savoir lesquels sont plus particulièrement responsables. Il est intéressant que des INs cholinergiques TJ^+ aient ainsi un rôle dans la contraction spécifique des muscles ventraux. Ce type de spécificité dans l'innervation de certains groupes de MNs pourraient dans ce cas particulier permettre la mise en œuvre de comportements locomoteurs bien particulier comme le roulement (rolling en anglais) que les larves effectuent pour échapper à un stimulus nocif (Burgos et al., 2018 ; Ohyama et al., 2015). Il serait tout à fait possible que les neurones cholinergiques TJ^+ soient impliqués dans les circuits neuronaux qui contrôlent ce comportement de roulement ; pour confirmer cette hypothèse, il serait nécessaire de mettre en évidence les connections entre les neurones-commandes qui contrôlent le roulement, appelés neurones Goro (Ohyama et al., 2015) par une technique de GRASP (GFP Reconstruction Across Synaptic Partners) par exemple.

Finalement, j'ai étudié les effets de l'activation des neurones GABAergiques TJ^+. Lorsque ces neurones sont activés, les larves semblent avoir une locomotion tout à fait normale, mais ralentie. En effet, les larves font un nombre de vagues péristaltiques inférieur aux contrôles, même si la propagation de la vague de contraction se fait tout à fait normalement. A partir de ce résultat, on peut faire l'hypothèse que les neurones GABAergiques TJ^+ contrôlent la vitesse de locomotion en changeant potentiellement la fréquence d'occurrence des vagues péristaltiques. Afin d'identifier parmi la population GABAergique TJ^+ quels neurones sont impliqués dans ce ralentissement de la locomotion, nous avons mis en place une expérience de triple intersection. Cette fois-ci, l'idée est de cibler des neurones en fonction de trois caractéristiques. En fonction des outils génétiques disponibles, je suis parvenue à visualiser les effets de l'activation de neurones TJ^+ qui sont à la fois GABAergiques et expriment *period*. L'activation de ces trois neurones par segment (sur 610 neurones localisés dans un segment) provoque une diminution du nombre de vagues péristaltiques avec une propagation des vagues péristaltiques apparemment normale. Ces trois neurones TJ^+ per^+ GABAergiques semblent donc être responsables de la régulation de la vitesse de locomotion. En les caractérisant mieux, je me suis aperçue que ces neurones se trouvent dans la partie médiane ventrale de la CNV, qu'ils font partie du domaine *sim*, qu'ils expriment les FTs *engrailed*, *forkhead* et *period.* Grâce à ces caractéristiques, on peut affirmer que ces 3 neurones GABAergic TJ^+ per^+ font partie des « midline cells », un groupe de cellules dont le développement a été particulièrement étudié mais dont la fonction est inconnue. Plus

particulièrement, parmi les « midline cells », les neurones TJ^{+} *per*$^{+}$ GABAergiques font partie des neurones « MNB progeny » (Fontana and Crews, 2012; Kearney et al., 2004; Manning et al., 2012; Pearson and Crews, 2014; Tio et al., 2011; Watson and Crews, 2012; Wheeler et al., 2006; Wheeler et al., 2008; Heckscher et al., 2014). En allant un peu plus loin dans la caractérisation moléculaire de ces neurones, je me suis rendue compte qu'elles expriment les FTs *grain* et *hlh3b*. Le code combinatoire trouvé dans les neurones TJ^{+} *per*$^{+}$ GABAergiques est donc le suivant : *fkh*, *grain* et *hlh3b*, ce qui rappelle le code combinatoire d'une population d'INs impliqués dans la locomotion chez les vertébrés : les V_{2b} (Andrzejczuk et al., 2018 ; Al-Mosawie et al., 2007). De façon encore plus intéressante, une sous-population des V_{2b} semble avoir un rôle dans la régulation de la vitesse de locomotion chez le Zebrafish (Fidelin et al., 2015; Wyart et al., 2009). Nous faisons donc l'hypothèse que les neurones TJ^{+} *per*$^{+}$ GABAergiques que nous avons identifié sont conservés au cours de l'évolution jusque chez les vertébrés. Bien évidemment, une caractérisation morphologique et des données moléculaires additionnelles sont requises pour pouvoir confirmer cette hypothèse.

Conclusion

Au cours de ce doctorat, j'ai effectué la caractérisation moléculaire et fonctionnelle des neurones TJ^{+}, une population neuronale encore jamais étudiée dans le système nerveux de la larve de Drosophile. Mes résultats montrent que cette population neuronale est diverse et qu'elle est impliquée de différentes façons dans le CPG locomoteur de la larve de Drosophile. Les neurones cholinergiques TJ^{+} par exemple, semblent innerver spécifiquement des MNs qui projettent sur des muscles ventraux ; par cette innervation différentielle d'un seul groupe de muscle, ils pourraient avoir un rôle dans le comportement de roulement. Les neurones GABAergiques TJ^{+} quant à eux, et plus particulièrement les neurones TJ^{+} GABAergiques qui expriment *period* semblent avoir une fonction dans la régulation de la vitesse de locomotion des larves. Ce résultat est particulièrement captivant, car les neurones GABAergiques TJ^{+} *per*$^{+}$ expriment un code moléculaire combinatoire similaire de celui trouvé dans une population d'INs présents chez les vertébrés, les V_{2b}, qui seraient également impliqués dans la régulation de la vitesse de locomotion chez le Zébrafish.

Abstract:

CPGs (Central Pattern Generators) are neural networks able to autonomously generate essential rhythmic behaviours such as walking or breathing. In *Drosophila* larvae, the locomotor CPG is made up of motoneurons (MNs) and a huge variety of interneurons (INs). How many are actually necessary to constitute a functional CPG and how they interact is not known. During the course of this PhD, I studied a discrete neuronal population singled out by its expression of the Maf transcription factor (TF) *Traffic Jam* (*TJ*). Thanks to an intersectional genetics approach and a *TJ-Flp* line generated during my PhD, I showed for the first time that TJ^+ neurons subpopulations have distinct functions in *Drosophila* larva locomotion. Functional subdivision of TJ^+ population eventually led to the identification of 3 TJ^+ per^+ GABAergic neurons that regulate the speed of locomotion. Thorough molecular characterization of this population permitted to identify them as mnb progeny neurons, a well-studied subgroup of midline cells whose function had never been described before. The TF combinatorial code expressed by these cells is highly reminiscent of the one found in V_{2b} INs, a population in vertebrates thought to regulate the speed of locomotion as well in vertebrates; this opens the possibility of a functional conservation across evolution. Preliminary results furthermore suggest that TJ^+ INs would have functional roles in the adult fly.

Key words: Central Pattern Generator; Locomotion; *Drosophila melanogaster* larva; *Traffic Jam*; Intersectional genetics; Interneurons ; speed of locomotion

Résumé:

Les CPGs (Central Pattern Generators) sont des circuits neuronaux capables de générer de façon autonome des comportements rythmiques essentiels à la vie tels que la respiration ou la locomotion. Chez la larve de Drosophile, le CPG locomoteur est composé de motoneurones (MNs) et d'une grande diversité d'interneurones (INs). Combien d'entre eux sont nécessaires pour former un CPG fonctionnel et comment ils interagissent reste un mystère. Au cours de mon doctorat, j'ai étudié une population neuronale restreinte caractérisée par son expression du facteur de transcription (FT) de la famille des Maf, *Traffic Jam* (*TJ*). En utilisant une technique d'intersection génétique et grâce à une lignée *TJ-Flp* générée au cours de mon doctorat, j'ai démontré pour la première fois que différentes sous-populations de neurones TJ^+ ont des fonctions distinctes dans le comportement locomoteur de la larve de Drosophile. Au travers de cette sous-division fonctionnelle, j'ai finalement identifié 3 neurones TJ^+ per^+ GABAergic par segment qui régulent la vitesse de locomotion des larves. Une caractérisation moléculaire poussée de ces cellules a permis de confirmer qu'elles appartiennent au groupe connu des « midline cells », et plus particulièrement des neurones MNB progeny, dont la fonction était jusqu'à maintenant inconnue. Par ailleurs, le code combinatoire de FTs trouvé chez ces MNB progeny rappelle celui exprimé par les V_{2b}, une population d'INs qui régulerait également la vitesse de locomotion chez les vertébrés. Ces similarités entre MNB progeny et V_{2b} laissent à penser que cette population de neurones pourrait être conservée au cours de l'évolution. En outre, des résultats préliminaires suggèrent que les INs TJ^+ ont également un rôle chez la mouche adulte.

Mots-clés: Réseau Locomoteur Spinal ; Locomotion ; Larve de Drosophile; *Traffic Jam*; Intersection génétique; Interneurones ; vitesse de locomotion

Institut des Neurosciences de Montpellier, INSERM U1051, 80 Rue Augustin Fliche, 34095 Montpellier